ISSN 0-825-491

PROCEEDINGS

TECHNOLOGY TRANSFER CONFERENCE No. 6

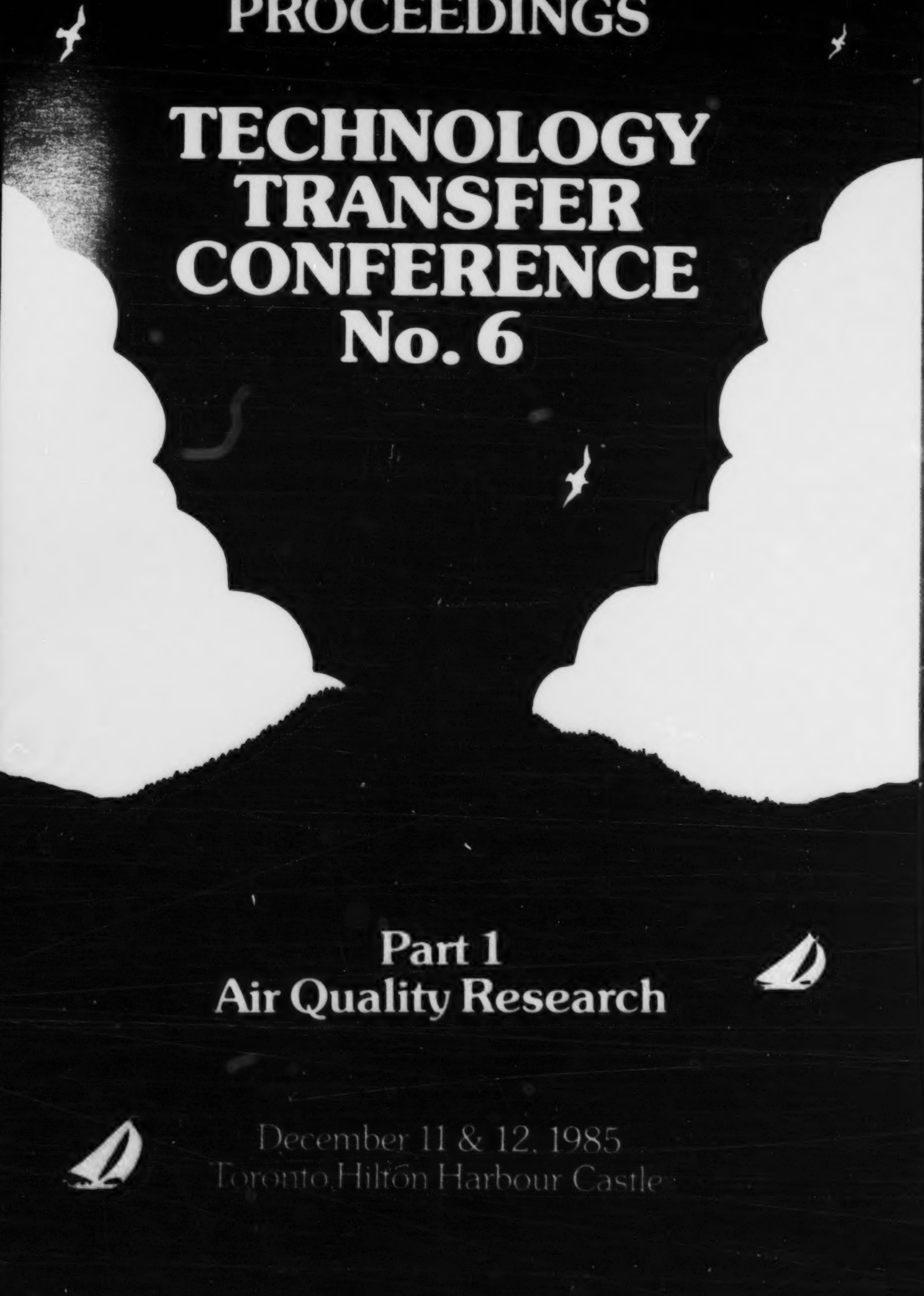

Part 1
Air Quality Research

December 11 & 12, 1985
Toronto Hilton Harbour Castle

ISSN 0-825-491

PROCEEDINGS

TECHNOLOGY TANSFER CONFERENCE NO. 6

December 11 & 12, 1985

Toronto Hilton-Harbour Castle

PART ONE

AIR QUALITY RESEARCH

Organized by
Research Advisory Committee

Sponsored by

Policy & Planning Branch
Ministry of the Environment
Ontario

Goal Statement

"To achieve and maintain a quality of the environment - including air, water and land - that will protect human health and the ecosystem and will contribute to the well-being of the people of Ontario."

ACKNOWLEDGEMENTS

The Conference Organization Committee would like to thank the invited speakers, investigators and the National Research Council of Canada for their valuable contributions.

DISCLAIMER

The views and ideas expressed in these papers are those of the authors and do not necessarily reflect the views and policies of the Ministry of the Environment, nor does mention of trade names or commercial products constitute endorsement or recommendation for use.

TABLE OF CONTENTS

Conference Paper No.		Page No.
	INTRODUCTION	xi
	PART 1: AIR QUALITY RESEARCH	
I	IDENTIFICATION AND COMPARATIVE RISK ASSESSMENT OF AIRBORNE CARCINOGENS FROM COMBUSTION SOURCES Joellen Lewtas; U.S.E.P.A., Research Triangle Park.	1
II	CHLORINATED DIOXINS AND DIBENZOFURANS IN ONTARIO - CRITERIA FOR DEVELOPING ENVIRONMENTAL STANDARDS Brendan Birmingham; MOE.	52
1	BIOLOGICAL AND CHEMICAL TESTING OF COKE OVEN EMISSIONS G. Thomas, J. Craigmile, B. Das, and A. Horton; Ontario Research Foundation.	76
2	EXPERIMENTALLY DETERMINED MUTATION RATES IN LUNG AND BRONCHIAL EPITHELIA AS A PRIMARY AIR POLLUTION STANDARD J.A. Heddle, K. Jain, H. Kaul, and D.B. Couch; Department of Biology, York University.	97
3	FACTORS THAT INFLUENCE ASSESSMENTS OF HEALTH EFFECTS OF AIR POLLUTION P. Corey, F. Silverman, A. Ayiomamitis, S. Mintz, and H.R. Husein; The Gage Institute, University of Toronto	114
4	ENVIRONMENTAL MODELLING OF TOXIC SUBSTANCES IN SOUTHERN ONTARIO D. Mackay, S. Peterson, W.Y. Shiu, and C. Charles; Department of Chemical Engineering and Applied Chemistry, University of Toronto.	137

Conference Paper No. Page No.

5 DIAGNOSTIC TESTING OF THE SWARU INSTALLATION IN HAMILTON 157
J. Trought, V. Ozvacic*, and S. Thorndyke**;
IMET, *Ministry of the Environment and
**Ontario Research Foundation.

6 CHEMICAL AND PHYSICAL CHARACTERIZATION OF AIRBORNE PARTICULATES AND THEIR SOURCES THROUGH MULTIELEMENT ANALYSIS AND RECEPTOR MODELLING 171
T.G. Pringle and R.E. Jervis; Department of
Chemical Engineering and Applied Chemistry
University of Toronto.

7 STUDY OF CONDITIONS FOR CONDENSATION AND DESORPTION OF PCDD ON PARTICULATE MATTER UNDER STACK SAMPLING CONDITIONS 191
F.W. Karasek and L.C. Dickson; Department of
Chemistry, University of Waterloo.

8 ASSESSMENT OF TOXICITY OF INGESTED AND INHALED HALOAROMATIC HYDROCARBONS 218
G.D. Sweeney, D.A. Clark and J. Gauldie;
Department of Medicine, McMaster University.

9 THE RAPID SCREENING OF MUNICIPAL REFUSE INCINERATOR FLY-ASH AND STACK GAS FOR PCDD/PCDF USING A TRANSPORTABLE TANDEM MASS SPECTROMETER (GC/MS/MS) SYSTEM 224
Boni Shushan and Angie Ngo; Sciex Ltd., Ontario

28 BLOOD LEAD AND ASSOCIATED RISK FACTORS IN ONTARIO CHILDREN - 1984 236
L. Smith, C. Duncan*, and J. O'Heany**;
Ministries of Health, *Environment and **Labour.

29 THE DISPERSAL OF AIR PARTICULATES ON A SHORT AND LONG-TERM TIME SCALE 245
J.D. MacArthur, G.R. Palmer, and Xin-Pei Ma;
Department of Physics, Queen's University.

30 DOSE-RESPONSE STUDIES OF GASEOUS POLLUTANTS ON FOOD CROPS 263
D. Ormrod, and J.M. Petitte;
Department of Horticultural Science,
University of Guelph.

31 USE OF THE DIRECT SAMPLE INSERTION DEVICE FOR SAMPLE VAPORIZATION IN THE INDUCTIVELY COUPLED PLASMA FOR ATOMIC AND MASS SPECTROMETRY 291
E. Salin, R.L. Sing, D.W. Boomer* and M. Powell*;
Department of Chemistry, McGill University, and
*Ontario Ministry of the Environment.

Conference Paper No. **Page No.**

32 IDENTIFICATION OF SELECTED PAHs IN A HAMILTON, ONTARIO AIR SAMPLE BY SHPOL'SKII SPECTROSCOPY 300
C.M. Sadowski*, S.P. Filseth*, G. Parnel and F. Morgan; Departments of Chemistry* & Physics, York University.

33 THE EXCHANGE OF AIR PARTICULATES BETWEEN THE INSIDE AND OUTSIDE OF A BUILDING 320
J.D. MacArthur, G.R. Palmer and Xin-Pei Ma; Department of Physics, Queen's University.

34 FEASIBILITY OF DETERMINING SO_2 MASS EMISSION FLUXES BY STACKSCANNING 335
R.C. Mitchner and R.A.H. Buxton; Moniteq Ltd., Ontario.

35 GAS-PHASE PHOTOCHEMISTRY OF POLYCHLORINATED BIPHENYLS 349
N. Bunce and Jo-Anne Langshaw; Department of Chemistry, University of Guelph.

36 A FUNDAMENTAL STUDY ON THE DEPOSITION OF AEROSOLS ON CYLINDERS IN TURBULENT CROSS FLOWS 379
P.L. Douglas and S. Ilias; Department of Chemical Engineering, Queen's University

Conference Paper No. | Page No.

PART 2: WATER QUALITY RESEARCH

IV TOXICOLIGICAL EVALUATION OF GREAT LAKES DRINKING WATER 1
Ian Munro; Canadian Centre for Toxicology.

10 TRACE ORGANIC CONTAMINANT REMOVAL FROM DRINKING WATER 13
J. Hilton and R. Machacek;
MacLaren Plansearch Inc.

11 PILOT TESTING PROGRAM FOR POTABLE WATER TREATMENT FOR COLOURED NORTHERN ONTARIO WATER 32
T. Constantine, K. Sakamoto and G. Lai;
M.M. Dillon Ltd.

12 DEFLUORIDATION OF AMABELLE TOWNSHIP GROUNDWATER 73
P. Haliday; Proctor & Redfern Ltd.

13 SEDIMENT AND POLLUTANT ACCUMULATION IN THE HUMBER RIVER MARSH 110
Jane Weninger and A. Jopling;
Department of Geography, University of Toronto.

14 REGIONAL GEOCHEMICAL STRATIFICATION OF SHALLOW GROUNDWATERS RESULTING FROM CATCHMENT URBANIZATION 160
K. Howard, P. Pilon, and H. Falk;
Scarborough College, University of Toronto.

15 THE EFFECTS OF TILE DRAINAGE AND OPEN DITCHES ON PEAK FLOWS AND DRY WEATHER FLOWS 184
W.E. Watt and J. Paine; Department of Civil Engineering, Queen's University.

16 PRE-FEASIBILITY STUDY ON EXPANSION AND UPGRADING OF PORT DOVER SEWAGE TREATMENT PLANT.... 198
Maria Kelleher and C. Papadopol;
MacLaren Engineers, Inc.

17 THE EFFECTS OF WASTEWATER QUALITY ON ULTRAVIOLET LIGHT DISINFECTION 226
G. Elliot Whitby*, G. Palmateer**, F. Boon*, and E. Janzen**; *Trojan Technologies and **Ministry of the Environment.

Conference Paper No. **Page No.**

18 THE TECHNICAL AND ECONOMIC FEASIBILITY OF RETROFITTING EXISTING MUNICIPAL TREATMENT PLANTS IN CANADA FOR BIOLOGICAL PHOSPHORUS REMOVAL 257
S. Nutt; Canivro Consultants Ltd.

37 THE ASSESSMENT OF A POINT SOURCE DISCHARGE OF SUSPECTED MUTAGENIC AND CARCINOGENIC CONTAMINANTS: AN EPIDEMIOLOGICAL APPROACH 285
I. Smith and H. Ferguson; Fish Pathology Laboratory, University of Guelph.

38 DEVELOPMENT OF PREDICTIVE ORGANIC CONTAMINANT STRUCTURE-PROPERTY-TOXICITY RELATIONSHIPS FOR AQUATIC ORGANISMS 333
D. Mackay, S. Abernethy, and C. Charles; Institute for Environmental Studies, University of Toronto.

39 THE SIGNIFICANCE OF NEOPLASIA IN FISH POPULATIONS 357
H. Ferguson, M. Hayes, J. Heeney, B. Hicks and I. Smith; Department of Pathology University of Guelph.

40 EPIDEMIOLOGICAL STUDY OF DISEASE INCIDENCE AND RECREATIONAL WATER QUALITY AT SELECTED CONSERVATION AREAS IN SOUTHERN ONTARIO 370
Patricia Seyfried and Nancy Brown; Faculty of Medicine, University of Toronto.

41 FINGERPRINTING THE TORONTO WATERFRONT: A METHOD FOR DETERMINING THE SOURCES OF BACTERIAL POLLUTANTS 414
W. Bradbury, M. Marko, D. Rego, M. Young, E. Harris, and P. Seyfried; Department of Microbiology, & Toronto General Hospital University of Toronto.

42 VALIDATION AND A POSSIBLE RE-ASSESSMENT OF CLAM CAGING EXPERIMENTS USING ELLIPTIO COMPLANATUS AS BIOMONITORS FOR TOXIC CONTAMINANTS IN WATER 427
P. Hebert, B. Muncaster, and C. Pugsley; Great Lakes Institute, University of Windsor.

Conference Paper No.		Page No.
43	REVISED MONITORING SCHEME FOR PERSISTENT AND TOXIC ORGANICS IN GREAT LAKES SPORTS FISH .... J. Coburn, H. Huneault, G.A. Rees* and G. Crawford; Zenon Environmental Inc., and *Ontario Ministry of the Environment.	441
44	DEVELOPMENT OF A COST EFFECTIVE PROTOCOL FOR ROUTINE ANALYSIS OF TRACE ORGANIC CONTAMINANTS IN MUNICIPAL WPCP RAW SEWAGES AND FINAL EFFLUENTS .... J. Martin, Cicillia Chan and D. Sutherland; Mann Testing Laboratories Ltd.	470
45	ANALYSIS OF CHEMICALS USED AT WATER TREATMENT PLANTS .... F. Karasek and T. Thompson; Department of Chemistry, University of Waterloo.	504

Conference Paper No. **Page No.**

PART 3: LIQUID & SOLID WASTE RESEARCH

Conference Paper No.		Page No.
III	VOLATILE ORGANIC CARBON FROM LAND DISPOSAL OF WASTE - MECHANISMS OF EMISSIONS AND CONTROL STRATEGIES .... Louis Thibodeaux; Louisiana St. University.	1
19	HAZARDOUS ORGANIC CHEMICALS IN GROUNDWATER AT ONTARIO LANDFILLS .... J. Cherry, J. Barker, M. Zapico, M. Moore and N. Gensky; Institute for Groundwater Research, University of Waterloo.	14
20	THE ACCURATE DETERMINATION OF IN-SITU CONCENTRATIONS OF VOLATILE HYDROCARBONS IN GROUNDWATERS AT THE GLOUCESTER LANDFILL SITE, OTTAWA, ONTARIO .... W. Gorman and R. Devlin; Department of Geological Sciences, Queen's University.	46
21	DESIGN OF GROUNDWATER MONITORING PROGRAMS FOR WASTE LANDFILL SITES .... R. Schwartz and P. Byer; Department of Civil Engineering, University of Toronto.	86
22	AN IN-SITU METHOD FOR DETERMINING RATES OF DENITRIFICATION IN GROUNDWATER .... D. Miller, R. Gillham and R. Starr; Institute for Groundwater Research, University of Waterloo.	87
23	SELECTION OF AERATION DEVICES .... J. Ganczarczyk; J. Ganczarczyk Ltd., Toronto.	107
24	COMPOSITION, MINERALOGY, AND MORPHOLOGICAL NATURE OF INDUSTRIAL WASTES AND THEIR LEACHIBILITY .... J. Kramer and O. Mudroch; Department of Geology, McMaster University.	132
25	MODELLING THE MOVEMENT OF VAPOURS FROM HAZARDOUS LIQUIDS IN SOIL .... R.A. Allan, G. Farquhar, and E. McBean; Department of Civil Engineering, University of Waterloo.	149

Conference Paper No. | Page No.

26 POSSIBLE EFFECTS ON GROUNDWATER QUALITY OF THE USE OF LIQUID INDUSTRIAL WASTES FOR DUST CONTROL ON ONTARIO ROADS 178
A. Abdul, R. Gillham, J. Barker, and R. Carter; Institute for Groundwater Research, University of Waterloo.

27 CODISPOSAL OF INDUSTRIAL AND MUNICIPAL WASTES 209
D. Kirk and M. Lau; Department of Chemical Engineering, University of Toronto.

46 EFFECTS OF INCREASING AMOUNTS OF NON-POLAR ORGANIC LIQUIDS IN DOMESTIC WASTE LEACHATE ON THE HYDRAULIC CONDUCTIVITY OF CLAY LINERS IN SOUTHERN ONTARIO 244
R. Quigley and F. Fernandez; Geotechnical Research Centre, University of Western Ontario.

47 GEOMECHANICAL INVESTIGATION OF NEAR-SURFACE FRACTURES IN CLAY TILLS 265
M. Dusseault and A. Vorauer; Department of Earth Sciences, University of Waterloo.

48 WASTE MANAGEMENT PLANNING FOR THE PHARMACEUTICAL INDUSTRY 292
R. Stairs and R. Makhija; Department of Chemistry, Trent University.

49 REFUSE PYROLYSIS EMISSIONS TESTING 298
S. Thorndyke; Ontario Research Foundation.

50 APPROACHES TO MINIMIZING SOLVENT EFFECTS IN MUTAGENICITY ASSAYS 309
D. Logan, S. Chiu, and M. Salsmone*; York University, *Ministry of the Environment.

51 LEACHING STUDIES OF PCDD AND PCDF FROM MUNICIPAL INCINERATOR FLYASH 321
F. Karasek, H. Tong, and G. Revel; Department of Chemistry, University of Waterloo.

52 DEVELOPMENT AND VALIDATION OF PROTOCOLS FOR SAMPLING SURFACE AND GROUNDWATERS FOR ORGANIC CONTAMINANTS 349
J. Barker and G. Travis; Institute for Groundwater Research, University of Waterloo.

Conference Paper No. Page No.

53 LABORATORY STUDY OF TILE DRAIN EFFICIENCIES FOR LEACHATE COLLECTION 370
R. Farvolden, A. Abdul, R. Carter and R. Gillham;
Institute for Groundwater Research,
University of Waterloo.

54 DEVELOPMENT OF DESIGN CRITERIA FOR OPTIMAL RECOVERY OF LEACHATE UNDER SANITARY LANDFILLS 397
A. Abdul, L. Arnaud, R. Gillham, and R. Farvolden;
Institute for Groundwater Research, University
of Waterloo.

INTRODUCTION

The Ontario Ministry of the Environment holds its annual Technology Transfer Conference to report and publicize the progress made on Ministry-funded projects. These studies are carried out in Ontario universities and by private research organizations.

The papers presented at Technology Transfer Conference No. 6, held in December 1985 are presented in Conference Proceedings. These Proceedings are divided into three parts corresponding to the conference sessions - Part 1 deals with air quality research, Part 2 with water quality research, and Part 3 with liquid and solid waste research. Papers dealing with analytical methods and instrument development are assigned to each of the three parts.

For further information on any of the projects, the reader is kindly referred to the Principal Investigators or to the Research Co-ordination Office at (416) 965-5788.

IDENTIFICATION AND COMPARATIVE RISK ASSESSMENT OF AIRBORNE CARCINOGENS FROM COMBUSTION SOURCES

Joellen Lewtas*, Marcia G. Nishioka+, and Bruce A. Petersen**
*Genetic Bioassay Branch, Health Effects Research Laboratory,
U.S. Environmental Protection Agency, Research Triangle Park, NC.

+ Batelle-Columbus Laboratories, Columbus, OH.

**Applied Technology and Mobile Environmental Analysis, Sciex Inc.,
Worthington, OH.

ABSTRACT

The identification and assessment of airborne carcinogens have been significantly advanced by the use of short-term genetic bioassays. Bioassay-directed fractionation, coupled with new organic characterization methods, has provided the tools needed for more efficient identification of potential carcinogens in complex combustion emissions and urban air samples. These studies have shown that a significant portion of the mutagenicity is found in fractions more polar than polynuclear aromatic hydrocarbons (PAHs). New mass spectrometry techniques have been developed to identify and quantify the more polar mutagens in these samples.

The comparative mutagenicity and carcinogenicity of a series of combustion emissions have been assessed using dose-response studies in bacteria, mammalian cells and rodents. This data base has been used to develop a comparative potency risk assessment methodology for a series of combustion emissions.

IDENTIFICATION AND COMPARATIVE RISK ASSESSMENT OF AIRBORNE CARCINOGENS FROM COMBUSTION SOURCES

Joellen Lewtas*, Marcia G. Nishioka†, and Bruce A. Petersen¶

*Genetic Bioassay Branch, Health Effects Research Laboratory,
U.S. Environmental Protection Agency, Research Triangle Park, NC
27711, U.S.A.
†Battelle-Columbus Laboratories, Columbus, OH 43201, U.S.A.
¶Applied Technology and Mobile Environmental Analysis, Sciex, Inc.,
100 East Wilson Bridge Rd., Suite 208, Wortington, OH 43085, U.S.A.

ABSTRACT

The identification and assessment of airborne carcinogens has been significantly advanced by the use of short-term genetic bioassays. Bioassay-directed fractionation coupled with new organic characterization methods has provided the tools needed to more efficiently identify potential carcinogens in complex combustion emissions and urban air samples. These studies have shown that a significant portion of the mutagenicity is found in fractions more polar than polynuclear aromatic hydrocarbons(PAHs). New mass spectrometry techniques have been developed to identify and quantify the more polar mutagens in these samples.

The comparative mutagenicity and carcinogenicity of a series of combustion emissions has been assessed using dose-response studies in bacteria, mammalian cells and rodents. This data base has been used to develop a comparative potency risk assessment methodology for a series of combustion emissions.

PART I: CHARACTERIZATION AND COMPARISON OF THE MUTAGENIC AND CARCINOGENIC ACTIVITY OF COMBUSTION EMISSIONS

INTRODUCTION

Incomplete combustion products from various sources contain carcinogenic polycyclic organic compounds and in several cases these combustion products have been recognized as human carcinogens (e.g., chimney soot, coal tars, and cigarette smoke). Polynuclear aromatic hydrocarbons (PAH's) and particularly benzo[a]pyrene (BaP) were implicated in the early 1900's as the major carcinogenic constituents of coal tars and soot extracts.[1-3] Since then, many PAH's have been isolated from combustion products, identified and evaluated as carcinogens in animals.[4-6] Although many other PAH's are carcinogenic, BaP was for many years considered the best indicator of PAH's and was monitored as a measure of both air pollution and occupational exposure to PAH's from combustion products.[5,7-9] Recent improvements in quantitative analytical methods for measuring many PAH's and other carcinogenic polycyclic organic matter (POM's) (e.g., aromatic amines, substituted PAH's, and heterocyclic compounds) have shown that BaP is not always well correlated with total PAH exposure or exposure to carcinogenic POM's.[10-12] Advances in bioassay-directed chemical fractionation and characterization techniques[13] when applied to different combustion products, also indicate that PAH's alone do not account for all the mutagenic or carcinogenic activity of these products.[14-16]

The relative mutagenic and carcinogenic activity of a series of these organic combustion emissions has recently been characterized and compared. The combustion emission sources include residential wood stoves and oil heaters,[17] utility power plants,[18] diesel and gasoline vehicles.[19] The relative activity of these emissions has been compared to the activity of complex organics from roofing tar pots, coke ovens, and cigarette smoke; emissions for which human lung cancer data are available.[20-22] This chapter reviews these recent studies designed to: 1) use short-term mutagenicity assays to characterize fractionated combustion products, 2) evaluate the relative mutagenic and carcinogenic activity of combustion emissions, and 3) develop a comparative potency method for estimating cancer risk from combustion products.

CHARACTERIZATION OF THE MUTAGENS AND CARCINOGENS EMITTED FROM COMBUSTION SOURCES

Combustion of either fossil fuels (e.g., oil, coal, gasoline, diesel fuel) or vegetative sources (e.g., wood, plant materials) results in the production and usually the emission of a very complex mixture of organic gaseous and particulate pollutants as well as some inorganic materials. The major gaseous pollutants CO, NO_x, and SO_x are known to produce a variety of acute and chronic non-carcinogenic health effects associated with the respiratory system. These and other gaseous emissions such as nitrous acid (HONO), are thought to react with many of the organic emissions to form oxidized and nitrated compounds such as epoxides, lactones, and nitrated polycyclic aromatic hydrocarbons (NO_2-PAH's).[23] A number of these epoxides (e.g., BaP-4,5-oxide),[24] lactones (e.g., 4-oxapyrene-5-one)[23] and NO_2-PAH's (e.g., nitropyrenes)[25] have been shown to be mutagens and in some cases carcinogens. Combustion of both fossil and vegetative fuels also results in the emission of gaseous compounds which have been shown to induce tumors in animals or have been implicated as carcinogens in human epidemiological studies including aldehydes (e.g., formaldehyde, acetaldehyde) and aromatic hydrocarbons (e.g., benzene).[26,27]

Virtually every combustion process in which carbonaceous fuels are burned results in the production of soot. Soot often consists of clusters of very small (~30nm) spheroids fused together to form particles with a 0.1-0.2 micrometer diameter.[28] These soot particles contain an organic fraction (solvent extractable) and an elemental carbon fraction which appears to be similar to graphite.[28] The combustion of diesel fuel, gasoline, coal, fuel oil, and wood have all been shown to produce soot particles with extractable organic matter which is mutagenic in short-term bioassays[17-19,29-31] and in several of these sources have been shown to be tumorigenic in animals.[32-34] Chemical characterization of these organics shows that they contain carcinogenic PAH's. Recently, chemical characterization studies of motor-vehicle emissions have identified the presence of methylated PAH's (e.g., methylphenanthrenes),[35] nitrated PAH's (e.g., nitropyrene),[36] oxidized PAH's (e.g., cyclopenta(c,d)-pyrene dicarboxylic acid anhydride),[37] and a variety of other polycyclic organic compounds not yet evaluated in animal cancer bioassays.

Bioassay-directed fractionation closely coupled to chemical characterization has been shown to be the most efficient and effective approach to identifying the biologically active compounds in a complex mixture. This approach has been used to identify tumor initiators and tumor promoters in cigarette-smoke condensates,[32] automotive exhaust emissions,[38] and urban-air particles.[14] More recently, this approach has been coupled with short-term genetic bioassays, including both microbial and mammalian-cell mutation assays, to identify mutagens and potential carcinogens in complex mixtures.[39] We first employed this method to identify the chemical classes and specific components associated with diesel particulate emissions that were mutagenic in the Ames *Salmonella typhimurium* mutagenesis assay.[40]

Diesel particles collected by the dilution-tunnel method[41] were Soxhlet®-extracted with dichloromethane and solvent-partitioned into organic acids, bases, and neutral components. The neutral components were further fractionated into paraffins (hexane), aromatics (1% ether/hexane to elute blue fluorescent material), transitional compounds (yellow non-fluorescent band eluted with 1% ether/hexane), and oxygenated compounds (50% acetone/methanol). The mutagenic activity of each fraction was determined using the Ames Salmonella typhimurium/-microsome assay in TA1535, TA1537, TA1538, TA98, and TA100[40]. The distributions of the mass of each fraction and of its mutagenic activity in TA98 are shown in Table 1 for the four-stroke V-8 Caterpillar 3208 engine used in urban service vehicles. The moderately and highly polar neutral compounds in the transitional (TRN) and oxygenated (OXY) fractions account for 89-94% of the mutagenic activity of the extractable organics and only 32% of the mass. Conventional gas chromatography/mass spectroscopy identified many nonmutagenic fluorenones and methylated fluorenones as major constituents of these fractions. None of these or other identified constituents accounted for the direct-acting frameshift mutagenic activity observed. Studies with nitroreductase-deficient strains of Salmonella typhimurium showed a reduction in the mutagenicity of these organics, suggesting that nitrated compounds are present.[42] Nitrated polycyclic aromatic hydrocarbons (NO_2-PAH's) are potent direct-acting frameshift mutagens detected in xerographic toners.[43] A series of NO_2-PAH's in diesel extracts were then identified and quantitated in order to estimate their contribution to the mutagenic activity of diesel particulate emissions.[44] Similar studies have also been conducted by Schuetzle.[45] These studies show that NO_2-PAH's, di-NO_2-PAH's, and hydroxyNO_2-PAH's together account for much of the mutagenicity observed in Salmonella typhimurium. Particulate emissions from catalyst-equipped gasoline-engine vehicles using unleaded fuel contain significantly less of these NO_2-PAH's.[44] The mutagenic activity of both leaded- and unleaded-gasoline emissions is substantially increased with the addition of an exogenous metabolic activation (MA) system, suggesting that the classical PAH's may play a more important role than do NO_2-PAH's in the mutagenicity and carcinogenicity of gasoline emissions.[46]

Characterization of the mutagenicity of emissions from both vegetative and fossil fuels show general similarities. Comparison of the distribution of mutagenic activity in different organic fractions extracted from an airtight woodstove burning pine and oak are compared to the emissions from a light-duty diesel vehicle in Table 2. In both wood and diesel combustion, 82-99% of the mutagenicity was in the neutral fraction. Very little mass or mutagenic activity was observed in the organic bases. Differences in these sources were observed in the distribution of mass and mutagenicity in the neutral subfractions.

Bioassay-directed fractionation and chemical characterization has also been used to characterize and compare the complex organic emissions from roofing tar pots, coke ovens, and cigarette smoke. To obtain a gross characterization of the chemical classes present in the samples, the chemical class distribution was determined by solvent partitioning the organics into acidic, basic, neutral, and cyclohexane insoluble (a highly polar fraction) fractions. The neutral fractions were further separated into the nonpolar neutrals, aromatics (nitromethane soluble) and polar neutrals. Characterization of the distribution of mutagenic activity (Ames _Salmonella_ _typhimurium_ bioassay) in each of these fractions[47] showed significant differences between the diesel, coke oven main, roofing tar, and cigarette smoke condensate samples. In the diesel samples, over 90% of the mutagenic activity is located in the aromatic and polar-neutral fractions, and a significant portion of this activity can be accounted for by NO_2-PAH's. The cigarette smoke condensate, coke oven main, and roofing tar samples did not contain detectable amounts of NO_2-PAH's.[48] Most of the mutagenicity of coke oven main sample was found in the basic fraction (37%) and polar neutral fraction (39%). The cigarette smoke condensate sample also had significant activity in the basic fraction (66%), but chemical analysis indicated that the components differed significantly from those of the coke oven main sample.[49] The roofing tar sample contained aromatic (14%) and polar (75%) mutagenic constituents that were not NO_2-PAH's. The PAH subfraction of each of these samples accounted for only a small portion of the mutagenicity (eg. diesel (0.2%), cigarette smoke condensate (0.1%), roofing tar (5%) and coke oven main (8%)).

Although the specific mutagens in these different sources are not identical, they all cause frameshift mutations and appear to be compounds that could be classified as polycyclic organic matter (POM). Chemical characterization suggests that in addition to nitrated NO_2-PAH's found in the slightly and moderately polar neutrals, hydroxylated and carboxylated polycyclic organics are found in the organic acid fraction, aromatic amines and nitrogen heterocycles are found in the organic bases and highly oxygenated quinones, diones, and nitro-oxygenated compounds are found in the polar neutral fractions.

RELATIVE MUTAGENIC AND CARCINOGENIC ACTIVITY OF COMBUSTION EMISSIONS

Mutagenic Activity

The mutagenic activity of dichloromethane extractable organics from diluted and filtered particulate emissions from different combustion sources has been evaluated in several short-term genetic bioassays. The short-term *in vitro* bioassays were performed according to standardized protocols, and when possible, in such a way that dose-response data demonstrated a positive increase (slope) above spontaneous levels for at least three doses. When such dose-response data were obtained, the slope of the response curve was determined using simple linear regression analysis. In several short-term bioassays described elsewhere[50,51] difficulties were encountered in obtaining good dose-response data which may be due in part to solubility problems in the aqueous cell culture media. In the following bioassays, dose-dependent increases in response were obtained for many of the combustion emission samples evaluated:

1. Reverse mutation in *Salmonella typhimurium* TA98 (Ames bioassay)[52]
2. Forward mutation at the thymidine kinase locus in L5178Y mouse lymphoma cells (mouse lyphoma bioassay)[53]
3. Sister chromatid exchange (SCE) in Chinese hamster ovary (CHO) cells (SCE bioassay)[53]
4. Enhancement of viral (simian adenovirus SA7) transformation in Syrian hamster embryo (SHE) cells (viral enhancement bioassay)[50]

Of the above four *in vitro* bioassays, the first three provided reproducible dose responses. The enhancement of viral transformation assay produced variable dose responses that may have been due to variation in primary embryo cell isolations.[54]

For the Ames, mouse lymphoma, and SCE bioassays, one or more preliminary range-finding assays were performed to determine the optimum dose range for defining the slope of the dose response. The bioassays were generally performed with duplicate or triplicate treatments at five to seven doses.

Although alternative methods of analyzing the dose-response data from short-term bioassays have been reported,[55] the linear slope of the dose-response determined from simple regression analysis is presented here for the Ames, mouse lymphoma, and SCE bioassays. The dose-response slopes were uniformly consistent with a linear nonthreshold pattern. In the *Salmonella typhimurium* bioassay, toxic doses (generally the highest two doses) were deleted from the regression analysis. In the three mammalian cell bioassays, doses that resulted in survivals below 10% were deleted. When data from several experiments were available, the data resulting in the best dose response as measured by the correlation coefficient (>0.8) were utilized in this study.[19] A determination of the coefficient of variation between separate bioassay slopes for the same sample has been reported elsewhere[19,56] and generally averaged 10-20%.

The slopes of each of these dose-response curves for each complex emission sample are summarized in Table 4. The diesel samples did not require an exogenous metabolic activation (MA) system in either the mouse lymphoma or the Ames bioassay, and in most cases, the addition of MA decreased the slope slightly. This was also true for the utility coal combustion emissions. The three human carcinogens, on the other hand, either required MA or were significantly enhanced in genetic activity as a result of the addition of MA. The emissions from gasoline powered vehicles, airtight woodstoves, and residential oil heaters were also enhanced by the addition of MA.

Carcinogenic Activity

Mouse skin tumorigenesis assays have had considerable use in determining the tumorigenic and carcinogenic effects of chemicals and complex mixtures.[57,58] Skin tumor initiation experiments were performed with the extractable organics from combustion particulate emissions in SENCAR mice. After administration of five single initiating doses (80 mice/dose), the mice were treated twice weekly with 12-O-tetradecanoylphorbol-13-acetate (TPA, 2.0 μg). Mice were scored individually at six months for papillomas and at one year for squamous cell carcinomas.[33,34] The carcinoma responses in the initiation assay were correlated with the papilloma responses; only the papilloma responses are referred to here.

A linear dose-response relationship for skin tumor initiation was observed for all samples up to a dose level of 1 mg. The extractable organics from fossil fuel combustion showed very similar potencies (0.12-0.59 papillomas/mouse/mg), however, the cigarette smoke condensate was much weaker (0.0024 papillomas/mouse/mg), and the coke oven samples were more potent (2.1 and 3.2 papillomas/mouse/mg) than the combustion emissions examined.

Human lung cancer unit risk estimates shown in Table 4 have been used as a basis of comparing carcinogenic potency for complex organic emissions containing polycyclic organic matter. The unit cancer risk is predicated on the linear non-threshold extrapolation model and is the individual lifetime excess lung cancer risk from continuous exposure to 1 μg carcinogen per m^3 inhaled air. The human lung cancer unit risks obtained from the epidemiologic data for coke oven workers, roofing tar applicators, and cigarette smokers were, respectively, 9.3×10^{-4}, 3.6×10^{-4}, and 2.2×10^{-6} per μg particulate organics per m^3 air.

Comparison of the Relative Potencies

The relative potencies of each of these extractable organics from combustion emissions can be directly compared to each other and to the human carcinogens by normalizing the slope data from each bioassay to one of the samples. The coke oven topside sample was selected and given a relative potency of 1.0. The relative potencies for the other samples were determined by normalizing to the coke oven topside activity for that assay (relative potency = slope normalized to coke oven topside = slope sample ÷ by slope of coke oven topside for each assay). The relative potencies are shown in Table 5.

The relative potency of the combustion emissions ranged from only a five-fold difference in the mouse skin tumorigenesis assay to a 150-fold difference in the mouse lymphoma gene mutation assay. The Ames *Salmonella typhimurium* mutagenesis assay showed approximately two orders of magnitude difference (100-

110-fold) from the weakest (wood and diesel combustion emissions) to the most potent (diesel and leaded gasoline samples). The cigarette smoke condensate, however was nearly three orders of magnitude less tumorigenic than the coke oven topside sample in the mouse skin tumorigenesis assay but not in the short-term bioassays. In the short-term bioassays the potency of the cigarette smoke condensate compared to coke oven topside was several orders of magnitude higher than that indicated by the epidemiologic data (Table 5). The relatively higher potency of the cigarette smoke condensate in the in vitro bioassays may be due to the presence of highly mutagenic heterocyclic amines (2-amino-9H-pyrido[2,3-b]indole and 2-amino-3methyl-9H-pyrido[2,3-b]indole).[59]

The mouse skin tumor initiation bioassay and mouse lymphoma bioassay (+MA) agreed closely on the relative potency of the Nissan diesel extract with respect to the coke oven topside sample. The Ames Salmonella typhimurium TA98 bioassay and the mouse lymphoma bioassay (-MA) yielded a higher relative potency by approximately one order of magnitude when compared to the skin tumor initiation bioassay (Table 5). The relatively high mutagenic activity of the diesel particulate extracts in the Ames bioassay compared to the human carcinogens may result from the presence of NO_2-PAH's in the diesel emissions. NO_2-PAH's have been estimated to account for a substantial portion of the Ames activity observed in diesel particulate extracts.[44] The decreased mutagenic activity of these diesel emissions in nitroreductase-deficient strains of Salmonella typhimurium[42] is additional evidence for the involvement of bacterial nitroreduction in the bacterial mutagenicity of diesel emissions.

Table 5 also presents the best estimates for the unit risk of lung cancer from epidemiologic data for roofing tar and cigarette smoke normalized to the coke oven topside sample. Roofing tar has about one-third the potency of coke oven topside, and cigarette smoke condensate had about one-four-hundredth the potency of coke oven topside. Mouse skin initiation data compared well with the human epidemiologic data, with roofing tar and cigarette smoke at about one-fifth and one-thousandth the potency of coke oven topside, respectively.

Comparison of Mutagenic Emission Rates for Various Combustion Sources

Since the mutagenic activity (potency) of the extractable organics from combustion particulate emissions from various sources were generally within two orders of magnitude (10^2) in order to directly compare the sources, organic and particulate emission rates must be considered. The emission rates for the particle-bound organics from these sources differ in some cases by as much as 5×10^5. To compare the mutagenicity of emissions from various sources, it is critical to compare the rates of mutagenic emissions on the same consumption, or yield as shown in Table 6. To compare rates of mutagenic emissions of mobile sources, the mutagenic activity per kilometer is often reported. The rates of mutagenic emissions from stationary sources are compared on the basis of fuel consumption or energy consumption. Although stationary and mobile sources could be directly compared on a fuel-consumption basis, the distribution of fuel is fixed by consumption demands based on the relative needs for transportation, home heating, or energy.

ESTIMATION OF CANCER RISK FROM COMBUSTION EMISSIONS BASED ON COMPARATIVE POTENCY

Due to the chemical nature of the polycyclic organics produced during combustion of many types of fuels, it is likely that these POM's on soot particles emitted from combustion sources will all exhibit mutagenic and carcinogenic activity. This poses a difficult problem for both the scientific assessment of risk and the regulatory decision making process aimed at risk management. To evaluate new or alternative combustion fuels and engines, a quantitative estimate of the cancer risk from these emissions is needed together with comparative estimates of cancer risks from existing technologies. We have described a comparative potency method for such a comparative cancer risk assessment[22] which is based on the hypothesis that there is a constant relative potency between two different carcinogens across different bioassay systems including animals and humans. The data base we have developed for conducting a comparative assessment of automotive (diesel and gasoline) emissions is summarized and expanded on here (Table 4) by the addition of oil, wood, and coal combustion emission data.

The underlying assumption of this comparative potency method is that the relative potency of two carcinogens in an _in vivo_ or _in vitro_ bioassay is directly proportional to the relative potency in humans. This assumption has been examined for three complex organic emission products from coke ovens, roofing tar, and cigarettes which are known to be human lung carcinogens.[22] For these three samples, the mouse skin tumor initiation relative potencies are within a factor of two, directly proportional to the relative potency estimated for these emissions from human lung cancer epidemiological data. The relative potencies, from the _in vitro_ bioassays as compared to the human data, were similar for coke oven and roofing tar, but for the cigarette smoke condensate the _in vitro_ tests predicted a higher relative potency. The mouse skin initiation bioassay was, therefore, used to determine the unit lung cancer risk for the most potent of the diesel emissions (Nissan).

In this comparative potency method, the risk of a suspect human carcinogen (e.g., diesel emissions) for which there are no epidemiologic cancer data was estimated by comparison to a known human carcinogen (e.g., coke oven emissions) according to the following equation:

$$\text{human risk}_{\text{diesel}} = \text{human risk}_{\text{coke oven}} \quad \text{relative bioassay potency } \frac{\text{diesel}}{\text{coke oven}} \qquad (1)$$

The relative bioassay potency as expressed by the term, ($\text{bioassay potency}_{\text{diesel}} \div \text{bioassay potency}_{\text{coke oven}}$), is obtained by the ratio of the slopes of the dose responses from the same *in vitro* or *in vivo* bioassays.

In the initial application of this method to the estimation of cancer risk from diesel emissions,[22] the unit risk of the most potent diesel sample (Nissan) was estimated using each of the human carcinogens. The estimated risks for this diesel sample ranged from 2.6×10^{-4} to 5.4×10^{-4} lifetime risk/µg organic/m^3 with an average of 4.4×10^{-4}. Since the skin tumor initiation activity of all the extractable organics from diesel and gasoline particulate emissions showed an excellent correlation with the short-term bioassay data, the human unit risk estimates for other diesel and gasoline combustion emission samples (x) were determined in relation to the average 4.4×10^{-4} lifetime risk/µg organic/m^3 estimated for the Nissan diesel sample according to the following equation:

$$\text{human risk}_{x} = 4.4\times10^{-4} \text{ (average relative short-term bioassay potency)} \qquad (2)$$

The relative bioassay potencies were determined for each of the short-term bioassays by dividing the mutagenicity (linear slope of the dose-response curve) of each combustion emission sample (x) by the mutagenicity of the diesel Nissan. The relative potencies for the mouse lymphoma, SCE, and Ames bioassays (+MA) were then averaged to obtain the average relative short-term bioassay potency term for equation (2) above. The final risk estimates based on short-term bioassays are shown in Table 7.

This method assumes that when comparing across combustion emissions with different chemical characteristics as described above, the mouse skin best predicts the relative potency compared to humans. Within both diesel and gasoline automotive emissions, since the mouse skin tumor initiating activity correlated so well with the short-term bioassay data, it is further assumed that an average relative potency in these short-term bioassays can be used to estimate the comparative human risk. This approach is extended here to estimate the unit-risk for several gasoline non-catalyst vehicles and residential oil heater emissions. Since we also have mouse skin tumor initiating activity for many of these emissions, the unit risk estimates are also presented for these samples basing the comparison on the relative risk in mouse skin tumorigenicity according to equation (1). The relative potencies were compared to each of the human carcinogens (coke oven, roofing tar, and cigarette smoke) and the final estimates based on each human carcinogen were averaged to give the value shown in Table 7 based on skin tumor initiation.

The residential wood and utility coal combustion emissions have only been evaluated in the Ames *Salmonella typhimurium* mutagenesis bioassay (Table 4), therefore, a range of estimated risks is presented in Table 7 determined from the relative potency in the Ames assay compared to each of the human carcinogens. These estimates range over 2-3 orders of magnitude because of the 2-3 orders of magnitude difference in human risk between the cigarette smoke and the other human carcinogens (a difference which is not reflected in the Ames assay). Using the Ames relative potency compared to the diesel Nissan results in 0.3×10^{-4} lifetime risk/µg organic/m^3 for wood and $1\text{-}4 \times 10^{-4}$ lifetime risk/µg organic/m^3 for the coal emissions. This limited bioassay data (Ames test alone) is insufficient to select the relative bioassay data which best fits the relative potency model.

The major assumption and main source of uncertainty in this comparative potency method is the validity of the constant relative potency hypothesis.

Interspecies differences that always plague efforts to extrapolate from animals to man (e.g., differences in absorption, distribution, metabolism, DNA damage and repair capabilities) may also effect the constant relative potency. By designing studies to test this hypothesis we may be able to determine the range of variation in potency for different bioassays and emission sources. For example, it is apparent from the existing data base that the relative potency of the diesel samples in the bacterial (Ames) assay are approximately one order of magnitude greater than the relative potency in mouse skin. This difference may be due to differences between mouse skin and bacteria in their ability to metabolize chemicals present in diesel emissions (e.g., nitrated PNA). Since we have assumed that the relative potency in mouse skin tumor initiating activity best predicts the relative potency in humans, it is possible that we have underestimated the human risk by approximately 10-fold. This would be the case if future additional data suggests that bacteria more accurately reflects the relative carcinogenic potency in humans than does the mouse skin tumor initiation assay. As additional human risk and animal cancer data (e.g., from intratrachael instillation) become available, this assumption and methodology should be re-evaluated.

When extrapolating from animal cancer data to human cancer risks for a single agent using classical methodology, bioavailability, tissue distribution, metabolism and target organ dosimetry data are utilized to relate exposure to dose. The comparative potency method does not eliminate the utility of such data but does provide a method for estimating risk with the simplified assumption that these factors are directly proportional or constant from one bioassay to another. Under this assumption, for example, the relative bioavailability of carcinogens from diesel particles in humans compared to coke oven particles would be directly proportional to the bioavailability of these carcinogens in the non-human bioassays. The most useful data to test this assumption would be the relative bioavailability of carcinogens from these different particles in different bioassays and in humans. Since such data are not now available, the validity of this assumption remains untested.

The constant relative potency model does not assume that the carcinogens being compared are chemically related. Future evaluation of this model may show that it is only valid for either very similar chemicals or for combustion emissions where the carcinogens present in these mixtures are identical and vary only in their concentration. Chemical characterization of the different complex mixtures show that all of the mixtures contain POMs which cause frameshift mutations in *Salmonella typhimurium* and in that sense these emissions are similar. Upon chemical fractionation, however, significant differences were observed in the distribution of mutagenic activity in various fractions indicating that although these compounds may generally be polycyclic aromatic compounds, the specific mutagenic chemicals are different (e.g., by substitution of nitro, amino, or oxygenated moieties).

SUMMARY

Short-term genetic bioassays have been useful in both characterizing and evaluating the complex organic emissions from many combustion sources. Identification of the specific mutagens and carcinogens in these complex organics has been greatly facilitated by the use of bioassay-directed chemical fractionation and characterization methods. Although all combustion emissions appear to contain neutral polycyclic organic compounds which are mutagenic and tumorigenic, the classical PAH's do not account for all of the potential carcinogens in these emissions. Substituted and oxidized PAH's appear to play a significant role in the mutagenic and tumorigenic activity of many of these combustion emissions.

Studies on the relative mutagenic and carcinogenic activity of the extractable organics from diluted and filtered soot particles, show that these organics from very different combustion sources differ at the most by two orders of magnitude (10^2). Comparison of mutagenic and organic emission rates for these different sources differ by four to five orders of magnitude (10^4-10^5). Utilizing a recently developed approach to evaluating the comparative potency of these emissions, the estimated cancer risk from the various combustion particles is similar and ranges only over two orders of magnitude except for utility power plants which have very low organic emission rates due to the high combustion efficiency of these sources.

DISCLAIMER

The research described in this paper has been reviewed by the Health Effects Research Laboratory, U.S. Environmental Protection Agency and approved for publication. Approval does not signify that the contents necessarily reflect the views and policies of the Agency nor does mention of trade names or commercial products constitute endorsement or recommendation for use.

REFERENCES

1. Kennaway, E. L., Experiments on cancer producing substances, Brit. Med. J., 1, 1, 1925.
2. Cook, J. W., Hieger, J., Kennaway, E. L., and Mayneord, W. V., The production of cancer by pure hydrocarbons, Proc. Roy. Soc. Biol., 111, 455, 1932.

3. Cook, J. W. and Kennaway, E. L., Chemical compounds as carcinogenic agents, Amer. J. Cancer, 33, 50, 1938.
4. Dipple, A., Polynuclear aromatic carcinogens, in Chemical Carcinogens, ACS Monograph 173, Searle, C. E., Ed., American Chemical Society, Washington, D.C., 1976, 245.
5. Shabad, L. M., Carcinogenic action of polycyclic hydrocarbons in animals and man, in Air Pollution and Cancer in Man, Vol. 16, Mohr, U., Schmahl, D. and Tomatis, L., Eds., IARC Scientific Publication, Lyon, 1977, 257.
6. IARC, IARC Monographs on the Evaluation of the Carcinogenic Risk of Chemicals to Man, Certain polycyclic aromatic hydrocarbons and heterocyclic compounds, Vol. 3, International Agency for Research on Cancer, Lyon, 1973.
7. Walter, R., The benzpyrene of town air, Brit. J. Cancer, 6, 8, 1952.
8. Pike, M. C., Gordon, R. J., Henderson, B. E., Menck, H. R., and Soo Hoo, J., Air pollution in Persons at High Risk of Cancer, Fraumeni, J. F., Ed., Academic Press, New York, 1975, 225.
9. National Research Council: Particulate Polycyclic Organic Matter. National Academy of Sciences, Washington, D.C., 1972.
10. Bjorseth, A., Determination of polynuclear aromatic hydrocarbons in the working environment, in Polynuclear Aromatic Hydrocarbons, Jones, P. W. and Leber, P., Eds., Ann Arbor Science, Ann Arbor, 1979, 371.
11. Bjorseth, A., Analysis of polycyclic aromatic hydrocarbons in particulate matter by glass capillary gas chromatography, Anal. Chem. Acta., 94, 21, 1977.
12. Speizer, F. E., Assessment of the epidemiological data relating lung cancer to air pollution, Environ. Health Persp., 47, 33, 1983.
13. Claxton, L. D., Review of fractionation and bioassay characterization techniques for the evaluation of organics associated with ambient air particles,

in Genotoxic Effects of Airborne Agents, Tice, R. R., Costa, D. L., Schaich, K. M., Eds., Plenum Press, New York, 1982, 19.

14. Hueper, W. C., Kotn, P., Tabor, E.C., Payne, W. W., Falk, H., and Sawicki, E., Arch. Pathol., 74, 89, 1962.

15. Alfheim, I., Lofroth, G. and Moller, M., Bioassay of extracts of ambient particulate matter, Environ. Health Persp., 47, 227, 1983.

16. Lewtas, J., Austin, A., Claxton, L., Burton, R. and Jungers, R., The relative contribution of PNA's to the microbial mutagenicity of respirable particles from urban air, in Polynuclear Aromatic Hydrocarbons, Jones, P. W. and Leber, P., Eds., Ann Arbor Science, Ann Arbor, 1979, 449.

17. Lewtas, J., Comparison of the mutagenic and potentially carcinogenic activity of particle bound organics from wood stoves, residential oil furnaces, and other combustion sources, in Residential Solid Fuels, Cooper, J. A., Malik, D., Eds., Oregon Graduate Center, Oregon, 1982, 606.

18. Mumford, J. and Lewtas, J., Mutagenicity and cytotoxicity of coal fly ash from fluidized-bed and conventional combustion, J. Tox. and Environ. Health, 10, 565, 1982.

19. Lewtas, J., Evaluation of the mutagenicity and carcinogenicity of motor vehicle emissions in short-term bioassays, Environ. Health Persp., 47, 141, 1983.

20. Lewtas, J., Bradow, R. L., Jungers, R. H., Harris, B. D., Zweidinger, R. B., Cushing, K. M., Gill, B. E., and Albert, R. E., Mutagenic and carcinogenic potency of extracts of diesel and related environmental emissions: study design, sample generation, collection and preparation, Environ. Int., 5, 383, 1981.

21. Nesnow, S. and Lewtas, J., Mutagenic and carcinogenic potency of extracts of diesel and related environmental emissions: summary and discussion of

the results, Environ. Int., 5, 425, 1981.

22. Albert, R. E., Lewtas, J., Nesnow, S., Thorslund, T. W., and Anderson, E., A comparative potency method for cancer risk assessment: Application to diesel particulate emissions, Risk Analysis, in press.

23. Pitts, J. N., Formation and fate of gaseous and particulate mutagens and carcinogens in real and simulated atmospheres, Environ. Health Persp., 47, 115, 1983.

24. Levin, W., Wood, A. W., Yogi, H., Dansette, P. M., Jerina, D. M., and Couney, A. H., Carcinogenicity of benzo(a)pyrene-4,5-, 7,8-, and 9,10-oxides on mouse skin, Proc. Natl. Acad. Sci. (U.S.), 73, 243, 1976.

25. Sugimura, T. and Takayama, S., Biological actions of nitroarenes in short-term tests on Salmonella, cultured mammalian cells and cultured human trachael tissues: possible basis for regulatory control, Environ. Health Persp., 47, 171, 1983.

26. Holmberg, B. and Ahlborg, U., Consensus report: Mutagenicity and carcinogenicity of car exhausts and coal combustion emissions, Environ. Health Persp., 47, 1, 1983.

27. Rudling, L., Ahling, B., and Lofroth, G., Chemical and biological characterization of emissions from combustion of wood and wood-chips in small furnaces and stoves, in Residential Solid Fuels, Cooper, J. A. and Malek, D., Eds., Oregon Graduate Center, Oregon, 1982, 34.

28. Wolff, G. T. and Klimisch, R. L., Particulate Carbon: Atmospheric Life Cycle, Plenum Press, New York, 1982.

29. Alfheim, I., Bergstrom, J. G. T., Jensson, D. and Moeller, M., Mutagenicity in emissions from coal- and oil-fired boilers, Environ. Health Persp., 47, 177, 1983.

30. Rannug, U., Data from short-term tests on motor vehicle exhausts, Environ.

Health Persp., 47, 177, 1983.

31. Merrill, R. G., Jr., Lewtas, J., and Hall, R. E., Source assessment sampling system (SASS) versus dilution tunnel sampling, in Short-Term Bioassays in the Analysis of Complex Environmental Mixtures III, Waters, M. S., Sandhu, S. S., Lewtas, J., Claxton, L., Chernoff, N. and Nesnow, S., Eds., Plenum Press, New York, 1983, 17.

32. Hoffmann, D. and Wynder, E. L., Environmental respiratory carcinogenesis, in Chemical Carcinogens, ACS Monograph 173, Searle, C. E., Ed., American Chemical Society, Washington, D.C. 1976, chap. 7.

33. Nesnow, S., Triplett, L., and Slaga, T. J., Comparative tumor-initiating activity of complex mixtures from environmental particulate emissions on SENCAR mouse skin, J. Natl. Cancer Inst., 68, 829, 1982.

34. Nesnow, S., Evans, C., Stead, A., Creason, J., Slaga, T. J., and Triplett, L. L., Skin carcinogenesis studies of emission extracts, in Toxicological Effects of Emissions from Diesel Engines, Lewtas, J., Ed., Elsevier Science Publishing Co., Inc., New York, 1982, 295.

35. Thilly, W. G., Longwell, J. and Andon, B. M., A general approach to the biological analysis of complex mixtures in combustion effluents, Environ. Health Persp., 48, 129, 1983.

36. Schuetzle, D., Lee, F. S. C., Prater, T. J. and Tejada, S. B., The identification of polynuclear aromatic (PAH) derivatives in mutagenic fractions of diesel particulate extracts, Int. J. Environ. Anal. Chem., 9, 93, 1981.

37. Rappaport, S. M., Wang, Y. and Wei, E. T., Sawyer, R., Watkings, B. E. and Rappaport, H., Identification of a direct-acting mutagen in diesel exhaust particulates, Environ. Sci. Technol., 14, 1505, 1980.

38. Grimmer, G., Naujack, K.-W., Dettbarn, G., Brune, H., Deutsch-Wenzel, R., and Misfeld, J., Analysis of balance of carcinogenic impact from emission

condensates of automobile exhaust, coal heating, and used engine oil by mouse-skin-painting as a carcinogen-specific detector, in Polynuclear Aromatic Hydrocarbons, Cooke, M., Dennis, A. J., and Fisher, G. L., Eds., Battelle-Columbus Press, Columbus, 1982, 335.

39. Epler, J. L., Clark, B. R., Ho, C.-h., Guerin, M. R., and Rao, T. K., Short-term bioassay of complex organic mixtures: part II, mutagenicity testing, in Application of Short-Term Bioassays in the Fractionation and Analysis of Complex Environmental Mixtures, Waters, M. D., Nesnow, S., Huisingh, J. L., Sandhu, S. S., and Claxton, L., Eds., Plenum Press, New York, 1978, 269.

40. Huisingh, J., Bradow, R., Jungers, R., Claxton, L., Zweidinger, R., Tejada, S., Bumgarner, J., Duffield, F., Waters, M., Simmon, V. F., Hare, C., Rodriguez, C., and Snow, L., Application of bioassay to the characterization of diesel particle emissions, in Application of Short-Term Bioassays in the Fractionation and Analysis of Complex Environmental Mixtures, Waters, M. D., Nesnow, S., Huisingh, J. L., Sandhu, S. S., and Claxton, L., Eds., Plenum Press, New York, 1978, 381.

41. Bradow, R. L., Diesel particle and organic emissions: engine simulation, sampling, and artifacts, in Toxicological Effects of Emissions from Diesel Engines, Lewtas, J., Ed., Elsevier Science Publishing Co., Inc., New York, 1982, 33.

42. Claxton, L. D., and Huisingh, J. L., Comparative mutagenic activity of organics from combustion sources, in Pulmonary Toxicology of Respirable Particles, Sanders, C. L., Cross, F. T., Dagle, G. E., Mahaffey, J. A., Eds., Department of Energy, U.S. Government Printing Office, CONF-791002, 1980, 453.

43. Rosenkranz, H. S., McCoy, E. C., Sanders, D. R., Butler, M., Kiriazides,

D. K., and Mermelstein, R., Nitropyrenes: isolation, identification, and reduction of mutagenic impurities in carbon black and toners, Science, 209, 1039, 1980.

44. Nishioka, M. G., Petersen, B. A., and Lewtas, J., Comparison of the nitroaromatic content and mutagenicity of diesel emissions, in Polynuclear Aromatic Hydrocarbons, Cooke, M., Dennis, A. J. and Fisher, G. L., Eds., Battelle-Columbus Press, Columbus, 1982, 603.

45. Schuetzle, D., Sampling of vehicle emissions for chemical analysis and biological testing, Environ. Health Persp., 47, 65, 1983.

46. Lewtas, J., Mutagenic activity of diesel emissions, in Toxicological Effects of Emissions from Diesel Engines, Lewtas, J., Ed., Elsevier Science Publishing Co., Inc., New York, 1982, 243.

47. Austin, A., Claxton, L. and Lewtas, J., Mutagenicity of particle-bound organic chemical fractions from diesel and comparative emissions, in Diesel Emissions Symposium Proceedings, EPA-600/9-82-014, National Technical Information Service, Springfield, 1982, 478.

48. Nishioka, M. and Petersen, B. A., personal communications.

49. Sparacino, C., Williams, R., Brady, K., and Jungers, R., Fractionation and characterization of the organics from diesel and comparative emissions, in Diesel Emissions Symposium Proceedings, EPA-600/9-82-014, National Technical Information Service, Springfield, 1982, 598.

50. Casto, B. C., Hatch, G. G., Huang, S. L., Huisingh, J. L., Nesnow, S., and Waters, M. D., Mutagenic and carcinogenic potency of extracts of diesel and related environmental emissions: in vitro mutagenesis and oncogenic transformation, Environ. Int., 5, 403, 1981.

51. Curren, R. D., Kouri, R. E., Kimi, C. M., and Schechtman, L. M., Mutagenic and carcinogenic potency of extracts from diesel related environmental

emissions: simultaneous morphological transformation and mutagenesis in BALB/c 3T3 cells, Environ. Int., 5, 411, 1981.

52. Claxton, L. D., Mutagenic and carcinogenic potency of diesel and related environmental emissions: Salmonella bioassay, Environ. Int., 5, 389, 1981.

53. Mitchell, A. D., Evans, E. L., Jotz, M. M., Riccio, E. S., Mortelmans, K. E., and Simmon, V. F., Mutagenic and carcinogenic potency of extracts of diesel and related environmental emissions: in vitro mutagenesis and DNA damage, Environ. Int., 5, 393, 1980.

54. Pienta, R. J., A hamster embryo cell model system for identifying carcinogens, in Carcinogenesis: Identification and Mechanisms of Action, Griffin, A. C. and Shaw, C. R., Eds., Raven Press, New York, 1979, 121.

55. Stead, A. G., Hasselblad, V., Creason, J. P., and Claxton, L., Modeling the Ames test, Mutat. Res., 85, 13, 1981.

56. Claxton, L. and Kohan, M., Bacterial mutagenesis and the evaluation of mobile-source emissions, in Short-Term Bioassays in the Analysis of Complex Environmental Mixtures II, Waters, M. D., Sandhu, S. S., Huisingh, J. L., Claxton, L., and Nesnow, S., Eds., Plenum Press, New York, 1981, 299.

57. Nesnow, S., Triplett, L. L. and Slaga, T. J., Mouse skin tumor initiation-promotion and complete carcinogenesis bioassays: mechanisms and biological activities of emission samples, Environ. Health Persp., 47, 255, 1983.

58. Pereira, M. A., Skin tumorigenesis research data base, J. Amer. Coll. Toxicol., 1, 47, 1982.

59. Sugimura, T., A view of a cancer researcher on environmental mutagens, in Proceedings of the Third International Conference on Environmental Mutagens, Tokyo, Japan, in press.

60. Harris, J. E., Diesel emissions and lung cancer, Risk Analysis, in press.

61. Dudney, C. S., Walsh, P. J., Jones, T. D., Calle, E. E., and Griffin, G. D.,

On the use of relative toxicity for risk estimation, in Short-Term Bioassays in the Analysis of Complex Environmental Mixtures III, Waters, M. D., Sandhu, S. S., Lewtas, J., Claxton, L., Chernoff, N. and Nesnow, S., Eds., Plenum Press, New York, 1983, 499.

62. Petersen, B. A. and Chuang, C. C., Methodology of fractionation and partition of diesel exhaust particulate samples, in Toxicological Effects of Emissions from Diesel Engines, Lewtas, J., Ed., Elsevier Science Publishing Co., Inc., New York, 1982, 51.

TABLE 1

Distribution of the Mass and Mutagenic Activity of Fractionated Diesel Particle Organics[a]

Fraction[b]	Mass	Specific Mutagenic Activity[c] (rev/mg)		Weighted Mutagenic Activity[d] (rev/mg)		Distribution of Mutagenic Activity[e] (%)	
	(%)	-MA	+MA	-MA	+MA	-MA	+MA
Organic acids	14.9	193	248	28.8	37.0	4.9	9.5
Organic bases	0.3	43.8	132	0.13	0.40	0.02	0.10
Ether insolubles	3.9	53.9	80.9	2.1	3.2	0.36	0.80
Paraffins	36.7	Neg.	Neg.	0.0	0.0	0.0	0.0
Aromatics	6.9	49.5	30.1	3.42	2.1	0.60	0.54
Transitionals	5.0	7520	2620	376	131	64.9	33.5
Oxygenates	26.9	629	798	169	215	29.2	55.4
Sum				579	389		

[a] Diesel particles obtained by the dilution tunnel method from a four-stroke V-8 Caterpillar 3208 engine operated on the standard 13 mode series of steady states.[40]

[b] Dichloromethane extractable organics were solvent-partitioned into acids, bases, and neutrals as previously described.[40] The neutral fraction was further fractionated on silica gel into four fractions by the following solvents: hexane (paraffins), 1% ether in hexane (aromatics and transitionals), and 50% acetone in methanol (oxygenates).

[c] Salmonella typhimurium mutagenesis assay performed with and without metabolic activation (MA). Slope determined from linear regression analysis of the initial portion of the dose-response curve.

[d] Weighted mutagenic activity of each fraction relative to the total extract is the product of distribution of mass in each fraction (% mass) and the specific mutagenic activity (rev/mg). The sum of these weighted mutagenic activities is used to determine the distribution of mutagenicity (%) as described below.

[e] Distribution of mutagenic activity is the percentage of weighted mutagenic activity in each fraction compared to the sum of the weighted mutagenic activities. This distribution assumes that any mutagenicity not recovered through the fractionation is equally distributed across all fractions.

TABLE 2

Characterization of Mutagenicity from Combustion of Pine and Oak in an Airtight Woodstove Compared to Diesel Combustion Emissions

Fraction[a]	Diesel[b]		Pine[c]		Oak[c]	
	mass %	mutagenicity[d] %	mass %	mutagenicity[b] %	mass %	mutagenicity[b] %
1. organic acids	7.6	17.9	47.0	0.0	44.0	0.0
2. organic bases	0.2	<0.1	2.3	1.3	2.2	4.8
3. neutrals	(92.2)[e]	(82.1)	50.7	98.7	53.7	95.2
A. aliphatics (hexane)	56.1	0.0	14.3	10.9	14.2	29.4
B. aromatics (hexane/benzene)	12.4	37.0	19.5	14.7	18.1	23.7
C. moderately polar (dichloromethane)	3.1	24.7	20.1	70.2	29.0	11.6
D. highly polar (methanol)	20.6	20.4	46.1	4.2	38.7	35.3

---

[a] The acids and bases were first separated by liquid-liquid partitioning to separate the acids and bases. The neutrals are partioned into four fractions by open column chromatography on 5% water deactivated silica gel utilizing the solvents designated in parenthesis.[62]

[b] Diesel particles collected by the dilution tunnel technique from a 1973 Datsun Nissan 220C diesel automobile operated on a chassis dynamometer using the highway fuel economy test cycle (HWFET).[20] The total exhaust was diluted (10:1) with filtered air prior to collection on 20 x 20 inch Teflon coated Pallflex T60-A20 filters. The particles were Soxhlet extracted with dichloromethane (DCM) for 48 hrs prior to fractionation.

[c] Pine and oak combustion particles collected by the dilution tunnel technique from an airtight woodstove (Johnson Energy Converter) during the constant burn phase.[17] The emissions were diluted, collected, and Soxhlet extracted by the same techniques employed for the diesel particles.

[d] Data from the *Salmonella typhimurium* plate incorporation assay in TA98 with metabolic activation was analyzed by the model slope method[19] to determine the specific mutagenic activity in revertants/µg of fraction tested. Distribution of mutagenic activity between each fraction (% mutagenicity) is the percentage of weighted mutagenic activity [mass (%) x specific mutagenic activity (rev/µg) of each fraction] of each fraction compared to the sum of the weighted mutagenic activities.

[e] Sum of the neutral subfractions shown in parenthesis.

TABLE 3

Comparison of the Distribution of Mutagenic Activity of Different Sources

Fraction[a]	Diesel[b]		Cigarette Smoke[c]		Coke Oven[d]		Roofing Tar[e]	
	mass %	muta-genicity[f] %	mass %	muta-genicity %	mass %	muta-genicity %	mass %	muta-genicity %
1. organic acids (A)	3.6	4.0	1.0	0.7	0.3	0.1	2.3	1.1
2. organic bases (B)	1.0	3.8	12.2	66.1	3.9	37.1	2.9	5.9
3. neutrals (sum of A, B,C) (N)	(95.4)	(92.1)	(86.8)	(33.1)	(95.8)	(62.8)	(94.8)	(93.0)
A. non-polar neutrals (NPN) (cyclohexane soluble)	75.1	1.4	0.6	2.2	13.9	6.6	40.4	3.9
B. aromatics (sum 1-4) (ARM) (nitro-methane soluble)	(4.5)[g]	(21.8)	(0.6)	(5.8)	(17.8)	(17.0)	(33.3)	(13.9)
1. PNA's (PNA1)	1.1	0.2	<0.1	0.1	9.0	7.9	31.8	4.9
2. slightly polar aromatics (PNA2)	1.4	13.6	0.0	0.0	0.0	0.0	1.2	7.9
3. moderately polar aromatics (PNA3)	0.7	7.8	<0.1	0.1	7.4	5.4	<0.1	0.1
4. highly polar aromatics (PNA4)	1.3	0.2	0.5	5.6	1.4	3.7	0.3	1.0
C. polar neutrals (sum 1&2)	(15.8)	(68.9)	(85.6)	(25.1)	(64.1)	(39.2)	(21.1)	(75.2)
1. methanol soluble (PN)	7.7	52.5	11.6	0.0	6.5	8.2	13.1	17.3
2. cyclohexane in-soluble (CI)	8.1	16.4	74.0	25.1	57.6	31.0	8.0	57.9

Footnotes for Table 3.

[a] Fractionation[49] by liquid-liquid partioning into the following fractions: bases (10% and 20% sulfuric acid), acids (1 N. sodium hydroxide), nonpolar neutrals (cyclohexane), aromatics (nitromethane), polar neutrals (methanol and water), and cyclohexane insolubles. The aromatics were further fractionated by preparative silica gel chromatography using sequentially more polar solvents to obtain the following fractions: PNA 1 (2% dichloromethane in hexane, PNA 2 (50% dichloromethane in hexane), PNA 3 (100% dichloromethane), PNA 4 (methanol in dichloromethane).

[b] Diesel particles from a 1978 Oldsmobile 350 diesel automobile, collected and extracted as described in Table 2.

[c] Cigarette smoke condensate from Kentucky Reference 2R1 cigarette collected as described previously.[20]

[d] Coke oven mains collected from a separator located between the gas collector main and primary coolers within the coke oven battery.

[e] Roofing tar emissions collected from pitch based coal tar as described previously.[20]

[f] *Salmonella typhimurium* TA98 plate incorporation assay with Aroclor induced rat liver S9 metabolic activation system. Mutagenicity (%) distribution determined as described in Table 1.

[g] Values shown in parenthesis are calculated sums of the subfractions shown below.

TABLE 4

Comparative Mutagenicity and Carcinogenicity of Extractable Organcis

	Human Epidemiologic Data	Bioassay Data							
		Animal *in vivo*	Short-Term *in vitro*						
Source[a]	Lung Cancer Unit Risks[b]	Mouse Skin Tumor Initiation[c]	Enhancement of Viral Transformation[d]	Mutation in L5178Y Mouse Lymphoma Cells[e]		SCE in CHO Cells[f]		Ames Salmonella typhimurium TA989	
				(-MA)	(+MA)	(-MA)	(+MA)	(-MA)	(+MA)
Comparative Emissions									
Human Carcinogens									
° Coke Oven Main[47,22]	--	3.2	--	0.38	27.0	0.20	0.19	0.11	6.7
° Coke Oven Topside[20]	9.3×10^{-4}	2.1	1.2	0.71	12.0	0.41	0.03	0.7	1.1
° Roofing Tar[20]	3.6×10^{-4}	0.41	0.87	0.39	17.0	0.12	0.02	Neg[h]	0.86
° Cigarette Smoke Condensate[20]	2.2×10^{-6}	0.0024	0.35	0.39	0.79	0.12	0.08	Neg	0.57
Combustion Emissions									
Diesels[19]									
° Mercedes		0.37	--	0.03	1.5	0.09	0.16	10.0	12.0
° Nissan		0.59	0.42	4.2	2.9	0.30	0.071	11.0	13.0
° Volkswagen Rabbit		0.24	0.14	0.98	0.72	0.075	0.030	3.8	3.0
° Oldsmobile		0.31	0.030	1.2	1.3	Neg	0.017	2.2	1.5
° Caterpillar		Neg	Neg	0.25	0.063	0.011	Neg	0.38	0.31
Gasoline Catalyst[19]									
° Mustang II		0.17	0.024	0.38	1.1	0.076	--	1.6	3.5
Gasoline Non-Catalyst[19]									
°Chevrolet 366		--	--	1.2	4.9	0.72	0.22	2.9	6.2
° Ford Van		--	--	2.1	5.7	0.62	0.47	17.0	32.0
Residential Heaters[17,31]									
° Oil		0.12	0.28	1.2	2.6	0.06	0.04	1.3	2.1
° Wood		--	--	--	--	--	--	0.15	0.93
Utility Power Plants[18]									
° Coal, Conventional		--	--	IP[i]	IP	IP	IP	3.1	--
° Coal, FBC		--	--	IP	IP	IP	IP	9.4	5.2

Footnotes for Table 4.

[a] References to the collection method and original bioassay dose-response data are indicated with each emission source.

[b] Lifetime risk/μg organics/m^3 calculated from the linear nonthreshold extrapolation model (Thorslund, T.W).

[c] Papillomas/mouse/mg based on papilloma multiplicity data in Sencar mice (Nesnow, S., Triplett, L.L., and Slaga, T.J.).

[d] Transformation frequency (transformed foci/10^6 surviving cells)/μg/ml.

[e] Mutation frequency (TK mutants/10^6 surviving cells)/μg/ml.

[f] SCE/cell/μg/ml, (-MA) was a 21.5 h exposure and (+MA) was a 2 hr exposure.

[g] Revertants/μg (from simple linear regression analysis).

[h] Neg = Negative.

[i] IP = In progress.

TABLE 5

Relative Mutagenicity and Carcinogenicity of Extractable Organics

	Human Epidemiologic Data	Bioassay Data								
		Animal Bioassay	Short-Term Bioassay							
Source	Lung Cancer Unit Risks^a	Mouse Skin Tumor Initiation^b	Enhancement of Viral Transformation^c	Mutation in L5178Y Mouse Lymphoma Cells^d		SCE in CHO Cells^e		Ames Salmonella *typhimurium* TA98^f		
				(-MA)	(+MA)	(-MA)	(+MA)	(-MA)	(+MA)
Comparative Emissions									
Human Carcinogens									
° Coke Oven Main	--	1.5	--	0.53	2.3	0.49	6.3	0.16	6.1
° Coke Oven Topside	1.0	1.0	1.0	1.0	1.0	1.0	1.0	1.0	1.0
° Roofing Tar	0.39	0.2	0.73	0.55	1.4	0.29	0.67	0.0	0.78
° Cigarette Smoke Condensate	0.0024	0.0011	0.29	0.55	0.066	0.29	2.7	0.0	0.52
Combustion Emissions									
Diesels									
° Mercedes		0.18	--	0.04	0.12	0.22	5.3	14.0	11.0
° Nissan		0.28	0.35	5.9	0.24	0.73	2.4	16.0	12.0
° Volkswagen Rabbit		0.11	0.12	1.4	0.06	0.18	1.0	5.4	2.7
° Oldsmobile		0.15	0.03	1.7	0.11	0.0	0.57	3.1	1.4
° Caterpillar		0.0	0.0	0.35	0.005	0.027	0.0	0.54	0.28
Gasoline Catalyst									
° Mustang II		0.08	0.02	0.53	0.09	0.19	--	2.3	3.2
Gasoline Non-Catalyst									
°Chevrolet 366		--	--	1.7	0.41	1.8	7.3	4.1	5.6
° Ford Van		--	--	3.0	0.48	1.5	16.0	24.0	29.0
Residential Heaters									
° Oil		0.06	0.23	1.7	0.22	0.15	1.3	1.9	1.9
° Wood		--	--	--	--	--	--	0.21	0.85
Utility Power Plants									
° Coal, Conventional		--	--	IP^h	IP	IP	IP	4.4	--
° Coal, FBC		--	--	IP	IP	IP	IP	13.4	4.7
Range of Combustion Emissions		5	18	150	96	67	9	110	100

Footnotes for Table 5.

[a] Lifetime risk/μg organics/m^3 calculated from the linear nonthreshold extrapolation model (Thorslund, T.W).

[b] Papillomas/mouse/mg based on papilloma multiplicity data in Sencar mice (Nesnow, S., Triplett, L.L., and Slaga, T.J.).

[c] Transformation frequency (transformed foci/10^6 surviving cells)/μg/ml.

[d] Mutation frequency (TK mutants/10^6 surviving cells)/μg/ml.

[e] SCE/celT/μg/ml, (-MA) was a 21.5 h exposure and (+MA) was a 2 hr exposure.

[f] Revertants/μg (from simple linear regression analysis).

[g] Neg = Negative.

[h] IP = In progress.

TABLE 6

Mutagenic Emission Rates for Various Combustion Sources

Source	Fuel type	Mutagen-[a] icity of Organics (rev/µg)	Organic Emission Rate (mg/km)	Organic Emission Rate (mg/kg)	Organic Emission Rate (ng/J)	Mutagenic Emission Rate (rev/km)	Mutagenic Emission Rate (rev/kg)	Mutagenic Emission Rate (rev/MJ)
Diesel engine								
Car (Mercedes)	diesel	12.0	19.2			240,000		
Truck (Mack)	diesel	2.3	143.0			320,000		
Bus (GM)	diesel	0.1	357.0			37,000		
Gasoline engine								
Non-catalyst (Ford Van)	unleaded gasoline	32.0	5.7			180,000		
Catalyst (Mustang II)	leaded gasoline	3.5	1.4	43		5,000	140,000	
Residential heaters								
Woodstove	Pine	1.3		8940	508.0		12,000,000	660,000
	Oak	0.9		3096	187.0		2,800,000	168,000
Residential oil								
furnace #1	No. 2 fuel oil	2.0		21	0.5		40,000	1,000
furnace #2	No. 2 fuel oil	5.1		70	1.5		360,000	7,600
Utility power plants (coal)	coal	3.1			0.01			31

---

[a] *Salmonella typhimurium* TA98 with metabolic activation

TABLE 7

Application of the Comparative Potency Method to Estimation of Lung Cancer Unit Risks for Combustion Emissions

Unit-Risk Estimates (Lifetime risk/μg/m^3)

Emission Sources	Organics		Particles	
	Relative Potency in Skin Tumor Initiation[a]	Relative Potency in Short-Term Bioassays[b]	Relative Potency in Skin Tumor Initiation	Relative Potency in Short-Term Bioassays
DIESELS				
Nissan	4.4×10^{-4}	---	3.5×10^{-5}	---
Volkswagen Rabbit	1.7×10^{-4}	1.3×10^{-4}	3.0×10^{-5}	2.3×10^{-5}
Oldsmobile	2.4×10^{-4}	1.2×10^{-4}	3.9×10^{-5}	2.0×10^{-5}
Caterpillar	---	0.066×10^{-4}	---	0.2×10^{-5}
GASOLINE CATALYST				
Mustang II	1.2×10^{-4}	1.4×10^{-4}	5.1×10^{-5}	6.0×10^{-5}
GASOLINE NONCATLYST				
Chevrolet 366	---	7.9×10^{-4}	---	1.6×10^{-5}
Ford Van	---	16.0×10^{-4}	---	30.0×10^{-5}
RESIDENTIAL HEATERS				
Oil	0.95×10^{-4}	2.4×10^{-4}	0.91×10^{-5}	2.3×10^{-5}
Wood	---	$(0.04\text{-}8\times10^{-4})$[c]	---	$(0.4\text{-}80\times10^{-5})$[c]
UTILITY POWER PLANTS				
Coal	---	$(0.1\text{-}40\times10^{-4})$[d]	---	$(0.2\text{-}80\times10^{-8})$[d]

---

[a] Based on relative mouse skin tumor initiation activity (Table 5) compared to the coke oven, roofing tar, and cigarette smoke. These three unit risks (2.6×10^{-4}, 5.2×10^{-4}, and 5.4×10^{-4} respectively have been averaged.

[b] Based on average relative activity in the mouse lymphoma, SCE, and Ames bioassays (+MA) compared to the Nissan diesel sample. This is determined by the average relative potency in the mouse lymphoma, SCE, and Ames bioassay (+MA).

[c] Based on relative activity in the Ames bioassay (+MA) compared to the relative human cancer risks for coke oven (8×10^{-4}), roofing tar (4×10^{-4}), and cigarette smoke (0.04×10^{-4}). Estimation based on Nissan diesel human risk (4.4×10^{-4}) and comparison of the relative Ames bioassay (+MA) of wood compared to Ames bioassay (+MA) of Nissan diesel results in 0.3×10^{-4} lifetime risk/μg organics/m^3.

[d] Based on relative activity in the Ames bioassay (-MA) compared to the relative human cancer risks for coke oven (40×10^{-4}), roofing tar (16×10^{-4}), and cigarette smoke (0.1×10^{-4}). Estimation based on Nissan diesel human risk (4.4x10-4) and comparison of the relative Ames bioassay (-MA) of utility coal combustion compared to the Ames bioassay (-MA) of Nissan diesel results in 1×10^{-4} to 4×10^{-4} lifetime risk/μg organics/m^3.

PART II: CONTRIBUTION OF NO_2-PAHS TO THE MUTAGENIC ACTIVITY OF AUTOMOTIVE EMISSIONS AND URBAN AIR PARTICLES

Several lines of evidence suggest that nitrated polynuclear aromatic hydrocarbons (NO_2-PAHs) are responsible for much of the "direct-acting" bacterial mutagenicity of extracts of diesel exhaust particules and urban air particulate matter.[1] Quantification of the concentration of a series of NO_2-PAHs and determination of their contribution to the direct-acting mutagenicity in Salmonella typhimurium TA 98 shows that the nomo-NO_2 PAHs make relatively minor contributions to the mutagenicity of the urban air particles (<2%). 1-Nitropyrene was present at the highest concentration (107-1590 ppm) in the diesel particle extracts, and yet it accounted for only 3-13% of the mutagenicity. Dinitropyrene isomers present at less than 1 ppm accounted for over 25% of the mutagenicity. In urban air particle extracts NO_2-PAHs where quantified at less than 1 ppm and accounted for less than 2% of the bacterial mutagenicity. The concentration of several of the NO_2-PAHs in a series of extracts of diesel and gasoline exhaust particles were highly correlated with their mutagenicity both in S. typhimurium and L5178Y mouse lymphoma cells and skin tumor initiating activity in Sencar mice.

Bioassay-directed fractionation studies have shown that over 80% of the mutagenic activity of the solvent extractable organic material from automotive particulate emissions and ambient urban particulate is found in a compound class fraction that is more polar than PAHs.[2] This polar organic fraction is mutagenic in bacteria without the addition of an exogenous metabolic activation system, which is required to detect the mutagenicity of unsubstituted PAHs [e.g., benzo(a)pyrene]. Studies using nitroreductase-deficient and nitroreductase-proficient strains of Salmonella typhimurium suggest that nitro-substituted compounds (e.g., NO_2-PAHs) are present in organic extracts of diesel particles and ambient air particles.[3] Many nitroarenes including nitropyrenes and other NO_2-PAHs are mutagenic in the Ames Salmonella typhimurium mutagenicity assay in the absence of exogenous metabolic activation, and are mutagenic in mammalian cells and carcinogenic in rodents.[4]

NO_2-PAHs have recently been qualitatively identified in extracts of diesel particles and urban air particulate matter.[5] However, the detection of these compounds at low levels and the quantification of NO_2-PAHs has posed problems for analytical chemists because the conventional analytical techniques for quantifying PAHs [e.g., high performance liquid chromatography (HPLC) with fluorescence detection and gas chromatography (GC)/mass spectrometry (MS) with electron impact ionization (EI)] are relatively insensitive to these nitro-substituted PAHs. The 1,3-; 1,6-; and 1,8-dinitropyrene isomers are so highly mutagenic in the Ames (TA98 -S9) assay that trace concentrations of these compounds, if present in diesel particulate extracts, could account for a major proportion of the observed mutagenic activity. A capillary column GC/MS analytical technique using on column injection and negative chemical ionization (NCI) detection was therefore developed to detect these and other nitro-PAHs at very low concentrations. The application of this technique to extracts of particles from four diesel vehicles, one gasoline catalyst vehicle and two urban air locations is reported here (Table 1). Twenty-three different NO_2-PAHs were identified in the diesel engine extracts five NO_2-PAHs in the urban air particle extracts, and only one, 1-nitropyrene was detected in the unleaded gasoline engine extract. 1-Nitropyrene was the NO_2-PAH detected in greatest quantity in the diesel extracts (107-1590 ppm, relative to the weight of the extract), followed by the nitrophenanthrene/anthracene isomers. The quantities of these detected nitro-aromatics, which varied from 0.1 ppm to 1590 ppm in the extracts are given in Table 1. Mono-nitro derivatives of the PAHs at molecular weight 228, such as benz(a)anthracene and chrysene, and molecular weight 252, such as benzo(a)pyrene, perylene and benzofluoranthenes, were also detected. Two nitropyrenone isomers were identified in diesel samples A, B, and D. The only dinitro-PAHs for which analytical standards were available, the dinitropyrene isomers, were detected in one diesel extract sample at sub-ppm concentrations (0.4-0.6 ppm).

The quantification of NO_2-PAHs in the particle extracts reported here allows estimation of the contributions that these quantified nitro-PAHs make to the mutagenicity. Although this may be done by using the mutagenicity values reported in the literature for individual NO_2-PAH, this approach is limited by the wide variation in mutagenic activity reported for many of these compounds apparently due to both the purity of the compounds and the variations in the metabolic state of the bacterial culture. In order to minimize these errors, the five automobile emission samples described here and the pure (>99%) nitro-PAH isomers (1-nitropyrene and 3-nitrofluoranthene) were assayed in the Ames _S. typhimurium_ plate incorporation assay simultaneously with the same resting bacterial culture of tester strain TA98 (-S9). These automotive particle emission extracts and urban air particle extracts are mutagenic in _S. typhimurium_ TA1538, TA1537, TA98, and TA100 and are non-mutagenic in TA1535.[3] Tester strain TA98 has been the most widely used to compare the mutagenicity of both automotive emissions and ambient air particulate matter and to compare the mutagenicity of different NO_2-PAHs and was therefore selected for this study. The calculated contribution that 1-nitropyrene, 3-nitrofluoranthene, and dinitropyrene isomers make to the "direct-acting" mutagenic activity (-S9) of the five particle extracts is shown in Table 2. Although 1-nitropyrene was present in the diesel extracts at concentrations ranging from 107 ppm to 1590 ppm (Table 1), this compound accounted for only 3% to 13% of the "direct-acting" (S-9) mutagenicity; 3-nitrofluoranthene present at 1 ppm to 7 ppm in the diesel samples accounted for 0.8% to 1.4% of the mutagenicity. By using the mutagenicity values determined in separate experiments for 2-nitrofluorene and those reported in the literature for 1-nitroaphthalene, these compounds were estimated to account for less than 0.01% of the mutagenic activity. Although the dinitropyrene isomers: 1,3; 1,6; and 1,8 were detected only in diesel sample C at 0.4-0.6 ppm, their mutagenic activity (496,000; 629,000; and 870,000 rev/μg, respectively)[6] was high enough to account for 26% of the mutagenicity of this sample. The total "direct-acting" mutagenic activity in *S. typhimurium* TA98 that can be accounted for by the 23 nitro-PAHs quantified in Diesel C is 40%. This estimation is supported by the loss of 50% of the mutagenic activity of this extract it was assayed in TA98FRI (renamed TA98NRD), a classical nitroreductase-deficient *S. typhimurium* tester strain obtained from H. Rosenkranz.[7]

The fact that dinitropyrenes at concentrations below the ppm level can account for nearly one-third of the mutagenic activity (-S9) suggests that the presence of other highly potent dinitro-PAHs may account for even more of the mutagenic activity (-S9) in the moderately polar neutral fraction. A recent application of S. typhimurium tester strains developed to exhibit resistance to dinitropyrenes (e.g., TA98/1,8DNP$_6$) has led to even larger estimations of the contributions of dinitropyrenes to the mutagenicity of diesel particle extracts.[10] The lack of quantitative data on the concentrations of the dinitropyrene isomers in such samples has previously made it impossible to confirm whether the concentrations of the dinitropyrenes are indeed sufficient to account for the contribution predicted by the resistant tester strains. Pederson[11] has reported that in several light-duty diesel particle extracts, 50% to 90% of the TA98 (-S9) mutagenicity is lost when the extracts are tested in TA98/1,8DNP$_6$. Since these strains may show a resistance to other dinitro-PAHs, it is possible that highly potent dinitro-substituted isomers of other parent PAHs present in the particle extracts may also contribute to the mutagenicity of the moderately polar neutral fraction.

The mutagenicity of the extractable organic material from these diesel and gasoline emissions has been reported for a battery of in vitro bioassays detecting gene mutations, DNA damage, chromosomal effects, and oncogenic transformations.[12] Skin tumor initiation and carcinogenic activity of these samples has also been reported in SENCAR mice.[13] Very good correlations ($r^2>0.90$) were observed when the slope of the dose-response for the mutagenic activity in S. typhimurium strain TA98(-MA) was plotted versus the mutagenic activity in the mammalian cell assays and the skin tumor initiating activity.

The correlation of mutagenic and skin tumor initiating activity with the concentration of selected nitro-PAHs was examined for these diesel and gasoline samples. Table 3 shows the high correlations observed between the concentrations of 1-nitropyrene, 3-nitrofluoranthene, and several other nitro-PAH isomers in these samples, and their mutagenic activity in S. typhimurium, L5178Y mouse lymphoma cells, and skin tumor initiating activity in SENCAR mice. The r^2 correlation coefficient for the relationship between the mutagenicity in S. typhimurium (-S9) and the 3-nitrofluoranthene concentration in the series of diesel and gasoline samples is particularly good, as shown in Figure 1.

The mutagenicity in S. typhimurium (-S9) correlated well ($r^2 \geq 0.90$) with the concentrations of 3-nitrofluoranthene, the nitro-252 isomer, 1-nitropyrene, and the nitro-228 isomers, nitromethylpyrenes and nitrofluorenes while no correlation was observed with several of the other less mutagenic, lower molecular weight nitro-PAHs (nitrophenanthrenes and nitronaphthalenes). The mutagenic activity in the absence of S9 activation in L5178Y mouse lymphoma cella at the thymidine kinase locus also correlated well with the concentrations of 3-nitrofluoranthene (r^2=.99) and somewhat less well with 1-nitropyrene (r^2=0.89), and these correlations decreased with the addition of S9. The skin tumor initiating activity[28] was also highly correlated with the concentration of certain nitro-PAHs (e.g., 3-nitrofluoranthene and nitrofluorenes) as shown in Table 3.

The quantified mono-NO_2-PAHs account for less than 20% of the direct-acting bacterial mutagenicity of these samples. The high correlations observed between the concentration of these compounds and the mutagenic activity of the total extract, therefore, suggest that the concentrations of the unidentified mutagens responsible for the remainder of the mutagenic activity and possibly the mutagenic and carcinogenic activity in other bioassays is directly related to the relative concentrations of these mono-NO_2-PAHs. Because the remaining unidentified mutagens appear to be primarily located in the chemical fractions that are more polar than the fraction which contains the unsubstituted and mono-NO_2-PAHs, it is possible that other di-NO_2-PAHs (e.g., dinitrofluoranthenes) or other oxygenated NO_2-PAH's (e.g., hydroxy-nitro-PAHs) species are primarily responsible for the major portion of the unidentified mutagenic activity.

We have recently identified and quantifed hydroxy-NO_2-PAHs in both a polar neutral fraction and acidic fraction of an ambient air particulate extract using bioassay-directed fractionation.

DISCLAIMER

The research described in this paper has been reviewed by the Health Effects Research Laboratory, U.S. Environmental Protection Agency and approved for publication. Approval does not signify that the contents necessarily reflect the views and policies of the Agency nor does mention of trade names or commercial products constitute endorsement or recommendation for use.

REFERENCES

1. Huisingh, J., Bradow, R., Jungers, R., Claxton, L., Zweidinger, R., Tejada, S. Bumgarner, J., Duffield, F., Waters, M., Simmon, V.F., Hare, C., Rodriguiz, C. & Snow, L. in *Application of Short-Term Bioassays in the Fractionation and Analysis of Complex Environmental Mixtures* (eds. Waters, M. D., Nesnow, S., Huisingh, J. L., Sandhu, S. S. & Claxton, L.) 381-418 (Plenum Press, New York, 1979).
2. Wei, E. T., Wang, Y. Y. & Rappaport, S. M. *APCA J.* *30*, 267-271 (1980).
3. Lewtas, J. *Environmental Health Perspectives* *47*, 141-152 (1983).
4. Nesnow, S., Triplett, L. L. & Slaga, T. J. *J. Natl. Cancer Inst.* *68*, 829-834 (1982).
5. Lewtas, Huisingh, J. *Bull. NY Acad. Med.* *57*, 251-160 (1981).
6. Claxton, L. D. & Huisingh, J. D. in *Pulmonary Toxicology of Respirable Particles* Dept. of Energy Symposium Series 53, CONF-791002, 453-465 (U.S. Government Printing Office, Washington, D.C., 1980).
7. Loforth, G. in *Short-Term Bioassays in the Analysis of Complex Mixtures II* (eds. Waters, M. D., Sandhu, S. S., Lewtas Huisingh, J., Claxton, L., and Nesnow, S.) 319-336 (Plenum Press, New York, 1981).
8. Mermelstein, R., Kiriazedes, D. K., Butler, M., McCoy, E. C. & Rosenkranz, H. S. *Mutat. Res.* *89*, 187-196 (1981).
9. Arlett, C. F., Cole, J., Broughton, B. C., Lowe, J. & Bridges, B. A. in *Genotoxic Effects of Airborne Agents* (eds. Tice, R. R., Costa, D. L. & Schaich, K. M.) 397-410 (Plenum, New York, 1981).
10. Sugimura, T. & Takayama, S., *Environmental Health Perspectives* *47*, 171-176 (1983).

11. Ohgaki, H., Motsukura, N., Morino, K., Kawachi, T., Sugimura, T., Morita, K., Tokiwa, H. & Hirota, T. *Cancer Lett.* *15*, 1-7 (1982).

12. Petersen, B. A., Chuang, C. C., Margard, W. L., and Trayser, D. A., *J. Air Pollution Control Assoc.*, *81*, 1-15 (1981).

13. Rappaport, S. M., Wang, Y. Y., Wei, E. T., Sawyer, B. E., Watkins, B. E. & Rappoport, H. *Environ. Science & Tech.* *14*, 1505-1509 (1980).

14. Schuetzle, D., Lee, F. S.-C., Prater, T. J. & Tejada, S. B. *Int. J. Environ. Anal. Chem.* *9*, 93-144 (1981).

15. Lewtas, J., Bradow, R. L., Jungers, R. H., Harris, B. D., Zweidinger, R. B., Cushing, K. M., Gill, B. E. & Albert, R. E. *Environ. Int.* *5*, 383-387 (1981).

16. Claxton, L. D. *Environ. Int.* *5*, 389-392 (1981).

17. Rosenkranz, H. S., McCoy, E. C., Mermelstein, R. & Speck, W. T. *Mutat. Res.* *91*, 103-105 (1981).

18. McCoy, E. C., Rosenkranz, H. S. & Mermelstein, R. *Environ. Mutag.* *3*, 421-427 (1981).

19. Pederson, T. C. in *Mobile Source Emissions: Recent Impacts and Research Needs* (eds. Cooke, M. & Rondia, D.) (Reidel, Dordrecht, in the press).

Table 1 Quantification of nitrated polynuclear aromatic hydrocarbons in particulate extracts

Compound	Concentration in extract (μg of species/g of extract) (ppm)						
	Diesel Auto A	Diesel Auto B	Diesel Auto C	Diesel Auto D	Gasoline Auto E	Urban Air F	Urban Air G
1-Nitronaphthalene	1.4	0.5	0.7	0.3	ND	0.1	0.2
Nitronaphthalene/azulene isomer	ND	0.1	0.6	0.2	ND	ND	ND
Nitronaphthalene/azulene isomer	1.7	0.9	1.2	0.3	ND	"	"
Nitrofluorene isomer	ND	ND	1.0	0.5	ND	"	"
2-Nitrofluorene	ND	ND	ND	0.4	ND	"	"
Nitrofluorene isomer	17.	1.9	1.4	1.1	ND	ND	ND
9-Nitroanthracene	ND	ND	ND	ND	ND	1.0	0.8
Nitrophenanthrene/anthracene isomer	272.	98.	285.	63.	ND	0.6	ND
Nitrophenanthrene/anthracene isomer	9.0	2.7	33.	25.	ND	ND	ND
3-Nitrofluoranthene	7.0	2.9	1.2	0.9	ND	ND	ND
Nitrofluoranthene/pyrene isomer	7.5	1.7	1.4	0.6	ND	0.8	0.4
1-Nitropyrene	1590.	407.	589.	107.	2.5	1.0	0.2
Nitromethylpyrene/methylfluoranthene isomer	233.	23.	46.	22.	ND	ND	ND
Nitromethylpyrene/methylfluoranthene isomer	11.	1.9	3.3	1.9	ND	"	"
Nitro-228	16.	3.0	1.1	1.4	ND	"	"
Nitro-228	7.	0.8	1.3	0.2	ND	"	"
Nitro-228	31.	3.9	5.6	1.2	ND	"	"
Nitromethyl 228	1.3	2.6	ND	ND	ND	"	"
Nitro-252	68.	29.	10.	1.1	ND	"	"
Nitropyrenone/fluoranthenone isomer	15.	5.	ND	2.1	ND	"	"
Nitropyrenone/fluoranthenone isomer	35.	12.	ND	3.9	ND	"	"
1,3-Dinitropyrene	ND	ND	0.6	ND	ND	ND	ND
1,6-Dinitropyrene	ND	ND	0.6	ND	ND	ND	ND
1,8-Dinitropyrene	ND	ND	0.4	ND	ND	ND	ND

Table 1 Legend

Diesel and gasoline particulate emissions were obtained by the dilution tunnel sampling technique from the following vehicles operated on a chassis dynamometer using the U.S. highway fuel economy test cycle (HWFET):[12] a preproduction 1973 Datsun-Nissan 220 C diesel vehicle (diesel samples A and B), a prototype turbocharged Volkswagen Rabbit diesel vehicle (diesel sample C), a 1978 Oldsmobile 350 diesel vehicle (diesel sample D), and a 1977 Ford Mustang II-302 gasoline spark ignition vehicle equipped with a catalytic converter and exhaust gas recirculation emission controls (gasoline sample E). The particle emission rates for these vehicles were 0.20 g/km (diesel A and B), 0.11 g/km (diesel C), 0.32 g/km (diesel C) and 0.0033 g/km (gasoline E). The particulate emissions collected on 20" x 20" Teflon coated Pallflex T60-A20 filters, were Soxhlet extracted with dichloromethane (DCM) to remove organic material. The percent of extractable organic material for each of these samples was 11% (A), 8% (B), 18% (C), 17% (D), 43% (E) 7.6% (F) and 6.1% (G). The extracted organic material was fractionated by open bed chromatography on 5% H_2O deactivated silica gel into the following four fractions by successively more polar solvents: aliphatic fraction (hexane), aromatic fraction (hexane/benzene), moderately polar fraction (DCM) and highly polar fraction (methanol). The aromatic fraction contained all the mononitro-PAHs of 2-4 rings and the moderately polar fraction contained mononitro-PAHs of greater than 4 rings and dinitro-PAHs. The highly polar neutral fraction contained substituted PAHs with more than one substitution (e.g., nitro and keto groups as in nitrofluorenones). Capillary column gas chromatography (HRGC)/mass spectrometry (MS) with chemical ionization (methane) and negative ion detection (NCI) was used to separate and identify the nitroaromatics. On-column chromatographic injection was used and found to be essential to eliminate thermal degradation during analysis. In order to quantify the NO_2PAHs, standard solutions containing the following compounds were analyzed over the concentration range 0.1-10 ng/µl for the calibration curve: 1-nitroaphthalene, 2-nitrofluorene, 9-nitroanthracene, 1-nitropyrene, 2,7-dinitrofluorene, 2,7-dinitrofluorenone, 1,6-dinitropyrene, and 1,3,6-trinitropyrene. D_7-nitronaphthalene, the internal standard, was spiked into all standards and samples at the level of 2.5 ng/µl. Additional standards of 3-nitrofluoranthene, 1,3-dinitropyrene, and 1,8-dinitropyrene were analyzed to determine the retention times of these compounds. The response factor for each compound relative to the internal standard was calculated over the calibration range. Nitro-aromatic compounds not present in the standard that were detected in samples were quantified by using the response factor of the most similar compound from the standard. The detection limit for all the NO_2-PAHs was 0.1 µg/g of extract (ppm)±10%. The compounds not detected are shown in the table as ND. The relative retention time (relative to d_7-nitronaphthalene) and mass spectrum of each standard compound was used to assign specific isomer identification. Nitro-PAH isomers of MW 228 [e.g., benz(a)anthracene, chrysene, benz(c)phenanthrene, etc.] and MW 252 [e.g., B(e)P, B(a)P, perylene, benzofluoranthe etc.] and other isomers detected for which standards were not available were identified on the basis of their mass spectra and GC retention.

Table 2 Contribution of NO_2-PAHs to the mutagenic activity of particle extracts in *Salmonella typhimurium* TA98(-S9)

Extract Sample	Mutagenic Activity (rev/µg)	Contribution to Mutagenic Activity (%)		
		1-nitropyrene	3-nitrofluoranthene	dinitropyrene isomers
Diesel Auto A	13.	11.	1.4	--
Diesel Auto B	6.2	5.9	1.2	--
Diesel Auto C	3.9	13.	0.8	26.
Diesel Auto D	3.5	2.7	0.8	--
Gasoline Auto E	1.6	0.1	--	--
Urban Air F	1.8	0.05	1.8	--
Urban Air G	4.4	0.004	0.4	--

Legend

The Ames S. *typhimurium* TA98 plate incorporation assay was performed as described by Claxton.[13] The diesel and gasoline extracts were bioassayed simultaneously with 1-nitropyrene (1-NP) and 3-nitrofluoranthene (3-NF) (both prepared by Midwest Research Institute to greater than 99.95% purity). The diesel and gasoline extracts were tested at the following 6 doses (10, 30, 50, 100, 300, 500 µg/plate) in triplicate plates in the absence of S9. The pure nitro-PAHs, 1-NP and 3-NF were tested at 7 doses (0.020-1.00 µg/plate and 0.010-0.060 µg/plate respectively) in triplicate plates in the absence of S9. 2-Nitrofluorene (3µg) was used as a positive control and the spontaneous plate counts were 15 ± 2 rev/plate. The initial slope of the dose response curve was determined using linear regression analysis and was 892 rev/µg for 1-nitropyrene and 25,200 for 3-nitrofluoranthene. The contribution of 1-NP, 3-NF and the dinitropyrene isomers to the mutagenic activity was calculated as follows: (concentration of nitro-PAH in µg/g extract) x (mutagenicity of the nitro-PAH in rev/µg) ÷ (mutagenicity of the extract in rev/g). The mutagenicity of the dinitropyrene isomers used in these calculations was 496,000 rev/µg (1,6-dinitropyrene) and 870,000 rev/µg (1,8-dinitropyrene). The contribution of the 1-nitronapthalene and 9-nitroanthracene to the mutagenicity of the urban air particles was <0.001%.

Table 3 Correlation coefficients (r^2) for NO_2-PAHs in automotive emissions vs. mutagenic and tumorigenic activity

Nitro-PAH	*S. typhimurium*		Mouse Lymphoma		Tumor Initiation
	-S9	+S9	-S9	+S9	SENCAR
1-nitropyrene	0.91	0.86	0.89	0.69	0.82
3-nitrofluoranthene	1.00	0.92	0.99	0.88	0.95
Nitro-252	0.98	0.96	0.96	0.86	0.89
Nitro-228 isomers (3)	0.93	0.95	0.97	0.87	0.91
Nitromethylpyrene isomers (2)	0.90	0.93	0.98	0.85	0.93
Nitrophenanthrene/anthracene isomers (2)	0.33	0.22	0.31	0.08	0.28
Nitronaphthalene/azulene isomers (3)	0.63	0.46	0.57	0.28	0.53
Nitrofluorene isomers (3)	0.91	0.93	0.99	0.90	0.95

Legend

The correlation coefficients (r^2) were determined by linear regression analysis of the NO_2-PAH concentrations from the diesel and gasoline automotive emissions in Table 1 versus the mutagenic and tumorigenic activity as shown in Fig. 1. Mutagenic activity in *S. typhimurium* TA98 was determined from linear regression analysis of the initial slope (revertants/µg) as shown in Table 3 in the absence of an S9 metabolic activation system (-S9). The *S. typhimurium* activity in the presence of S9 (+S9) in rev/µg was 13 (A), 3 (C), 1.5 (D), and 3.5 (E) as previously reported.[2] Mutagenic activity in L5178Y mouse lymphoma cells at the thymidine kinase locus as determined from linear regression analysis (mutation frequency/10^6 cells/µg/ml) (2) for -S9 and +S9 respectively was 4.2, 2.9 (A); 0.98, 0.72 (C); 1.2, 1.3 (D); 0.38, 1.1 (E). Tumor initiating activity in SENCAR mice (papillomas/mouse/mg) (3) was 0.59 (A), 0.24 (C), 0.31 (D), 0.17 (E). See Table 1 for an explanation of the nitro-PAH designations (e.g., nitro-252). Where more than one isomer was quantified [e.g., nitro-228 isomers (3)], all the isomers were summed (number shown in parenthesis) and the sum used in the linear regression analysis to determine the r^2.

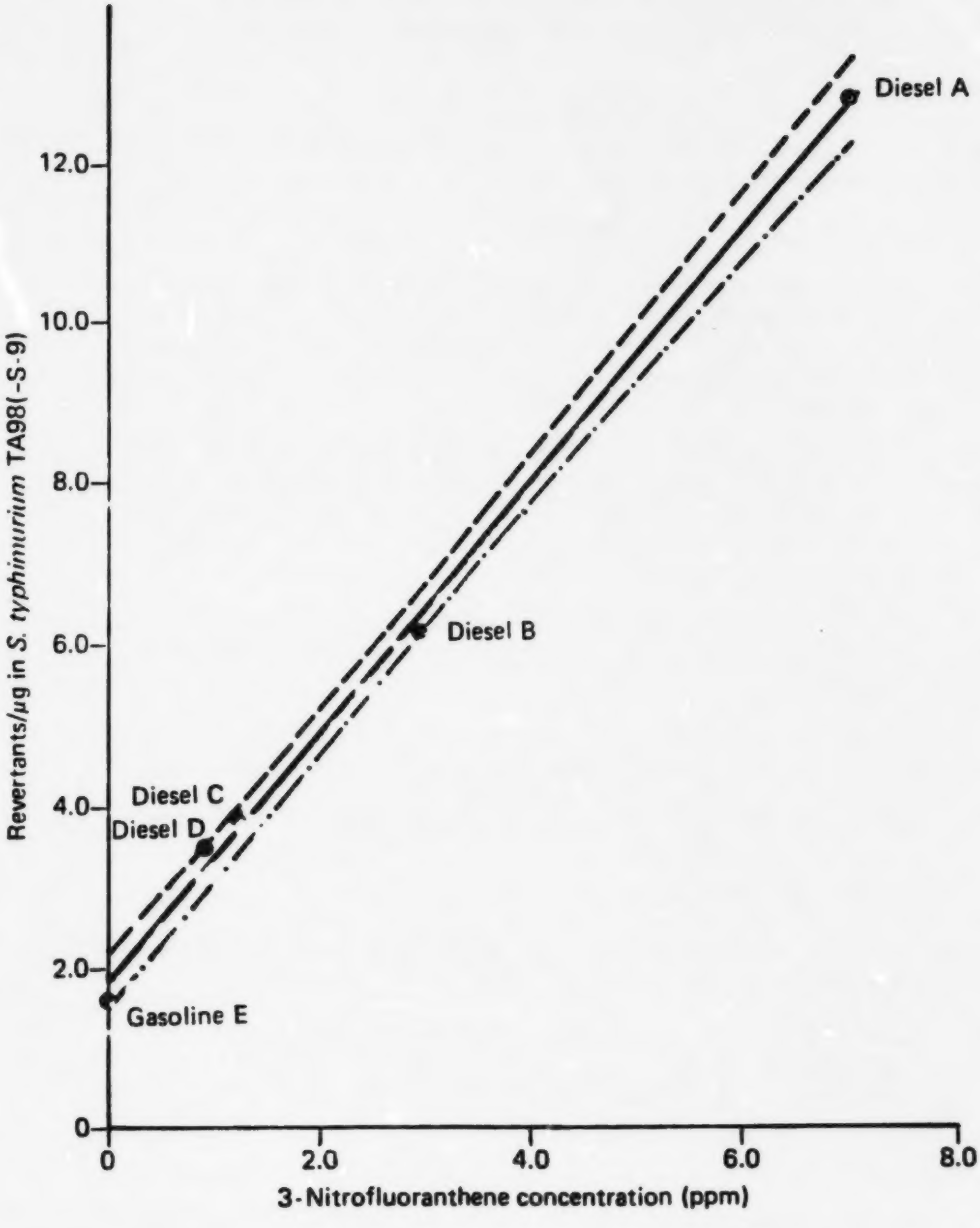

Figure 1. Correlation analysis of the concentration (PPM) of 3-nitrofluoranthene in the diesel (A-D) and gasoline (E) particulate extracts plotted versus the mutagenic activity. The mutagenic activity was determined from the linear slope of the dose-response in Salmonella typhimurium TA98 (-S9).

CHLORINATED DIOXINS AND DIBENZOFURANS IN ONTARIO - CRITERIA FOR DEVELOPING ENVIRONMENTAL STANDARDS

B. Birmingham
Ontario Ministry of the Environment, Intergovernmental Relations & Hazardous Contaminants Co-ordination Branch

ABSTRACT

In Ontario, dioxins and furans occur as complex mixtures (not as pure 2,3,7,8-T_4CDD), especially in incineration sources. These were determined to be a major source of exposure in Ontario. Since 2,3,7,8-T_4CDD is not prevalent in Ontario, concern was principally for isomers other than 2,3,7,8-T_4CDD.

Since the time required to accumulate toxicological data on other isomers may run into decades, the decision was made to use the apparent toxic potency relationships of other PCDDs and PCDFs to 2,3,7,8-T_4CDD in order to proceed with a control strategy for PCDDs and PCDFs at this time.

A risk analysis approach was taken with the toxicological assessment being conducted in parallel with the environmental/sources/fate/exposure assessment.

The conclusion of the environmental sources/fate assessment was that the major sources of PCDDs and PCDFs in the Ontario environment were:

(1) combustion sources including municipal refuse and sewage sludge incineration, and
(2) the use of chlorinated phenols.

Based on the exposure assessment, the major routes of exposure are in order of decreasing contribution:

(i) ambient air in the vicinity of incineration sources;
(ii) diet, especially some sport fish from Lake Ontario;
(iii) atmospheric PCDDs/PCDFs deposited on soil, mainly to children.

B. Birmingham, et al.
Ontario Ministry of the Environment,
Intergovernmental Relations & Hazardous
Contaminants Coordination Branch
135 St. Clair Avenue West
Toronto, Ontario, Canada M4V 1P5

CHLORINATED DIOXINS AND DIBENZOFURANS IN ONTARIO - CRITERIA FOR DEVELOPING ENVIRONMENTAL STANDARDS

Polychlorinated dibenzo-p-dioxins (PCDDs) and chlorinated dibenzofurans (PCDFs) have been identified as a high priority for standard setting in response to public concern about analytical tests showing PCDDs and PCDFs present in incinerator emissions, some Lake Ontario fish and leachate from chemical landfills in upper New York State discharging to the Niagara River.

In 1983, the Minister appointed an international panel of experts to the Ontario Scientific Advisory Committee on Dioxins and Furans (O.S.A.C.) who provided scientific direction and review to a staff expert committee.

The task of this staff committee was to review published literature and MOE monitoring data and prepare a scientific criteria document for new standards which would take into account human health considerations. Human health advice was provided by the Ministry of Labour.

A risk analysis approach was taken with the toxicological assessment being conducted in parallel with the environmental/sources/fate/ exposure assessment.

The conclusion of the environmental sources/fate assessment was that the major sources of PCDDs and PCDFs in the Ontario environment were:

(1) combustion sources including municipal refuse and sewage sludge incineration, and
(2) the use of chlorinated phenols.

Based on the exposure assessment the major routes of exposure are in order of decreasing contribution:

(i) ambient air in the vicinity of incineration sources;
(ii) diet, especially some sport fish from Lake Ontario;
(iii) atmospheric PCDDs/PCDFs deposited on soil, mainly to children

The toxicological assessment focused on 2,3,7,8-T_4CDD. In Ontario, PCDDs and PCDFs occur as complex mixtures not as pure 2,3,7,8-T_4CDD. Therefore, concern was principally for isomers other than 2,3,7,8-T_4CDD. The apparent toxic potency relationships of other PCDDs and PCDFs to 2,3,7,8-T_4CDD was used in order to proceed with a control strategy for PCDDs and PCDFs at this time.

The Scientific Criteria Document recommends an umbrella maximum allowable daily intake of 2,3,7,8-T_4CDD or its toxic equivalent from all exposure pathways based on NOEL from rodent cancer bioassays and an explicit safety factor of 100. The next step is to allocate this ADI amongst the routes of exposure to develop environment standards for the various media.

CHLORINATED DIOXINS AND DIBENZOFURANS IN ONTARIO - ANALYSING AND CONTROLLING THE RISKS

DEVELOPMENT OF SCIENTIFIC CRITERIA DOCUMENT LEADING TO MULTI-MEDIA STANDARDS FOR POLYCHLORINATED DIBENZO-P-DIOXINS (PCDDS) AND DIBENZO POLYCHLORINATED DIBENZOFURANS (PCDFS)

B. Birmingham*, R. Clement, D. Harding, R. Pearson, D. Rokosh,
W. Smithies, A. Szakolcai, B. Hanna Thorpe, H. Tosine and
D. Wells.
*Ontario Ministry of the Environment, Intergovernmental
Relations and Hazardous Contaminants Coordination Branc
135 St. Clair Avenue West
Toronto, Ontario, Canada M4V 1P5

Introduction

Ontario, Canada is located beside the Great Lakes, on the border with the U.S. Being close to the U.S. of course, has greatly sensitized the citizens of Ontario to the dioxin issue through the various events associated with the publicity of the Agent Orange issue, and the Times Beach soil contamination issue (8). Lake Ontario is downstream of the Niagara River. This river is the location of several infamous chemical dump sites, such as Love Canal and Hyde Park and currently the province is very concerned about the potential leaching of material from these sites into the Lake Ontario ecosystem (4).

Because of public concern about the presence of PCDDs and PCDFs in in incinerator emissions (1,22,23,30), Great Lakes fish (15,21,29) and the threat of the leachate from the chemical landfills in Upper New York State (4), PCDDs and PCDFs were identified as a high priority for standard setting. In 1983, a special branch, now called the Intergovernmental Relations and Hazardous Contaminants Coordination Branch was formed to coordinate the development of multi-media environmental standards. This presentation will cover the high- lights from a scientific criteria document (20) produced by this Branch as part of the standard setting process. This document is 536 pages long so that only the briefest of outlines is possible.

Approach

The approach taken in the development of this particular document, was to initially form an internal expert committee, utilizing staff from the Ministry of the Environment (Table 1). Human health advice was provided by the Ministry of Labour. The task of this Internal Committee was to review existing guidelines for these substances, to review current literature and monitoring data for PCDDs and PCDFs in the province, and to develop the scientific criteria document with human health considerations in mind, since clearly the receptor of interest was human.

To assist and direct them in the production of this document, the Minister appointed a panel of international scientists to the Ontario Scientific Advisory Committee on Dioxins and Furans (OSAC) (Table 2). The job of the external committee of international experts was to ensure a high quality of scientific direction and peer-review of the material produced by the internal committee.

Figure 1 is an outline of the approach to the scientific criteria document. The risk analysis approach (24) used is defined as assessing the toxicological hazard and the exposure hazard separately and then comparing them to come up with an estimate of the toxicological risk. The exposure assessment indicates whether a risk exists or not. Basically, determination of an acceptable level of exposure or acceptable level of risk was based on the review of the toxicity data. This level (the proposed standard) would be used as an umbrella number for total exposure including diet.

Toxicological Assessment

There are 210 PCDD and PCDF isomers, however, chronic toxicity data only exists for 3 of them (9,14,16-19). All available toxicity information on all PCDDs and PCDFs was reviewed. The focus of the review was the 2,3,7,8-T_4CDD isomer, since this is clearly the isomer with the greatest amount of toxicological data.

The review of 2,3,7,8-T_4CDD included all data on the acute responses such as LD_{50}, enzyme induction, immunotoxicity, short term mutagenicity tests and environmental toxicity tests; chronic responses such as cancer bioassays and reproductive studies in animals; and available human and epidemiological data.

The purpose of this toxicological review was to identify reliable, well-validated data; to determine the most sensitive end-point and the most appropriate species if human data is unavailable; and to derive a dose-response relationship from which an appropriate level of protection could be chosen.

A problem that surfaced was related to the fact that 2,3,7,8-T_4CDD is often not detectable in the PCDD and PCDF mixtures analysed in Ontario (1,13,22,23,28,30) and that there is a very wide range of toxicities amongst the different isomers (10,11). Clearly to assume that all other PCDDs and PCDFs in such mixtures are equally toxic to 2,3,7,8-T_4CDD is no longer scientifically justifiable or necessary. Consequently, all acute and sub-chronic data was used to construct a matrix of all the known effects of the other PCDDs and PCDFs. Also, the fact that there seems to be a strong structurally-related basis to the activity of these compounds, with substitutions in the 2,3,7,8 positions being involved (25), was taken into consideration.

Since it is clear that it will take decades to accumulate sufficient chronic toxicological data to set a standard for most of the other dioxins and furans found in the environment, the decision was made to utilize these apparent toxic potency relationships as a basis for proceeding with some sort of interim control strategy for PCDDs and PCDFs.

The toxicity ranking scheme developed is shown in Table 3. This toxic equivalent ranking scheme involves a number of assumptions. One is that the effects of all the PCDDs and PCDFs in the mixtures are considered additive. Another assumption is that the toxic equivalent factor for each group of PCDDs and PCDFs is based on the most toxic member of the group. This gives a very large implicit safety factor since in most cases, the most toxic fraction of each isomer group is usually less than 50% and often only represents 1/10 to 1/100 of the analysed content. Of course it is recognized that as new scientific information becomes available, this interim approach to estimating the toxicity of these substances will of course have to be modified.

Rationale for Standard

The most important points in the toxicological overview of the 2,3,7,8-T_4CDD data which forms the basis of our proposed standard are outlined in Table 4.

(1) The acute toxicity data indicates extreme toxicity with a wide range of sensitivities in different species;
(2) The mutagenicity tests are in general negative or inconclusive;

(3) A direct mode of action involving direct binding to or direct action on chromosomes or the DNA has not been indicated;

(4) 2,3,7,8-T_4CDD is teratogenic and fetotoxic in animal tests but no effect levels (NOEL) are indicated in these tests;

(5) The animal cancer tests with rodents are positive, however a NOEL is also indicated;

(6) In terms of the human health effects, the major acute effect is that of chloracne, generally only observed in people who are occupationally or accidentally exposed to relatively high concentrations;

(7) Evidence for chronic effects of PCDDs and PCDFs on the incidence of cancer or reproductive problems in the human population is negative or at best, inconclusive. PCDDs and PCDFs always occur as contaminants of other chemicals, and currently effects in the human population cannot be specifically nailed down as being caused by only the PCDD or PCDF component.

(8) The toxic criterion for the proposed standard was the study of Kociba et al., 1978 (9). This study is well designed and well validated. The data also indicates a no effect level. As far as we are aware, there are no other chronic toxicological effects that are more sensitive than these cancer bioassays using rodents.

(9) Based on knowledge of the activity of PCDDs and PCDFs in mutagenic tests, and the general lack of evidence for the direct action on DNA or chromosomes, it was the conclusion of our committees that a threshold for tumours exist in the rodents examined, that humans are no more sensitive than rodents and that a reasonable doubt exists that 2,3,7,8-T_4CDD will cause cancer in humans at levels below those which have no effect in animals. Consequently a 100-fold explicit safety factor would provide an adequate margin of safety and that the toxicity of other PCDDs and PCDFs can be pro-rated to that of 2,3,7,8-T_4CDD using appropriate toxic equivalent factors.

A basic assumption behind these deliberations was that Ontario citizens are generally exposed to PCDDs and PCDFS other than 2,3,7,8-T_4CDD. Therefore, the proposed umbrella maximum allowable daily intake derived is 10 pg (picogram) of 2,3,7,8-T_4CDD or its toxic equivalent/kilogram body weight/day.

Environmental assessment

Estimates of the quantities of PCDDs and PCDFs in Ontario for the environmental assessment are based on Ontario monitoring data, and where this does not exist, extrapolations have been made from Canadian or international data sets (Table 5). One area not monitored directly is ambient air. As yet, the Ministry does not have reliable technology to permit direct sampling of ambient air. Therefore estimates of ambient air concentrations were based on standard dispersion models (5).

To quickly summarize the environmental assessment, the sources determined to be of importance are:

(1) the use of chemical products, contaminated with PCDDs and PCDFs. These are principally chlorinated phenols such as pentachlorophenol where the bulk of the PCDDs and PCDFs from this source are the hepta- and octa-chlorinated forms (7,27). The total PCDD/PCDF quantity input to the province has been estimated to be on the order of about 500 kg per year. There is no 2,3,7,8-T_4CDD in these chemical sources at this time. Application of toxic equivalent factors from Table 3 indicates that the equivalent toxicity of this quantity of PCDDs and PCDFs is quite a bit lower-on the order of about 4 kg per year.

The second major source, is combustion. This source is divided into two major categories; the first category is that of municipal refuse and sewage sludge incineration (1,22,23,30).

These are processes over which a fair amount of control can and is being applied. The other category is all other combustion processes.

Estimates of what is produced by the incineration of refuse and sludge are reasonably accurate. Since a percentage of the isomers in these emissions are 2,3,7,8-substituted, the equivalent toxicological quantity of these substances being emitted is comparable with that from all chemical products. Our estimates for the other combustion sources are of necessity, a lot less precise.

The third source that could lead to PCDDs and PCDFs coming into the province, is termed transboundary. This includes long range atmospheric transport of PCDFs and PCDDs on air particulate matter (2,3), and, waterborne dioxins and furans. No estimates of air transported quantities are available. The principal transboundary source of concern to this province is through the Niagara River. Federal estimates released about 2 years ago, suggest that somewhere in the range of 2-20 kg per year of unspecified PCDDs and PCDFs may be flowing into Lake Ontario via the Niagara River (4). At this time, it is not clear what the toxic equivalent of this material is.

Another source considered was that of sewage. Sewage is the end point of much human and industrial activity, and there is evidence that low levels of PCDFs and PCDDs are found in this material (12). Our reason for being concerned about this material is the very large quantity which is produced by municipalities every year.

Figure 2 outlines the type of approach taken in the exposure pathway assessment. Since PCDDs and PCDFs are persistent environmental contaminants that have penetrated most media, the assessment of exposure becomes quite complex and by its nature, a multi-media situation. Using ambient level data estimated from the environmental assessment, human exposure was modelled via inhalation, ingestion, and dermal contact pathways using fairly standard models based on the surface area of the body, the volume of air inhaled, the quantity of food and the quantity of water ingested.

The exposure assessment which of necessity was a preliminary one, indicated the major routes of exposure outlined in Table 6. The primary one of concern in Ontario is that of ambient air in the vicinity of incineration sources. Another important exposure pathway is that of diet. It is clear that PCDDs and PCDFs are being found in food basket items, especially the higher chlorinated hepta and octa chlorinated isomers (15,26,27). 2,3,7,8-T_4CDD has also been found in some sport fish from Lake Ontario (15,21,29).

Another source of exposure is that of soil (13). The soil itself is presumably contaminated by deposition of airborne PCDDs and PCDFs from incineration activities. Concern was mainly with young children playing in soil who might transfer soil to their mouths during play activity.

The surface water exposure pathway is minor and only applies to people dependent on untreated tapwater near a source of pollution (28). The majority of people in Ontario drink treated water out of the tap (6).

It should be pointed out of course that the major and probably the most significant source of human exposure would occur in the occupational context where people who handle PCDD and PCDF contaminated chemicals would be exposed to the highest concentrations, however, this matter was not pursued, since occupational exposure falls outside the mandate of the Ministry of the Environment.

Conclusion

In summary, this 536 page criteria document has developed an umbrella maximum allowable daily intake using risk analysis. Using a multi-media approach major sources and problem exposure pathways have been identified. Now having developed an umbrella number, the next step is to partition this number into individual standards or guidelines for ambient air, water, and waste in such a manner that these guidelines and standards together do not exceed the overall intake of 10 pg 2,3,7,8-T_4CDD or its toxic equivalent/kg body weight/day.

TABLE 1 - INTERNAL EXPERT COMMITTEE

Member	Ministries	Expertise
Dr. B. Birmingham (Chairman)	Environment	Environmental Toxicology
Dr. D. Harding	Labour	Human Health
Mr. R. Pearson	Environment	Phytotoxicology
Dr. D. Rokosh	Environment	Mutagenesis
Dr. A. Szakolcai	Environment	Environmental Chemistry
Ms. H. Tosine/ Dr. R. Clement	Environment	Analytical Chemistry
Mr. D. Wells	Environment	Aquatic Toxicology
Mr. W. Smithies	Environment	Policy
Ms. B. Hanna Thorpe (Secretary)	Environment	Environmental Assessment

TABLE 2 -
ONTARIO SCIENTIFIC ADVISORY COMMITTEE ON DIOXINS AND FURANS

Prof. O. Hutzinger	University of Bayreuth, Germany
Prof. G. Plaa	Universite de Montreal
Prof. S. Safe	Texas A & M University
Dr. E.Y. Spencer (Chairman)	University of Western Ontario
Dr. B. Birmingham (Secretary)	Ministry of the Environment

TABLE 3 - ESTIMATED RELATIVE TOXICITY OF PCDD AND PCDF ISOMERS TO 2,3,7,8-T_4CDD

Isomer Groups	Toxicity factor relative to 2,3,7,8-T_4CDD
DD	non-toxic
M_1CDD	0.0001
D_2CDD	0.001
T_3CDD	0.01
T_4CDD*	0.01
P_5CDD	0.1
H_6CCC	0.1
H_7CDD	0.01
O_8CDD	0.0001
DF	non-toxic
M_1CDF	0.0001
D_2CDF	0.0001
T_3CDF	0.01
T_4CDF	0.5
P_5CDF	0.5
H_6CDF	0.1
H_7CDF	0.01
O_8CDF	0.0001

* excluding 2,3,7,8-T_4CDD

TABLE 4 - RATIONALE FOR PCDD AND PCDF STANDARD

TOXICOLOGICAL OVERVIEW (Standard based on 2,3,7,8-T_4CDD)

Acute Toxicity Tests	- extremely toxic (wide range of sensitivity)
Mutagenicity Tests	- negative (inclusive) - indirect mode of action
Animal Reproduction Tests	- positive (NOEL indicated)
Animal Cancer Tests	- positive (NOEL indicated) - indirect non-genetic mode of action.

Human Health Effects

Short term effect - chloracne (high exposure)

Chronic effects (cancer or reproduction)
- negative (inconclusive)

TOXIC CRITERION FOR STANDARD (Most sensitive effect)

Incidence of liver tumours in female rats (Kociba et al, 1978)
- well designed, well validated study
- NOEL (0.001 ug 2,3,7,8-T_4CDD/kg body weight/day)

ASSUMPTIONS

- threshold for liver tumours exists (NOEL)
- humans are no more sensitive than rodents
- 100-fold safety factor will provide adequate margin on safety
- toxicity of other PCDDs and PCDFs can be prorated to that of 2,3,7,8-T_4CDD using appropriate factors.

RECOMMENDED MAXIMUM ALLOWABLE DAILY INTAKE

10 pg 2,3,7,8-T_4CDD or its equivalent/kg body weight

TABLE 5 - ENVIRONMENTAL ASSESSMENT (ESTIMATED QUANTITIES OF PCDDS AND PCDFS ENTERING THE ONTARIO ENVIRONMENT)

	Estimated Current Quantity (kg/year)	
Source	Total PCDD + PCDF	2,3,7,8-T_4CDD Toxic Equivalents
1. CHEMICAL PRODUCTS (No.2,3,7,8-T_4CDD now)		
A. Phenoxy herbicides		
B. Chlorinated Phenols		
C. Polychlorinated Biphenyls	> 500	> 4
D. Chemical Wastes from A,B and C		
E. Commercial/Domestic Products		
2. COMBUSTION		
A. Municipal Refuse/ Sewage Sludge	29 - 37	8 - 10
B. All other Combustion Sources	100 - 200	20 - 50
3. TRANSBOUNDARY		
A. Airborne	Unknown	Unknown
B. Waterborne	2 - 20	<2 - 20
4. SEWAGE	Unknown	Unknown

TABLE 6 EXPOSURE ASSESSMENT

- Ambient air near incinerators
- Diet (Lake Ontario fish)
- Soil
- Surface water (no PCDDs or PCDFs in treated drinking water)
- Occupational exposure

TABLE 7

IN VIVO TOXICOLOGICAL EFFECTS OF 2,3,7,8-T_4CDD ON MAMMALIAN SPECIES

SPECIES	DOSE	EFFECT
Acute Responses	(ug/kg)	
Hamster	1157 - 5051	LD_{50}
Mouse	114 - 284	LD_{50}
Rabbit	115	LD_{50}
Monkey	50 - 70	LD_{50}
Guinea Pig	0.6 - 2.0	LD_{50}
Rat/Mouse/Rabbit	0.1	NOEL-Reproductive Effects
Rabbit	0.01 - 0.1	LEL-Keratinization
Mouse	(0.016)	LEL-Immune Suppression
Rat	0.002	LEL-AHH Induction
Chronic Responses	(ug/kg/day)	
Rat	0.007	LEL-Tumour Production
Monkey	0.002	LEL-Reproductive Effects
Mouse	0.0017	LEL-Tumour Production
Rat	0.001	NOEL-Reproductive Effects (3-generation study)
Rat	0.001	NOEL-Tumour Production

REFERENCES

1. Clement. R.E., Tosine, H.M., Osborne, J., Ozvacic, V., and G. Wong. (In press). Levels of chlorinated organics in a municipal incinerator. In Chlorinatd dioxins and dibenzofurans in the total enviornment - II. Keith, L., Choudhary, G., and C. Rappe (eds.).

2. Czuczwa, J.M., and R.A. Hites. 1984. Environmental fate of combustion-generated polychlorinated dioxins and furans. Environ. Sci. Technol. 18:444-450.

3. Czuczwa, J.M., McVeety, B.D., and R.A. Hites. 1984. Polychlorinatd dibenzo-p-dioxins and dibenzofurans in sediments from Siskiwit Lake, Isle Royale. Science 226:568-569.

4. Environment Canada. 1983. Evidence of "S" area leaks found in the Niagara River. News Release, December 9, 1983.

5. Government of Ontario. 1982. Regulations under the Environmental Protection Act, 1971. General-Air Pollution. Ontario Regulation 308, June 1982.

6. Health and Welfare Canada. 1981. Tap water consumption in Canada. Cat. No. H46-2/82-80E. 83 pages.

7. Jones, P.A. 1981. Chlorophenols and their impurities in the Canadian environment. EPS, Environment Canada, EPS 3-EC-81-2 (1981).

8. Kimbrough, R.D., Carter, C.D., Liddle, L.A., and R.E. Clene. 1977. Epidemiology and pathology of a tetrachlorodibenzo-dioxin poisoning episode. Arch. Environ. Health 32(2):77-86.

9. Kociba, R.J., Keyes, D.G. Beyer, J.E., Carreson, R.M., Wade, E.E., Dittenber, D.A., Kalmins, P.O., Franson, L.F., Park, P.N., Barnard, S.D., Hummel, P.A., and C.G. Humiston. 1978. Results of a two year chronic toxicity and oncogenicity study of 2,3,7,8-tetrachlorodibenzo-p-dioxin (TCDD) in rats. Toxicol. Appl. Pharmacol. 46:279-303.

10. Kociba, R.J., and B.A. Schwetz. 1982a. Toxicity of 2,3,7,8-tetrachlorodibenzo-p-dioxin (TCDD). Drug Metabolism Reviews 13:387-406.

11. Kociba, R.J., and B.A. Schwetz. 1982b. A review of the toxicity of 2,3,7,8-tetrachlorodibenzo-p-dioxin (TCDD) with a comparison of the toxicity of other chlorinated dioxin isomers. Assoc. Food Drug Officials Quart. Bull. 46:168-188.

12. Lamparski, L.L., Nestrick, T.J., and V.A. Stenger. 1984. Presence of chlorodibenzodioxins in a sealed 1933 sample of dried municipal sewage sludge. Chemosphere 13:361-365.

13. McLaughlin, D.L., and R.G. Pearson. 1984. Concentrations of PCDD and PCDF in soil from the vicinity of the SWARU incinerator, Stoney Creek, July, 1983. Air Resources Branch, Ontario Ministry of the Environment. 22 pages.

14. Murray, F.J., Smith, F.A., Nitschke, K.D., Humiston, C.G., Kociba, R.J., and B.A. Schwetz. 1979. Three generation reproduction study of rats given 2,3,7,8-tetrachlorodibenzo-p-dioxin (TCDD) in the diet. Toxicol. Appl. Pharmacol. 50:241-252.

15. National Research Council of Canada. 1981. Polychlorinated dibenzo-p-dioxins: Criteria for their effects on Man and his Environment. NRCC Publication No. 18574, 251 pages.

16. National Toxicology Program. 1982a. Carcinogenesis bioassay of 2,3,7,8-tetrachlorodibenzo-p-dioxin in Osborne-Mendel rats and B6C3Fl mice (gavage study). NIH Publication No. 82-1765.

17. National Toxicology Program. 1982b. Carcinogenesis bioassay of 2,3,7,8-tetrachlorodibenzo-p-dioxin in Osborne-Mendel rats and B6C3Fl mice (dermal study). NIH Publication No. 82-1757.

18. National Toxicology Program. 1980c. Bioassay of 1,2,3,6,7,8- and 1,2,3,7,8,9-hexachlorodibenzo-p-dioxin (gavage) for possible carcinogenicity. DHHS Publication No. (NIH) 80-1754.

19. National Toxicology Program. 1980d. Bioassay of 1,2,3,6,7,8- and 1,2,3,7,8,9-hexachlorodibenzo-p-dioxin for possible carcinogenicity (dermal study). DHHS Publication No. (NIH) 80-1758.

20. Ontario Ministry of the Environment. 1985. Scientific Criteria Document for Standard Development. No. 84-4. Polychlorinated dibenzo-p-dioxins (PCDDs) and polychlorinated dibenzofurans (PCDFs). September 1985. 536 pages.

21. Ontario Ministry of the Environment and Ministry of Natural Resources. 1983. Guide to eating Ontario sportfish.

22. Ozvacic, V., Wong, G., Tosine, H., Clement, R., Osborne, J., and S. Thorndyke. 1984a. *Determination of chlorinated dibenzo-p-dioxins, chlorinated dibenzofurans, chlorinated biphenyls, chlorobenzenes and chlorophenols in air emissions and other process streams at SWARU in Hamilton*. Joint Report by Air Resources and Laboratory Services and Applied Research Branches, M.O.E. and Ontario Research Foundation. Report No. ARB-02-84-ETRD.

23. Ozvacic, V., Wong, G., Tosine, H., Clement, R.E., and J. Osborne. 1984b. Emissions of chlorinated organics from two municipal incinerators in Ontario. Presented at 77th APCA Meeting. San Francisco. June.

24. Piche, E.W. 1984. Risk and Resposnibility: Managing toxic substances in the environment. Presented to 1st Conference on Toxic Substances, April, 1984, Montreal, Quebec.

25. Poland, A., and J.C. Knutson. 1982. 2,3,7,8-tetrachlorodibenzo-p-dioxin and related halogenated aromatic hydrocarbons: Examination of the mechanisms of toxicity. *Ann. Rev. Pharmacol. Toxicol.* 22:517-524.

26. Ryan, J.J., R. Lizotte, T. Sakuma and B. Mori, 1985. Chlorinated dibenzo-p-dioxins, chlorinated dibenzofurans and pentachlorophenol in canadian chicken and pork samples. *J. Agric. Food Chem*. (in press).

27. Ryan, J.J., and J.C. Pilon. 1982. Chlorinated dibenzodioxins and dibenzofurans in chicken litter and livers arising from penta chlorophenol contamination of wood shavings. In *Chlorinated Dioxins and Related Compounds, Impact on the Environment*. Hutzinger, O., Frei., R.W., Merian, E., and F. Pocchiari (eds.). Pergamon Press, Oxford. pp. 183-189.

28. Tosine, H., Clement, R.E., and R. Hunsinger. 1984. *A Survey of Selected Drinking Water Supplies in Ontario for Chlorinated Dibenzo-p-dioxins and chlorinated Dibenzofurans*. Laboratory Services and Applied Research Branch, Ontario Ministry of the Environment. 74 pages.

29. Tosine, H., Smillie, D., and G.A.V. Rees. 1983. Comparative monitoring and analytical methodology for 2,3,7,8-TCDD in fish. In Human and Environmental Risks of Chlorinated Dioxins and Related Compounds, Tucker, R.E., Young, A.L., and A.P. Gray (eds.). Plenum Publishing Corp. pp. 127-139.

30. Tosine, H., Clement, R.E., Osborne, J., Ozvacic, V. and G. Wong. 1983b. Levels of chlorinated organics in a municipal incinerator. American Chemical Society, Division of Environmental Chemistry. 186th National Meeting, Washington, D.C. Preprinted Extended Abstract 23:260-262.

FIGURE 1. RISK ANALYSIS

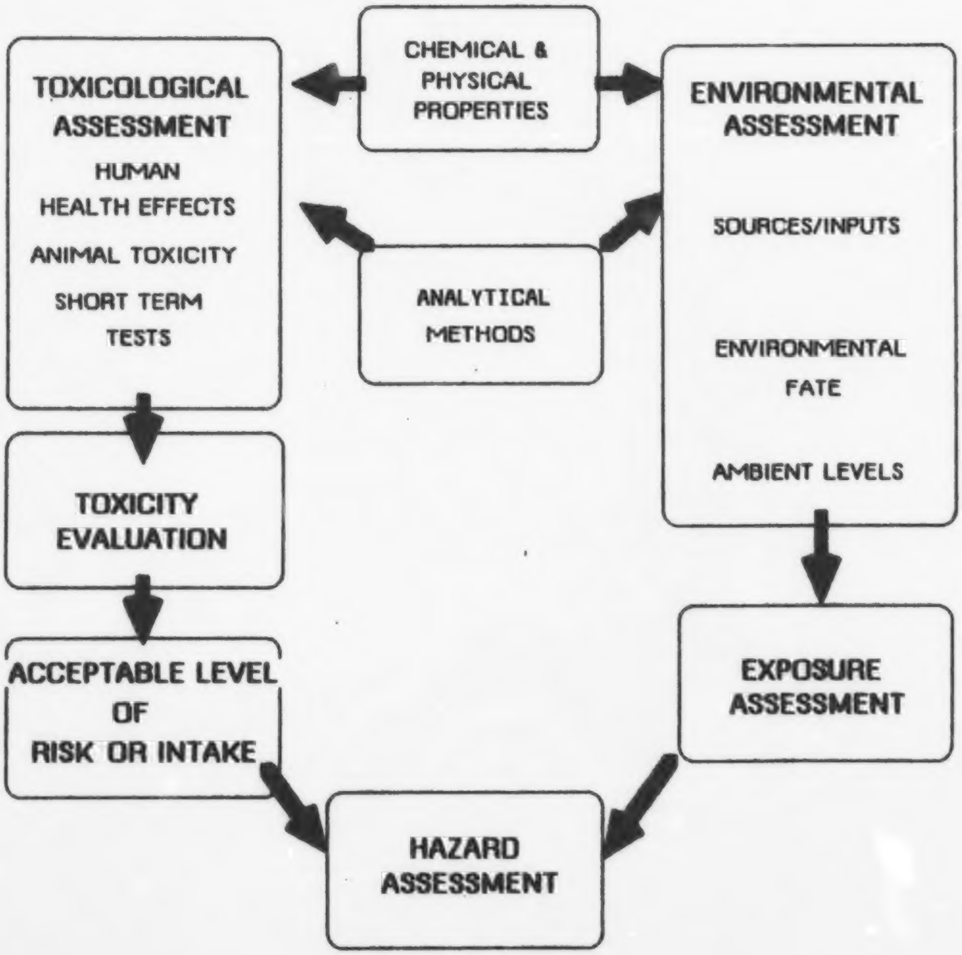
CHEMICAL &
PHYSICAL
PROPERTIES
TOXICOLOGICAL
ASSESSMENT
HUMAN
HEALTH EFFECTS
ANIMAL TOXICITY
SHORT TERM
TESTS
ENVIRONMENTAL
ASSESSMENT
SOURCES/INPUTS
ANALYTICAL
METHODS
ENVIRONMENTAL
FATE
AMBIENT LEVELS
TOXICITY
EVALUATION
ACCEPTABLE LEVEL
OF
RISK OR INTAKE
EXPOSURE
ASSESSMENT
HAZARD
ASSESSMENT

FIGURE 2. EXPOSURE ASSESSMENT

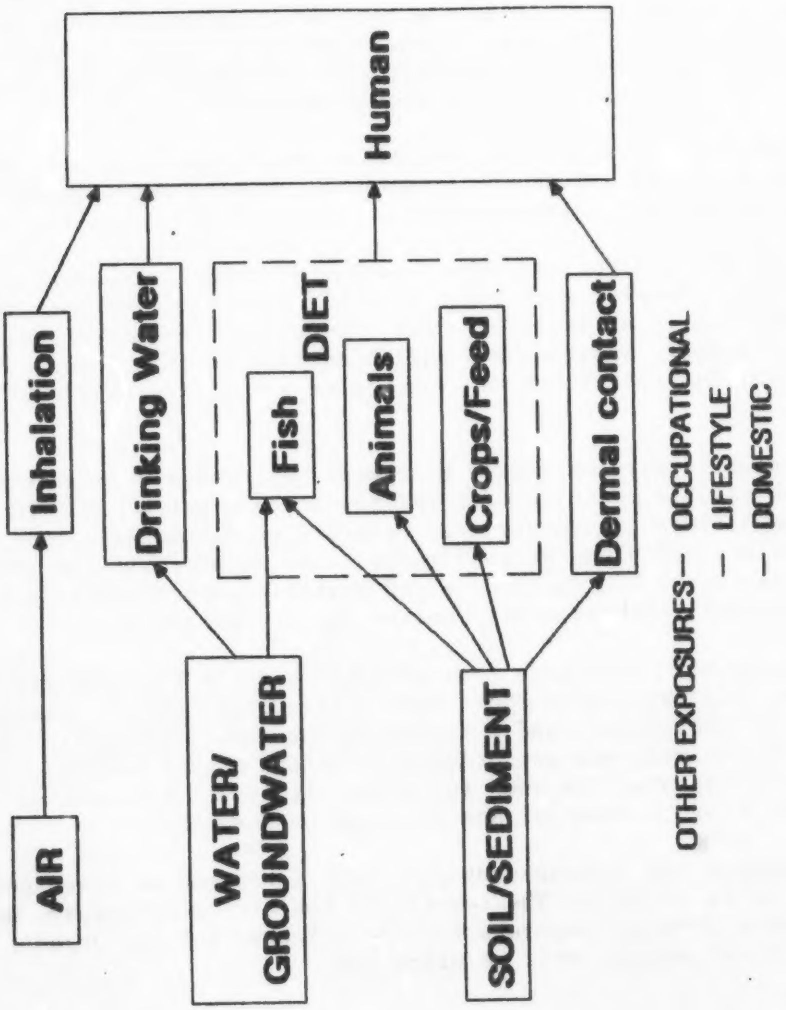
AIR
WATER/ GROUNDWATER
SOIL/SEDIMENT
Inhalation
Drinking Water
Fish
Animals
Crops/Feed
DIET
Dermal contact
Human
OTHER EXPOSURES— OCCUPATIONAL
— LIFESTYLE
— DOMESTIC

BIOLOGICAL AND CHEMICAL TESTING OF COKE OVEN EMISSIONS

G. Thomas, J. Craigmile, B. Das and A. Horton
Ontario Research Foundation

Key words: PAH, Coke Oven Emissions, Air Pollution, Mutagenicity, Organic Analysis.

ABSTRACT

Ambient air studies in Ontario and elsewhere have shown that polycyclic aromatic hyrdocarbons (PAH) are present in urban and rural air. In some areas coke ovens are a significant contributor to the ambient PAH concentrations, but it is difficult to assess the degree of hazard this poses to the populations in surrounding areas.

This study relates to coke oven emissions, especially with respect to the mutagenicity and chemical nature of solvent extractable fractions of collected particulate material.

Representative HiVol and LoVol samples of coke oven emissions have been collected. Samples were taken directly from the coke oven through a hole drilled in a lid, every hour throughout a complete coking cycle. Simultaneously, samples were collected from on top of the coke oven. The HiVol sample filters were backed up by polyurethane (PUF) foam plugs.

LoVol filters were extracted with benzene. These data provided the benzene soluble fraction of total particulate matter (BSFTPM) to be used as markers to compare with existing occupational data. HiVol filters and PUF plugs were extracted with dichloromethane (DCM). The decision to use DCM was made after suitable experimentation (bioassay and chemical) with separate benzene and DCM extracts.

Organic soluble fractions from selected Lid and Top Side HiVol samples were used in two-tiered short-term mutagenicity assays, namely, a bacterial test (Ames) and a tissue culture test (SCE-CHO). Concurrent chemical analysis was performed on portions of the samples used for the biological assays. In some instances, limited fractionation of the samples prior to chemical analysis was performed.

The sampling and testing protocols were performed at three coke oven locations in Ontario. The results of the biological assays and the concurrent chemical analyses for the selected soluble organic fractions of the HiVol samples will be discussed.

Technology Transfer Conference No. 6
December 11, 1985
Toronto Hilton Harbour Castle

Presentation:

"Biological and Chemical Testing of Coke Oven Emissions"

by: J. Craigmile, B. S. Das, A. J. Horton, G. H. Thomas
Ontario Research Foundation, Mississauga, Ontario.

R. S. Gupta, Department of Biochemistry
McMaster University, Hamilton, Ontario.

INTRODUCTION

The potential environmental hazards of polycyclic aromatic hydrocarbons (PAH) are well known. They represent the largest known group of chemical carcinogens found in airborne particulates. Many PAH have cytotoxic, mutagenic, carcinogenic and co-carcinogenic effects. Monitoring and controlling emissions of PAH compounds and assessing their potential hazards to human health resulting from exposures is of great importance to Government and regulatory agencies.

The presence of PAH in the environment results largely from the incomplete combustion of carbonaceous material. Though widespread at low levels in Ontario, some locations display elevated concentrations. These locations include workplace atmospheres associated with industrial high temperature processes involving carbonaceous material, viz. gas and coke oven workers, steel workers, etc.

Coke workers have been singled out from other by-product workers as having the highest incidence of lung cancer. It is alleged that the cause for this is exposure to PAH compounds present in the emissions generated during the coking process.[1-4] Coke oven emissions are a combination of gaseous and fine/heavy particulate material resulting from the destructive distillation of coal during the production of coke. The presence of known carcinogens, e.g. benzo[a]pyrene, B[a]P, and benzo[a]anthracene, B[a]A, has been demonstrated in coke oven emissions. Epidemiological studies for coke oven workers[5,6] also demonstrated that the job-site of coke workers within the coking operation had a significant health risk.

Coke oven emissions have been measured in terms of total particulate matter emitted; as well as its organic solvent soluble fraction known as coal tar pitch volatiles (CTPV). Since benzene was usually the solvent of choice the soluble fraction is often referred to as the benzene soluble fraction of total particulate matter (BSFTPM). In the reported epidemiological studies exposure was measured by the BSFTPM of coke oven emissions.

Due to the pattern of lung cancer experience of coke oven workers which displays an increase in excess risk with length of employment at the ovens, and a dependency of the magnitude of the mortality on the area of employment, the relationship between some measurement of the coke oven emissions and the risk of developing this disease needs to be investigated. In areas where coke ovens are a significant contributor to ambient PAH concentrations, it is difficult to assess the degree of hazard this poses to the populations of surrounding areas.

Many PAH are mutagenic, and although mutagenicity cannot directly predict carcinogenicity the fact that a compound is mutagenic is cause for concern. Short-term biological tests are attracting interest as a basis for possible regulatory purposes. The reason for this is that these tests assess mutagenicity, and thus provide some predictive value regarding health effects. It is generally agreed that more than one short-term bioassay test should be used to prescreen chemicals for potential carcinogenic activity.

The objective of this study was to collect and determine pertinent data related to coke oven emissions. The intent was to determine whether a possible correlation exists between the soluble organic fraction (SOF) of collected coke oven emissions and short-term mutagenicity tests. In addition, concurrent detailed chemical analyses of the SOF was to be performed.

SAMPLING PROTOCOL

It was decided to sample at both old and new coke ovens in Ontario both on top and at the side of the ovens.

Initially, sampling equipment consisted of three high Hi-Vols, two Lo-Vols and a filter tape sampler. The high volume sample filters were backed up by polyurethane foam (PUF). Because of the low ambient temperatures at the time of sampling it was felt that the ozone levels would be relatively low and there was no need for an ozone denuder before the filter. The samplers were sited both on the top and at the side of coke ovens.

It had been estimated that sampling times of 2 to 4 hours would provide sufficient extractable material for biological testing.

However, it turned out that this sampling procedure provided insufficient material for the proposed biological testing protocol. It was found that there were only between seven and ten per cent of extractable organic material in the collected sample. There was an exception to this where the sample had been taken near a leaking lid. This sample contained 33% soluble organic fraction.

The initial biological assay protocol called for a nine strain Ames assay of organic extracts obtained using benzene and dichloromethane, in order to determine the most suitable solvent and tester strain combination. In order to provide sufficient material, sampling was performed on a cat walk slightly elevated above the top of the coke oven. These samples were collected over a 45 hour time period.

Significant changes were made in the sampling protocol after the initial results had been evaluated and discussions had taken place with steel company staff. In the new protocol, samples were taken at hourly intervals directly from the coke oven through a hole drilled in a lid. Hi-Vol and Lo-Vol samples were collected on top of the coke oven at the same time. These samples provided sufficient material to do all the tests required.

Samples have been collected and analyzed from three steel mills in Ontario. The soluble organic fractions from the Hi-Vol samples were divided into two portions for biological and chemical testing, respectively. Some ambient air samples have also been taken outside the steel mill property, both upwind and downwind.

Extraction Solvents

Lo-Vol filters were extracted with benzene. These data provided the BSFTPM, benzene soluble fraction of total particulate matter, which will be used as markers to compare with existing occupational standards.

The Hi-Vol filters and PUF plugs were extracted with dichloromethane (DCM). DCM extracts were tested in comparison with benzene extracts in a nine strain Ames assay and essentially the same results were obtained from both methods of extraction. Chemical analysis also showed similar compositions in extracts obtained using the two different solvents.

BIOLOGICAL TESTING

The bioassays employed were the Ames *Salmonella* mutagenicity assay and the sister chromated exchange assay in Chinese hamster ovary cells (SCE-CHO).

In the preliminary Ames work nine *Salmonella* tester strains were used to select the most sensitive strains for use in this test program. The five standard *Salmonella* tester strains, TA-1535, TA-1537, TA-1538, TA-98 and TA-100 were used. Tester strain TA-102 and the three nitro-reductase deficient strains TA-98NR, TA-98, 1,8DNP6 and TA-988NR/1,8DNP6 were also used. The nitro-reductase deficient strains were used because of the sensitivity of the *Salmonella* tester strains to nitro-PAHs. In fact, the nitro-reductase deficient strains did not show any significant differences in tests on coke oven samples or samples taken in the surrounding area outside the steel company.

Results of the preliminary assay indicated that TA-98 was the most active tester strain for Hi-Vol filter extracts. TA-98 and TA-1537 were active on PUF extracts. TA-98, TA-100, and TA-1537 were selected as testing strains.

All SCE induction studies were carried out with Chinese hamster ovary (CHO) cells.

Sample preparation for testing was as follows:

An aliquot of a Hi-Vol filter SOF calculated to contain sufficient material for the tiered biological testing was transferred to a small tray and allowed to dry at room temperature in a fume hood. The weight of the dry extract was determined. The extract was dissolved in a suitable volume of dimethylsulphoxide (DMSO) to give a concentration of 10,000 µg/mL.

Samples for sister chromatid exchange tests (SCE) were prepared the same way except the dry extract was dissolved in DMSO to a concentration of 5,000 µg/mL. A sample volume of 25 mL was prepared and immediately frozen on dry ice. The samples for SCE testing were transported frozen on dry ice to Dr. R. Gupta at McMaster University in Hamilton.

All quality assurance samples were prepared as a single sample, divided into equal parts, frozen on dry ice and transported to the participating laboratories. The MOE biohazard laboratory acted as the reference lab for both Ames assays and SCE tests on reference compounds and samples.

CHEMICAL TESTING

Aliquots (10 mL) of all SOF from the Hi-Vols and PUFs were sealed in hypo-vials, labelled and stored at 4°C prior to chemical analysis. Preliminary chemical data were obtained by direct injection of suitable aliquots (1-3 µL) of the samples into a gas chromatograph-mass spectrometric (GC-MS) system. The systems used were:

(i) HP Model 5992B with a HP 18740B capillary column interface/control, and equipped with a HP desk top computer (9825A) plus a flexible disk system (9885).

(ii) HP Model 5790A series capillary GC with a HP 5970A Mass Selective Detector.

Instrument Parameters

(i) GC Conditions

Column : 30 m x 0.25 mm fused silica column (SP B5)
Injection : 250°C
GC-MS Interface : 250°C
Column Program : 50°C for 1 min; 10°C/min to 275°C
Carrier : He at 1.5 mL/min

(ii) MS Conditions

Source : Electron Impact with 70 eV
Electron Multiplier : 2000-2400 volts
Scan : 380 amu/sec; 4 samples per 0.1 amu
Mass range scanned : 35-400 amu

Selected extracts (mainly those used for the tiered biological testing) were separated into compound type concentrates of saturates, monoaromatics, diaromatics, polyaromatics and polar aromatics on a dual-packed silica gel-alumina liquid solid chromatographic system (LSC).

RESULTS

Extraction Data

Extraction data in terms of total particulate matter (TPM) and soluble organic fractions (SOF) for comparative Hi-Vol and Lo-Vol samples is presented in Tables 1, 2 and 3. Table 1 gives data for lid samples collected throughout a coking cycle. Table 2 gives representative data for lid samples collected at the three mills. Table 3 gives corresponding data for the coke oven topside (COTS) samples collected from the three mills.

TABLE 1

Lid Samples Mill #1
TPM, SOF and VOF for Hi-Vol/Lo-Vol Samples
(mg/m^3)

Coke Cycle Time	Hi-Vol Filter Samples and PUF			Lo-Vol Filter Samples	
	Dichloromethane Extracts			Benzene Extracts	
	TPM	SOF	VOF	TPM	SOF
0	1435	390*	88	1091	644
2	1665	1343	145	1747	1642
6	678	580	232	989	767
8	617	518*	236*	942	783
10	662	507	232	551	449
12	512	342*	229*	1011	698
14	234	186*	75	105	204

* Tested for Mutagenicity

TABLE 2

TPM and SOF of Hi-Vol/Lo-Vol Lid Sets from 3 Mills
(mg/m^3)

Mill #	Coke Cycle Time	Hi-Vol DCM		Lo-Vol Benzene	
		TPM	SOF	TPM	SOF
1	0	1435	390	1091	644
	8	617	518	942	783
	14	234	186	-	-
2	1	687	490	377	290
	8	356	299	255	106
	16	606	33	169	48
3	1	302	175	119	81
	8	1532	219	424	414
	15	837	109	280	231

TABLE 3

TPM and SOF of Hi-Vol/Lo-Vol Coke Oven Top Sets from 3 Mills

(mg/m^3)

Mill #	Filter Sample #	Hi-Vol DCM		Lo-Vol Benzene	
		TPM	SOF	TPM	SOF
1	101	1.3	0.4	0.7	0.5
	105	2.8	0.6	2.2	0.7
	108	8.6	2.5	3.6	2.6
	118	3.2	2.6	1.4	0.7
2	249	7.0	2.0	5.0	2.7
	237	5.6	2.9	5.0	3.3
	229	12.2	4.0	5.1	3.9
	222	4.4	1.7	6.9	5.4
3	305	3.0	0.4	1.8	0.3
	319	4.2	0.2	1.7	1.1

BIOLOGICAL TESTING

All positive and negative control test data indicated that the assay systems were functioning and capable of detecting mutagenicity.

The lid samples submitted for biological testing represented samples collected at the beginning, middle and near the end of a coking cycle. The coke oven top samples (COTS) were collected concurrently with the lid samples for periods of time ranging from 4-6 hours. Summaries of the biological test results are presented in Table 4 (Lid Samples) and in Table 5 (COTS).

TABLE 4

Summary of Biological Tests on Lid Samples

Mill #	Coke Cycle Time	Filter #	Ames	SCE-CHO
1	0	128	-	+
	8	112	+	+
	14	122	-	/
2	1	238	+	+
	8	225	+	+
	16	246	+	/
3	1	308	+	+
	8	317	+	+
	15	327	+	+

/ = not tested

TABLE 5

Summary of Biological Tests on COTS

Mill #	Filter Sample #	Ames	SCE-CHO
1	AM 19 (combination 101 & 105)	+	+
	101	+	/
	105	+	/
	108	+	+
	AM 20 (combination 118, 124 & 126)	+	/
2	220	-	/
	229	-	/
	237	(+) not confirmed	/
	241	-	+
	249	-	+
3	305	+	+
	319	+	/

/ = not tested

CHEMICAL ANALYSIS

The types of compounds associated with coke oven emissions have been studied by many workers.[7,8,9] In general the majority of compounds identified have been polycyclic aromatic hydrocarbons (PAH). In the present study fused silica glass capillary gas chromatography (GC)[2] with mass spectrometric detection was used for the qualitative analysis of the SOF of the coke oven emissions.

Using GC-MS we were able to determine that virtually all the components passing through the GC column were PAH. As an additional means of facilitating chemical analysis a conventional solid/liquid column chromatographic technique using adsorption on silica gel/alumina was performed. Elution with solvents of increasing polarity yielded fractions consisting of alkanes, non-polar PAH (divided into mono- and di-aromatics and polyaromatics) and a moderately polar PAH. The polar fraction contained mainly aza-arene type PAH. The use of an extensive range of eluting solvents did give an effective separation, especially of the heteroatomic components. However, there was still considerable overlap between compound classes as experienced by other authors.[10,11]

It was possible to tentatively identify most of the peaks present in the unfractionated SOF. The principal findings are summarized in Table 6. This table contains a listing of the compound types together with formulae and molecular weights, for the respective compounds identified.

The unfractionated samples in all cases ranged in colour from dark yellow to dark brown. In the fractionation procedure performed on selected samples the major portion of the coloured material was retained as a brown band on the adsorption columns. The benzene extracts were light yellow in colour. The later polar solvent fractions did contain a portion of the original colour and were generally dark brown in colour. Some colour material remained on the column even after solvent stripping, and is presumed to be high molecular weight material. The various fractions obtained were also analyzed using GC-MS. The data obtained were used to confirm the tentative assignments made from the unfractionated GC-MS data. In the case of the methanol fraction, which was dark brown in colour the GC-MS data indicated that the majority of the compounds present were probably nitrogen containing PAH (aza-arenes). The principal findings for these aza-arene compounds are summarized in Table 7. This table contains a listing of the compound types together with formulae and molecular weights for the respective compounds identified.

Only a limited number of PUF extracts were subjected to the Ames test. The results indicated that the samples were positive both with and without metabolic activation. The chemical data obtained on the PUF extracts showed that they consisted mainly of the low molecular weight PAH together with large amounts of the alkylated derivatives. There were also phenolic materials present especially in the COTS extracts.

TABLE 6

M.Wt.	Compound	Formula
94	Toluene	C_7H_8
134	Benzothiophene	$C_{10}H_{14}$
128	Naphthalene	$C_{10}H_8$
142	C_1-alkyl	$C_{11}H_{10}$
156	C_2-alkyl	$C_{12}H_{12}$
154	Acenaphthene	$C_{12}H_{10}$
152	Acenaphthyene	$C_{12}H_8$
168	Dibenzofuran	$C_{12}H_8O$
182	C_1-alkyl	$C_{13}H_{10}O$
166	Fluorene	$C_{13}H_{10}$
178	Phenanthrene	$C_{14}H_{10}$
178	Anthracene	$C_{14}H_{10}$
192	C_1-alkyl	$C_{15}H_{12}$
206	C_2-alkyl	$C_{16}H_{14}$
184	Dibenzothiophene	$C_{12}H_8S$
190	4H-cyclopenta[def]phenanthrene	$C_{15}H_{10}$
202	Pyrene	$C_{16}H_{10}$
202	Fluoranthene	$C_{16}H_{10}$
216	C_1-alkyl	$C_{17}H_{12}$
216	Benzofluorene	$C_{17}H_{12}$
228	Benz[a]anthracene	$C_{18}H_{12}$
228	Chrysene	$C_{18}H_{12}$
228	Triphenylene	$C_{18}H_{12}$

Continued ...

TABLE 6

M.Wt.	Compound	Formula
Continued...		
242	C_1-alkyl	
226	Benzo[ghi]fluoranthene	$C_{18}H_{10}$
240	C_1-alkyl	
252	Benzo[b]fluoranthene	$C_{20}H_{12}$
252	Benzo[j]fluoranthene	$C_{20}H_{12}$
252	Benzo[k]fluoranthene	$C_{20}H_{12}$
252	Benzo[a]pyrene	$C_{20}H_{12}$
252	Benzo[e]pyrene	$C_{20}H_{12}$
252	Perylene	$C_{20}H_{12}$
266	C_1-alkyl	$C_{21}H_{14}$
266	Dibenzo[ac]fluorene	$C_{21}H_{14}$
276	Indeno[1,2,3,cd]pyrene	$C_{22}H_{12}$
276	Benzo[ghi]perylene	$C_{22}H_{12}$
276	Anthanthrene	$C_{22}H_{12}$
278	dibenz[ac]anthracene	$C_{22}H_{14}$
278	dibenz[ah]anthracene	$C_{22}H_{14}$
278	benzo[b]chrysene	$C_{22}H_{14}$
278	Picene	$C_{22}H_{14}$
300	(Coronene (Dibenzo[ghi,per]perylene	$C_{24}H_{12}$
302	Dibenzo[e,l]pyrene	$C_{24}H_{14}$

TABLE 7

M.Wt.	Compound	Formula
129	Quinoline	C_9H_7N
129	Isoquinoline	C_9H_7N
143	C_1-quinoline	$C_{10}H_9N$
157	C_2-quinoline	$C_{11}H_{11}N$
171	C_3-quinoline	$C_{12}H_{13}N$
167	(Azafluorene	$C_{12}H_9N$
	(Carbazole	
169	Azadibenzofuran	$C_{12}H_{11}N$
169	C_1-aza-acenaphthene or diphenyl	$C_{12}H_{11}N$
179	2,3-benzoquinoline	
	3,4-benzoquinoline	$C_{13}H_9N$
	5,6-benzoquinoline	
	(7,8-benzoquinoline	
	(Acridine	
181	C_1-azafluroene	$C_{13}H_{11}N$
183	C_1-azadibenzofuran	
	C_2-aza-acenaphthene or diphenyl	$C_{13}H_{13}N$
185	Azadibenzothiophene	$C_{11}H_7NS$
191	Phenanthro[bcd]pyrrole	$C_{14}H_9N$
193	C_1-benzoquinoline	$C_{14}H_{11}N$
199	C_1-azadibenzothiophene	$C_{12}H_9NS$
203	Azafluoranthene/pyrene	$C_{15}H_9N$
205	C_1-aza-cyclopenteno[def] phenanthrene	$C_{15}H_{11}N$
207	C_2-benzoquinoline	$C_{15}H_{13}N$

Continued ...

TABLE 7

M.Wt.	Compound	Formula
Continued...		
217	C_1-azofluoranthene/pyrene	$C_{16}H_{11}N$
229	3,4-Benzacridine	$C_{17}H_{11}N$
229	Dibenzoquinoline	$C_{17}H_{11}N$
253	Azabenzofluoranthene/pyrene	$C_{19}H_{11}N$
267	Dibenzo[ai]carbazole	$C_{20}H_{13}N$
279	Dibenz[ah]acridine	$C_{21}H_{13}N$
168	Azacarbazole	$C_{11}H_8N_2$
194	C_1-azaphenanthrene	$C_{13}H_{10}N_2$

6. REFERENCES

1) Reed, D.D. and C. Buck. Brit. J. Ind. Med. 13:265 (1965).

2) Doll, R. et al. Brit. J. Ind. Med. 22:1 (1965).

3) Hucper, W.C. Environmental and Occupational Cancer. Public Health Report. Supplement 209.

4) Lloyd, J.W. J. Occup. Med. 13:53, February, 1971.

5) Wallingford, K.M. and S.S. QueHee. 8th Int. Symp. on PAH, Columbus, Ohio, October, 1983.

6) Fanninck, N., L.T. Gonslor and J. Schockley. Am. Ind. Hyg. Ass. J., 33, pp. 461-468 (1972).

7) Lao, R.C., R.S. Thomas and J.L. Minkima. J. Chromatogr. 112, pp. 681-700 (1975).

8) U.S. Environ. Prot. Agency - Carcinogen Assessment of Coke Oven Emissions. EPA-600/6-82-003, November, 1982.

9) Eisenhut, W., E. Langer and C. Meyer. 6th Int. PAH Symposium, pp. 255-261 (1981).

10) Farcasiu, M. Fuel, 56, pp. 9-14 (1977).

11) Sawatzky, H., A.E. George, G.T. Smiley and D.S. Montgomery. Fuel, 55, pp. 16-20 (1976).

EXPERIMENTALLY DETERMINED MUTATION RATES IN LUNG AND BRONCHIAL EPITHELIA AS A PRIMARY AIR POLLUTION STANDARD

J.A. Heddle, K. Jain, H. Kaul, and D.B. Couch
Department of Biology, York University

Key words: Mutagenicity Assays, Air Pollution, Mutation Rates, Health Effects, Inhalable Particulates, Exposure.

ABSTRACT

One of the health hazards arising from the inhalation of polluted air is cancer of the lung and trachea. Since epidemiological studies of exposed populations and animal cancer bioassays are too cumbersome to be used as primary standards for air pollution, a more practical standard must be used. This project is dedicated to developing a more relevant biological standard than raw particle counts or benzpyrene determinations. The central role played by mutation in the carcinogenic process suggests that measurement of mutation rates in the lung and tracheal cells could provide such a standard.

Normally, mutation rates are measured by determining the proportion of cells that can form colonies under conditions that permit mutant cells to grow but not unmutated cells. This restricts the cells in which measurements of mutation frequency can be made to those for which there are excellent culture conditions available. Recently, however, we have developed a technique designed to bypass these difficulties and to permit measurement of mutation rates in a variety of primary cell types that can be maintained in culture but not cloned efficiently, such as those of lung and trachea. The concept has been shown to work successfully in the CHO cell line where a wide variety of mutagens were detected and the assay validated. The assay detects mutation to diphtheria-toxin-resistance, one of the standard loci used in the traditional colony-formation assays. The resistance to the toxin, which acts by inhibiting protein synthesis, is detected not by colony formation but rather autoradiographically after exposure of the intoxicated cell population to tritiated leucine. Mutants resistant to the toxin will continue to synthesize protein and thus will be labelled, whereas cells that have been killed by the toxin will not. The conditions for a successful assay were indicated by the work in CHO cells, which has been published [Ronen et al, PNAS 81 (1984)].

Since then, work has proceeded on the mammary, colonic, and lung epithelia which are at various stages of development. In the mammary and colonic epithelia, the conditions for the assay have been worked out and the assay applied to model carcinogens active in these tissues. In the lung and trachea, which work was begun much more recently, we have succeeded in developing and standardizing the isolation and culture techniques sufficiently well so as to permit commencement of the experiments that will determine the appropriate selection conditions.

EXPERIMENTALLY DETERMINED MUTATION RATES IN LUNG AND BRONCHIAL EPITHELIA AS A PRIMARY AIR POLLUTION STANDARD: METHOD DEVELOPMENT

J.A. Heddle, K. Jain, H. Kaul, and D.B. Couch
Department of Biology,
York University,
Toronto (Downsview), M3J 1P3

ABSTRACT

One of the health hazards arising from the inhalation of polluted air is cancer of the lung and trachea. Since epidemiological studies of exposed populations and animal cancer bioassays are too cumbersome to be used as primary standards for air pollution, a more practical standard must be used. This project is dedicated to developing a more relevant biological standard than raw particle counts or benzo(a)pyrene determinations. The central role played by mutation in the carcinogenic process suggests that measurement of mutation rates in the lung and tracheal cells could provide such a standard.

Normally mutation rates are measured by determining the proportion of cells that can form colonies under conditions that permit only mutant cells to grow. This restricts the cells in which measurements of mutation frequency can be made to those for which there are excellent culture conditions available. Recently, however, we have developed a technique to bypass this restriction so as to permit measurement of mutation rates in a variety of cell types that can be maintained in culture but not cloned efficiently, in this case, the cells of the lung and trachea. The assay detects mutation to diphtheria-toxin-resistance, one of the standard loci used in the colony-formation assays. The resistance to the toxin, which acts by inhibiting protein synthesis, is detected autoradiographically after exposure of the intoxicated cell population to tritiated leucine. Mutants resistant to the toxin will continue to synthesize protein and thus will be labelled whereas cells that have been killed by the toxin will not. The conditions for a successful assay were indicated by the work in CHO cells, which has been published (Ronen, et al., Proc. U.S. Natl.

Acad. Sci. 81:6124-6128 (1984)).

Since then work has proceeded on the application of this approach to cells in vivo. In the lung and trachea, we have succeeded in developing and standardizing the isolation and culture techniques sufficiently well so as to permit determination of the appropriate selection conditions. Some data, originally anticipated in the second year, are reported.

I. INTRODUCTION

A. NEED FOR THE ASSAY

There is a long-standing need for air pollution standards that are relevant to human health. Chief among the hazards to human health is the threat of lung cancer, now the most common cancer in Ontario in men, and second only to breast cancer in women. In spite of the enormous contribution of cigarette smoking to the incidence of this disease, about 15% of all lung cancers arise in non-smokers and there is a marked excess of lung cancers in urban populations as compared to rural ones even among people smoking the same number of cigarettes per day. An appropriate standard for air-borne carcinogens is one that reflects the true carcinogenic risk of the polluted air with all of its complexities. Unfortunately it is impossible to set air pollution standards based on epidemiological studies of exposed populations. Similarly the animal cancer bioassay is much too cumbersome and expensive to be used as a monitoring method or even as a primary standard against which cheaper and more sensitive chemical methods can be calibrated. The revolution in our understanding of the carcinogenesis and the established role of mutation of oncogenes as one of the critical and rate-controlling steps suggests that the measurement of mutation rates in the lung tissue of experimental animals would provide an appropriate standard.

The current assays for mutagenesis have been surprisingly successful given their inherent defects. In the bacterial assays such as the Ames test, for example, the complex processes of uptake, metabolism, distribution, inactivation, and excretion of the carcinogen in vivo are either unrepresented or are mimicked by the addition of S-9, an extract of mammalian liver capable of metabolizing xenobiotics. Furthermore, the Ames Salmonella/mammalian microsome test gives no indication of the tissue-specificity of the carcinogen. Positive results may thus be obtained for air pollutants that would be liver carcinogens if administered intraperitoneally but that are inactive by inhalation at any site. In addition, only a very rough estimate of potency can be made from the Ames test results. Of course, for in vivo assays, the route of exposure can be comparable to the human route so that the normal metabolic uptake, metabolism, etcetera will be reflected in the outcome of the assay. Unfortunately, in vivo assays use of tissues of convenience rather than target tissues and thus could also give false positives. (For example, air particulates might contain a carcinogen that produces colon cancer when administered intraperitoneally but that is innocuous when inhaled.) The solution we propose is to measure mutation rates in the target tissues themselves and thus to turn this disadvantage, which is inherent in most in vivo assays, into an advantage.

B. CONCEPT OF THE ASSAY

Until recently, all assays for mutation required dividing cell populations because mutants were detected by their ability to form colonies under selective conditions, ie conditions under which non-mutant cells were killed. This made the assays inappropriate for the measurement of mutation rates in trachea and lung since the cells cannot be cloned with high efficiency. Recently however, we have developed an autoradiographic assay in Chinese hamster ovary cells which is independent of their ability to divide. The assay detects as wide spectrum of DNA-damaging agents; indeed, all that have been tested with it have been detected. The selective agent used was diphtheria toxin, a protein which acts by shutting down protein synthesis in sensitive cells. It is known that resistance to the toxin can arise by mutation at three or more loci.

C. REQUIREMENTS FOR THE ASSAY

Since cancer develops primarily in the epithelial cells of the lung and bronchus, it is important to measure mutations in these cells. An important requirement of the assay, therefore, is that methods be available to isolate the epithelial cells of interest and to maintain them in culture for the time required to identify cells with the mutant (toxin-resistant) phenotype. A second requirement for the assay is then to be able to distinguish sensitive from resistant cells. As sensitive cells can be killed by exposure to toxin, there are only two major variables of the selection to be worked out, concentration of toxin and duration of exposure although other factors such as pH, culture medium, may also influence the intoxication. In CHO cells the frequency of spontaneous mutants detected is about 4 per 100,000. Obviously the microscopic examination of each of 100,000 cells would be very tedious and time-consuming. Accordingly we developed a rapid means of detecting the mutants by means of darkfield illumination. Under these conditions, only the highly refractile grains of the autoradiogram are visible; the cells themselves are not seen. Mutant cells are readily detected since they are covered with grains. The frequency of mutants is determined by counting the number of labelled cells in a defined area and knowing the total number of cells in the same area. Once assay conditions have been established, animals will be exposed to known mutagens/carcinogens. Cells which become toxin-resistant through genetic alteration will require some time to express the mutant phenotype, and so another requirement of the assay is that this expression time be determined. It is likely that in the slowly growing lung epithelium expression will take considerably longer than in the rapidly growing CHO cells.

The research program has three phases, (1) development of the technical ability to handle the cells of interest, (2) determination of the assay conditions, and (3) validation with known tissue-specific carcinogens, each phase corresponding to one year of the grant. This is a report of the first year in which the detailed objectives were to establish experimentally each of the first three techniques required for the assay; namely, the isolation, culture, and examination of the epithelial cells of the lung and trachea. A necessary part of this was the specific identification of the epithelial cells within which the cancers of the lung and trachea arise.

II. METHODS USED

A. LUNG CELL ISOLATION

Epithelial cells were isolated from lungs of Chinese hamsters. The animals were anesthetized with sodium pentobarbital or Nembutal (0.1 ml). The heart and lungs were removed intact and placed in a petri plate containing MEM medium. The lungs were perfused with medium intravascularly via the right ventricle until the lung became bleached. Three to four animals were used in each experiment. The outer portion of the tubular part of the trachea was freed of blood capillaries and other adherent tissues and then trachea separated from the pulmonary region and processed separately as follows.

The pulmonary region of the lung from Chinese hamsters was minced in an Erlenmeyer flask containing 20 ml of MEM medium with ascorbic acid (5 ug/ml) and glutathione 5 ug/ml). The mince was degassed under vacuum while being stirred until the tissue pieces sank, followed by rinsing and filteration through nylon cloth (220 um) to remove the macrophages and remaining blood cells. The tissues were then incubated at 4°C overnight in modified MEM (MMEM) medium containing 0.25% trypsin (GIBCO) or other enzymes.

Next morning, a concentrated solution of DNASE was added to the mince to give a final concentration 10 ug/ml. The mince was left at room temperature for 10 minutes and then triturated gently with a blunt siliconized pipette to mobilize the cells. The supernatant was collected in cold tubes in MMEN with 2% albumin. This procedure was repeated four times, after which the cells were pooled together and pelleted by centrifugation (as described later for tracheal cells in more detail). The cell pellet was twice resuspended in modified D-Valine medium and centrifuged again. The final pellet was resuspended in modified D-Valine medium containing 10% fetal bovine dialyzed serum and plated in the same medium. The cells were incubated at 37°C in a humidified atmosphere of 5% Co_2 in air.

B. PREPARATION OF CULTURES FROM TRACHEAE:

Each trachea was rinsed three times with medium and split into two halves longitudinally. Split tracheae were washed 2-3 times with fresh medium with gentle agitation and then placed in a tube containing 0.125% trypsin or 1% pronase in MEM which contained 5 ug/ml ascorbic acid and 5 ug/ml glutathione. Tracheae were incubated at 4°C overnight. In the morning, the enzyme containing medium was removed gently without disturbing the tracheae and 10 ml of fresh medium without trypsin were added to the tubes. The tracheal cells were then gently mobilized with the help of blunt siliconized pipettes. When this procedure was repeated 3-4 times, the majority of the epithelial cells came off as sheets if trypsin was used as a dissociating enzyme. Some islands of cells and some single cells were also found.

These islands of the cells were layered on the top of a 5% albumin gradient in MEM in tubes that were placed vertically on ice for 20 minutes. During this incubation the islands of cells settle down in the albumin gradient, leaving the single cells in the supernatent. The supernantent containing single cells was transferred to another tube and centrifuged for 10 min at 1000 rpm. The islands of cells and single cells were plated separately in maintenance medium: D-Valine medium containing 10% dialyzed fetal bovine serum, ascorbic acid (5 ug/ml), and glutathione (5 ug/ml). The plates were incubated at 37°C in an atmosphere of 5% CO_2 in air.

PREPARATION OF CELLS FOR ASSAY:

In order to select a suitable method of preparing tracheal and lung cells for examination in the autoradiographic assay for resistance to diphtheria toxin, cells were prepared by using the following methods:

(1) Following isolation cells were plated (a) in 60 mm petri plates, (b) in one chamber Lab Tek tissue culture slides, (c) on regular precleaned glass slides, or (d) cells were kept in suspension either in the glass vials or plastic tubes. The cells were intoxicated either immediately after isolation or after

24 hours of incubation in their maintenence medium, by which time the majority of the cells had attached.

(2) Isolated cells were plated in 60 mm petri plates and incubated for 48h. Floating cells were removed by rinsing the cultures twice with PBS. The cells were then trypsinized (0.25% trypsin, GIBCO) and plated (a) into the petri plates, (b) into chamber slides, or (c) on to the surface of regular precleaned glass slides.

D. ASSAY FOR DT RESISTANT CELLS

Cells from lung and trachea were isolated and seeded (1.8 - 3) x 10^5 cells) in 60 mm petri plates in their maintenence medium 24 hours prior to assay. After 24 hours, the medium was removed and replaced with fresh medium containing DT for 24, 48 or 72 hours. At the end of the incubation, the cells were rinsed with Hank's balanced salt solution and covered with 2 ml of labelling medium: Hank's balanced salt solution supplemented with 25 mm Hepes, 1 mg/ml bovine serum, and 10 uCi of [4, 5-^{3} H(N)] leucine. After 2 hr incubation at 37^{o}C, the labelling medium was removed and the cells were rinsed twice with phosphate-buffered saline and fixed in ethanol/acetic acid (3:1 vol/vol) for at least 1 hr. Each preparation was then washed in 100% ethanol, dried, and coated with Kodak NTB-2 photographic emulsion (diluted 1:1 vol/vol in water) and left at room temperature in complete darkness overnight. Kodak D-19 was used to develop the exposed autoradiographs. Plates were developed in a specially designed and constructed plate holder, made in the York University machine shop (see enclosed photographs Fig 1A) and were stained for 10 min with 4-5% Gimsa.

The scoring of DT-resistant cells was done on plates which were marked in squares (32) and were held in specially designed microscope stage holder (see photograph Fig 1B). The labelled cells were scored with a microscope equipped with a dark-field condensor using the 10 or 20x objective lenses. Under these conditions, the labelled cells shine brightly while the unlabelled ones appear dark against the somewhat paler background. All of the labelled cells which were in petri plates were scored.

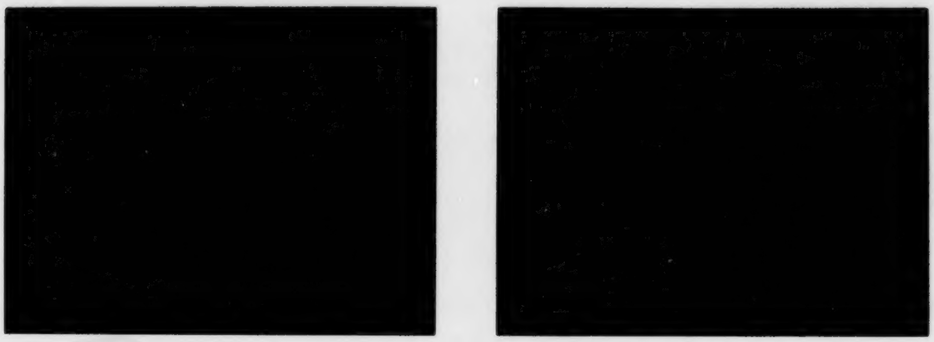

FIGURE 1. Photographs of specially constructed apparatus. A. Holder for autoradiography of 60 mm petri plate bottoms. B. Holder for microscopic examination of petri plate bottoms.

III. RESULTS

A. LUNG CELLS

Cell preparations obtained from the pulmonary region contained a mixed population of cells, including large numbers of ciliated cells, of two quite different sizes. Between 36 and 48 hours after plating, the majority of the cells attached to the petri plates. Most of the unattached cells were ciliated. The attached cells flattened and formed mixed population monolayers with epithelial morphology. Under the inverted microscope, cells differed in their appearance: in some cells the granulated appearance was only perinuclear, while in others it was localized at one side or was uniform. Some smaller cells had uniform cytoplasm with a distinct nucleus. Ciliated cells in these cultures retained their beating cilia for 6-7 days. Cells remained in good condition for 10 days, during which incubation, fibroblastic growth was not observed.

1. Effect of various media on lung cell attachment and maintenance of monolayers.

Of the several media tried the maximum number of cells were attached when

D-Valine medium (supplemented with ascorbic acid (5 ug/ml), glutathione (5 ug/ml), insulin 1 ug/m), hydrocortisone (0.1 ug/m), and 5% dialyzed calf serum) was used. On this medium monolayers remained unchanged for a week, without overgrowth of fibroblasts or muscle cells. Further, macrophages failed to proliferate in this medium. However, when alpha medium was used, fibroblast and muscle cells started to proliferate after 3 days as did macrophages.

2. Effect of trypsin, elastase and elastase-trypsin on the yield, viability and monolayer forming efficiency of the lung cells.

The results are summarized in Table 1. Large numbers of cells were obtained when trypsin (0.25% & 0.5%) was used as a dissociating enzyme. Although trypan blue viability was above 80%, only a few cells attached to the petri plates and formed monolayers; the remaining cells remained unattached and slowly disintegrated. When trypsin (0.125%) or elastase (10 units/ml) when used alone, it took longer to liberate cells and the mobilization process had to be repeated several times, which injured the cells. When elastase and trypsin were used together, cells came off easily and majority of them (mostly from bronchioles) were obtained as islands of cells. When plated these cells were form monolayers. Thus for further studies for isolation of lung cells from Chinese hamster the elastase-trypsin combination was used.

Table 1:- Effect of trypsin, elastase and trypsin-elastase on the yield and viability of lung cells of Chinese hamster.

Enzyme	Cells obtained per animal lung	Viability by trypan blue	Attachment efficiency of cells, forming monolayers*
Trypsin (0.5%)	65×10^7	85	+
Trypsin (0.25%)	62×10^7	89	+
Trypsin (0.125%)	45×10^7	85	++
Elastase (4 u/ml)	31×10^7	83	++
Elastase (4 u/ml)+ Trypsin (0.1%)	62×10^7	90	+++

* + less than 20% of cells attached; ++ about 50% of the cells attached; +++ more than 50% of cells attached.

B. Tracheal cells

1. Viability.

The viability of the harvested cells both from trachea and lungs of Chinese hamsters was 70-85%; the majority of the tracheal cells that were trypan blue positive were ciliated. Tracheal cells required 36-48 hours to attach completely and form monolayers. (Fairly large numbers of cells remained unattached, and slowly disintegrated.) Initially cell islands formed patchy monolayers, with a characteristic epithelial morphology but comprising a mixed population of cells including ciliated, mucin containing, and basal cells. Some of the cells were polygonal, relatively larger in size, and granulated, while others were more cuboidal with homogeneous cytoplasm. Initially patchy monolayers slowly established contacts with neighbouring cells, coalesced together, and formed a contigous sheet. Chinese hamster cells remained undeteriorated for 2 weeks, the maximum tried to date, without fibroblasts.

2. Effect of pronase and trypsin on the yield of tracheal cells.

When trypsin was used as a dissociating enzyme for tracheal cell isolation, the majority of the cells came off as sheets, which beating cilia showed towards the periphery of the sheet. However, when pronase was used as a dissociating enzyme, the majority of the cells appeared as clumps of 2-50 cells (Table 2). When monolayers formed from trypsin digests, large numbers of cells with beating cilia were present whereas from pronase digests there were few cells with beating cilia. When trypsin liberated cells were incubated for two weeks fibroblasts or muscle cells did not appear. In contrast, when pronase was used as a dissociating enzyme both fibroblastic cells and muscle cells made their appearance after the third day of incubation. For these reasons trypsin (0.125%) was selected as the dissociating enzyme for tracheal cell isolation.

Table 2:- Effect of trypsin (0.125% and Pronase (1%) on the number, viability, appearance and type of tracheal epithelial cells of Chinese hamster.

Protease used	Cells obtained trachea*	Viability	Appearance of cells	Monolayers Appearance after 48h		
				Ciliated cells	Other epithelial cells	non-epithelial cells
Trypsin	2.3×10^6	79	As a sheet	Many	Many	None
	1.8×10^6	72	As a sheet	Many	Many	None
Pronase	2.7×10^6	70	Clumps of cells (2-50)	Few	Many	Many
	2.4×10^6	65	Clumps	Few	Many	Many

* each number represents the results from a different animal.

3. Effect of different media on the cell attachment and maintenence of Chinese hamster treacheal cells as a monolayers.

The results are summarized in Table 3. The maximum number of cells attached in the shortest incubation period (24 hours) when Ham's F12 medium (supplemented with 2% fetal calf serum, insulin, and hydrocortisone) and conditioned medium were used in equal proportions. On this media monolayers remained unchanged for two weeks. During the first week of incubation the cells appeared more cuboidal and compact; later, the cells enlarged in size and gave rise to monolayers with a different appearance. When cells were plated in the same medium but plates were coated with collagen gels however, the cells in monolayers were small and cuboidal and remained morphologically unchanged for at least a whole month. A few cells also appear to divide on collagen gels. In further studies, tracheal cells were always plated on a plastic surface containing Ham's F12 medium (with 2% fetal calf serum, insulin (1 ug/ml), hydrocortisone (0.1 ug/ml), plus conditioned medium in the ratio of 1:1.

Table 3:- Effect of different media on the cell attachment and maintenance of Chinese hamster tracheal cells as a monolayer.

S. No.	Media	Approximate cell attachment time (hours)	Attachment efficiency*	Maintenance of monolayers
1	Alpha medium + 5% fetal bovine serum	48	+	> 1 week
2	Alpha medium + 10% fetal bovine serum	48	+	> 1 week
3	D-valine medium + 10% dialyzed calf serum	48	+	> 1 week
4	Ham's F12 medium + 2% fetal calf serum + Insulin (1 ug/ml) + hydro-cortisone (0.1 ug/ml)	48	++	Two weeks
5	Medium as in 4 plus conditioned medium in ratio of 1:1	24	+++	Two weeks
6	Medium as in 5 plated on collagen gel plates	24	+++	> 4 weeks

* + 10-20% cells attached; ++ 20-50% cells attached; +++ 50% or more cells attached.

4. Reproducability

In order to examine the reproducability of the isolation procedure tracheal cell isolations were conducted using 10 tracheae, 4 as controls and 6 for intoxication. Each trachea was separately processed by the standard method described earlier. Cell yields varied from $2.1 \times 10^5 - 3.9 \times 10^5$ cells per trachea with a viability of 76-85%. Cells obtained from all the ten tracheas attached within 24 hours of incubation. When these cells were labelled at 24, 48, or 72 hours after their attachment, all the attached cells were labelled. In order to make sure that all the cells were labelled, cells were counted randomly selecting different areas on the plates. The results. presented in Table 4, indicated that at all incubation times the unintoxicated cells were able to incorporate radioactive leucine. It was quite noticeable that the cells were not uniformly labelled: some cells were more heavily labelled cells than other cells from the same area showed. This may be due to the heterogeneous population of cells present in the monolayers rather than to different metabolic states. These results indicate that our isolation procedures show a consistency in the yield, attachment, and labelling of the cells.

Table 4:- Patterns of 3H-leucine incorporation in isolated tracheal cells of Chinese hamster after 24, 48 and 72 hours after attachment.

	Patterns of 3H-leucine incorporation at different intervals of time in hours					
	24		48		72	
Animal number	cells examined	% labelled cells	cells examined	% labelled cells	cells examined	% labelled cells
1	450	100	450	100	320	100
2	330	100	240	100	250	100
3	291	100	245	100	180	100
4	277	100	263	100	242	100
5	264	100	325	100	170	100

5. Methods used for the preparation of cells for diphtheria toxin (DT) intoxication assay

When cells were plated directly after isolation onto the surface of chamber slides or onto the surface of ordinary slides, the majority of the cells failed to attach uniformly to the chamber slides. When the cells were first plated onto the surface of 60 mm petri plates and then trypsinized 24 hours later when most of the cells are attached and seeded onto the surface of chamber slides or ordinary slides, there was no further increase in the attachment efficiency of the cells. The most suitable method is to plate cells directly onto the surface of petri plates, because this has several advantages over all the other methods tried. The advantages are as follows:

(i) Within 24 hours after isolation, the cells are ready for the assay.

(ii) There is no need to trypsinize and plating repeatedly, which saves time and material.

(iii) The cells are well spread and attached, is advantageous for scoring DT resistant cells.

(iv) Under similar conditions, the autoradiographic procedure, gives a low background.

The only problem encountered with this method was how to handle these plates during the autoradiographic procedures and subsequent examination of the plates under the microscope to score the cells. We overcame this problem by designing a holder and a stage which could hold these plates easily (see photograph Fig 1). Thus for further studies, the cells were plated directly on the surface of petri plates and challenged with Diphtheria toxin within 24 hours.

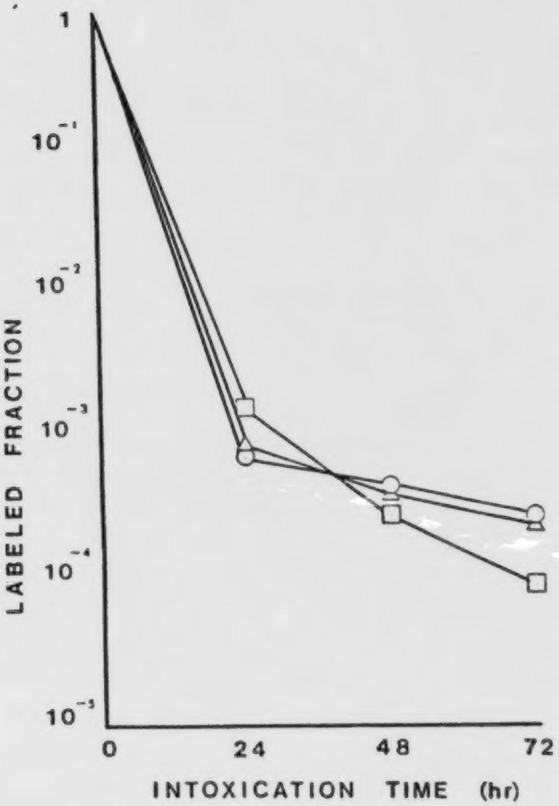

FIGURE 2: Fraction of labelled cells of the tracheal as a function of time in diphtheria toxin, 100 LF/ml. Three replicates are shown by the different symbols.

6. DT intoxication assay

The results of an experiment to determine the effect of 100 LF/ml of diphtheria toxin on the labelling index are presented in the Table 5 and Fig 2.

All of the control plates at all times showed 100% labelled cells, Table 4, whereas the cells exposed to DT showed a progressive decrease in the labelling index with time. The final index reached is similar to that expected for spontaneous mutants and suggests that a satisfactory concentration and time has been found.

Table 5:- Effect of diphtheria toxin on incorporation of 3H-leucine into Chinese hamster tracheal cells at different intervals of time after intoxication. For each experiment 230,000 cells were plated.

Time in hours after DT intoxication	No. of cells labelled		
	Experiment 1	Experiment 2	Experiment 3
0	All the cells	All the cells	All the cells
24	179	208	314
48	100	98	67
72	61	59	21

An experiment was also conducted to determine the variability of the results. Cells from each trachea were isolated and plated separately. After 24 hours of seeding cells were intoxicated with 100 LF of DT and incubated for 24 hours or more. The results obtained are also presented in Table 6.

Table 6:- Effect of Diphtheria toxin (100LF) on the labelling index of Chinese hamster tracheal cells [cells were isolated from individual animals and plated separately] during 72 hours of incubation - A test of reproducability.

Trachea No.	No. of cells plated from individual trachea	No. of cells labelled	Fraction labelled
1	1.9×10^5	25	1.3×10^{-4}
2	1.9×10^5	22	1.2×10^{-4}
3	2.3×10^5	36	1.6×10^{-4}
4	2.6×10^5	52	2.0×10^{-4}
5	2.2×10^5	42	1.9×10^{-4}
6	1.8×10^5	28	1.5×10^{-4}

E. SUMMARY OF ACCOMPLISHMENTS

. In summary it can be said that we have achieved virtually all of the first year's objectives. We can now isolate, culture, and examine the cells of interest from both lung and trachea. Indeed, we have even been able to obtain reproducable intoxication curves for these cells, which is the first requirement of the second year program. We have the imunofluorescent tagging of melanin-body keratin technique working well, and even have a single observation of cells double-labelled with tritiated leucine and fluorescent antibody. The fluorescent tagging indicates that non-epithelial cells are an insignificant fraction of the cells prior to intoxication so that it is very likely that they will not prove to be a significant fraction after intoxication.

FACTORS THAT INFLUENCE ASSESSMENTS OF HEALTH EFFECTS OF AIR POLLUTION

P. Corey, F. Silverman, A. Aviomamitis, S. Mintz, and H.R. Hosein
The Gage Research Institute, Departments of Medicine and Preventive
Medicine and Biostatistics, University of Toronto

Key words: Health Effects, Air Monitoring, Air Pollution, Exposure, Air Particulates.

ABSTRACT

Health effects of air pollution were examined in 30 asthmatics and 14 healthy non-asthmatics. The objectives were: (1) to assess exposure in 4 ways - personal (P), inside (I) and outside (O) the home, and at a fixed air pollution monitoring site (GMOE) in downtown Toronto; (2) to examine the relationship among the estimates of exposure; and (3) to assess the relative strength of the four estimates of exposure as demonstrated by its association with measures of health effects. Small portable multipollutant samplers for nitrogen dioxide (NO_2), sulphur dioxide (SO_2) and particulate matter were carried by the subjects, placed inside and outside the home and at a downtown Toronto air pollution monitoring station. Subjects were each visited on approximately 20 days; pulmonary function (spirometry) was assessed in the morning at the beginning of sampling, and again at the end of the day when sampling was terminated; a questionnaire was completed (symptoms, medications, daily activities and exposure to other potential irritants).

Analyses have been performed to measure the relationship between estimates of pollution exposure, home and lifestyle characteristics, and season of the year on symptoms and pulmonary function. The effect of season is very strong both for pulmonary function and symptom frequency. Furthermore, the relationship between pollutant exposure and pulmonary function is strongly dependent on season.

Regression analyses have been performed to determine whether the estimate of exposure using the personal monitor, our gold standard, can be replaced with a linear combination of 2 or 3 of the other three exposure estimates (I, O, GMOE). On days when an individual had spent a large proportion of his indoor time away from home, the predictive ability of the regression model was weak, as would be expected. However, for the subset of days on which the time spent indoors was only at home, the multiple correlation coefficient for the predictive model was 0.81. This finding has the potential for greatly reducing the costs of exposure monitoring in epidemiologic studies.

FACTORS THAT INFLUENCE ASSESSSMENT OF HEALTH EFFECTS OF AIR POLLUTION

P. Corey, F. Silverman, A. Ayiomamitis,
S. Mintz and H.R. Hosein

presented at
Ontario Ministry of the Environment
Technology Transfer Conference No. 6
December 11, 1985
Sessior A

INTRODUCTION

There is evidence to suggest an association of air pollution with an increased incidence of respiratory diseases and asthmatic attacks. Persons with chronic respiratory disease (e.g. asthma) may be more sensitive. However, there are difficulties involved in clearly defining health effects of air pollution, particularly at low levels of exposure. Two major areas require clarification.

In the first place, most studies to date utilize imprecise assessments of each person's exposure to air pollution. Although man can spend about 70-90% of his time indoors, relatively few studies have been carried out on either the quality of indoor air or its health effects. Until recently, studies of effects of air pollution have relied on pollution exposure measurements obtained from fixed location air pollution stations monitoring outside air. Such stations most commonly have been established in order to evaluate compliance with air quality standards, rather than to examine population exposure. The implicit assumption is that these measurements are representative of an individual's exposure to air pollution. However, there can be substantial differences between air pollution levels separated in space and time. Among numerous factors that contribute to such differences are meteorologic conditions and, proximity of air pollution sources. Thus, the actual levels encountered by an individual carrying out his/her daily activities, i.e. "personal exposure" can be quite different than the pollutant concentrations measured at fixed outdoor monitoring stations.

Another set of problems in previous studies has occurred in the area of assessment of health effects. For instance, the use of severe symptoms or signs as indicators of response could ignore minor (but potentially important) fluctuations in disease. Objective assessments of response such as pulmonary function have not always been included.

Health effects of air pollution were examined in a group of asthmatics in Toronto, Canada. Asthmatics were chosen since previous evidence has suggested that they might be more sensitive to adverse effects of inhaling air pollution. This report is concerned only with some results related to the asthmatics.

METHODS

Nineteen asthmatics were selected for the study from the patient population of The Gage Research Institute Asthma Clinic, a tertiary referral centre for patients with obstructive airway disease. The subjects carried a personal multipollutant sampler for a 6-8 hour period between 8 or 9 A.M. and 4 or 5 P.M. for approximately 20 week days (∿ 10 days in the winter or heating season, 10 days in the summer or non-heating season). On each day pulmonary function (spirometry) was assessed in the morning when the sampler was switched on and at the end of the air pollution sampling period; a questionnaire was also completed which documented symptoms, medications, daily activities and exposure to possible airborne irritants.

Air pollution exposure assessment

Subjects carried a portable personal multipollutant sampler for SO_2, NO_2 and respirable suspended particulates (RSP). Air pollution sampling was carried out from Monday to Friday each week, for a total of 4 weeks for each participant. The design was such that subjects be monitored on each day of the week over approximately four weeks with sampling in both seasons of the year on each subject. The "personal" sampler was worn either on a shoulder strap or belt around the waist. Three other samplers were also employed at fixed sites. One was placed in the subject's home (Indoor), one outside his home (Outdoor) and the third at a site used by the Ministry of the Environment (MOE).

The sampler used for these studies was designed and developed at The Gage Research Institute and is a small, portable, multi-pollutant sampler for SO_2, NO_2 and respirable suspended particulate matter (RSP). It is a battery-operated pump system, consisting of a filter assembly leading to 2 impingers, each containing appropriate absorbing reagent. The samplers were prepared and checked in the laboratory each day before they were taken into the field for use, then the air flow through the bubbling systems for SO_2 and NO_2 were recorded and the timer started. Subjects were instructed on the use and care of the personal sampler. At the end of the sampling period, the flows and elapsed times of each sampler were recorded. The filters were stored flat in small Petri dishes until conditioning and weighing could be completed. The SO_2 concentration was assessed by the method of West & Gaeke and the US EPA NAAQS. The NO_2 concentration was assessed by the TGS-ANSA method. Calibration & quality assurance procedures have been reported previously. As part of our ongoing quality control program, a Gage sampler was set up at a central Ministry of the Environment monitor network station so that a direct comparison between the Gage results and the Ministry's results could be made. The Gage sampler was placed inside an insulated chest with a filter holder protruding from the chest. The chest provided temperature control for the absorbing solutions. Analyses were performed in a routine manner for SO_2, NO_2 and particulates. These values were compared to the 08:00 to 16:00 hour average pollutant concentrations provided by the Ministry. This also provided us with the data to compare personal sampling with fixed site sampling using the same techniques in both cases.

Pulmonary function. Spirometric tests of lung function were performed on the subjects at the beginning and end of each monitoring period using a wedge-balloon spirometer (Vitalograph). Measurements made included: forced vital capacity (FVC), forced expiratory volume in one second (FEV_1) and forced expiratory flow during the middle half of a maximum expiratory manoeuvre ($FEF_{25\%-75\%VC}$). The tests were administered according to standard recommended procedures. At each test session at least 3 maximum expiratory manoeuvres were performed by the subjects until 2 spirograms were obtained which were reproducible to within 5% for both flow and volume. The Vitalograph was calibrated monthly for volume (using a 1 litre syringe) and time.

RESULTS

The correlation coefficients between the 4 sites of NO_2 sampling, (personal, indoor, outdoor and MOE) are given in Table 1. The indoor sampler gave estimates that had the highest correlation with those obtained from the personal sampler ($r = 0.57$). Although large and statistically significant this correlation does not recommend strongly the use of the indoor estimate alone as a substitute for the value obtained using the personal sampler even though the mean levels at the different sites are similar. For completeness the means and correlations are given for SO_2 and RSP in Tables 2 and 3.

Although the personal estimate was not strongly predicted by any single fixed site estimate it may be predicted by a linear combination of the 3 fixed site estimates. To derive such a predictive equation multiple regression analysis was employed.

On each day the subject was asked to record the amount of time spent in one of four categories: home outdoors, home indoors, away outdoors and away indoors. A fixed site sampler was available to measure exposure for all but the last of these 4 categories. Therefore it was anticipated that any predictive equation that could be derived with this data would be strongest for that subset of days on which the percentage of time spent indoors away from home was low. For this reason the multiple regression analysis was performed on 5 mutually exclusive subsets of the data defined by a range of percentage of time spent indoors away from home. The results given in Table 4 are in accordance with our expectations. The multiple correlation coefficient (R) of the predictive equation is largest (R > 0.81) for the two subsets in which the percentage of time spent indoors away from home is less than 20% and lowest for those individuals who spent all of their time indoors away from home (R = 0.35). The statistical significance associated with the indoor home sampler is at first extremely high (p = 0.0001) dropping to insignificance with increasing percentage of time spent indoors away from home. This indicates the importance of the indoor sample in predicting the personal sample in two ways. First when the percentage of time spent indoors away from home is low the percentage of time that the subject is not where a fixed site sampler is available to measure exposure is low. In these cases, not only is the significance associated with the indoor sampler high but the multiple correlation coefficient is high. Second when the percentage of time spent indoors away from home is high then we know that the subject is spending a large percentage of time where one of the fixed site samplers is unavailable to estimate his exposure. The importance of the indoor sample is again illustrated but in this case by the low multiple correlation coefficient associated with the predictive equation.

The almost monotonic decline in the regression coefficient associated with the indoor NO_2 sample is portrayed in Figure 1 for cumulative overlapping deciles of the data defined by the percentage of time spent indoors away from home. This relationship is also plotted for SO_2 and RSP. For RSP the decline in the indoor regression coefficient is not as dramatic and for SO_2 the relationship is more erratic.

The predictive equations using only the indoor and MOE sites and using only those subjects who spent no time indoors away from home are shown in Table 5. These results suggest the possibility at least for NO_2 of using the indoor estimate and the MOE estimate to predict the personal estimate.

An attempt to further simplification involved the creation of an index which weighted the indoor and MOE estimates by the percentage of time spent indoors and outdoors. The correlation coefficients of these indices with the personal sample are given in Table 6. The index for NO_2 gave the highest correlation with the personal estimate (R = 0.78) dropping only slightly from the R of 0.81 obtained from the multiple regression that used the same 2 fixed site estimates (Table 5). The SO_2 index has a very low correlation with the personal estimate.

It is probably unfair to judge the NO_2 index by measuring how strongly it relates to any health effects since in the complete dataset a large percentage of time is spent indoors away from home. In fact as shown in Table 7 the subjects used in this study spent a large percentage of their time indoors. This result, coupled with the very low SO_2 levels found indoors relative to outdoors (Table 2) probably explains the inability to create a strong SO_2 index for this group of subjects.

The relationship between pollutant and health effect is illustrated using the daily mean MEFR and the corresponding daily mean NO_2.

One approach to the assessment of the effect of NO_2 and MEFR would have been to calculate for each patient the mean MEFR and the corresponding mean NO_2 across the same days on which the daily MEFR was calculated. The correlation between the patient mean MEFR and NO_2 is shown in Table 8 for the summer and winter seasons. Note that the correlations are positive and statistically significant. This must not be interpreted as indicating that high concentrations of NO_2 lead to better, i.e. higher MEFR. These correlations can only be interpreted at face value namely that patients with high MEFR are exposed to high NO_2.

One possible interpretation would be that the sicker patient, that is, the patient with a lower mean MEFR seeks out a cleaner environment, which happens to be one with lower levels of NO_2.

The proper analysis involves the measurement of the relationship between daily NO_2 and MEFR within each patient. One approach is to use regression analysis of all person-days that incorporates a classification factor which takes into account the heterogeneity among the patients. The results of such an approach are shown in Table 9. Notice that the sign of the relationship is negative in accordance with our scientific notion that a patient's MEFR will be lower for days on which the NO_2 is higher. However the slope is significant only for the winter season. Included in the analysis is a medication index devised to account for the voluntary and variable drug intake of the patient. Notice that there is a strong positive correlation between the amount of drug intake on a given day and the corresponding mean MEFR.

Replacing the personal estimate of NO_2 with the NO_2 index results in the non-significant slopes shown in Table 10. The strong positive associations with the medication index remain.

It must not be concluded from these results that it is not possible to develop a NO_2 index that will replace the actual personal estimate of NO_2. This index was used in a situation in which a large proportion of the days involved a large percentage of time indoors away from home. A study could be designed in which a group of individuals spent their indoor time at home or primarily in an office or other workplace. One would want to test how well a predictive equation using 3 fixed site samplers (INDOOR HOME, OFFICE, MOE) could estimate the personal sample. Because the index involves the percentage of time spent in these 3 categories such a study would give close attention to the accurate recording of this information on the questionnaire.

TABLE 1

NO2 CORRELATIONS (N = 330)

	Indoor	Outdoor	MOE	Mean (ppb)
Personal	0.57	0.36	0.31	22
Indoor		0.43	0.29	18
Outdoor			0.58	21
MOE				26

TABLE 2

SO_2 CORRELATIONS (N = 330)

	Indoor	Outdoor	MOE	Mean (ppb)
Personal	0.45	0.53	0.36	1.3
Indoor		0.43	0.34	0.6
Outdoor			0.67	6.0
MOE				8.9

TABLE 3

RSP CORRELATIONS (N = 330)

	Indoor	Outdoor	MOE	Mean (μg/m^3)
Personal	0.50	0.31	0.16	51
Indoor		0.25	0.19	43
Outdoor			0.42	32
MOE				38

TABLE 4

REGRESSION COEFFICIENTS OF THE EQUATION USING THE 3 FIXED SITE NO_2 SAMPLES TO PREDICT THE PERSONAL SAMPLE

Percentage of time spent indoors away from home	N	INDOOR		OUTDOOR		MOE		R*
		β	P	β	P	β	P	
0	84	0.890	0.0001	-0.025	0.82	0.225	0.029	0.81
0<-20	52	0.833	0.0001	0.138	0.19	-0.0055	0.95	0.85
20-90	80	0.429	0.0001	0.065	0.48	0.218	0.024	0.64
90-<100	55	-0.023	0.85	0.426	0.007	-0.034	0.79	0.42
100	59	0.125	0.51	-0.211	0.21	0.452	0.03	0.35
TOTAL SAMPLE	330	0.52	0.0001	0.08	0.18	0.121	0.033	0.59

* R is the multiple correlation coefficient of the predictive equation

TABLE 5

RELATIONSHIP BETWEEN PERSONAL SAMPLED POLLUTANT AND SAMPLES FROM AN INDOOR AND MOE SITE (N = 84)*

	Indoor		Outdoor		R
	Slope	P	Slope	P	
NO_2	0.88	0.0001	0.21	0.02	0.81
SO_2	0.72	0.0001	0.08	0.0001	0.75
RSP	0.62	0.0001	-0.09	0.50	0.70

* 84 days sampled on which individuals spent no time away from home indoors.

TABLE 6

RELATIONSHIP BETWEEN PERSONAL SAMPLED POLLUTANT AND INDEX* (N = 84)**

Index for	Slope	P	R
NO_2	0.94	0.0001	0.78
SO_2	0.27	0.0001	0.19
RSP	0.62	0.0001	0.49

* Weighted combination of indoor and MOE estimates.

** 84 days sampled on which individuals spent no time away from home indoors.

TABLE 7

PERCENTAGE OF TIME SPENT INDOOR, OUTDOORS AT AND AWAY FROM HOME

Percentage of time spent AWAY indoors	Indoor		Outdoors		Total
	Home	Away	Home	Away	
0	94.6	0	2.7	2.7	100.0
0 - 20	82.9	11.2	0.6	5.3	100.0
20 - 80	51.0	46.7	0.5	1.8	100.0
80 - < 100	8.1	90.8	0.2	0.9	100.0
100	0	100	0	0	100.0

TABLE 8

RELATIONSHIP BETWEEN SUBJECT MEAN MEFR AND MEAN NO_2 (N = 19)

	Summer	Winter
Slope	0.074	0.050
P	0.012	0.017
R	0.57	0.54

TABLE 9

RELATIONSHIP OF DAILY MEAN MEFR AND NO_2* AND AMI**

	Summer		Winter	
	Slope	P	Slope	P
NO_2	- 4.2	0.24	- 7.3	0.016
AMI	0.018	0.0001	0.010	0.0001

* NO_2 measured with the portable personal sampler

** Medication index

TABLE 10

RELATIONSHIP OF DAILY MEAN MEFR AND NO_2 INDEX* AND AMI**

	Summer		Winter	
	Slope	P	Slope	P
NO_2 Index	5.0	0.22	- 1.5	0.69
AMI	0.017	0.0001	0.010	0.0001

* Weighted combination of indoor and MOE estimates

** Medication index

FIGURE 1

RELATIONSHIP BETWEEN THE REGRESSION COEFFICIENT ASSOCIATED WITH THE INDOOR SAMPLE AND THE PERCENTAGE OF TIME SPENT INDOORS AWAY FROM HOME

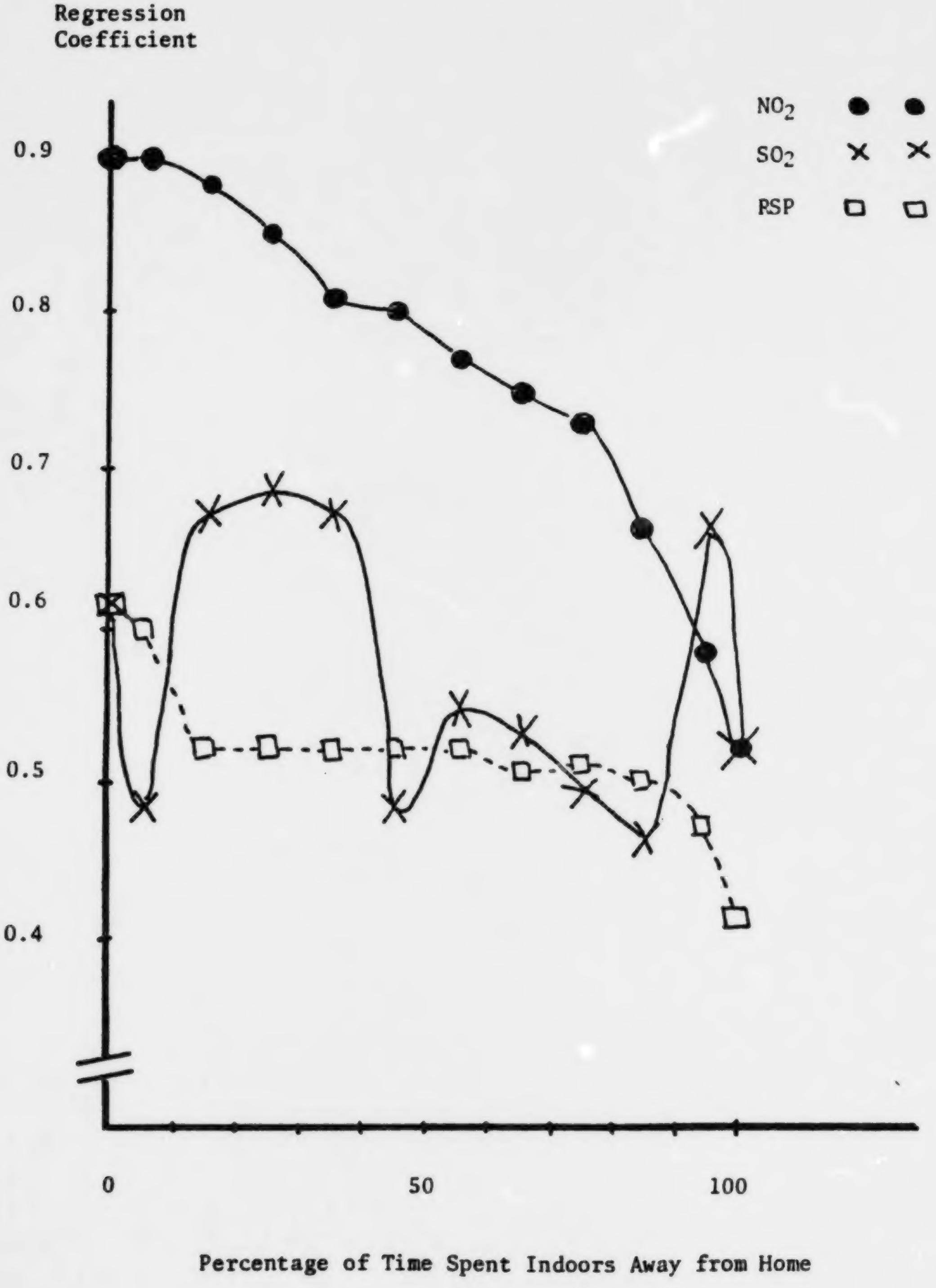

ENVIRONMENTAL MODELLING OF TOXIC SUBSTANCES IN SOUTHERN ONTARIO

Donald Mackay, Sally Paterson, Wan-Ying Shiu, and Christina Charles
Department of Chemical Engineering and Applied Chemistry
University of Toronto

Key words: Southern Ontario, Organics, Environmental Fate, Partitioning Model.

ABSTRACT

It is possible to develop methods of predicting the concentration of organic contaminants in the Southern Ontario Region from a knowledge of:

(i) the magnitude of local emissions to air, water and soil, both past and present;

(ii) the magnitude of advective inflows in air and water from other regions;

(iii) the physical-chemical properties of the chemicals as they influence partitioning tendencies between the media of air, water, soil, sediment and various biota;

(iv) the reactivity of the chemicals in these media which controls the chemicals' persistence; and

(v) the intermedia transport properties of the chemical, especially air-water, air-soil and sediment-water exchange.

A Level IV fugacity model has been devised which attempts to predict the time-dependent concentrations of specific chemicals in the Region from these input data. The model has been applied to a number of chemicals for which approximate emission data and prevailing concentration data are available. Reconciling the model with the prevailing concentrations requires comparison of the single predicted mean concentrations with a distribution of environmental concentrations in each medium. The Weibull distribution function has been found to be particularly advantageous. The principal difficulties are uncertainties about emission rates and prevailing concentrations.

If the model can be calibrated and validated, it could be an invaluable tool for exploring and documenting the behaviour of these contaminants, for elucidating dominant human exposure routes, for testing the effects of emission control measures and for determining, with the help of monitoring data, if a particular region is suffering from an unusually high concentration of a specific contaminant.

ENVIRONMENTAL MODELLING OF TOXIC SUBSTANCES IN SOUTHERN ONTARIO

Donald Mackay

Sally Paterson

Wan Ying Shiu

Christina Charles

Department of Chemical Engineering and Applied Chemistry

University of Toronto

ENVIRONMENTAL MODELLING OF TOXIC SUBSTANCES IN SOUTHERN ONTARIO

by

Donald Mackay, Sally Paterson, Wan Ying Shiu and Christina Charles

Department of Chemical Engineering and Applied Chemistry
University of Toronto

ABSTRACT

A steady state Level III and an unsteady state Level IV model, based on the fugacity concept, have been developed for Southern Ontario. Monitoring and emission data for a number of organic contaminants have been gathered for this region in an effort to validate the models. The data have been subjected to statistical treatment and fitted to a Weibull function to obtain mean concentrations and spread factors in water, fish and sediments. Data for air, soil and food will be treated similarly. Ultimately, the models should be capable of generating concentrations which lie under the envelope described by the distribution function.

The fugacity concept has also been successfully applied to a physiologically based unsteady state pharmacokinetic model of human tissue concentrations of styrene produced via inhalation. A steady state version of this model is currently being developed which also includes a food exposure pathway. This multi-exposure route pharmacokinetic model will ultimately facilitate correlation of environmental and human tissue concentrations of contaminants and aid in exploration of the effect of regulatory or remedial measures.

ABSTRACT

A steady state Level III and an unsteady state Level IV model, based on the fugacity concept, have been developed for Southern Ontario. Monitoring and emission data for a number of organic contaminants have been gathered for this region in an effort to validate the models. The data have been subjected to statistical treatment and fitted to a Weibull function to obtain mean concentrations and spread factors in water, fish and sediments. Data for air, soil and food will be treated similarly. Ultimately, the models should be capable of generating concentrations which lie under the envelope described by the distribution function.

The fugacity concept has also been successfully applied to a physiologically based unsteady state pharmacokinetic model of human tissue concentrations of styrene produced via inhalation. A steady state version of this model is currently being developed which also includes a food exposure pathway. This multi-exposure route pharmacokinetic model will ultimately facilitate correlation of environmental and human tissue concentrations of contaminants and aid in exploration of the effect of regulatory or remedial measures.

INTRODUCTION

During the last five years we have developed various models describing the behaviour of toxic substances in the environment. In particular, we have sought to devise models which will be useful for assessing toxic substance behaviour in Ontario. In this report we describe recent progress in this area and outline the nature of our current and future work.

It has become evident that no one modelling system will emerge as dominant;

rather there will be suites of models which can be called upon as required with different levels of accuracy and complexity and spheres of applicability, and with differing needs as regards input data. There is a growing tendency for these models to be user-friendly and to be suitable for use on personal computers, rather than main-frame computers. It appears that these models may become as widely used in environmental circles as mathematical software.

Figure 1 is an attempt to display a taxonomy of models, the four principal categories being evaluative models, real or site-specific models, human exposure models, and pharmacokinetic models.

EVALUATIVE MODELS

The evaluative models are of hypothetical environments containing reasonable volumes of selected phases with typical properties. The behaviour of the chemical can then be explained as it partitions, reacts and is transported under steady or unsteady state conditions. In the last year we have published our Level III fugacity model (Mackay et al., 1985) which has the aim of describing the broad behaviour profile of a chemical. The model output appears to be in good accord with observations and we believe that it can be used in its present form for preliminary evaluation of chemical behaviour. Figures 2 and 3 give illustrative outputs for such models. A Level IV unsteady state version has been devised in the last year which allows the time responses of concentrations to be explored. This is somewhat similar in concept to the model developed by Cohen and Ryan (1985).

An interesting recent development is that of evaluative soil models (Jury et al., 1983) for use with agro-chemicals.

We have also completed recently a model describing the exchange of toxic chemicals between air and water by simultaneously quantifiying the rates of wet

Figure 1. A taxonomy of environmental models with those being developed in this work designated*

Evaluative	Real	Exposure	Pharmacokinetic
Fugacity level I-IV*	Air-gaussian	Fugacity*	Fugacity*
EXAMS	Water dispersion	Rosenblatt	Ramsey-Andersen
Jury et al (soil)	Long range air	Nuclear	Tuey-Matthews
Cohen-Ryan	Multi-box lake	and others	and others
Kloppfer	Groundwater		
McCall	QWASI*		
and others	Bioconcentration		
	and others		

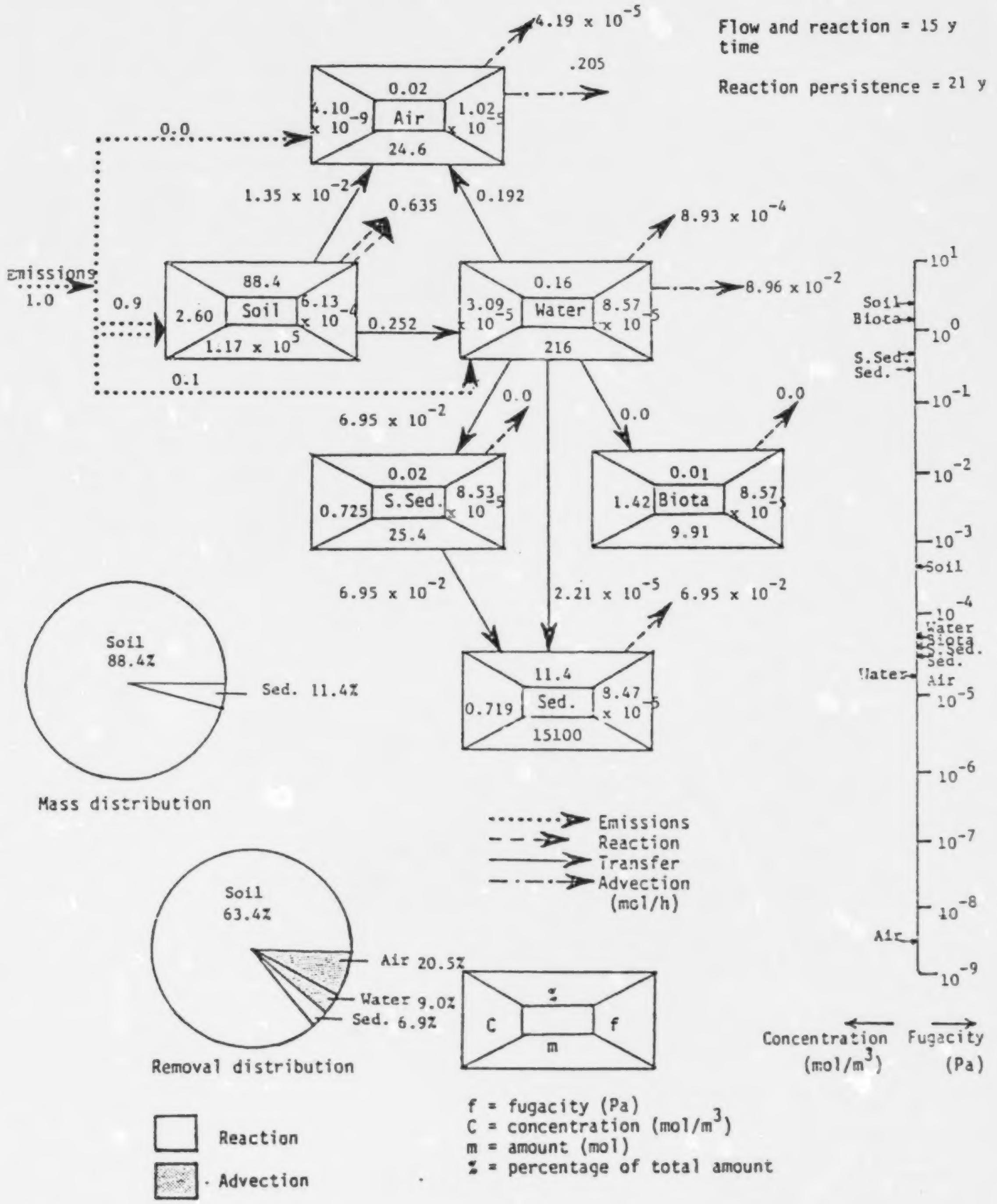
4.19 x 10^-5
.205
0.02
4.10 x 10^-9
Air
1.02 x 10^-5
24.6
0.0
1.35 x 10^-2
0.635
0.192
8.93 x 10^-4
Emissions 1.0
0.9
88.4
2.60
Soil
6.13 x 10^-4
1.17 x 10^5
0.252
0.16
3.09 x 10^-5
Water
8.57 x 10^-5
216
8.96 x 10^-2
0.1
6.95 x 10^-2
0.0
0.0
0.0
0.02
0.725
S.Sed.
8.53 x 10^-5
25.4
0.01
1.42
Biota
8.57 x 10^-5
9.91
6.95 x 10^-2
2.21 x 10^-5
6.95 x 10^-2
11.4
0.719
Sed.
8.47 x 10^-5
15100
Soil 88.4%
Sed. 11.4%
Mass distribution
Soil 63.4%
Air 20.5%
Water 9.0%
Sed. 6.9%
Removal distribution
Reaction
Advection
Emissions
Reaction
Transfer
Advection
(mol/h)
%
C
f
m
10^1
Soil
Biota
10^0
S.Sed.
Sed.
10^-1
10^-2
10^-3
Soil
10^-4
Water
Biota
S.Sed.
Sed.
Air
Water
10^-5
10^-6
10^-7
10^-8
Air
10^-9
Concentration (mol/m^3)
Fugacity (Pa)

Flow and reaction = 15 y time

Reaction persistence = 21 y

f = fugacity (Pa)
C = concentration (mol/m^3)
m = amount (mol)
% = percentage of total amount

Figure 2: Evaluative Model Behavior Profile for DDT

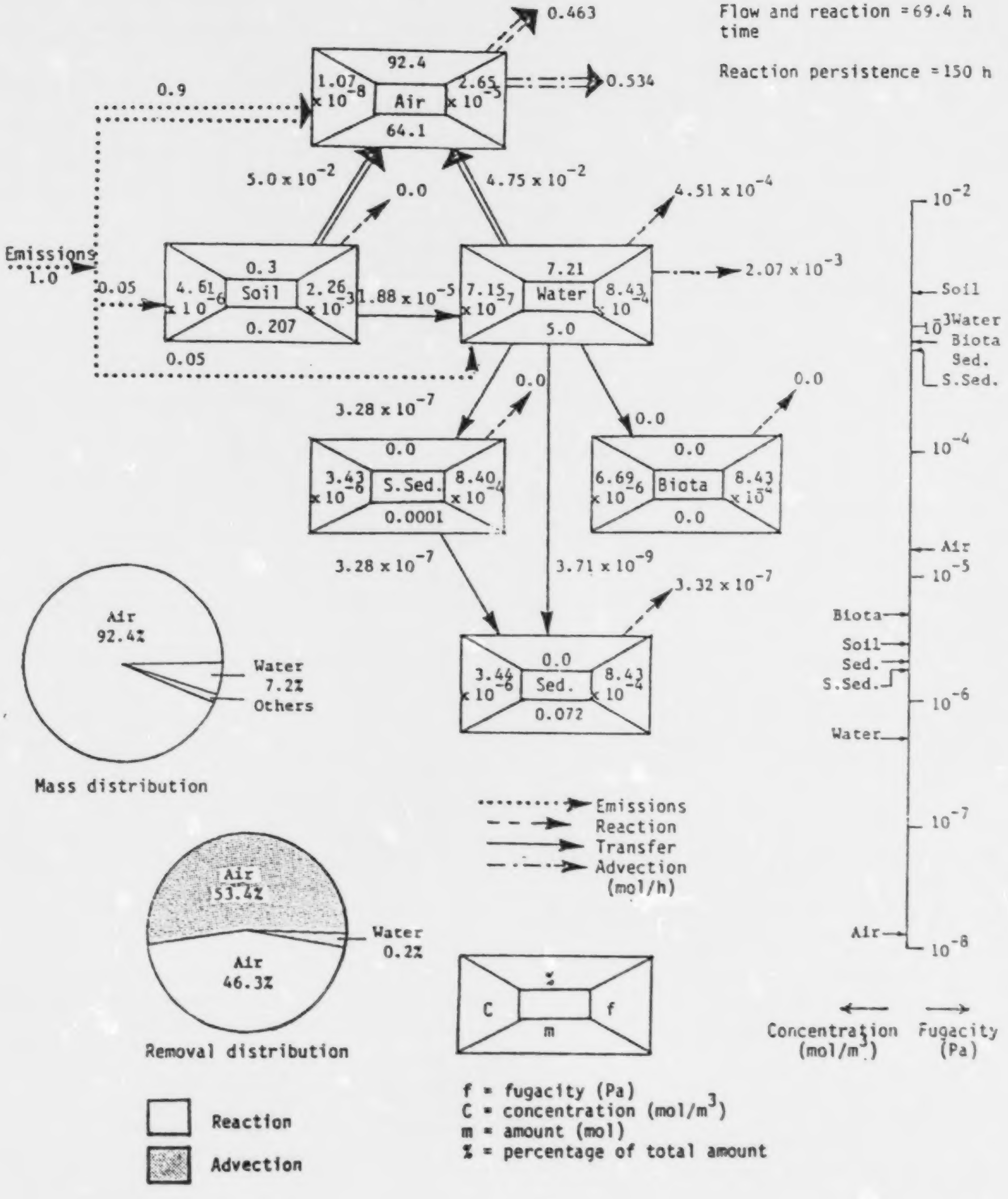
0.463
Flow and reaction time = 69.4 h
Reaction persistence = 150 h
92.4
1.07 x 10-8
Air
2.65 x 10-5
64.1
0.534
0.9
5.0 x 10-2
0.0
4.75 x 10-2
4.51 x 10-4
Emissions 1.0
0.05
0.3
4.61 x 10-6
Soil
2.26 x 10-3
0.207
1.88 x 10-5
7.21
7.15 x 10-7
Water
8.43 x 10-4
5.0
2.07 x 10-3
0.05
0.0
3.28 x 10-7
0.0
0.0
0.0
3.43 x 10-6
S.Sed.
8.40 x 10-4
0.0001
0.0
6.69 x 10-6
Biota
8.43 x 10-4
0.0
3.28 x 10-7
3.71 x 10-9
3.32 x 10-7
0.0
3.44 x 10-6
Sed.
8.43 x 10-4
0.072
10-2
Soil
10-3 Water
Biota
Sed.
S.Sed.
10-4
Air
10-5
Biota
Soil
Sed.
S.Sed.
10-6
Water
10-7
Air
10-8
Concentration (mol/m3)
Fugacity (Pa)
Air 92.4%
Water 7.2%
Others
Mass distribution
Air 53.4%
Water 0.2%
Air 46.3%
Removal distribution
Reaction
Advection
Emissions
Reaction
Transfer
Advection
(mol/h)
%
C
f
m
f = fugacity (Pa)
C = concentration (mol/m3)
m = amount (mol)
% = percentage of total amount

Figure 3: Evaluative Model
Behaviour Profile for Trichlorethylene

and dry deposition and volatilization/absorption or vapor exchange (Mackay et al., 1985).

The difficulty with evaluative models is that they can not be readily validated, although they can be applied to specific situations such as a stretch of river or a pond for which experimental data exist. Some success has been gained applying the U.S. EPA EXAMS model to specific situations.

REAL MODELS

The real models tend to fall into two subcategories. First are those describing the detailed concentration variations in space and time within one phase such as air or water. The well established air Gaussian dispersion models are an example. Numerous hydrodynamic models are also available describing behaviour in rivers, lakes, estuaries and oceans. Considerable success has been obtained applying these models to substances such as phosphorus. Recently there has been increasing interest in soil and groundwater models. The second class is the multimedia models in which an attempt is made to describe not only fate within a medium but also the transfer kinetics between phases. Examples are soil runoff models, sediment-water exchange models and various evaporation models applicable to lakes, rivers, soil (especially with applied agrochemicals) and landfill sites.

The difficulty with real models is that they are usually site-specific and of limited general use. A attractive approach is to link the evaluative and real models in order that the evaluative models become partially validated and the real models more general. Essentially, this implies using the same mathematical expression in both models wherever possible thus minimizing the differences and facilitating translation. The net effect is a mutual increase in credibility.

We have sought to do this by developing versions of the fugacity models for air-water-sediment systems termed the QWASI (Quantitative Water Air Soil Interaction) models which contain the same basic expressions as the evaluative models but are applied to the real situations. In the last year we have successfully applied the QWASI River model to the description of linear alkylbenzene sulfonate (LAS) fate in a river (Holysh et al., 1985). In this work we also undertook an evaluative assessment of LAS fate. Figures 4 and 5 show the results of model simulation of LAS behaviour in the river and in an evaluative environment. It is clear that the results are consistent.

In a parallel effort we have developed a Level III fugacity model applicable to the region of Southern Ontario. This model has been applied to PCBs but the results are unsatisfactory, because conditions for this compound in this area are far from steady state. Accordingly a Level IV fugacity model has been devised for Southern Ontario and applied to PCBs. The aim is to apply this model to PCBs over a period of some decades with decreasing emissions in the recent past. This has necessitated making some computational changes to make the numerical integration more robust and suitable for longer time steps. This greatly reduces computing time, but at the expense of some accuracy. We later discuss some activities involving the gathering and processing of environmental emission and concentration data for use in calibrating and validating the Southern Ontario model. This has proved to be a major task.

EXPOSURE MODELS

The third class of models concerns the quantification of multiple routes of human exposure. If concentration data are available for air, water, soil and various foodstuffs, it is possible to determine the relative importance of each route by assigning average properties such as inhalation rate or water drinking rate to a population. Often one route dominates; for example, for PCBs it is

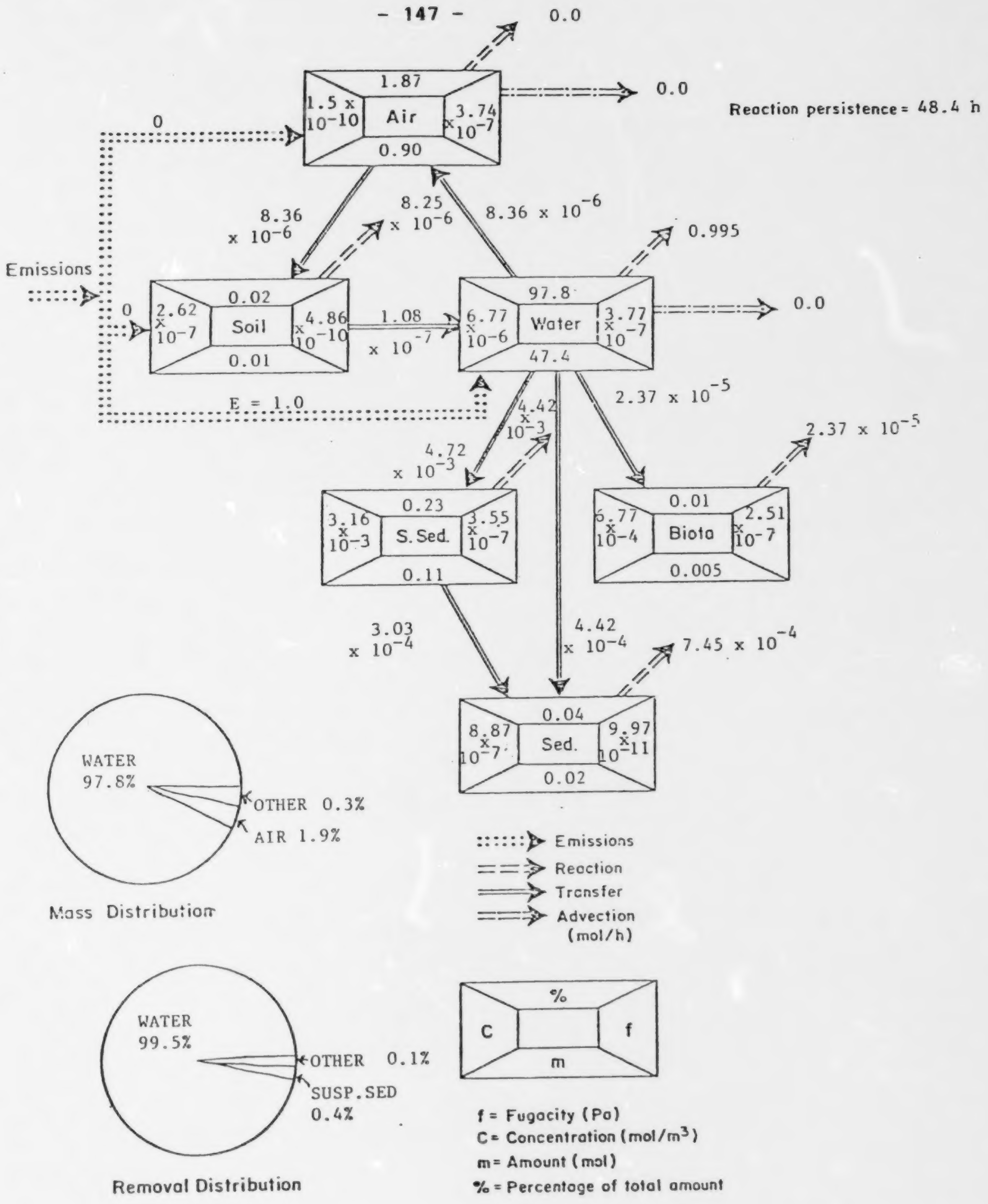
0.0
1.87
1.5 x 10-10
Air
3.74 x 10-7
0.90
0.0
Reaction persistence = 48.4 h
0
8.36 x 10-6
8.25 x 10-6
8.36 x 10-6
0.995
Emissions
0
2.62 x 10-7
0.02
Soil
4.86 x 10-10
0.01
1.08 x 10-7
97.8
6.77 x 10-6
Water
3.77 x 10-7
47.4
0.0
E = 1.0
4.42 x 10-3
2.37 x 10-5
4.72 x 10-3
2.37 x 10-5
0.23
3.16 x 10-3
S. Sed.
3.55 x 10-7
0.11
0.01
6.77 x 10-4
Biota
2.51 x 10-7
0.005
3.03 x 10-4
4.42 x 10-4
7.45 x 10-4
0.04
8.87 x 10-7
Sed.
9.97 x 10-11
0.02
WATER 97.8%
OTHER 0.3%
AIR 1.9%
Mass Distribution
Emissions
Reaction
Transfer
Advection (mol/h)
WATER 99.5%
OTHER 0.1%
SUSP.SED 0.4%
Removal Distribution
%
C
f
m
f = Fugacity (Pa)
C = Concentration (mol/m³)
m = Amount (mol)
% = Percentage of total amount

Figure 4: Evaluative Model
Behaviour Profile for LAS

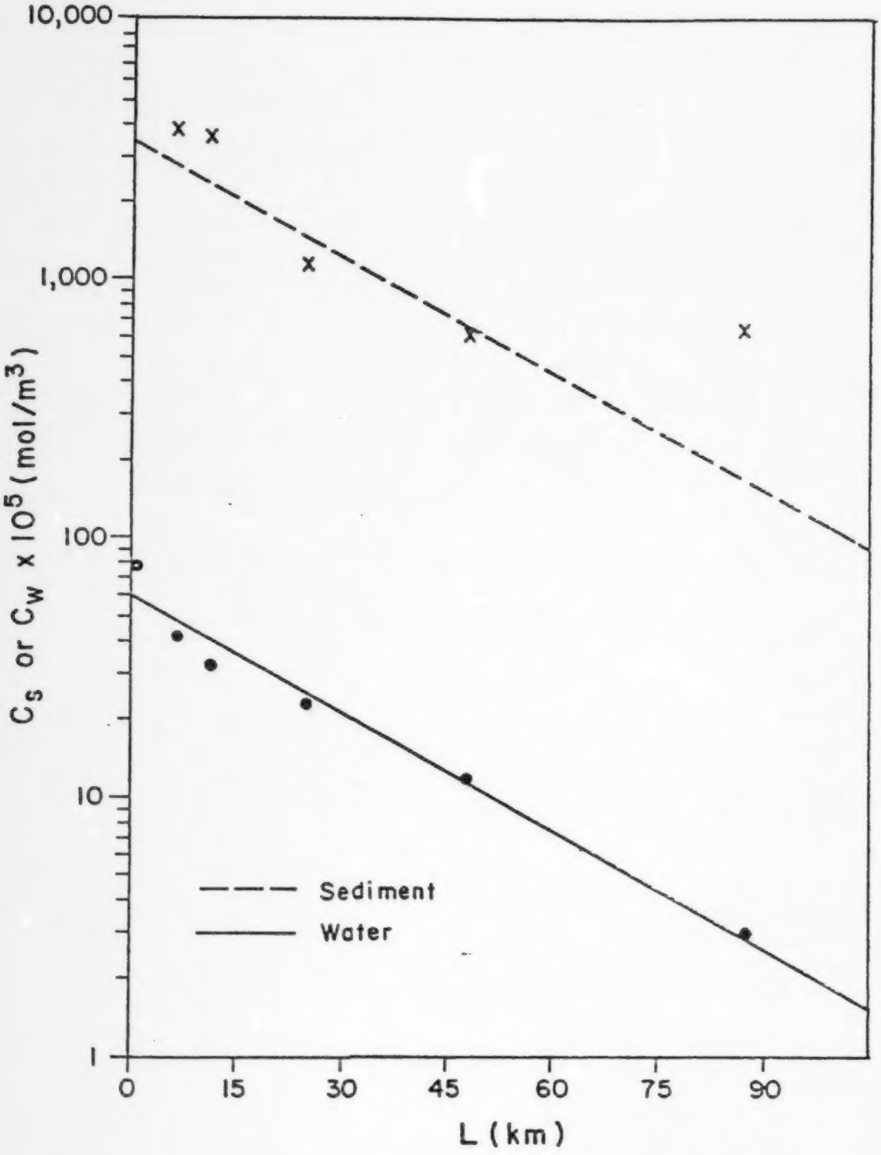

Figure 5

Plot of Sediment and Water Concentrations for LAS in Rapid Creek fish ingestion. In some cases dermal contact may be included, as may ingestion of soil. A logical extension of this type of modelling is to include exposure in the workplace and indoor environments. It is clear that certain populations are exposed to unusually large concentrations of industrial solvents and other chemicals, to domestic and agricultural pesticides and to radon. We do not suggest that high exposure under such conditions be used as an excuse to relax environmental standards, but it is helpful to place these exposures in perspective especially for epidemiological studies.

An obvious step is to extend the real or environmental models to include human exposure. We are attempting this with the Level III fugacity model and we plan to attempt it with the Southern Ontario model. An attractive feature of this extension or linkage is that data are available for concentrations of many chemicals in foodstuffs. These data often reflect the state of contamination of the environment in which the food was grown, which may of course be distant from the region of consumption.

The most highly developed models of this type are those for radionuclides (eg. Zach, 1982). This literature provides an invaluable background for toxic substances.

PHARMACOKINETIC MODELS

There is a growing body of opinion that the use of exposure concentration or even dosage of a chemical gives an inadequate description of the toxic effects. In many cases there is a highly non-linear relationship between external concentration or dosage and incidence of disease or other adverse effect. Presumably the ultimate objective is to reduce the toxic effects of chemicals present in the environment to "acceptable" levels. A logical step is then to extend the exposure analysis to treat chemical fate within the body and calculate concentrations of the chemical in critical tissues. It is likely that toxic effects are much better correlated with tissue concentration than with air or food concentration.

A considerable literature exists on pharmacokinetic modelling, especially for drugs and in connection with occupational exposure to substances such as industrial solvents. Most of these models describe the time course of decay of concentration after an administered dose rather than chronic or steady state exposure. One of the most significant recent developments is the Ramsey-Anderson (1984) pharmacokinetic model which has been applied to military and industrial personnel exposure to fuel and solvent vapours. This model is attractively simple and shows promise of being invaluable for environmental assessment purposes. In its existing form it is not conveniently compatible with environmental models but with some modification it could be compatible.

We have recently rewritten the Ramsey-Anderson model in fugacity format introducing what we believe are some algebraic simplifications and insights obtainable by the use of fugacity in addition to concentration (Paterson and Mackay, 1985). We are currently developing a steady state version of this model which can be linked to the human exposure assessment and ultimately to the evaluative or Southern Ontario models. It is then possible to compute the entire "toxic journey" from source to target tissue. This is an exciting development because it then becomes possible to explore the effects of various regulatory or remedial measures on target tissue concentration and the entire picture of environmental toxicology becomes clearer.

We note (ruefully) that the toxic chemical is apparently unaware that it is trespassing between jurisdictions of departments of industry, labour, environment, agriculture and food, and ultimately health. It also trespasses across Provincial and National boundaries. The implication is that comprehensive source-to-target-tissue models may create a bureacratic nightmare.

Figure 6 is a diagram describing the current pharmacokinetic model. It can be scaled to apply to humans, rats and mice. We also believe that it can be readily adapted to apply to fish.

ENVIRONMENTAL DATA

Environmental Emissions

There are few data for emissions of toxic chemicals in the Southern Ontario region. The most comprehensive study has been by Acres (1980) in which by applying emission factors to various industrial activities it is possible to estimate emissions. Table 1 lists 10 chemicals that we are attempting to model for Southern Ontario and the type of data available.

Environmental Concentrations

A number of environmental concentration data bases exist which purport to contain large quantities of data. In fact much of the data is not useful, it is inaccurate or it is simply not accessible. The inherent difficulty is that such data bases rarely receive the support they deserve because they are infrequently used. Ideally, the data should be gathered and immediately scrutinized to determine if they are consistent with some model or hypothesis. These models and hypotheses rarely exist, thus the data lie ignored except for revealing "hot spots". A related difficulty is that few background measurements are made of non-polluted environments thus using the available data directly reflects a bias in favour of more contaminated regions.

We have gathered data for a number of chemicals listed in Table 1 and have subjected them to statistical treatment. Briefly, the concentration data are fitted to a Weibull distribution function and mean concentrations and spread factors deduced. Data for fish, water, air, soil sediments, foodstuffs and

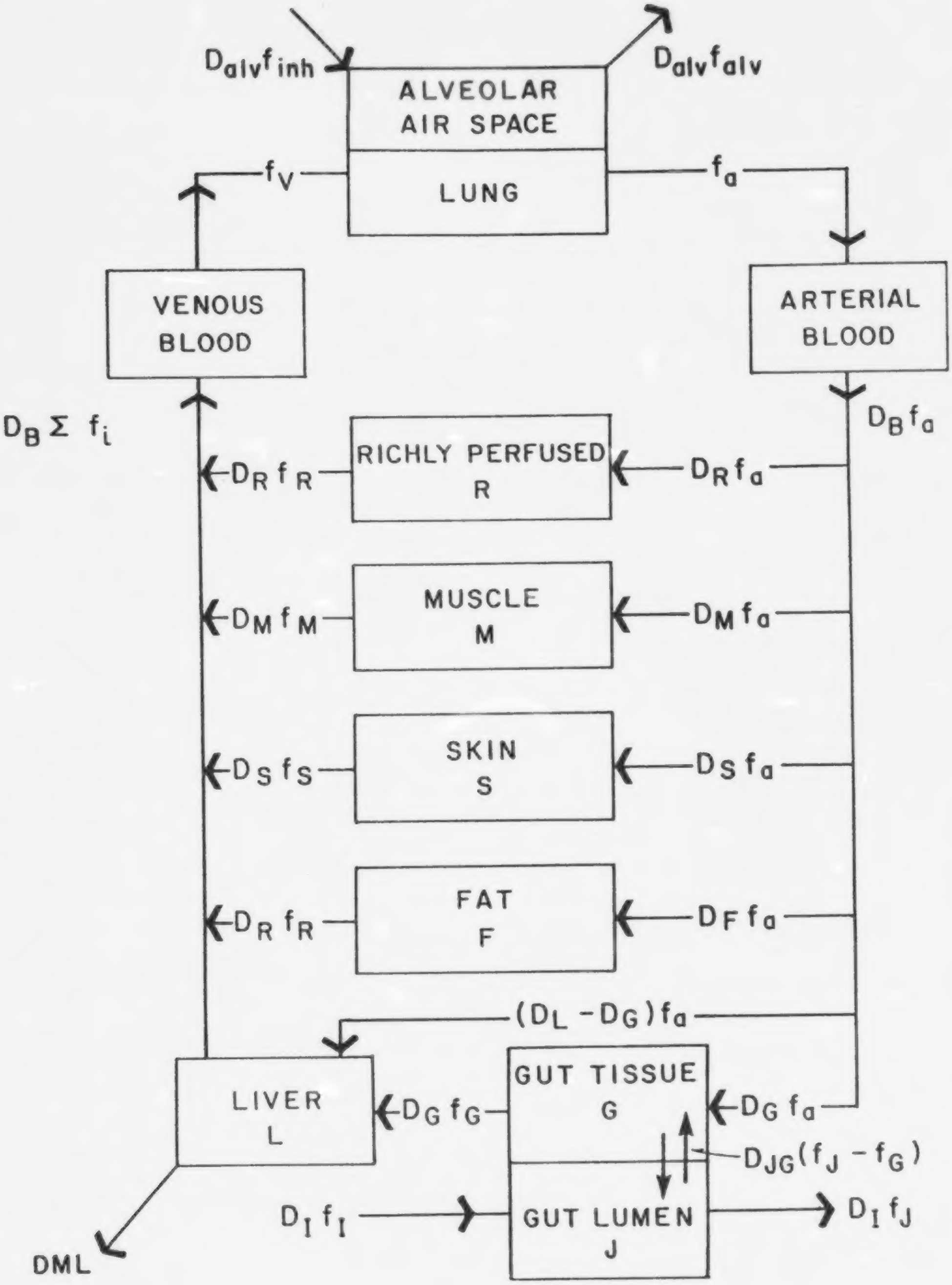
$D_{alv}f_{inh}$
$D_{alv}f_{alv}$
ALVEOLAR AIR SPACE
LUNG
f_V
f_a
VENOUS BLOOD
ARTERIAL BLOOD
$D_B \Sigma f_i$
$D_B f_a$
RICHLY PERFUSED R
$D_R f_R$
$D_R f_a$
MUSCLE M
$D_M f_M$
$D_M f_a$
SKIN S
$D_S f_S$
$D_S f_a$
FAT F
$D_R f_R$
$D_F f_a$
$(D_L - D_G) f_a$
LIVER L
GUT TISSUE G
$D_G f_G$
$D_G f_a$
$D_{JG}(f_J - f_G)$
GUT LUMEN J
$D_I f_I$
$D_I f_J$
DML

Figure 6: Steady State Fugacity-Based Pharmacokinetic Model with Simultaneous Multiple Exposure Routes

TABLE 1. List of Chemicals and available data

	Emissions	Physical Chemical properties	Ambient Concentrations						
			air	water	soil	sediment	biota	food	humans
PCB's	Y	X	X	X	X	X	X	X	X
Hexachlorobenzene	Y	X	--	X	--	X	X	--	--
Trichloroethylene	--	X	Y	X	--	X	--	--	--
Benzo (a) pyrene	Y	X	X	Y	X	X	Y	X	--
Styrene	X	X	--	--	--	--	--	Y	Y
Toluene	X	X	X	--	--	--	--	--	--
Ethylbenzene	--	X	X	--	--	--	--	--	--
Atrazine	X	X	--	X	--	--	--	--	--
Mirex	X	X	--	X	--	X	X	--	--
Benzene	Y	X	X	--	--	--	--	--	--

X = satisfactory data

Y = some or questionable data

-- = no data

human tissue are being, or will be, treated in this manner illustrated in Figure 7.

Ultimately the models should be capable of generating concentrations which lie under the envelope described by the distribution function.

PHYSICAL CHEMICAL PROPERTIES

It is self-evident that successful models must have reliable physical chemical property data for the chemicals of interest. We have continued our work in this area determining and correlating these properties, especially data for water solubility and octanol water partition coefficient. We have recently published a novel correlation between these properties (Miller et al., 1985).

CONCLUSIONS

Our work for the Ministry is proceeding down several parallel paths as follows:

1. Acquisition and processing of relevant physical chemical property data.
2. Acquisition and processing of environmental data on emissions and concentration distributions.
3. Construction and improvement of evaluative models describing chemical behaviour.
4. Construction and validation of models of real environmental situations in which chemical fate data are available for defined conditions. These models use the same calculation procedures as the evaluative models.

In addition, using support from other agencies we are extending these models to include exposure routes and pharmacokinetic models, thus tracking the toxicant from source to target.

In this paper our aim has been to describe the current status of this program of work, provide examples of the findings, and give references to the

Figure 7

Relationsnip of predicted environmental concentration distributions to toxic effect concentrations

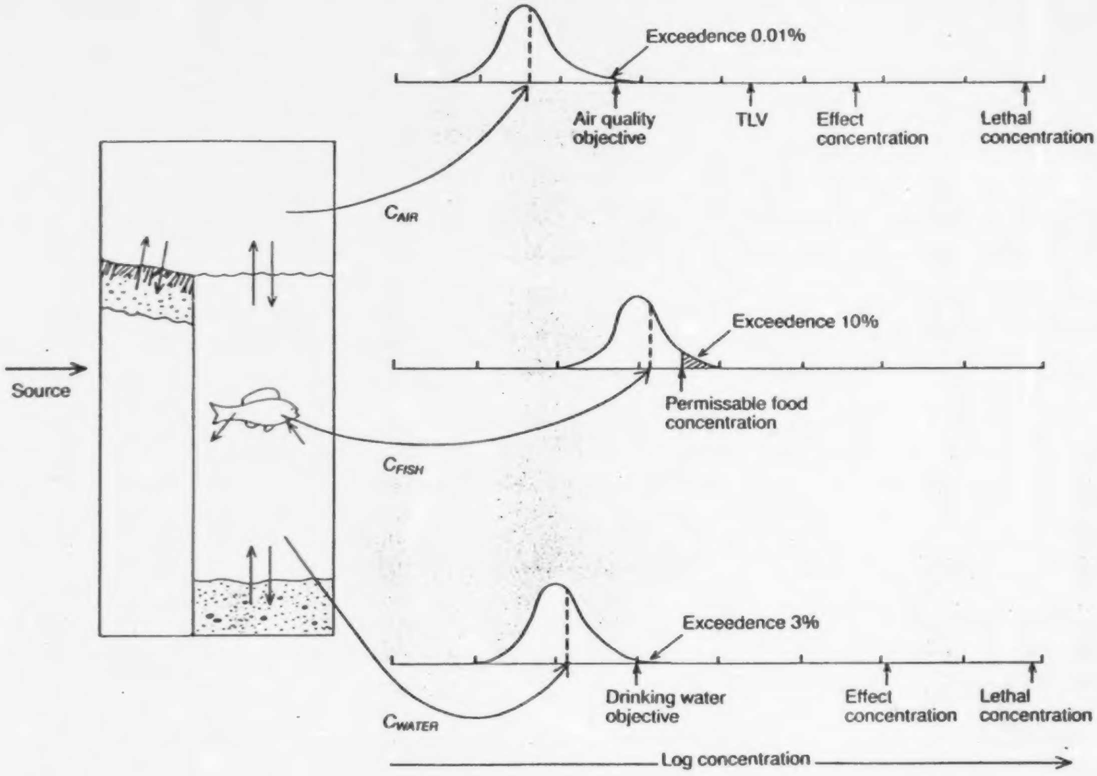
Exceedence 0.01%
Air quality objective
TLV
Effect concentration
Lethal concentration
C_{AIR}
Exceedence 10%
Permissable food concentration
Source
C_{FISH}
Exceedence 3%
Drinking water objective
Effect concentration
Lethal concentration
C_{WATER}
Log concentration

REFERENCES

Acres Consulting Services Ltd., "Methodology for an Environmental Risk Analysis Southern Ontario", Report prepared for Ontario Ministry of the Environment. (1980).

Cohen, Y. and Ryan, P.A., "Multimedia Modelling of Environmental Transport: Trichloroethylene Test Case", Environ. Sci. Technol. 19, 412-417. (1985).

Holysh, M., Paterson, S., Mackay, D., Bandwiraga, M.M., "Assessment of the Environmental Fate of Linear Alkylbenzene sulphonates", Chemosphere (in press, 1985).

Jury, W.A., Spencer, W.F. and Farmer, W.J., "Behaviour assessment model for trace organics in soil: I Model Description", J. Environ. Qual., 12 558-564, also 13, 573-579, 13, 580-586. (1983)

Mackay, D., Paterson, S., Cheung, B., Neely, W.B., "Evaluating The Environmental Behaviour of Chemicals with a Level III Fugacity Model, Chemosphere, 14, p 335-374 (1985).

Mackay, D., Paterson, S. and Schroeder, W.H., "A Model Describing the Rate of Transfer Processes of Organic Chemicals Between Atmosphere and Water", submitted to Environ. Sci. Technol., 1985.

Miller, M.M., Wasik, S.P., Huang, G.L., Shiu, W.Y., and Mackay, D., "Relationships Between Octanol-Water Partition Coefficient and Aqueous Solubility", Environ. Sci. Technol., 19, 522-529. (1985).

Paterson, S. and Mackay, D., "A Pharmacokinetic Model of Styrene Inhalation Using the Fugacity Approach", Toxicol. Appl. Pharmacol. (in press, 1985).

Ramsey, J.C. and Andersen, M.E., "A Physiologically Based Description of the Inhalation Pharmacokinetics of Styrene in Rats and Humans", Toxicol. Appl. Pharmacol. 73, 159-175. (1984).

Zach, R., "LIMCAL: A Comprehensive Food Chain Model for Predicting Radiation Exposure to Man in Long-Term Nuclear Waste Management", Atomic Energy of Canada Ltd. Report AECL-6827. (1982).

DIAGNOSTIC TESTING OF THE SWARU INSTALLATION IN HAMILTON

J. Trought[1], V. Ozvacic[2], and S. Thorndyke[3]
[1]IMET, [2]Ministry of the Environment, [3]Ontario Research Foundation

Key words: SWARU, Hamilton, Diagnostic Testing, Waste Incineration, Organics, Dioxins, PCBs, Stack Emissions.

ABSTRACT

The first measurements of the stack emissions of dioxins and furans at the SWARU installation were done in three tests in 1982, as part of a study progam on the formation of these species at municipal incinerators in Ontario. The test emissions were in excess of the limits set by the Provisional Guideline for stacks, and consequently, the plant was ordered to cut back on the refuse incineration rate. A comprehensive program, known as diagnostic testing, was carried out in 1983 to establish the limits for safe operation of the incinerator. The program was designed conceptually by the personnel of the Ministry's Air Resources and Laboratory Services Branches and contracts were let to Envirocon and the Ontario Research Foundation to work out the details and execute the field work.

The Ontario Research Foundation was responsible for the collection and preparation of stack and process stream samples for analyses on dioxins, furans, chlorobenzenes, PCBs and chlorophenols. The Laboratory Services Branch performed the analyses and the Air Resources Branch was responsible for co-ordinating the field work. Envirocon was responsible for process monitoring.

As a result of the study, new operating limits for incineration were established, maintenance procedures were modified, and installation of additional process gas monitors and of additional control equipment for the removal of particulates from the stack emissions were recommended.

DIAGNOSTIC TESTING METHODOLOGY
FOR THE
SWARU INSTALLATION IN HAMILTON

November 1985

Independent Measurement
and Technology Inc.
58, 1271 Denison Street
Markham, Ontario
L3R 4B5

Mr. J. Trought
Mr. D. Law

Ontario Ministry of the Environment
Air Resources Branch
880 Bay Street
Toronto, Ontario
M5S 1Z8

Mr. V. Ozvacic

ABSTRACT

A diagnostic testing program was performed on the **Solid Waste Reduction Unit (SWARU)** in Hamilton, Ontario. The objective of the program was to determine conditions under which SWARU could be operated while satisfying the Ontario Ministry of the Environment (MOE) Provisional Guidelines for polychlorinated dibenzo-p-dioxins (dioxins) and polychlorinated dibenzofurans (furans). This paper deals with the methodology employed in the diagnostic testing program.

A previous test program conducted in 1982 indicated emissions levels of dioxins and furans in excess of the Provincial Guidelines as set by the MOE and consequently, a restraint order was applied on refuse incineration rate. The of MOE formed a Liaison Committee and four technical committees to address the issue of trace organic emissions at the SWARU plant. The concept of diagnostic testing was developed by these committees and contracts were let to Envirocon (Eastern) Ltd. and Ontario Research Foundation to execute the field work.

The diagnostic test program involved a phased approach of a pre-testing program, a process characterization program and full diagnostic tests.

The overall study showed that operating conditions can be maintained within limits to reduce emissions of trace organics to levels below the MOE Provisional Guidelines. As a result of this and other studies, new operating limits for incineration were established, maintenance procedures were modified, installation of additional process gas monitors and additional control equipment for the removal of particulates from the stack emissions were recommended.

INTRODUCTION

A 1982 municipal incinerator testing program indicated that emission of polychlorinated debenzo-p-dioxins (dioxins) and polychlorinated dibenzofurans (furans) from the SWARU plant were in excess of the MOE Provisional Guidelines. This resulted in a restraint order restricting incineration rate being applied to SWARU and the formation at the MOE of a Liaison Committee and four technical committees to address the emission problem.

The overall objective of the committees was to determine how SWARU could be operated while satisfying the guidelines.

The concept of diagnostic testing was developed based on acquiring an understanding of the incineration process, reducing emissions and minimizing costs. The specific requirements to fullfill the objective were:

(1) To review equipment and operating procedures.

(2) To investigate how operating procedures affect combustion.

(3) To determine performance under a limited set of operating conditions and identify desirable operating conditions.

(4) To select and monitor operating conditions concurrent with obtaining a series of samples for dioxin and furan analysis.

The diagnostic test program was developed as a phased approach including pre-tests, characterization tests and full diagnostic tests.

The phased approach was employed to assess and troubleshoot the system before costly diagnostic testing and analysis were performed.

Pre-test Program

The objectives of the pre-testing was to become familiar with the system, identify and correct any system equipment problems and develop a characterization test matrix.

The pre-test program consisted of site visits by the Sampling Co-ordinator and the Boiler Co-ordinator to complete the following:

(1) Review drawings and performance specifications of the unit and auxiliaries.

(2) Observation of the operation of the fuel preparation system, boiler and auxiliaries.

(3) Internal inspection of the test unit, including grates, seals, control dampers, heat absorption surfaces, ducts and flues.

(4) Specification of additional sampling facilities.

(5) Performance of cold flow tests.

(6) Development of characterization test matrix.

As part of the pre-testing, the cold flow tests determined the gas flow patterns in the furnace and the interaction of undergrate and overfire air flows. This was accomplished by entering the furnace under cold conditions and varying the overfire and undergrate airflows. Flow velocities were measured using vane and hot wire anemometers. Flow patterns were observed using smoke bombs and light paper ribbons. Flow measurements, observed patterns and photographs were combined to produce isometric models of gas flow patterns.

Characterization Program

The objectives of the characterization/combustion tests were to measure boiler parameters under different operating conditions, assess the performance of the unit and develop a realistic test matrix of operating conditions for the diagnostic tests.

To fully monitor process conditions, additional equipment was used by the testing team. Figure 1 illustrates the furnace, boiler and dust collector portion of the SWARU plant. Combustion air temperatures and flows were measured. Flue gas temperatures, flows and composition were measured. Control room data was recorded. Fuel and ash samples were collected but not analyzed. The specific methods used will be described in the diagnostic test section.

The main parameters that were varied were boiler load, undergrate air flow and overfire air flow. Figure 2 illustrates the Diagnostic Test Matrix developed as a result of the characterization program.

FIGURE 1
Facility Isometric Drawing

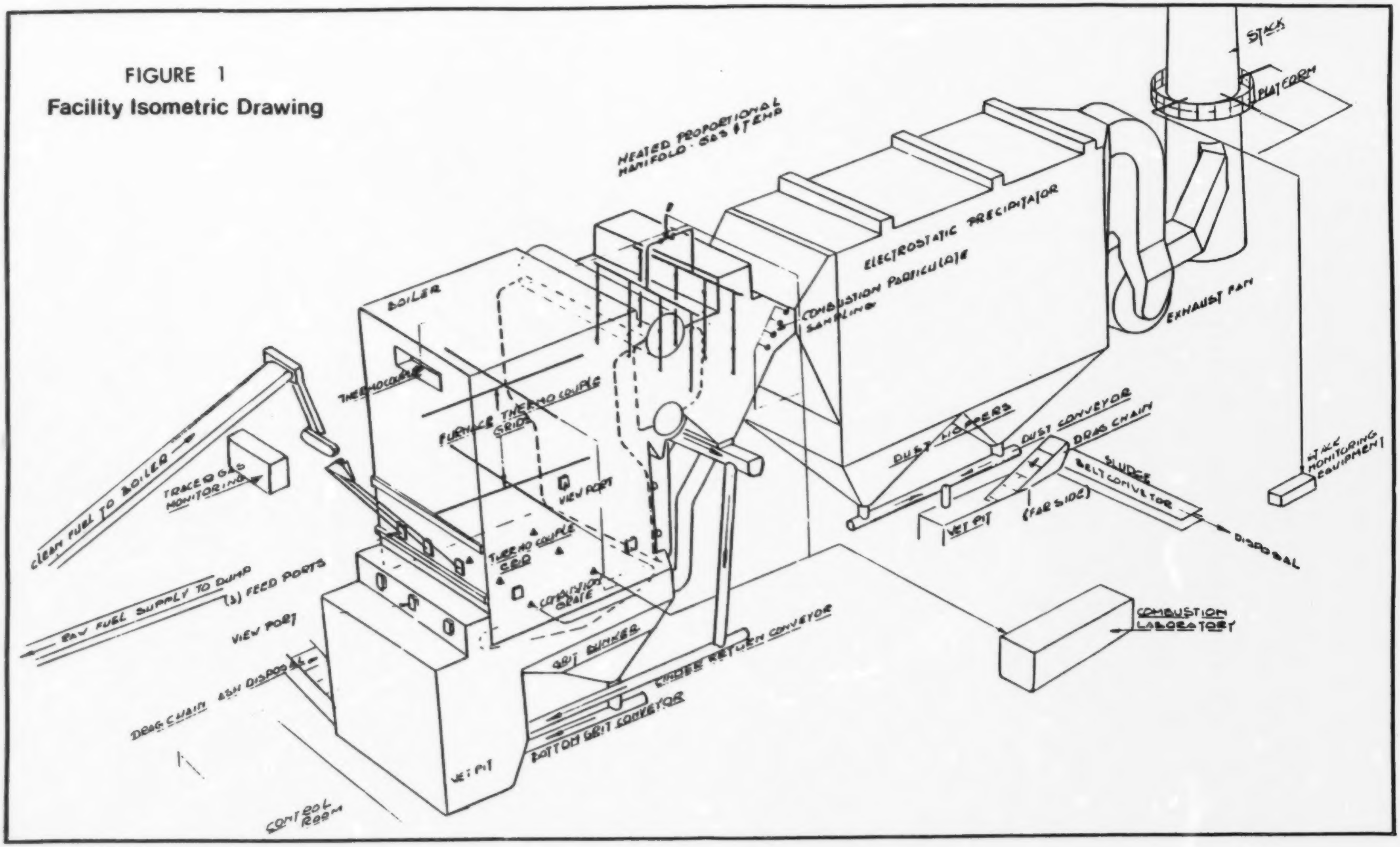
STACK
PLATFORM
HEATED PROPORTIONAL MANIFOLD · GAS & TEMP
ELECTROSTATIC PRECIPITATOR
COMBUSTION PARTICULATE SAMPLING
EXHAUST FAN
BOILER
THERMOCOUPLE
FURNACE THERMOCOUPLE GRIDS
VIEW PORT
THERMOCOUPLE GRID
COMBUSTION GRATE
DUST HOPPERS
DUST CONVEYOR
DRAG CHAIN
SLUDGE BELT CONVEYOR
(FAR SIDE)
WET PIT
DISPOSAL
STACK MONITORING EQUIPMENT
CLEAN FUEL TO BOILER
TRACER GAS MONITORING
RAW FUEL SUPPLY TO DUMP
(3) FEED PORTS
VIEW PORT
DRAG CHAIN ASH DISPOSAL
GRIT BUNKER
CINDER RETURN CONVEYOR
BOTTOM GRIT CONVEYOR
WET PIT
CONTROL ROOM
COMBUSTION LABORATORY

FIGURE 2

Diagnostic Test Matrix

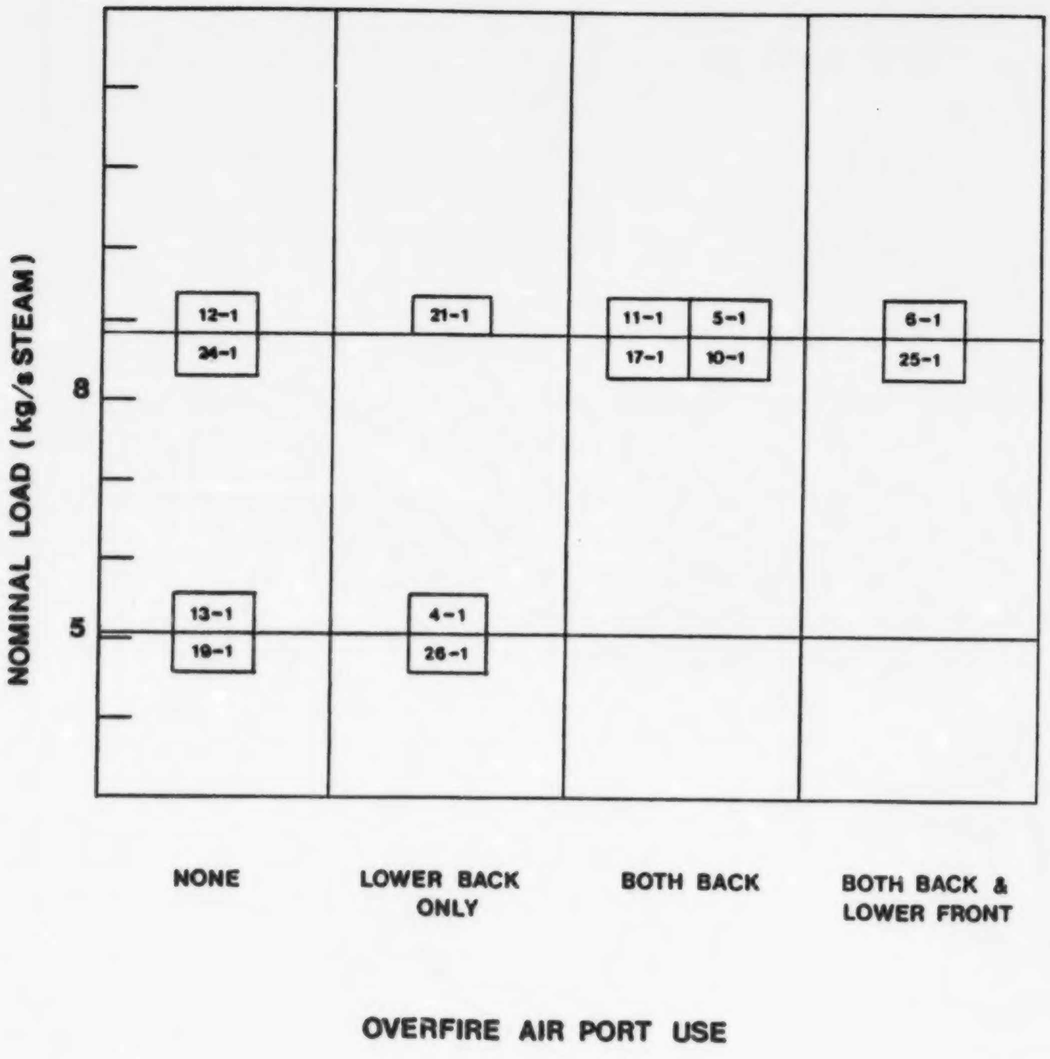

Diagnostic Tests

The objectives of the diagnostic tests were to monitor process conditions and sample for dioxin, furan and precursors. The trace organic sampling was performed by Ontario Research Foundation at the stack. One sampling train was used for dioxin and furan analysis, while a second train was used for precursor analysis. The two trains were necessary to collect sufficient sample for all analysis during a four hour test period. The following discusses in detail the actual measurements and sampling performed during the diagnostic tests.

Control Room Data

Pertinent control room data was recorded at 10 minute intervals during testing periods. This provided a log of such variables as steam flow, steam pressure, undergrate air flow and overfire air flow.

Combustion Air

Combustion air temperatures and flows were monitored. The combustion air temperature was measured by a guide of six thermocouples peened to the undergrate support structure. The air flows were measured by a helium tracer gas system. The pressures in the overfire air plenums and inlet chutes were monitored by water tube manometers installed adjacent to the control room.

Flue Gas

Flue gas was monitored for temperature, gaseous composition and entrained particulate composition and concentration. The flue gas temperature was monitored at two levels in the furnace zone, before the air heater and after the air heater.

Air cooled furnace temperature probes with Type K thermocouples at one foot intervals criss-crossed the furnace at two levels. The furnace top temperature was monitored as this was a controlling input in the control system. A thermocouple grid attached to the gas sampling manifold before and after the air heater also provided temperature measurement.

Flue gas composition was monitored continuously by instruments mounted in the Mobile Combustion and Emission Laboratory (MOCEL) from samples extracted from the gas sampling manifold. Constituents measured were carbon monoxide, carbon dioxide, total hydrocarbons and oxygen. Figure 3 illustrates a typical strip chart of CO and THC concentrations in the flue gas. Flue gas moisture was determined by condensation. Flue gas particulate was sampled using an Isojet sampling system at the inlet to the precipitator. This system allows for isokinetic collection of a large sample of particulate while steam quenching any burning particles to prevent sample spoilage.

Fuel

The fuel moisture, composition and particle size was monitored. Fuel was sampled at a conveyor transfer point at the rate of three shovels every fifteen minutes. The sampler swept the shovel through the complete width of the falling stream of waste to maintain consistent sampling procedures. The samples were air dryed and sieved to determine the moisture content and the particle size. Figure 4 illustrates fuel air dry moisture contents for discrete 15 minute samples. The fuel moisture content was also measured by an Infra-red moisture analyzer mounted above the fuel steam on the inlet conveyor. Ultimate, calorific, dioxin, furan and precursor analysis was done on fuel samples.

FIGURE 3 - CO AND THC CONCENTRATION FOR RUN 19-1

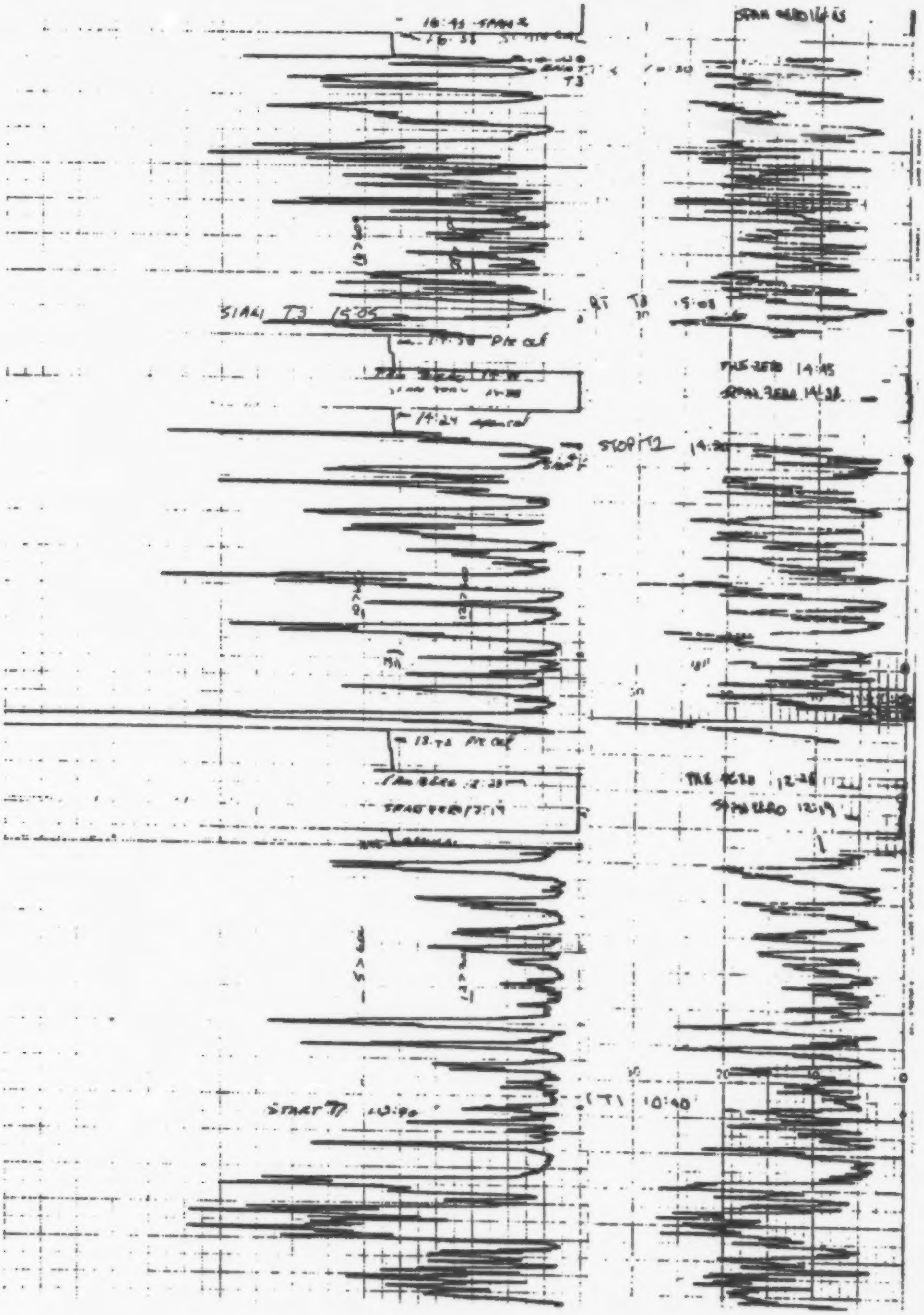

FIGURE 4 - AIR DRY MOISTURE RESULTS FOR TESTS 10-1 and 19-1

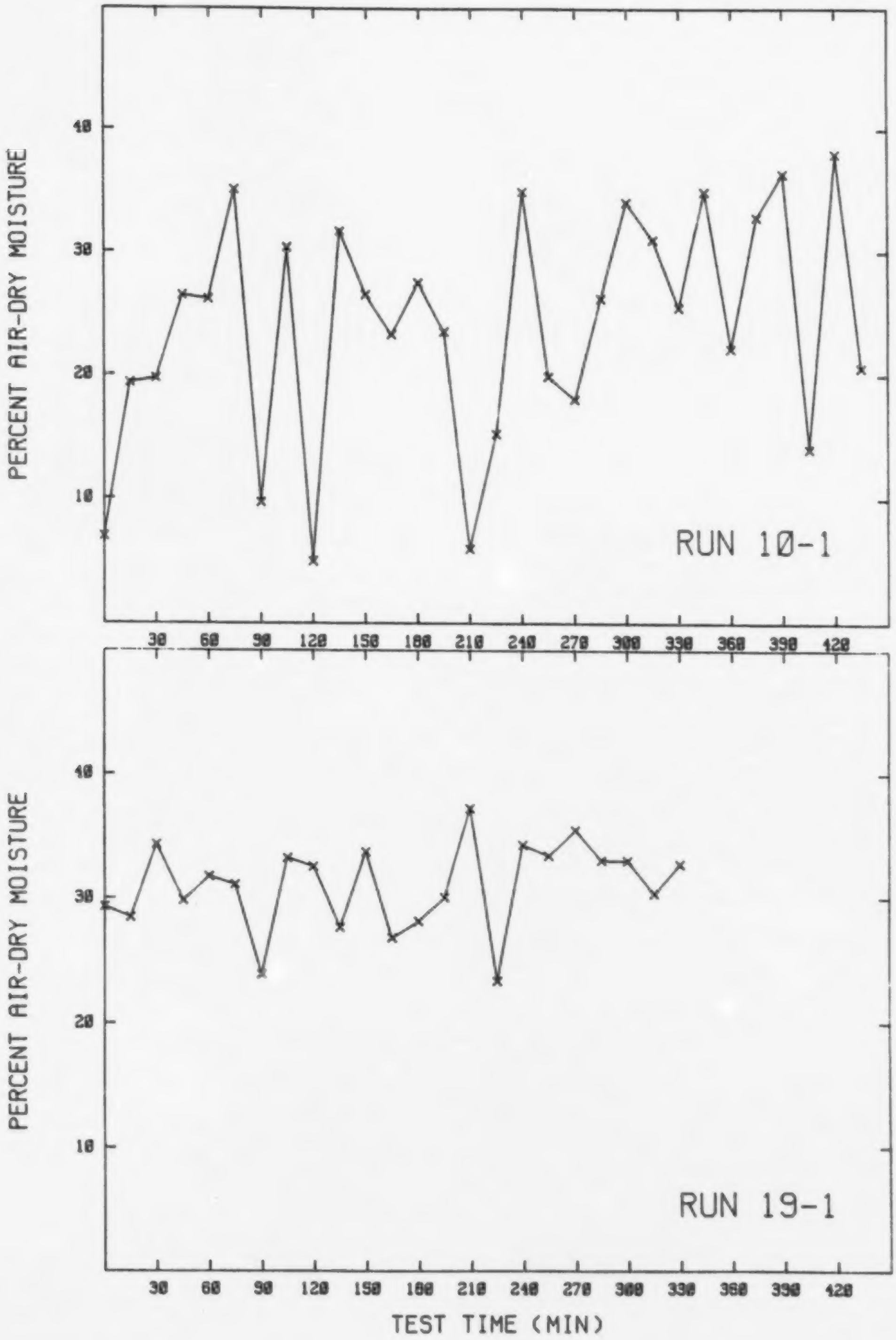

Ash

Ash samples were collected at the grate and the precipitator for moisture and combustibles, dioxin, furan and precursor analysis. Ash flow rates were determined using collection bins at the discharge of the grate and precipitator ash conveyors.

Data Handling

Owing to the quantities of data collected, vigourous data handling procedures were developed. All flue gas thermocouples and flue gas continuous monitors were scanned at three minute intervals by a datalogger and the data stored on floppy discs and on hard copy. This data was statistically reduced by computer for the test periods. All other periodic data was also manually reduced for test intervals.

RESULTS

The diagnostic testing program showed that with careful operation of the system, trace organic emissions can be reduced and brought below MOE Provisional Guidelines.

As a result of this and other studies new operating limits for incineration were established, maintenance procedures were modified and additional process gas monitoring and control equipment for removal of particulates were recommended.

REFERENCES

(1) Ministry Report No. ARB-02-84-ETRD

Title:

Determination of Chlorinated Dibenzo-p-dioxins, Chlorinated Dibenzofurans, Chlorinated Biphenyls, Chlorobenzenes and Chlorophenols in Air Emissions and Other Process Streams at SWARU in Hamilton.

Authors:

V. Ozvacic (ARB), G. Wong (ARB), H. Tosine (LSB), R. Clement (LBS), J. Osborne (LSB) and S. Thorndyke (ORF)

Names of Organizations:

Air Resources Branch, Laboratory Services Branch, Ontario Research Foundation

(2) Ministry Report No. ARB-43-84 ETRD

Title:

Report on Combustion Testing Program at the SWARU Plant, Hamilton-Wentworth

Authors:

P.G. Complin (Project Manager)

Names of Organizations:

Envirocon Limited, W.J. Howell Engineering Ltd.

CHEMICAL AND PHYSICAL CHARACTERIZATION OF AIRBORNE PARTICULATES AND THEIR SOURCES THROUGH MULTIELEMENT ANALYSIS AND RECEPTOR MODELLING

T. Glenn Pringle and R.E. Jervis
Department of Chemical Engineering and Applied Chemistry, and
Institute for Environmental Studies, University of Toronto

Key words: Particulates, Air Pollution, Multielement Analysis,
Receptor Modelling.

ABSTRACT

Source identification and apportionment of ambient airborne particulates is important if air pollution is to be more stringently controlled in urban, industrialized regions. These are locations where traditional air pollution dispersion models are at a disadvantage because of the investment of time, funds and manpower required to diligently characterize all the major contributing emission sources. On the other hand, receptor models utilize measurements at just one or a few limited receptor sites, and the contributing sources are then statistically evolved by analysis of a set of data factors: detailed chemical composition of ambient particulates, meteorological data, particle-size distributions and site locations.

In this research, radioanalytical methods are being applied for the simultaneous analysis of about 30-35 chemical elements in airborne particulate matter sampled in the greater Metropolitan Toronto area during the period from January 1984 to the present. In the first one and a half years of the funded project, all the results obtained together with the relevant meteorological data were subjected to statistical factor analysis with the objective of deducing, from the multielemental chemical composition data itself, the major contributing sources of air pollution in the Toronto atmosphere. Factor analysis indicated that six sources were distinguishable: wind-blown soil grains, automobile exhaust, refuse incineration, winter road salt, oil combustion and an unidentified source of arsenic. Elemental concentration profiles for the several elements that characterized each of these six sources were input into a comprehensive chemical element mass balance calculation to determine quantitatively the relative contribution of each source to the ambient Toronto aerosol.

The results showed that re-entrained soil contributed 67% to the inorganic portion of atmospheric air particulate matter, automobile exhaust contributed 15%, road salt 12%, and the other sources lesser amounts. A limited additional study of particle-size distributions, especially for Al, Fe, Sc, As, Br, Cl, Zn, Mn and V, provided some additional details on aerosol characterization.

MULTI-ELEMENT CORRELATIONS FOR AIRBORNE PARTICULATE SOURCE ATTRIBUTION

T. Glenn Pringle and Robert E. Jervis

Department of Chemical Engineering and Applied Chemistry
University of Toronto, Toronto, Canada. M5S 1A4

Abstract

Photon and thermal neutron activation analysis were used to analyze airborne particulate matter obtained during the period January to March of 1984 for up to thirty elements. Elemental concentrations and meteorological data from the Toronto, Ontario area were subjected to factor analysis and the major sources of particulate deduced. Elemental profiles for six sources, viz. crustal soil, automobile exhaust, road salt, refuse incineration, oil combustion and an unidentified arsenic source, were used in a chemical element balance to quantitatively determine the contribution of each source to the ambient aerosol. Re-entrained soil contributed 67%, automobile exhaust contributed 15% and the other sources contributed lesser amounts to the inorganic particulate matter. Particle-size distributions for nine elements, viz. Al, Fe, Sc, As, Br, Cl, Zn, Mn, V, are presented as an argument for the development of receptor models involving particle-size distribution data. The characterization of the cascade impactors used in this study, and the importance of this characterization are also discussed.

Introduction

In the past decade there have been many studies of air particulates, a number of which have involved the use of receptor models to identify the sources of airborne particulate matter and to apportion ambient particulate matter amongst the contributing sources [1 2 3]. This source identification and apportionment is important if air pollution is to be controlled in urban centres, a location where traditional pollution dispersion models are at a disadvantage because of the time, money and manpower required to properly characterize all major contributing sources. Receptor models utilize measurements at one or more receptor sites and the contributing sources are then statistically evolved from a set of any or all of: chemical composition of particulate matter, meteorological data, particle-size distribution and site location.

In the analysis of airborne particulates it is essential that the elemental analytical method be able to utilize the small amounts of sample which can be collected in a reasonable sampling period. Because of the statistical nature of receptor models it is also important to minimize the amount of variance in the data due to analysis and consequently a multi-elemental, instrumental method is desirable. Given these requirements, activation analysis is an ideal technique to analyze particulates for receptor model studies since it is non-destructive, instrumental, sensitive and multi-elemental. The use of thermal neutron and photon activation analyses as complimentary methods allows determination of most elements in addition to providing two different techniques for some elements as a method of quality control.

In order to allow routine application of receptor models, it is necessary that such models be shown to be applicable to sites of widely varying geography, number and type of pollutant sources and source composition. The research reported in this paper represents the application of contemporary receptor model methodology to air particulate data from the Toronto area in Ontario. Emphasis was placed on confirmation of the utility of the methodology in the study area and identification of source types as a prelude to model evolution. This research is part of a more extensive study involving the inclusion of particle-size distributions in receptor models.

Methods

Analytical Aspects

Air particulate samples were taken during the period January to March, 1984 using a high volume air sampler located in Port Credit, Ontario (see Fig. 1). The sampler was operated for 24 hour periods at a flow rate of 0.76 m^3/min (30 scfm) for a total collected air volume of approximately 1100 m^3. Whatman #41 cellulose filters were used because of their low trace element content [4]. Glass fibre, the standard high volume filter media, was particularly unsuitable because of high sodium and ash levels. Each exposed filter was divided into fourths and the edges trimmed to remove contamination from handling and from the filter cartridge. Two portions were analyzed by instrumental photon activation analysis (IPAA) and the two remaining portions by instrumental neutron activation analysis (INAA).

The IPAA work was performed at the National Research Council linear accelerator facility (LINAC) in Ottawa, Canada. Six samples and two multielement standards were placed in aluminum vials located in a rotating circular carousel and irradiated for 3-4 hours. All analyses were conducted at an electron energy of 30 MeV and a typical beam current of 35-50 μA, measured at the converter (3 mm tungsten). Using one, intermediate electron energy for all irradiations reduced nuclear and spectral interferences from unwanted reactions while still allowing determination of concentrations for Pb, Ni, As, Ca, Ti, Sb, Br, U, Zr, Mg, and Na, some of which are not susceptible to INAA (Pb, Ni, Zr) and others of which could be used for quality control comparisons. Further details on these irradiation parameters, the accuracy and precision and the interferences relevant to IPAA have been discussed elsewhere [5]. After irradiation the samples were transferred from the aluminum foil to clean polyethylene vials for counting, typically for 2 hours after 24 hours decay.

The two remaining portions of filter were then subjected to thermal neutron activation analysis (INAA) at the University of Toronto SLOWPOKE-2 reactor. Sequential irradiations for short-lived and long-lived radionuclides resulted in data for the concentrations of Al, Ag, As, Br, Ca, Ce, Cl, Co, Cr, Cs, Cu, Eu, Fe, Hf, I, In, K, La, Mn, Na, Sb, Sc, Se, Sm, Th, Ti, U, V, W and Zn. Irradiation parameters varied widely with irradiation times ranging from 2 min. to 16 hours, a neutron flux ranging form 2.5 x 10^{11} to 10^{12} n/cm^2s, decay times from 1 min. to 21 days and counting times from 5 mins to 12 hours.

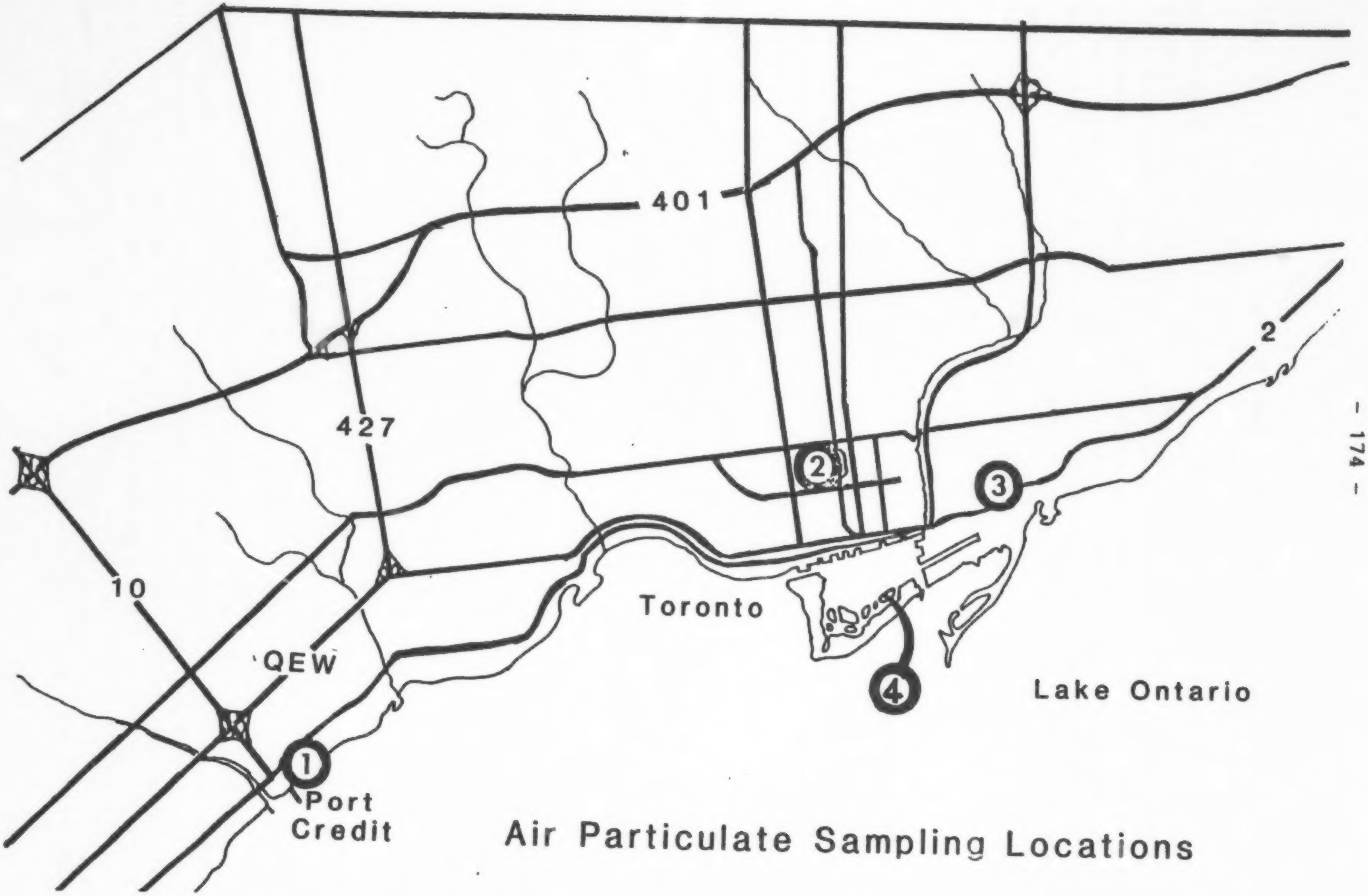
401
2
427
10
QEW
Toronto
Lake Ontario
①
Port
Credit
②
③
④

Air Particulate Sampling Locations

A U.S. National Bureau of Standards reference material, SRM 1632a, was used as a multi-elemental standard in both INAA and IPAA. The air particulate reference material, SRM 1648, and a flyash reference material, SRM 1633a, were also used to verify analytical accuracy.

To measure particle-size distributions, Sierra and Anderson-style high-volume cascade impactor heads were attached to the basic high-volume sampler. The particle-size cut-off diameters at 50% collection efficiency are listed in Table 1. These figures were verified by scanning electron microscope photographs of exposed impactor substrates. Anderson impactor experiments were performed at the downtown Toronto location (see Figure 1) at a flowrate of 0.5 m^3/min. Sierra impactor experiments were conducted at both the downtown locatin and the Toronto Island location at a flowrate of 0.85 m^3/min. Several samples were collected with each impactor for 4-24 hours at a time. Separate quarters of each Anderson stage substrate were analyzed by IPAA and INAA. Between one-half and a whole of each Sierra stage substrate was analyzed by INAA.

Statistical Aspects

The receptor models used in this study are based on the assumption that the concentration of any element (**i**) at a receptor is a linear sum of the contributions of that element from j sources (Eqn. 1). It is assumed that mass is conserved so that the chemical profile of the contribution from a

$$a_i = \sum_j b_{ij} c_j \qquad \text{Eqn. 1}$$

source remains unchanged from source to receptor. Depending on the information desired, Equation 1 can be interpreted in two different ways which represent the two most common receptor models, factor analysis (FA) and the chemical element balance (CEB).

Factor analysis requires no **a priori** assumptions about the number and type of sources contributing to the aerosol sample taken at the receptor. Thus it can be used to determine such information for later application to the CEB which does require these assumptions. For factor analysis, Equation 1 would be altered to a matrix format (Eqn 2) wherein A is an **i x n** matrix containing the measured concentrations of **i** elements (variables) on **n** air filters (observations). Matrix B is an **i x m** matrix containing the

$$A = B\ C \qquad \text{Eqn. 2}$$

factor loadings which represent correlation coefficients relating elements to pollution sources. The contributions of each source to each observation constitute C, an **m x n** matrix. The analysis procedure first normalizes all concentrations to their respective means so that the magnitude of concentration does not influence the results. The factor pattern is then calculated such that all the original variables essentially become functions of a smaller number of hypothetical factors. Finally, the matrix of factors is rotated to maximize the alignment between each factor and the variable with which it is most strongly correlated. Examination of the factor loadings can indicate the number and type of prominent sources of airborne particulate matter which contributed to the samples [7].

Once the sources have been identified the CEB model is used to calculate the actual contribution of each suspected source to the receptor. The b_{ij} in Equation 1 represent the elemental source profiles which were indicated by the factor analysis. A least squares regression of a and b produces the contribution of each source to each sample (c). This is done separately for each filter and the results are then averaged over all the filters to find the mean contribution of each source to the ambient particulate matter. A more thorough review of receptor model principles has been written by Watson [8].

Results and Discussion

The mean concentrations of fifteen elements in the Port Credit aerosol are presented in Table 2. Although the concentrations of up to thirty-five elements were determined, these concentration means were considered to be the most useful for comparison. Also presented are the results both from recent studies conducted in Washington [3] and Chicago [9] and from a previous study conducted in Toronto [10]. Immediately apparent are the lower concentrations of most elements in the Port Credit data. This can be attributed to a combination of winter sampling, a more surburban sampling site than in the other studies and the trend to lower levels of airborne particulate evident in recent years. The high concentrations of Na, Cl and Ca are all evidence of the use of de-icing salt in winter months.

Factor analysis of the aerosol data, augmented by wind direction information, resulted in the factor pattern given in Table 3. The variables included in the statistical analysis were each used because they were considered to be representative of the major sources found. This is consistent with the finding of Gordon et al.[11] that the inclusion of extra elements does not significantly improve a stable receptor model. Testing of all elements and several other possible variables, viz. precipitation, depth of snow cover, weekday and sample number, confirmed this conclusion: no further significant correlations were found. Of the seven factors in Table 3, five represent recognizable sources of airborne particulate matter, one represents a negative correlation of opposing wind directions and the identity of the seventh has not yet been ascertained.

Factor number one is strongly correlated with the elements Sc, Ca, Mn and Ti, which are normally associated with lithophyllic elements indicative of entrained soil. Such soil could be a combination of one or all of: windblown soil from nearby agricultural activity, construction activity or street dust. Other elements correlated with this factor but not listed in Table 3 are aluminum and the rare earths. The only direction dependency of factor one is a negative correlation with south-east winds (SA), the direction of Lake Ontario.

Factor two is assumed to represent road-salt because of the strong correlation between this factor and Na and Cl. Since there is an expressway and a major arterial road to the north-west of the sampling site the moderate correlation with north-westerly winds (NW) is not surprising.

Factor three, because of its association with lead and bromine, is considered to represent automobile exhaust. The existence of correlations with zinc, a result of car tire wear (Cradle et al.)[12], and Mn, a constituent of a gasoline octane-booster (MMT) used in unleaded gasoline (Daniel)[13] bear out this conclusion. The presence of a uranium correlation is thought to be a result of the Zn/U association in factor four since U is not commonly associated with particulate matter emissions from vehicular activity. It is, however, often associated with particulate matter emitted from coal-fired generating stations as are selenium and iodine which are correlated with factor four. Selenium and zinc are also associated with refuse incineration so this factor is assumed to be primarily the result of refuse incineration with the possible addition of some emissions from coal combustion. The lack of a lithophyllic association in this factor indicates a weak or distant fossil-fuel contribution.

A strong negative correlation between two wind directions is the basis for factor five. The low correlation coefficient for northeast winds (NE) is a result of the connection between NE and vanadium in factor six. Vanadium is associated with the combustion of vanadium-rich fuel oil refined primarily on the east coast of N. America from imported crude oil. It stands to reason that this factor should line up with the direction of the largest nearby urban centre, Toronto, which is located northeast of Port Credit. The moderate negative correlation with northwest winds indicates a potential easterly or south-easterly contribution to this factor, possibly long-distance aerosol from the eastern seaboard of the United States where a lot of vanadium-rich crude oil (Rahn and Lowenthal)[14] is used.

The final factor is associated only with arsenic. This unique factor indicates either a strong source only of particulate As or an analytical error of some sort. The low communality of As in the model and a lack of a readily identifiable source of As are strong arguments for the existence of an analytical error. However, careful checking has failed to pinpoint such an error. Rahn and Lowenthal[14] suggested a profile with relatively high arsenic and indium concentrations as an elemental signature for non-ferrous smelters located in the Sudbury basin of Ontario. The predominantly sub-micron arsenic (see Figure 2) measured in Toronto indicates a high-temperature, anthropogenic source such as these smelters. However, no wind direction correction (N wind) is evident to confirm any such conclusion. It is equally possible that this As factor can be attributed to a lead-battery manufacturer, located to the north of the sampling site, which uses arsenic as a hardening agent for lead.

Given the probable identity of the major contributors of particulate matter to the Port Credit aerosol, as indicated by the above factor analysis, a chemical element balance can be applied to the aerosol data to quantitatively apportion the aerosol among sources. The six source profiles used in the CEB are presented in Table 4. The profiles for refuse incineration, oil combustion and automobile exhaust were taken from the study of Scheff et al.[9] in Chicago. The selenium concentration in the refuse profile was increased to reflect sewage sludge incineration [16] since initial usage of the profile of Scheff et al. indicated gross under-estimation of selenium. The automobile profile was altered by increasing the Mn concentration to reflect the use in Canada of Mn-containing MMT in unleaded gasoline. The soil profile was derived from data obtained during a study of urban dust in Toronto and Port Credit which was conducted by this laboratory (Daniel, 1985)[13]. The salt profile was derived from the molecular formula of salt with a Ca component included to represent the use of calcium chloride in conjunction with sodium chloride as a road de-icing agent. The arsenic factor was an arbitrary choice to obtain a rough estimate of the contribution of the unknown source to the model. The lack of correlation between most elements and this factor in the factor analysis indicated that the actual composition of this factor would do little to destabilize the CEB model. The measured elemental concentrations were weighted by $1/\sigma^2$ where σ is the analytical precision.

The percentage contribution of each source to the inorganic aerosol is listed in Table 5. Soil, contributing 67% of the inorganic particulate matter, is by far the dominant source despite the winter time-frame of sampling and the accompanying snow cover. This is an important finding since dust levels are very difficult to control, whereas refuse incineration (3%), oil combustion (1.4%) and automobile exhaust (15%) are more easily controlled through legislation. The use of road salt, which contributed 12% of the aerosol, can also be controlled somewhat. Not surprisingly, the arsenic source contributes very little.

The accuracy of the balance can be assumed to be quite good since only two out of 108 source coefficients were negative and also because the ratio of predicted-to-observed elemental concentrations is quite low. In Table 6 are listed the larger/smaller ratios (L/S) for several CEB studies. The L/S ratio is used because large and small values of the predicted-to-observed ratio tend to cancel each other when averaged [3]; the L/S ratio is therefore a more representative measure of the accuracy of the CEB prediction. The present study, while not as accurate as the more extensive work of Kowalczyk et al.[3], is still a reasonably accurate fit compared to other work in the literature. This is important since this study is going to be used as a starting point for receptor model evolution.

One of the most persistent problems with conventional receptor models is the inability of such models to differentiate between sources which have similar elemental profiles. Coal combustion and soil is one pair of such sources [9], automobile exhaust and secondary lead smelters, another [10]. In some cases of this type the sources can be better identified by the characteristic particle-size distributions of their particulate emissions as is the case for the two examples mentioned above. Both coal flyash and automobile exahust are derived from combustion sources and consequently consist of predominantly fine particles whereas entrained soil and secondary lead smelter emissions both have a prominent large particle component. In Figure 2 and Figure 3 are size-distributions of nine elements sampled from the downtown Toronto aerosol by Anderson and Sierra cascade impactors respectively. The Al, Sc, and Fe distributions are typical of entrained soil; they consist of predominantly large particles. Bromine, arsenic and chlorine are representative of anthropogenic combustion sources with the expected predominance of small particles. The last three elements, Zn, V and Mn, are typical of elements produced from both physical (large particle) and combustion/condensation (fine particle) processes. Zinc, which exists in large particles from car tire wear and in small particles from refuse incineration, is a perfect candidate for a size-differentiating receptor model.

Several studies [11] [17] [18] have adopted this approach but have restricted the analysis to separate models for each of two size fractions (< 2 µm and 2-10 µm particle diameter). This approach assumes that the unique portion of the elemental nature of a particular source exists in one size fraction only and thus uses only a part of the particle-size information. Instead it is proposed in this study that all size information be included in the receptor model through the introduction of a new set of variables, i_1, i_2, i_3, i_4 to replace each original variable I. Each new variable would represent one size fraction of the element I in the ambient aerosol. These variables can then be treated in the CEB and factor analysis procedures in a fashion similar to the original element variables.

Some analysis of impactor samples has been performed to determine the parameters for routine sampling and analysis. One of the difficulties in the past with the use of cascade impactors, and noticed in these initial analyses, is the inability of such equipment to properly fractionate the aerosol. A factor analysis performed for this study using previously collected Anderson impactor data [10], and using the statistical approach outlined in the previous paragraph, failed to differentiate significantly between a large particle lead source and a fine particle lead source. The correlations between size fractions of the same element were often greater than those between similar size groups of different elements presumed to emanate from the same source. From these results it was concluded that bounce-off of large particles, and their subsequent transport to the fine-fraction backup filter, was confounding the analysis. Even a few large particles of lead on the backup filter will change variations formerly attributed to the automotive lead component.

In Figure 2 an increase in the concentrations of predominantly crustal elements (Al, Fe, Sc) can be seen in the backup filter. In contrast, the vaseline-coated filters used with the Sierra impactor, shown in Figure 3, have no evidence of such bounce-off. All future sampling will be performed using the Sierra impactor and vaseline-saturated substrates.

The collection of a set of cascade impactor filter samples is now underway to test the model presented above. Sampling is being performed on Algonquin Island and in the East Harbour area (sites 3,4 on Figure 1) and results are expected in the summer of 1986.

The use of nuclear analytical techniques will prove to be even more necessary for this next stage of the project since each size fraction will have only a small percentage of the total aerosol mass and to maintain useful sampling periods, it will be necessary to have a very sensitive analytical technique. The non-destructive and multi-elemental nature of INAA and IPAA will also prove useful by allowing multiple determinations to be performed on the limited amounts of sample available.

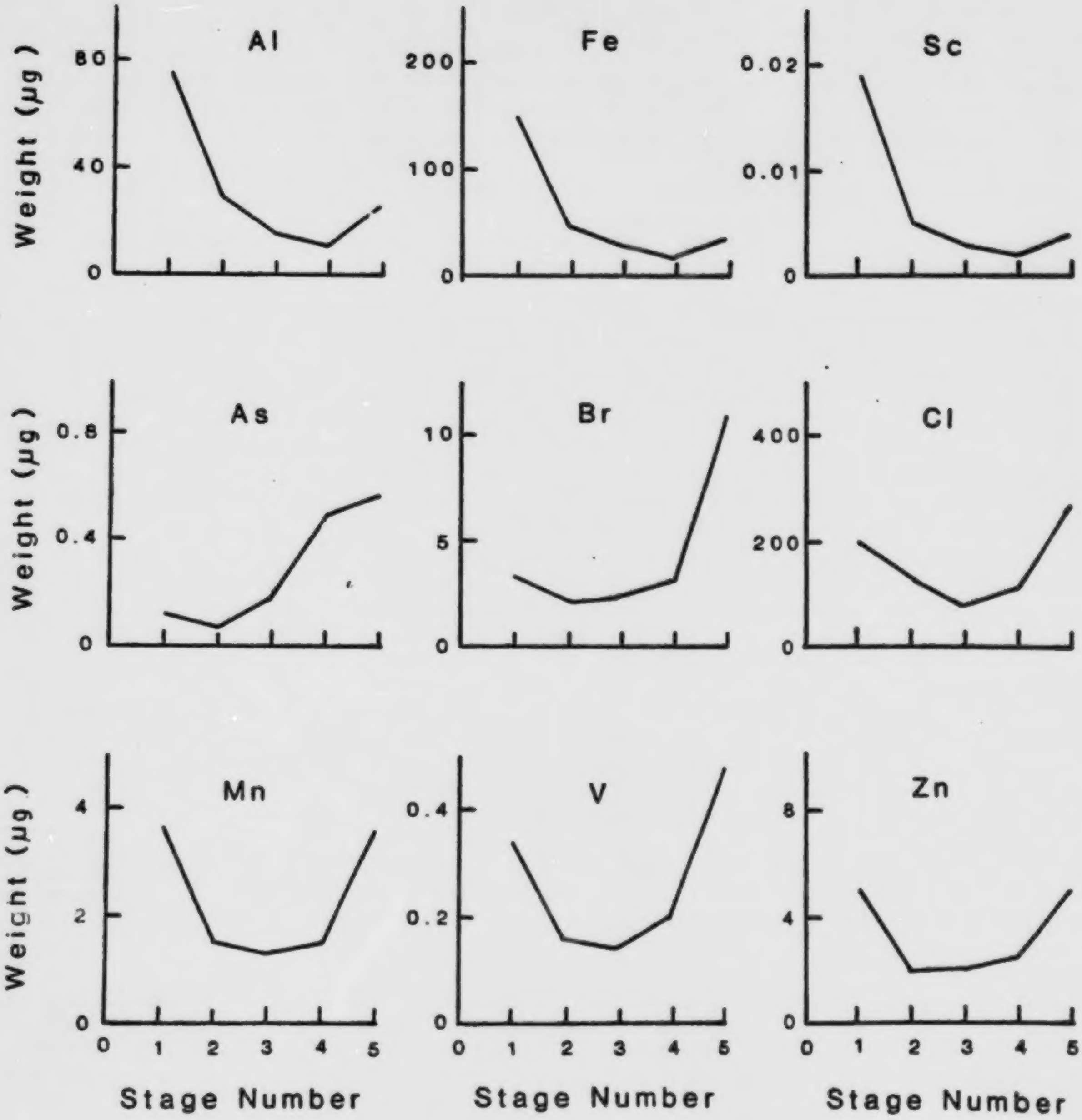
Al
Fe
Sc
As
Br
Cl
Mn
V
Zn
Weight (μg)
Weight (μg)
Weight (μg)
0
40
80
0
100
200
0.02
0.01
0
0.8
0.4
0
10
5
0
400
200
0
4
2
0
0.4
0.2
0
8
4
0
0
1
2
3
4
5
Stage Number
Stage Number
Stage Number

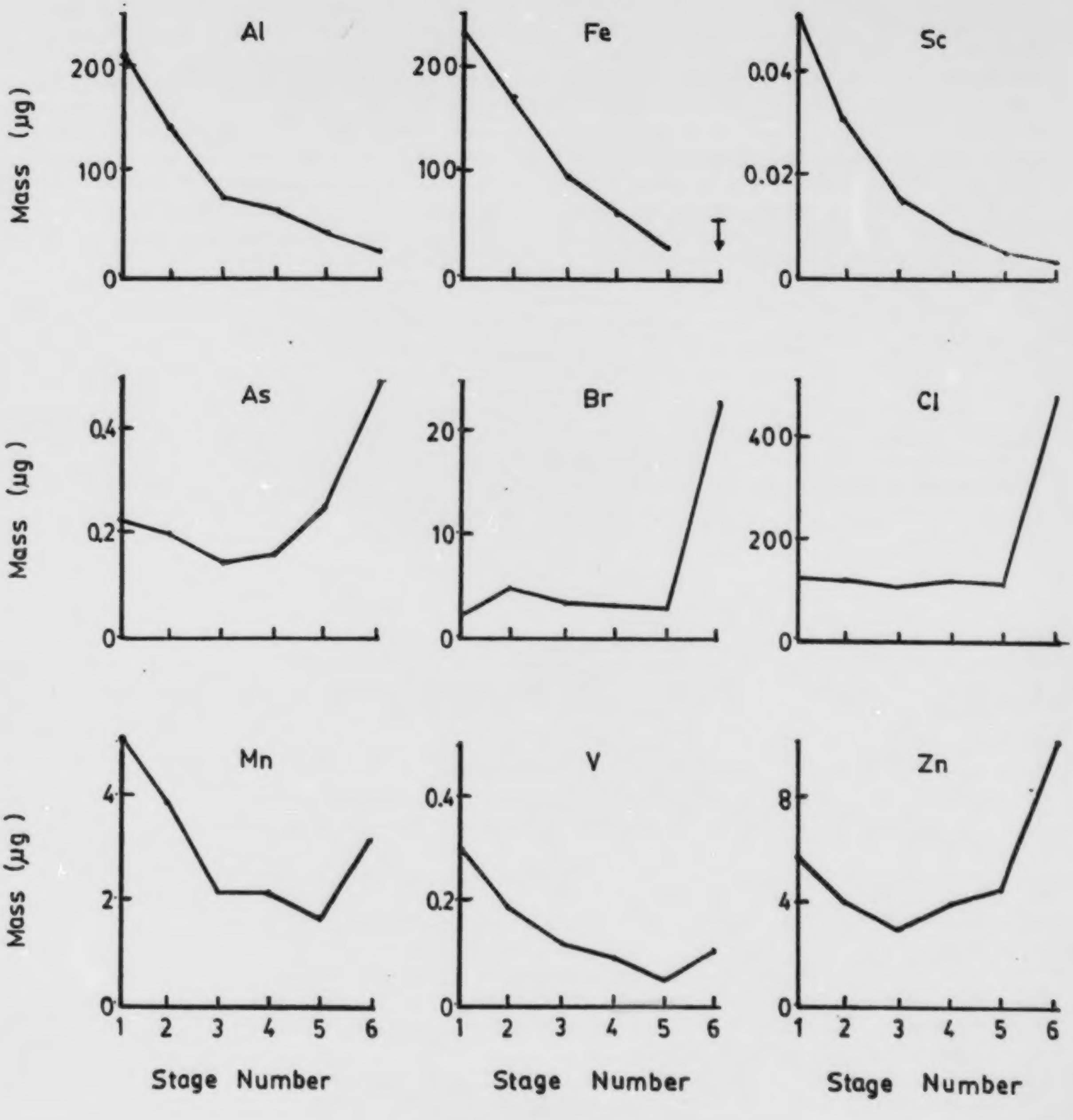
Al
Fe
Sc
As
Br
Cl
Mn
V
Zn
Mass (μg)
Mass (μg)
Mass (μg)
0
100
200
0
100
200
0
0.02
0.04
0
0.2
0.4
0
10
20
0
200
400
0
2
4
0
0.2
0.4
0
4
8
1
2
3
4
5
6
Stage Number
Stage Number
Stage Number

Conclusions

The concentrations of up to 30 elements were determined in airborne particulate matter from the Toronto area through the use of photon and thermal neutron activation analysis. Using this data both the factor analysis and chemical element balance receptor models were successfully applied to the Toronto area aerosol. Five prominent sources of particulate were deduced and their contributions to the ambient particulate levels quantified. The sources in order of descending contribution were: entrained soil, automobile exhaust, road salt, refuse incineration and oil combustion. A sixth source was evident but not identified. While this study is useful in confirming the utility of receptor models, much work has yet to be done in differentiating between sources of similar elemental profile. It is hoped that the proposed model involving particle-size distributions will address this problem in the next phase of this work.

Acknowledgements

The authors would like to express their appreciation to Dr. W.F. Davidson and A. Nowak of the LINAC facility at the National Research Council, the staff of the University of Toronto SLOWPOKE facility and to acknowledge the financial assistance provided by the Ontario Ministry of the Environment and the Natural Sciences and Engineering Rsearch Council of Canada.

References

1. G.E. GORDON, Environ. Sci. Technol., 14 (1980) 792.
2. D.F. GATZ, Atmos. Environ., 9 (1975) 1.
3. G.S. KOWALCZYK, G.E. GORDON, S.W. RHEINGROVER, Environ. Sci. Tech. 16 (1982) 79.
4. R. DAMS, K.A. RAHN, J.W. WINCHESTER, Environ. Sci. Tech., 6 (1972) 441.
5. T.G. PRINGLE, S. LANDSBERGER, W.F. DAVIDSON, R.E. JERVIS, J. Radioanal. Chem. Articles, 90 (1985) 383.
6. H. SIEVERING, M. DAVE, P. MCCOY, K. WALTER, Environ. Sci. Technol., 12 (1978) 1435.
7. B.A. ROSCOE, P.K. HOPKE, S.L. DATTNER, J.M. JENKS, JAPCA, 32 (1982).
8. J.G. WATSON, JAPCA, 34 (1984) 619.
9. P.A. SCHEFF, R.A. WADDEN, R.J. ALLEN, Environ. Sci. Technol. 18 (1984) 923.
10. J.J. PACIGA, Ph.D. Thesis, University of Toronto, 1975.
11. G.E. GORDON, W.H. ZOLLER, G.S. KOWALCZYK, S.W. RHEINGROVER, Atmospheric Aerosol: Source/Air Quality Relationships, American Chemical Society Symposium Series #167, Washington, D.C., (1981), 51.
12. S.H. CRADLE, R.L. WILLIAMS, Rubber Chem. and Tech. 53 (1980), 903.
13. C.DANIEL, M.A.Sc. Thesis, University of Toronto, 1985.
14. K.A. RAHN, D.H. LOWENTHAL, Science 228 (1985), 275.
15. P.K. HOPKE, E.S. GLADNEY, G.E. GORDON, W.H. ZOLLER, A.G. JONES, Atmos. Environ. 10 (1976), 1015.
16. R.L. BENNET and K.T. KNUPP, Environ. Sci. Technol. 16 (1982), 831.
17. G.D. THRUSTON, J.D. SPENGLER, Presented at 74th Annual Meeting of Air Pollution Control Assoc., New Orleans, 1982.

18. S-N. CHANG, P.K. HOPKE, S.W. RHEINGROVER, G.E. GORDON, Presented at 74th Annual Meeting of Air Pollution Control Assoc., New Orleans, 1982.

Fig. 1. Air particulate sampling sites in the Toronto area.

Fig. 2. Particle-size distributions for the Toronto aerosol determined by Anderson cascade impactor.

Fig. 3. Particle-size distributions for the Toronto aerosol determined by Sierra cascade impactor using vaseline-impregnated substrates.

TABLE 1

Cascade Impactor Particle-Size Cut-Offs at 50% Collection Efficiency (μm)

Stage	Anderson Manufacturer	Sierra Manufacturer
1	7	7.2
2	3.3	3.0
3	2	1.5
4	1.1	0.95
5	<1.1	0.49
6		<0.49

TABLE 2

Elemental Concentrations in Airborne Particulate Matter (ng/m^3)

Element	Toronto This study 1985	Toronto [10] Paciga 1975	Washington [3] Kowalczyk et al 1982	Chicago [9] Scheff et al 1984
Al	600	2100	1170	1630
As	5.3	12	4.6	4.3
Br	70	290	190	--
Ca	2150	5300	910	3420
Cl	2340	1200	--	--
Fe	640	2200	910	2310
I	3.2	<4	1.3	--
Mn	34	75	23	89.1
Na	1520	650	340	2540
Pb	300	970	520	490
Sc	0.13	0.27	0.26	--
Se	3.3	—	2.4	2.01
Ti	64	170	94	--
V	5.9	14	30	8.74
Zn	108	320	77	304

TABLE 3

Factor Pattern for the Port Credit Aerosol (Factor Loadings)

Soil	Road Salt	Mobile Sources	Refuse	Wind	Oil	Arsenic Source
Sc(0.93)	Na(0.95)	Pb(0.87)	Se(0.79)	SW(0.83)	NE(0.63)	As(0.66)
Ca(0.86)	Cl(0.92)	Br(0.82)	U (0.57)	NE(-0.5)	V (0.58)	
Mn(0.77)	NW(0.66)	Zn(0.65)	Zn(0.55)		NW(-0.56)	
Ti(0.72)	SA(-0.66)	Mn(0.55)				
SA(-0.5)		U (0.47)				

TABLE 4

Chemical Element Balance Source Profiles (μg/g)

Element	Soil	Mobile Sources	Refuse	Oil	Road Salt	Arsenic Source
Al	29100	7100	14000	4700	0	0
As	5	0	240	35	0	300000
Ca	109100	11000	17000	26000	50000	6000
Co	8	6	20	3	0	0
Cr	65	75	490	580	0	0
Fe	29300	8000	6500	14000	0	0
Mn	620	1000	730	270	0	0
Na	9900	0	82000	28000	350000	0
Ni	60	80	150	14500	0	0
Pb	60	100000	81000	490	0	7500
Se	1	8	1000	43	0	0
V	100	0	31	12200	0	0
Zn	490	1700	120000	730	0	0

TABLE 5

CEB Source Contributions

Source	Contributions (%)
Soil	67
Automobile Exhaust	15
Road Salt	12
Refuse Incineration	3
Oil Combustion	1.4
Arsenic Source	0.05

TABLE 6

Comparison with Other CEB Studies

Study	Author	Larger/Smaller Ratio
Pasadena	Friedlander (1973)[3]	9.6
Chicago	Gatz (1975)[3]	7.0
Washington	Kowalczyk et al.[3] (1982)	1.9
Toronto	Pringle and Jervis (1985)	2.3

STUDY OF CONDITIONS FOR CONDENSATION AND DESORPTION OF PCDD ON PARTICULATE MATTER UNDER STACK SAMPLING CONDITIONS

F.W. Karasek and L.C. Dickson
Chemistry Department, University of Waterloo

Key words: Incineration, Flyash, Dioxin, GC-MS.

ABSTRACT

Municipal incinerator flyash was heated in a pyrex tube under a flow of high-purity nitrogen. The levels of polychlorinated dibenzo-p-dioxins (PCDD) in the heated samples were determined using gas chromatography/mass spectrometry (GC/MS) and compared to levels in unheated samples.

In a time and temperature study where temperatures from 100° to 200°C and heating times from 16 to 48 hours were investigated, PCDD levels decreased to 10 to 30 per cent of the levels in unheated samples. The PCDD levels were independent of heating time and temperature under the above conditions. About 10 per cent of the PCDD could not be desorbed and are thought to be chemisorbed on the surface of the flyash particles. Heating the flyash at 120°C for 2 to 6 hours desorbed 15 to 38 per cent of the PCDD. The desorption rates for the PCDD congeners were estimated to be 0.037, 0.086, 0.15 and 0.23 ng/g/hr/L for tetrachloro-,pentachloro-, hexachloro- and heptachlorodibenzo-p-dioxins respectively. At constant temperature, these rates appear to depend mainly on the amount of the particular PCDD congener originally present on the flyash, not on physiochemical properties such as vapour pressure or dipole moment. When expressed as per cent/hr/L, desorption rates for the PCDD congeners were not significantly different from each other. The average value was 0.78 per cent/hr/L. Desorbed PCDD were adsorbed onto exhaustively extracted flyash placed in the tube downstream of the heated sample. There was no evidence of decomposition of the PCDD under the experimental conditions.

STUDY OF CONDITIONS FOR CONDENSATION AND DESORPTION OF PCDD ON PARTICULATE MATTER UNDER STACK SAMPLING CONDITIONS

by

F.W. Karasek and L.C. Dickson
The Guelph-Waterloo Centre for Graduate
Work in Chemistry, Waterloo Campus,
University of Waterloo,
Waterloo, Ontario,
N2L 3G1

SUMMARY

Municipal incinerator flyash was heated in a pyrex tube under a flow of high-purity nitrogen. The levels of polychlorinated dibenzo-p-dioxins (PCDD) in the heated samples were determined using gas chromatography/mass spectrometry (GC/MS) and compared to levels in unheated samples.

In a time and temperature study where temperatures from 100° to 200°C and heating times from 16 to 48 hours (h) were investigated, PCDD levels decreased to 10 to 30 percent of the levels in unheated samples. The final PCDD levels were independent of heating time and temperature under the above conditions. About 10 percent of the PCDD could not be desorbed and are thought to be chemisorbed on the surface of the flyash particles. Heating the flyash at 120°C for 2h to 6h desorbed 15 to 38 percent of the PCDD. The desorption rates for the PCDD homologues were estimated to be 0.037, 0.086, 0.15 and 0.23 ng/g/h/L for tetrachloro-, pentachloro-, hexachloro- and heptachlorodibenzo-p-dioxins respectively. At constant temperature these rates appear to depend mainly on the amount of the particular PCDD homologue originally present on the flyash, not on physiochemical properties such as vapour pressure or dipole moment. When expressed as percent/h/L, desorption rates for the PCDD homologues were not significantly different from each other. The average value was 0.78 percent/h/L. Desorbed PCDD were adsorbed onto exhaustively extracted flyash placed in the tube downstream of the heated sample. There was no evidence of decomposition of the PCDD under the experimental conditions.

INTRODUCTION

Polychlorinated dibenzo-p-dioxins (PCDD) and polychlorinated dibenzo-furans are groups of compounds which are among the most toxic. Since 1977 it has been know that PCDD are a by-product of municipal garbage incineration (1-6). Sampling of stack gases from incinerators has shown that PCDD are emitted into the atmosphere (7). As a result, the Ontario Ministry of the Environment has set provisional guidelines for PCDD emissions from incinerators (8).

For many years in the United States and Canada the EPA Method 5 Sampling Train has been used to monitor the gaseous and particulate emissions of incinerators (9). With the inclusion of a cartridge with suitable solid sorbent, the Method 5 Trains can be used for PCDD sampling. In the sampling train a glass fiber filter to trap particulates is placed upstream of impingers and adsorbant cartridges. This filter is maintained at 120°C for the duration of sampling which can last anywhere from one to twenty four hours. In the majority of sampling tests, a large portion of all PCDD is found in the impingers and adsorbant cartridges. Because of the unknown behaviour of adsorption and desorption of organic compounds on the trapped particulates it is not known whether the relative amounts of PCDD found on the filter and in the impingers is indicative of the relative amounts in the stack effluent. Sampling artifacts could be introduced by adsorption or desorption of PCDD on the particulate matter on the filter. It is important to know the true distribution between gas and particles as gaseous state PCDD are possibly a more potent health hazard than the particulate PCDD. Also, this information will aid in understanding the mechanism of formation of PCDD during incineration and in specifying equipment for air emission abatement.

Therefore the purpose of this study was to investigate adsorption and desorption behaviour of PCDD on flyash particles. This report presents the results and recommendations for further studies into this problem.

MATERIALS AND METHODS

Materials

Flyash from a municipal incinerator was supplied by the Ontario Ministry of the Environment. All solvents were "distilled in glass" UV grade. Unlabelled PCDD standards were purchased from Ultra Scientific Inc. and Cambridge Isotopes. Labelled PCDD standards, $[^{13}C_{12}]$TCDD and $[^{13}C_{12}]$OCDD were supplied by the Ontario Ministry of the Environment.

Pyrex tubes 45 cm x 2 cm I.D. were constructed with a medium porosity glass frit.

All glassware was washed in an ultrasonic bath using mild detergent, rinsed with deionized water and dried overnight at 275°C. Before use glassware was rinsed with solvent.

Time and temperature studies

About 15g of flyash was placed in the Pyrex tube on the upstream side of a glass frit. The tube and contents were placed in a modified gas chromatograph oven. The flyash was heated under a flow of 100 mL/min. high purity dry nitrogen at temperatures of

100, 150, and 200°C. At each temperature the flyash was heated for 16h, 32h and 48h.

Time studies at constant temperature

Flyash was sieved and the 170-200 Mesh fraction was used for these experiments. About 15g of the unextracted flyash was placed in the Pyrex tube on the upstream side of the glass frit. About 12g of exhaustively extracted flyash was placed downstream of the unextracted flyash against the glass frit. The flyash was retained with glasswool plugs. The tube and contents were heated at 120°C for 2h, 4h, and 6h in duplicate under a 100mL/min flow of high purity nitrogen. Any desorbed organic compounds not absorbed by the trap flyash were absorbed by a florisil guard trap. A flowchart of the experiment is shown in Figure 1.

Extraction and concentration

The flyash was transferred to a glass thimble with a medium porosity glass frit. 20 ng of $[^{13}C_{12}]$TCDD and 14 g of $[^{13}C_{12}]$OCDD internal standards in isooctane were added to the flyash in the time studies. Organic compounds were extracted with 200 mL benzene in a Soxhlet extractor for 18h. The extract was reduced to several mL by rotary evaporation under reduced pressure. Final concentration to 300 uL was achieved by blowing a gentle stream of high purity nitrogen over the surface of the sample in a calibrated reacti-vial.

Gas chromatographic analysis

Total organic compounds (TOC) were estimated by using gas chromatography - flame ionization detector (GC-FID) techniques. TOC were estimated using a response factor of 8 area counts/ng, based on average response factors for different compound classes (10).

Gas chromatography/mass spectrometry analysis

Analyses were carried out on a Hewlett-Packard 5987A gas chromatograph/mass spectrometer (GC/MS) with an HP1000 data system. The instrument was equipped with a cool on-column injector, a fused silica 30 m x 0.32 m I.D. DB-5 column and a direct inlet GC/MS interface. Instrument operating parameters are given in Table 1.

RESULTS AND DISCUSSION

Extraction of organic compounds

The precision of the extraction step was estimated by extracting the raw flyash in triplicate and determining the TOC in each extract. Two one-uL aliquots of each extract were injected into the GC.

The TOC analyses of the flyash extracts are presented in Table 2. The method of estimating TOC is quite reproducible for replicate analyses of the same sample but can only be considered semiquantitative because the response factor will vary between samples. Since the test indicated no difference between extractions, the pooled variance was used to determine the relative error of the extraction step, which was 4.3 percent.

Time and temperature study

There were few qualitative changes in the organic content of the flyash due to heating. A major peak identified as molecular sulphur (S_8) in the unheated sample was missing in the heated sample. This compound likely decomposed during heating. Some of the major components detected in the undesorbed flyash were detected in the trap flyash chromatogram. A large peak which appeared in the heated sample was identified as a phthalate ester. This likely desorbed from the Tygon tubing used to connect the nitrogen gas supply to the flow meter.

The percent loss data for each PCDD congener is shown in Table 3 and presented graphically in Figure 2. The data were tested for temperature and time effects by a 2-Way Model 1 analysis of variance (ANOVA) without replication (11). Within each group of PCDD congeners there was no significant effect due to temperature or heating time at the ninety-five percent confidence level. The relative precision of the quantitation procedure was estimated from the ANOVA to be eight percent relative.

It had been expected that the amount of PCDD desorbed would be directly related to both heating time and temperature. Such a dependence was not observed under these conditions. The high amount of material desorbed, between 68 and 89 percent, and the lack of time and temperature dependence suggests that the PCDD were desorbed in a time shorter than 16h. Since all the PCDD were not desorbed even after heating for 48h at 200°C it is possible that some of the PCDD are more tightly bound (chemisorbed) to the surface of the flyash and would not desorb under the experimental conditions. The majority is just adsorbed through van der Waals forces (physisorbed). The presence of two different types of adsorption is supported by the data of rordorf and Eiceman (12,13). Rordorf measured the vapour pressure of 2,3,7,8-TCDD to be 3.9-15.9 x 10^{-2} Pa at 100°C and found its decomposition temperature in nitrogen to between 850°C and 1100°C. If this model is correct, the apparent rate of desortion (ng/g/h/L) would have a finite value at the start of heating and would approach zero as the amount of physisorbed material approached zero. An Illustration of this proposed model is shown in Figure 3.

Time study at constant temperature

The percent loss of PCDD at 120°C after heating at 2h, 4h, and 6h in a 100 ml/min stream of dry nitrogen is presented in Table 4 and shown in Figure 4. There are no apparent differences in PCDD lost after heating for 2h and 4h, which may be due to the relative errors of the analyses, which vary from 0.11 to 0.44. The data possess an interesting feature. The percent loss of PCDD due to heating decreases in order of TCDD, H_6CDD, P_5CDD, H_7CDD. If the desorption of physisorbed material is governed solely by vapour pressure, the order would be expected to be that of increasing molar mass i.e. TCDD, P_5CDD, H_6CDD, H_7CDD. The switching of the order for P_5CDD and H_6CDD could be due to dipolar interactions. Both TCDD and H_6CDD homologue classes posses an even number of chlorine and hydrogen atoms and can form structures which posses no net dipole moment. Conversely, P_5CDD and H_7CDD have odd numbers of chlorine and hydrogen atoms and therefore are unable to form structures without a net dipole moment. We speculate that an increased average level of the van der Waals forces between the molecules results in greater retention of P_5CDD and H_7CDD congener classes. More exact and precise desorption data for each congener class is needed before any reliable conclusions can be reached.

A plot of desorption data taken from both studies is presented in Figure 5. The three sets of points below 10h, shown as circles, are taken from the time study at 120°C while points shown by squares are from the time and temperature study. The latter data are averages of data taken at the three temperatures. The data for 48h is omitted for clarity. The plot resembles the proposed model for PCDD desorption presented in Figure 3. The rising portion of the desorption curve represents the loss of physisorbed material from the flyash. The plateau of the curve for heating times greater than 16h represents the retention of material chemisorbed onto the surface of the flyash particles.

Desorption rates for PCDD have been estimated from data taken from both studies. Table 5 presents the PCCD loss data (ng/g) used to calculate desorption rates (ng/g/h/L). The data from the 2h experiments was suspect and therefore omitted. The calculated desorption rates for each congener class are presented in Table 6. The slope was calculated using linear regression techniques. The values listed under intercept do not have any physical meaning as no PCDD would be desorbed at 0 hours. The regression lines and confidence belts for the regression analysis of this data is presented in Figure 6. The 95% confidence belts are calculated for mean predicted values. The desorption rates increase from TCDD to H_7CDD. This increase is more likely due to the relative amounts of each congener found on flyash rather than an effect of increasing molar mass.

Table 7 presents desorption data, expressed as percentages of the original amount on the flyash. The data selected corresponds to the desorption data presented in Table 5. These data were used to calculate desorption rates, expressed as percent/h/L, and are shown in Table 8. The desorption rates for the congener are equal, within experimental error. Therefore, the data for the four congener classes were combined and a desorption rate based on the combined data was calculated. These data and the best-fitting line are presented in Figure 7. The 95% confidence belts were calculated for mean predicted values. These data show that desorption rates in percent/h/L are equal for each congener. This confirms our speculation that desorption rates expressed as ng/g/hr/L are more dependent upon the amount of physisorbed material in the flyash than on the molar mass.

Table 9 shows the amount of PCDD found on the trap flyash just downstream of the desorbed flyash. The listed values are from single analyses so the variances are high. The apparent trend follows the desorption data, with increasingly larger amounts recovered with an increasingly larger amount desorbed.

Table 10 compares the amount desorbed to the amount absorbed on unextracted flyash. These data indicate that the PCDD were desorbed from flyash and reabsorbed downstream without significant decomposition. It is far more difficult to obtain reliable adsorption data than to obtain desorption data due to condensation of PCDD on the surface of the flow tube and absorption by the glass frit. Further experiments must be carefully designed before useful adsorption data can be produced.

ACKNOWLEDGEMENTS

Financial Assistance from the Ontario Ministry of the Environment is gratefully acknowledged. We would like to thank Dr. Chris Young of the Statistics Consulting Service, Faculty of Mathematics, University of Waterloo for his helpful discussions.

REFERENCES

1. K. Olie, P.L. Vermeulen, and O. Hutzinger, Chemosphere 6, 455 (1977)
2. G.A. Eiceman, R.E. Clement, and F.W. Karasek, Anal. Chem. 51, 2343 (1979)
3. R.E. Clement, G.A. Eiceman, F.W. Karasek, W.D. Bowers, M.L. Parsons, J. Chromatogr. 189, 53 (1980)
4. G.A. Eiceman, R.E. Clement, and F.W. Karasek, Anal. Chem. 53, 955 (1981)
5. R.E. Clement and F.W. Karasek, J. Chromatogr. 234, 395 (1982)
6. F.W. Karasek, Canadian Research, 13(5) (1980)
7. A.S.M.E. Research Comm. on Industrial and Municipal Wastes, "Study on the State of the Art of Dioxin from Combustion Sources" (1980).
8. Ministry of the Environment, "Ambient Air Quality Provisional Guideline Criterion and Point of Impingement Provisional Guideline for Chlorinated Dibenzodioxins and Dibenzofurans".
9. Ministry of the Environment, Report #ARB-TDA-66-80, "Source

Testing Code Version #2", November 1980.

10. H.Y. Tong and F.W. Karasek, Anal. Chem., 56, 2124 (1984)

11. J.H. Zar, "Biostatistical Analysis", Prentice-Hall, New York, 1974.

12. B.F. Rordorf, "Thermodynamic and Thermal Properties of Polychlorinated Compounds: The Vapour Pressures and Flow Tube Kinetics of Ten Dibenzo-p-Dioxins", Abstracts of 4th International Symposium on Chlorinated Dioxins and Related Compounds, Ottawa, Ontario, Canada, October 1984.

13. G.A. Eiceman, and V.J. Vandives, Atmosph. Environ. 17, 461 (1983)

TABLE 1: Instrument Operating Parameters

Chromatographic Conditions

Fused silica WCOT column 30 m x 0.32 mm I.D.

Stationary phase DB-5, 0.25 μm thickness

Helium carrier gas flow 2.5 mL/min.

Temperature program 90°C to 300°C at 6°C/min.

Linear Scan Mass Spectrometry

Scan range 50 amu - 500 amu

Scan rate 630 amu/s

Selected Ion Monitoring Mass Spectrometry

Ions	M/Z	dwell (ms)
TCDD $[M+2]^+$	321.9	100
$[^{13}C_{12}]$TCDD $[M+2]^+$	333.9	100
P_5CDD $[M+2]^+$	355.9	100
H_6CDD $[M+2]^+$	389.8	100
H_7CDD $[M+2]^+$	425.8	100
OCDD $[M+2]^+$	459.7	100
$[^{13}C_{12}]$OCDD $[M+2]^+$	471.7	100

TABLE 2: Total Organic Carbon in Flyash Extracts

Extract		MOE I	MOE II	MOE III
Injection	1	16540[a]	18250	16170
	2	16220	16320	17680

---

[a] ng/g flyash

Average TOC is 17030 ng/g; pooled standard deviation (S.D.) is 738 ng/g; relative standard deviation (R.S.D.) is 0.043.

TABLE 3: Percent of Dioxins Lost due to Heating Time and Temperature Study

	100°C			150°C			200°C		
Time	16h	32h	48h	16h	32h	48h	16h	32h	48h
Dioxin									
TCDD	76[a]	82	74	81	78	68	76	86	83
P_5CDD	73	87	79	81	81	70	77	88	85
H_6CDD	78	86	78	80	81	68	73	89	86
H_7CDD	82	86	78	83	81	70	74	87	89

[a] Percentage of Original Amount

TABLE 4: Dioxins Desorbed due to Heating Time Study at Constant Temperature

Dioxin Loss (Percent of Original Amount)

Time	TCDD	P_5CDD	H_6CDD	H_7CDD
2h	24 ± 6[a]	16 ± 5	21 ± 4	15 ± 6
4h	25 ± 6	15 ± 5	22 ± 4	15 ± 6
6h	38 ± 6	33 ± 5	35 ± 4	20 ± 6

[a] Standard Error of the Mean estimated from error mean square of analysis of variance, 2 replicates per sample.

TABLE 5: Dioxins Desorbed due to Heating Selected Data from Both Studies

Dioxin Loss (ng/g)

Time	TCDD	P_5CDD	H_6CDD	H_7CDD
4h	1.5	1.4	4.5	4.3
	1.2	2.0	4.2	3.9
6h	2.2	3.8	7.2	7.5
	1.9	3.4	6.6	8.1
16h	4.0[a]	7.8	15.5	21.5
	4.3	8.7	15.9	22.0
	4.0	8.3	14.4	19.4

[a] Data from Time and Temperture Study are averages of the losses at the three temperatures at N_2 flow of 6 L/min.

TABLE 6: Desorption Rate of Dioxins[a]

Dioxin	Desorption Rate (ng/g/hr/L)	Slope (ng/g/hr)	Intercept
TCDD	0.0368 ± .006[b]	0.221[c] ± .037[d]	0.584
P_5CDD	0.0865 ± 0.016	0.519 ± .094	0.016
H_6CDD	0.147 ± 0.019	0.884 ± .113	1.169
H7CDD	0.229 ± 0.020	1.374 ± .177	-0.965

[a] Data taken from Table 5

[b] 95% confidence interval for desorption rate

[c] slope of corresponding best-fitting line in Figure 13.

[d] 95% confidence interval for slope

TABLE 7: Dioxins Desorbed due to Heating Selected Data from both Studies

	Dioxin Loss (Percentage of Original Amount)			
Time	TCDD	P_5CDD	H_6CDD	H_7CDD
4 hr	28	13	23	16
	23	19	21	15
6 hr	42	35	36	29
	36	32	33	31
16 hr	76[a]	73	78	82
	81	81	80	84
	76	77	73	74

[a] Data from Time and Temperature Study are averages of the losses at the three temperatures.

TABLE 8: Desorption Rate of Dioxins[a]

Dioxin	Desorption Rate (percent/hr/L)	Slope (percent/hr)	Intercept
TCDD	0.694[b] ± .112[c]	4.164[b] ± .673[d]	11.01
P_5CDD	0.803[b] ± .146	4.815 ± .873	0.114
H_6CDD	0.745[b] ± .093	4.471 ± .556	5.86
H_7CDD	0.870[b] ± .112	5.217 ± .669	-3.65
Combined	0.778[e] ± .067	4.667 ± .404	3.33

[a] Data taken from Table 7

[b] 7 data points

[c] 95% confidence interval for desorption rate

[d] 95% confidence interval for slope

[e] 28 data points

TABLE 9: Amount of Dioxins on Trap Flyash Dioxin (ng/g)[a]

Time	TCDD	P_5CDD	H_6CDD	H_7CDD
2 hr	ND[b]	ND	ND	6
4 hr	2	3	5	8
6 hr	2	4	8	11

[a] OCDD not quantitated

[b] Not detected

TABLE 10: Amount of Dioxins Desorbed Compared to Amount of Dioxins Absorbed on Unextracted Flyash

Time	TCDD		P_5CDD		H_6CDD		H_7CDD	
	Loss	Trap	Loss	Trap	Loss	Trap	Loss	Trap
2 hr	18[a]	ND[b]	26	ND	61	ND	56	75
4 hr	15	25	22	29	56	48	51	76
6 hr	31	26	55	52	106	104	118	143

[a] ng dioxin
[b] not detected

FIGURE CAPTIONS

Figure 1: Flowchart of the flyash analysis. Flyash was heated at 120°C for 2, 4 and 6 hours under a 100 mL/min flow of high-purity nitrogen.

Figure 2: Data from GC-MS-SIM analyses of heated flyash showing the percentage of TCDD, P_5CDD, H_6CDD and H_7CDD lost due to desorption. The percentage lost was independent of heating time and temperature.

Figure 3: A proposed model of PCDD desorption from flyash. Physisorbed material could desorb under stack sampling conditions but tightly-bound chemisorbed material would not desorb.

Figure 4: Data from GC_MS-SIM analyses of flyash heated at 120°C for 2, 4 and 6 hours showing the percent loss for TCDD, P_5CDD, H_6CDD and H_7CDD congeners.

Figure 5: Percent loss desorption data selected from both studies shows that PCDD is desorbed at heating times less than 16 hours while some PCDD remains adsorbed even after heating for 32 hours. The plot is similar to the proposed model of PCDD desorption shown in Figure 4.

Figure 6: Plot of PCDD loss (ng/g flyash/L nitrogen) versus heating time at 120°C. The data is taken from Table 5. The linear regression lines and 95% confidence belts for mean predicted values are overlayed on the data points.

Figure 7: Plot of percent PCDD loss per L of nitrogen versus heating time at 120°C. The data is taken from Table 7. The linear regression line and 95% confidence belts for mean predicted values are overlayed on the data points.

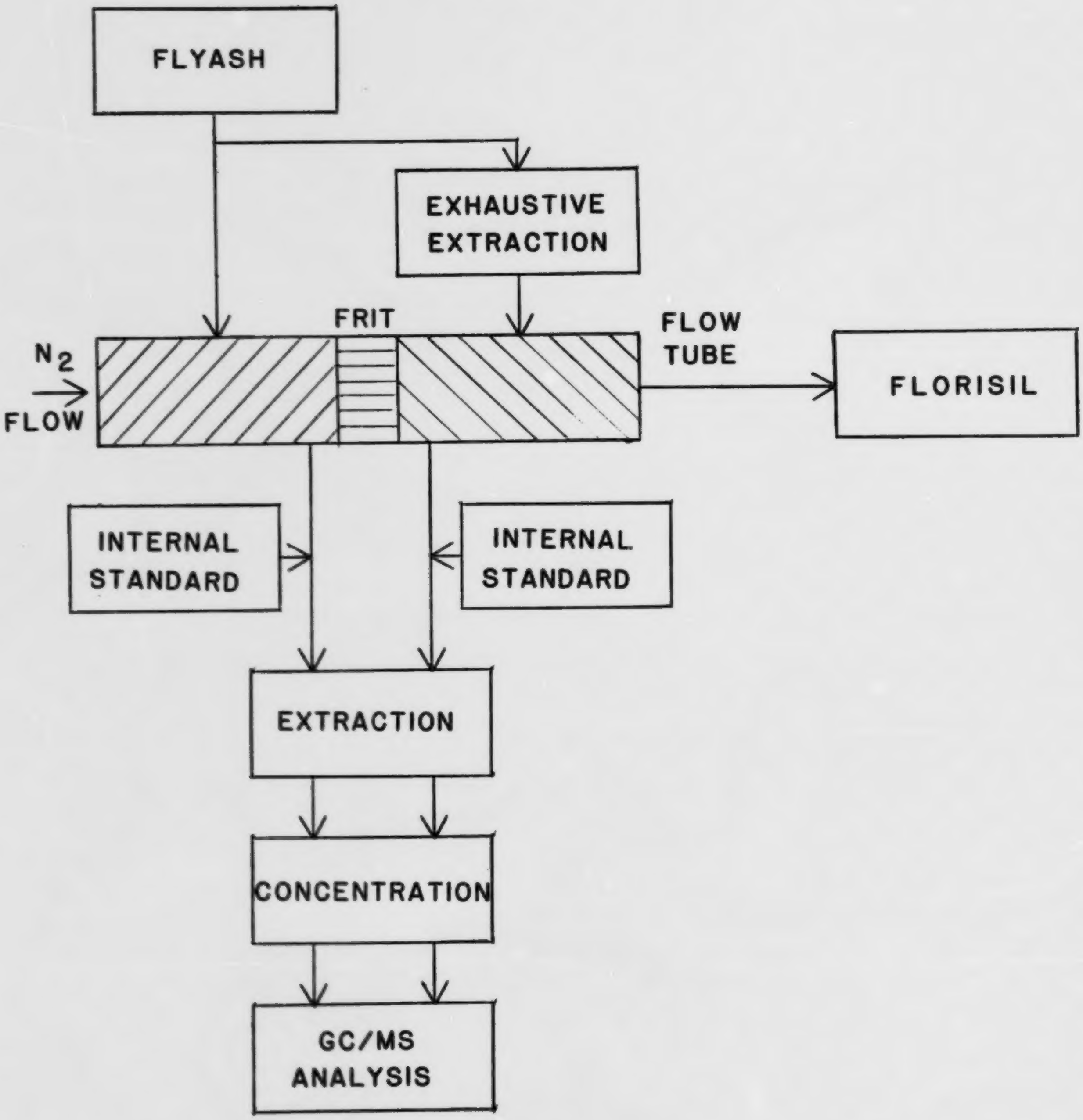
FLYASH
EXHAUSTIVE EXTRACTION
FRIT
FLOW TUBE
N_2 FLOW
FLORISIL
INTERNAL STANDARD
INTERNAL STANDARD
EXTRACTION
CONCENTRATION
GC/MS ANALYSIS

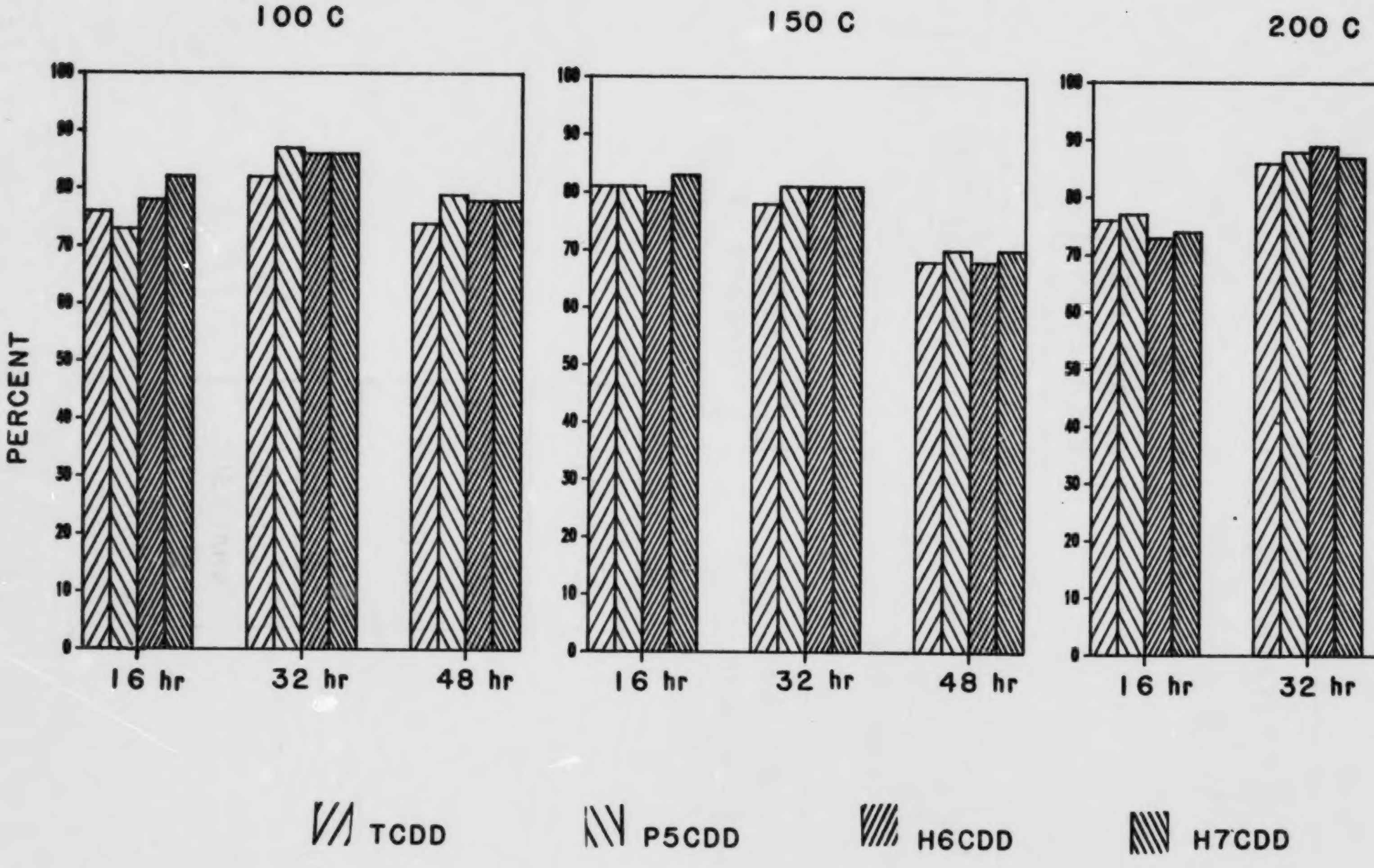
100 C
150 C
200 C
PERCENT
0
10
20
30
40
50
60
70
80
90
100
16 hr
32 hr
48 hr
TCDD
P5CDD
H6CDD
H7CDD

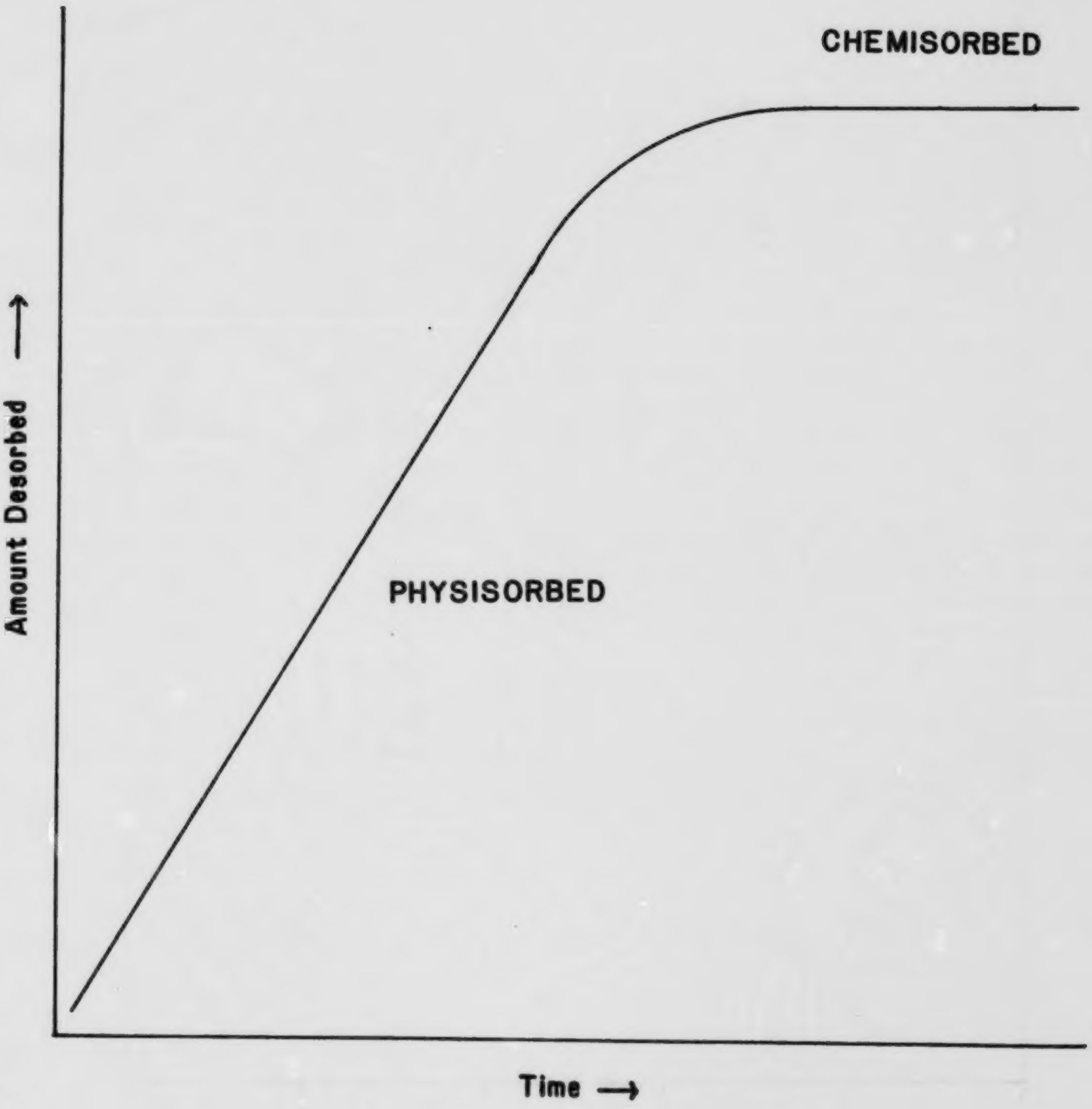
CHEMISORBED
PHYSISORBED
Amount Desorbed ⟶
Time ⟶

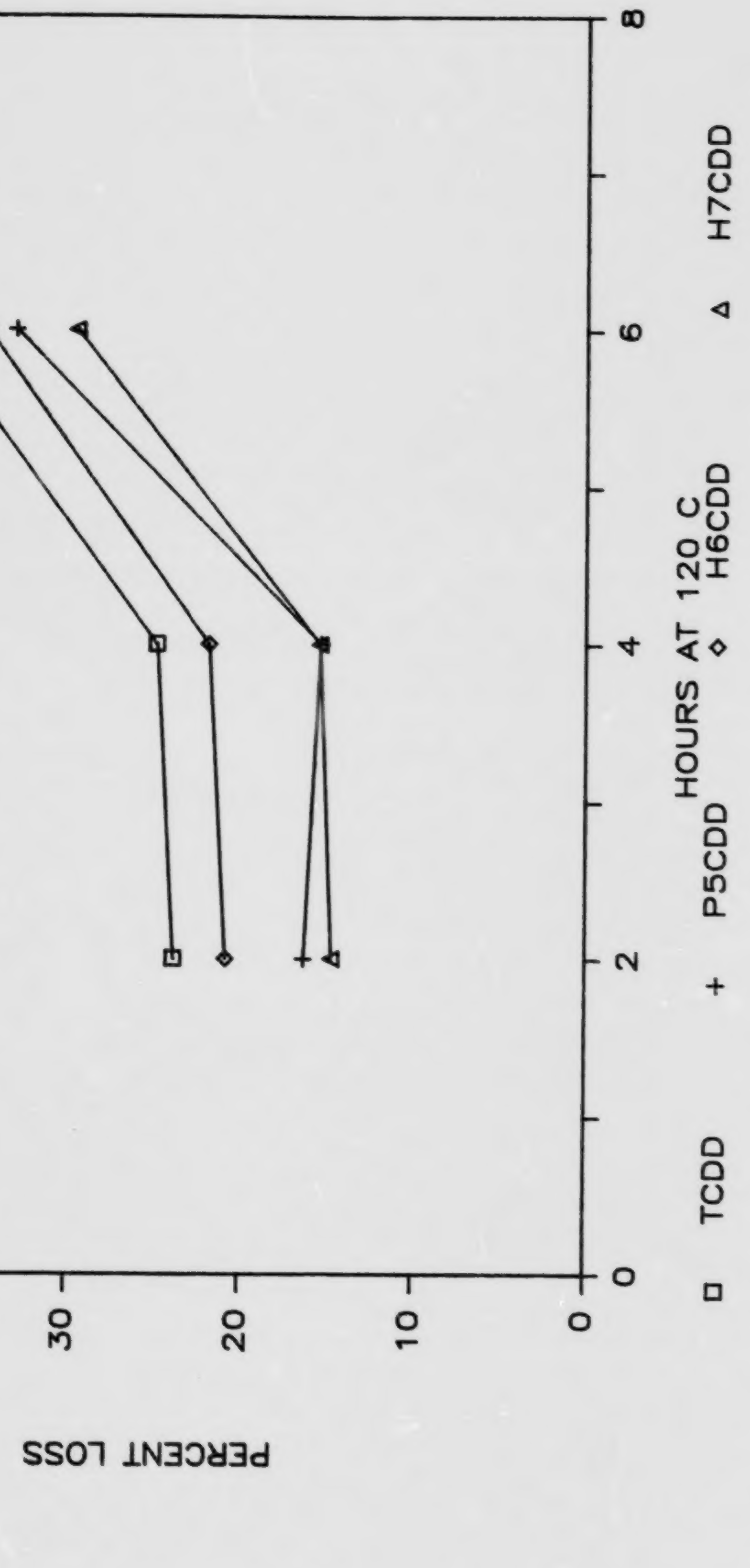
PERCENT LOSS
0
10
20
30
40
50
0
2
4
6
8
HOURS AT 120 C
□ TCDD
+ P5CDD
◇ H6CDD
△ H7CDD

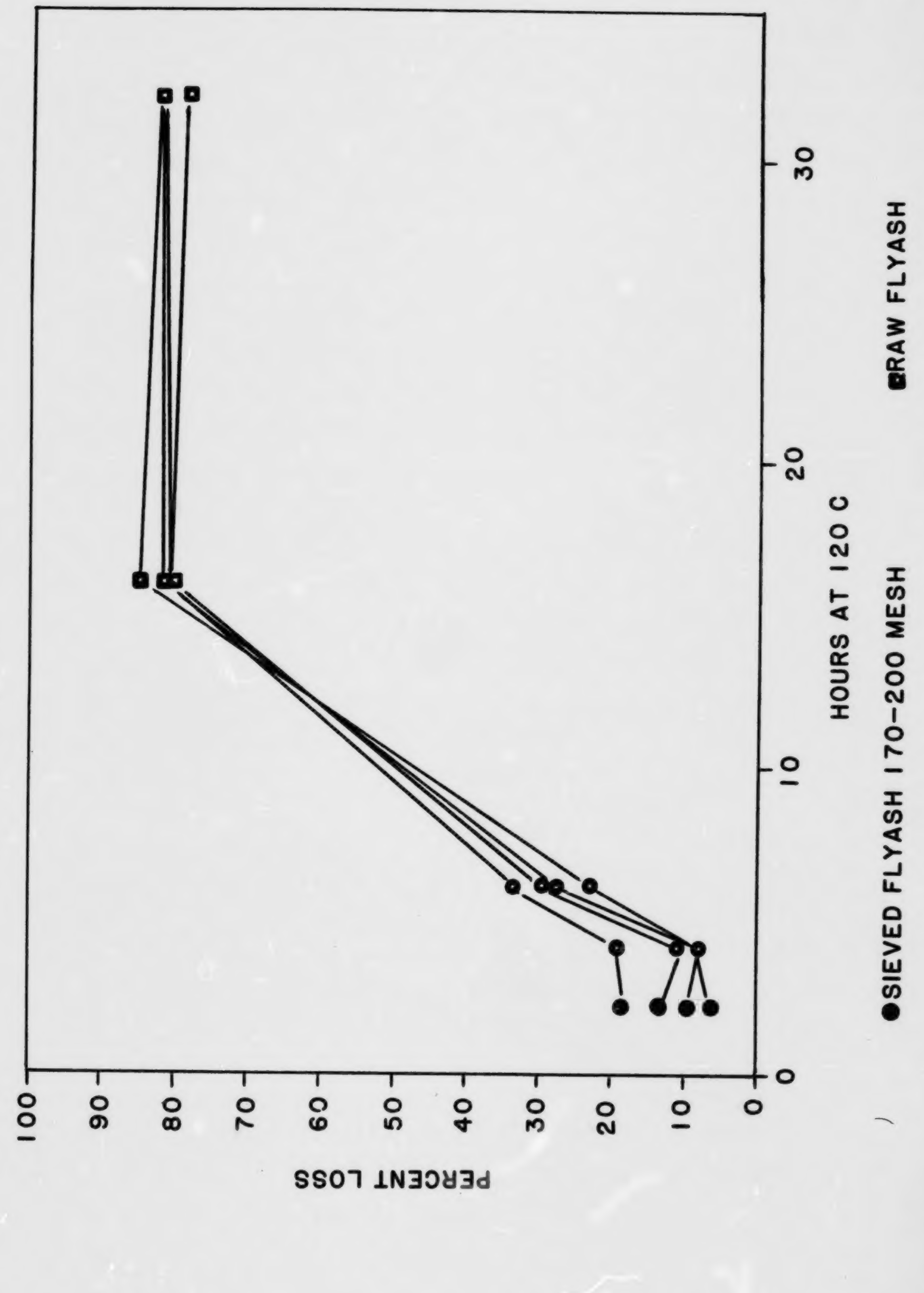
PERCENT LOSS
100
90
80
70
60
50
40
30
20
10
0
HOURS AT 120 C
0
10
20
30
●SIEVED FLYASH 170-200 MESH
▣RAW FLYASH

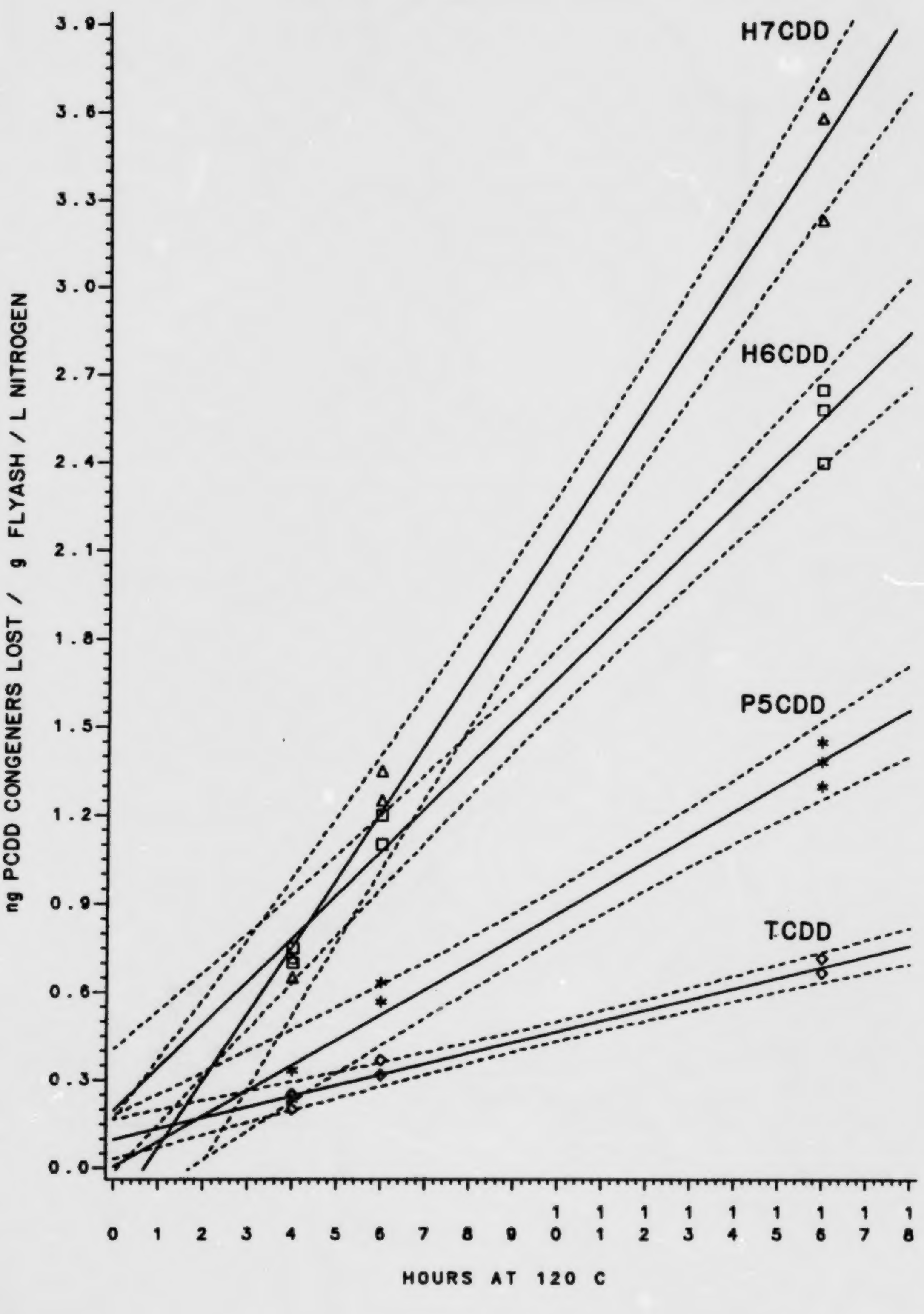
H7CDD
H6CDD
P5CDD
TCDD
ng PCDD CONGENERS LOST / g FLYASH / L NITROGEN
0.0
0.3
0.6
0.9
1.2
1.5
1.8
2.1
2.4
2.7
3.0
3.3
3.6
3.9
0
1
2
3
4
5
6
7
8
9
10
11
12
13
14
15
16
17
18
HOURS AT 120 C

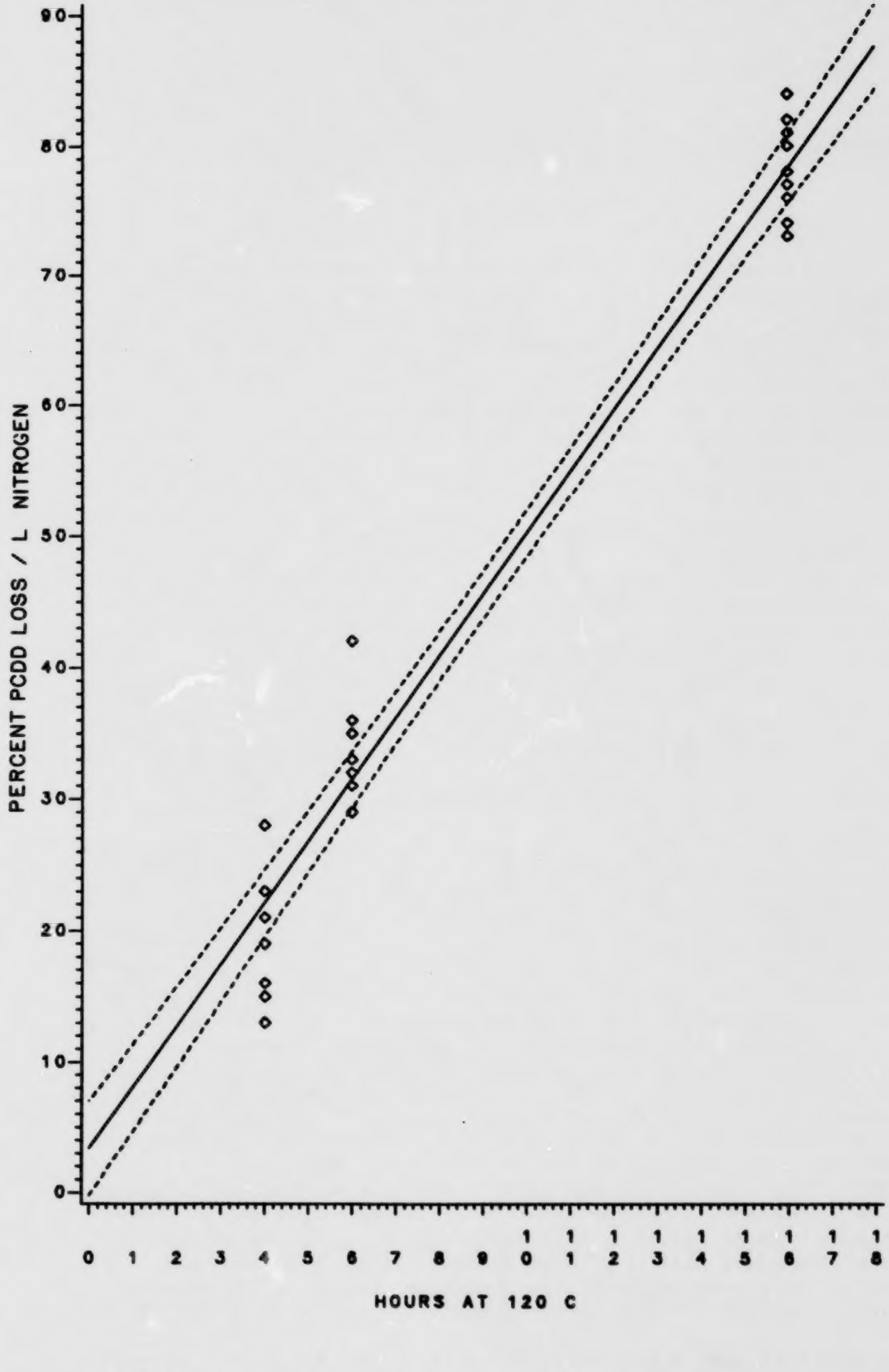
PERCENT PCDD LOSS / L NITROGEN
0
10
20
30
40
50
60
70
80
90
0
1
2
3
4
5
6
7
8
9
10
11
12
13
14
15
16
17
18
HOURS AT 120 C

ASSESSMENT OF TOXICITY OF INGESTED AND INHALED HALOAROMATIC HYDROCARBONS

Dr. G.D. Sweeney, Dr. D.A. Clark, Dr. J. Gauldie
McMaster University

Key words: Organics, Toxicity, Dioxins, Health Effects, Immunosuppression.

ABSTRACT

Previous studies in our laboratory have shown that 2,3,7,8-TCDD and related haloaromatic hydrocarbons such as Aroclor 1254 and 3,4,3',4'-tetracholorobiphenyl suppress the immune response. In the case of TCDD, suppression of the generation of cytotoxic T cells (CTL) occurred at a cumulative dose of 0.004 ug/kg (12 pM or 4 parts in 10^{12}) in chronically treated inbred laboratory mice. This immunosuppression proved to be 100-1000 times more sensitive an index of TCDD effect than was induction of hepatic P_T450 and related enzyme systems. Further, inhibition of CTL generation by TCDD was associated with an increased mortality following challenge with herpesvirus type 2.

Studies designed to elucidate the mechanism of immunosuppression by TCDD have shown that TCDD promotes the production of suppressor T cells. Sensitivity to TCDD is determined in part by genes at the Ah locus in mice and, using chimeric mice created by replacing the lymphocyte component of the immune system of TCDD-sensitive mice with cells from TCDD-resistant mice and vice versa, we were able to show that immunosuppression by TCDD is mediated through the non-lymphoid cells of the host. Since T cells develop in the thymus gland under the influence of thymic epithelium, and since epithelial cells have been noted to be particularly sensitive to TCDD, we proposed that TCDD acted via the thymic epithelia to promote suppressor T cell production.

Results from current studies have provided several new and relevant pieces of information:

1. Removal of the thymus gland from 6- to 8-week old mice renders them totally resistant to immunosuppression by low level TCDD exposure. The importance of the thymus is thus confirmed.
2. Thymus function declines with age. We found that 8-month old TCDD-sensitive mice that had achieved 20%-25% of their life span (roughly equivalent to a 15- to 17-year old human) were readily suppressed by 12 pM TCDD, whereas 13-month old mice that had completed approximately 36% of their life span (roughly equivalent to 22- to 28-year old individuals) and 22-month old mice were completely resistant to suppression by TCDD. These data have an interesting parallel in that in the study by Knutsen of humans exposed to 20 - 100 ppb for 2 years (or to 100 ppb for 6 months) in Time's Beach, Mo., evidence of immunosuppression was seen primarily in the group under the age of 18.
3. While TCDD administered orally in food has been shown to suppress CTL generation, a further experiment has indicated that a substantially greater amount of TCDD must be given orally to achieve the same immunosuppressive effects as 12 pM injected parenterally. A preliminary dose-response study suggests that the difference in oral vs parenteral dose required may be on the order of 1000 fold.

These data have significant implications for the setting of zero biological effect exposure limits for different groups of individuals who may be exposed to TCDD and related haloaromatic hydrocarbons by different routes. Further, since the thymus-mediated immunosuppressive effects appear to be reflected in alterations in the surface markers on blood T lymphocytes both in mice and in humans, it may be possible to monitor exposed individuals using a simple non-invasive technique.

QUANTITATIVE ASSESSMENT OF IMMUNOTOXICITY OF HALOAROMATIC HYDROCARBONS: KEY ROLE OF THE THYMUS GLAND IN SUSCEPTIBILITY TO DIOXIN AND IMPLICATIONS FOR DEFINITION OF "NO EFFECT" EXPOSURE LEVELS.

D.A. Clark, G.D. Sweeney, J. Gauldie, Departments of Medicine & Pathology, Host Resistance Program, McMaster University, Hamilton, Ontario, Canada.

2,3,7,8-tetrachlorodibenzo-p-dioxin (TCDD or "dioxin"), a toxic halogenated aromatic hydrocarbon found in the environment, can produce harmful effects on a variety of organs in the body including the liver, nervous system, skin and immune system. The toxic effects appear to be mediated by the binding of TCDD to a "receptor" protein in the cell, the concentration of which is genetically determined. A variety of halogenated aromatic hydrocarbons such as PCB's and PBB's that can bind to this "receptor" with sufficient affinity produce pathological changes similar to those seen with TCDD (reviewed in 1).

We have been particularly interested in the toxic effects of haloaromatic hydrocarbons on the immune system. To study the mechanism of these effects, we have injected TCDD into inbred laboratory mice over a 4 week period and then have tested the animal's immune response. This approach was taken because the immune system of mice is similar to that of man, simple assays exist that enable the different types of immune response of mice to be measured, and mouse strains exist that are relatively "susceptible" or relatively "resistant" to TCDD toxicity due to genetically-determined variation in the affinity of the cellular "receptor" for TCDD. Although the results from our studies have previously been published (2,3), several points deserve reiteration.

1. TCDD-"susceptible" mice such as C57Bl/6 develop suppression of immune function after a dose of 12 pM TCDD (4 parts per trillion). This suppression is restricted to the generation of cytotoxic T lymphocytes (CTL) that play an important role in resistance to viral infections. Antibody responses are spared. We have shown that suppression of the CTL response is due to the induction of suppressor T cells.

2. Immunosuppression occurs at TCDD doses 1000 fold lower than those required to alter liver function. The induction of hepatic enzymes such as arylhydrocarbon hydroxylase and cytochrome $P_1$450 required a substantially larger dose of TCDD (1,3).

3. It has been possible to create 'chimeric mice' by replacing the lymphocytes of the immune system of a TCDD-resistant mouse with bone marrow cells from a TCDD-susceptible strain and vice versa. In these studies, the recipient was irradiated to destroy its immune system and the immune system was restored by grafting bone marrow cells that would differentiate into immunocompetent lymphocytes in the recipient's thymus (2). We found that sensitivity to TCDD depended on the type of recipient host and

not upon the type (TCDD "resistant" or TCDD "susceptible) of cells grafted. We suspected, on the basis of these studies, that the thymus might represent the site at which TCDD acted on the immune system to cause suppression. In support of this concept, two further observations are relevant:

(a) TCDD acts preferentially on epithelial tissues, and thymic epithelium plays an important role in the development of the T cells that regulate the immune system.

(b) TCDD-treated mice show an increased proportion of T cells bearing the surface markers typical of short-lived suppressor cells that are produced by the thymus gland.

Nevertheless, it was still possible that TCDD might have been acting on the immune system to promote suppressor T cell production via radioresistant tissue other than thymus in the chimeras.

To test whether the thymus gland played a key role in mediating suppression by TCDD, we examined the susceptibility of thymectomized C57Bl/6 mice to suppression of CTL generation by 12 pM TCDD. As shown in Table 1, thymectomized C57Bl/6 mice proved to be completely resistant to TCDD. Taken together with the data otained using chimeras, we concluded that TCDD acts via radioresistant thymic epithelium to induce the development of suppressor T cells. Although direct evidence for such a conclusion has not yet been obtained, it has recently been shown that TCDD can act directly on cultured thymic epithelium in vitro to alter lymphocyte responses(4), and that certain epithelial cell lines show altered growth and differentiation when exposed in vitro to TCDD concentrations of 10-20 pM (5,6).

Table 1

Cells Tested	% Suppression of CTL Generation per CTL Precursor (CTLp) by TCDD Treatment	
	Thymectomized	Non-thymectomized Control
Spleen Lymphocytes	0 %	78.6 %**[a]
Lymph Node Lymphocytes	0 %	37.5 %**

a) The yield of CTL precursor was determined in vitro using a culture system described in detail elsewhere (1,2,3). The decrease in yield in TCDD-treated mice compared to mice receiving an injection of vehicle (corn oil) was used to calculate % suppression. ** denotes a statistically significant effect $P < 0.025$.

The thymus gland normally undergoes atrophy with age, and in humans, loses its function by the early 20's. In view of the results shown in Table 1, we asked whether aged mice might be resistant to the effects of TCDD. The age-dependent activity of thymic epithelium can be quantified by the assay of thymic humoral factor (FTS) in the blood, and data had already been published relating this activity to age in C57Bl/6 mice (7). Figure 1 shows the result of our study of CTL/CTLp yield from lymph nodes of TCDD-treated vs control mice that had received only corn oil. It is apparent that susceptibility to suppression by TCDD persisted until about 8 months of age and was then lost. The dotted line shows the activity of thymic epithelial cells as quantified by the titer of circulating thymic hormone level (FTS) (▲) or by the number of FTS-positive cells per 100 microscope fields (■) in the thymus as replotted from (7). It is readily apparent that the loss of susceptibility to suppression with TCDD correlated with age-dependent decline in thymic epithelial activity.

Figure 1

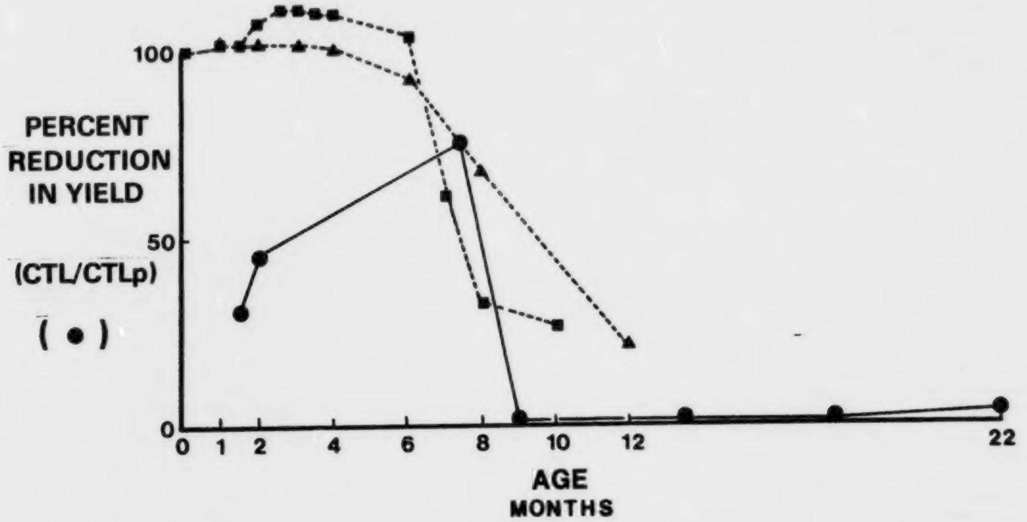

A number of practical implications derive from the result shown in Figure 1. It would be predicted that the group of humans most at risk of immunosuppression by TCDD would be children and adolescents who still have actively functioning thymic epithelial tissue. If one assumes that a 3 year lifespan of a C67Bl/6 mouse corresponds to a 75 year old human, then 7 1/2 month old mice (that are still susceptible to TCDD) would correspond to 15-18 year old humans, and 7-13 month old mice that are resistant to TCDD would correspond to humans aged > 20 years. Whilst it is always difficult to make extrapolations from one species to another, it is interesting that in the immunological evaluation of humans exposed to TCDD in Times Beach, Missouri, (20-100 ppb over 2 years or 100 ppb for six months), it was those persons under the age of 17 who showed immunological abnormalities (8,9). Further, a proportion of individuals exposed to low dose TCDD in Times Beach showed altered T cell surface markers in their blood similar to the findings we have reported in studies of TCDD-treated mice (3,9). Taken together, these data would imply that the no-effect exposure level for TCDD may be substantially higher in adults as compared to children and adolescents; this has implications for the definition of "safe levels" of TCDD exposure in the workplace. However, dependence of susceptibility to suppression by low dose TCDD on the thymus does not imply absolute resistance to immune system effects in thymus-deficient persons. In mice, higher doses of TCDD can exert direct suppressive effects on those lymphocytes that produce antibodies (10). The effects of higher doses of TCDD in thymus-deficient and aged mice has not yet been tested. Studies on aged mice would be valuable in prediting susceptibility of adult humans to suppression by TCDD and would identify which types of responses should be used to monitor the effects of TCDD-exposure in adults. With respect to younger individuals, the quantitation of circulating suppressor T cells of the 'short lived' variety using surface marker techniques holds the greatest promise as a highly sensitive assay for monitoring exposed individuals.

References

1. Clark, D.A., Gauldie, J., & Sweeney, G.D. 1983. Suppression of Immune Defences by Halogenated Aromatic Hydrocarbons. In Proc.. Technology Transfer Conference #4. Ministry of Environment of Ontario, ISBN-0-7743-8797-1, p.301.

2. Nagarkatti, P.S., Sweeney, G.D., Gauldie, J., & Clark, D.A. 1984. Sensitivity to suppression of cytotoxic T cell generation by 2,3,7,8-tetrachlorodibenzo-p-dioxin is dependent on the Ah genotype of the murine host. Toxicol. & Appl. Pharmacol. 12:169.

3. Clark, D.A., Sweeney, G.D., & Gauldie, J. 1985. Dose response, time-course, and mechanism for suppression of cytotoxic T cell generation by 2,3,7,8-tetrachlorodibenzo-p-dioxin. In Banbury Report #18: Biological Mechanisms of Dioxin Action. (A. Poland & R.D. Kimrough, eds.) Cold Springarbor Laboratories, p. 421.

4. Greenlee, W.F., Dold, K.M., Irons, R.D. & Osborne, R. 1985. Evidence for a direct action of 2,3,7,8-tetrachlorodibenzo-p-dioxin on thymic epithelium. Toxicol. Appl. Pharmacol. 79:112.

5. Gierthy, J.E. & Crane, D. 1984. Reversible inhibition of *in vitro* epithelial cell proliferation by 2,3,7,8-tetrachlorodibenzo-p-dioxin. Toxicol. Appl. Pharmacol. 74:91.

6. Dencker, L., Hassoun, E., D'Argy, R. & Alm, G. 1985. Fetal thymus organ culture as an *in vitro* model for the toxicity of 2,3,7,8-tetrachlorodibenzo-p-dioxin and its congeners. Molec. Pharmacol. 27:133.

7. Savind, W., Dardenne, M. & Bach, J.F. 1983. Thymic hormone containing cells. II. Evolution of cells containing serum thymic factor (FTS or thymulin) in normal and autoimmune mice as revealed by anti-FTS monoclonal antibodies. Relationship with Ia bearing cells. Clin. Exp. Immunol. 52:1.

8. Kimbrough, R.D. 1984. The epidemiology and toxicology of TCDD. Bull. Environ. Contam. Toxicol. 33:636.

9. Knutson, A.P. 1984. Immunologic effects of TCDD exosure in humans. Bull. Environ. Contam. Toxicol. 33:673.

10. Luster, M.I., Tucker, A.N., Hong, L., Patterson, R. & Greenlee, W. 1984. *In vivo* and *in vitro* effects of tetrachlorodibenzo-p-dioxin (TCDD) on B cell and stem cell differentiation. J. Leuk. Biol. 36:392.

THE RAPID SCREENING OF MUNICIPAL REFUSE INCINERATOR FLY-ASH AND STACK GAS FOR PCDD/PCDF USING A TRANSPORTABLE TANDEM MASS SPECTROMETER (GC/MS/MS) SYSTEM

Bori I. Shushan[1], Angie Ngo[1], V. Osvacic[2], G. Wong[2],
G. DeBrou[2], B. Bobbie[2] and R.E. Clement[2]

[1]SCIEX
[2]Ministry of the Environment

Key words: Refuse, Incineration, Flyash, Stack Gas, Dioxins, Furans, GC-MS.

ABSTRACT

The formation of polychlorinated dibenzo-p-dioxins and dibenzofurans (PCDD/PCDF) is strongly linked to the incineration of municipal refuse. To date, there has been no study which demonstrated clearly what, if any , incinerator operation parameter(s) this production correlates with. Part of the problem in determining such correlations is that testing for PCDD/PCDF is an expensive and time-consuming effort. This paper describes a rapid analytical approach using gas chromatography (GC) coupled to tandem triple quadrupole mass spectrometry (MS/MS). This combination has been demonstrated to be more specific than conventional GC/MS while requiring less time per analysis. Furthermore, the instrument used in the present work (the TAGA 6000E manufactured by SCIEX) is fully transportable, permitting it to be driven to the incinerator for rapid on-site PCDD/PCDF analysis. The analysis of fly-ash and stack gas will be described and analytical results compared to GC/MS analyses performed on the same samples.

THE RAPID SCREENING OF MUNICIPAL REFUSE INCINERATOR FLY-ASH AND STACK GAS FOR PCDD/PCDF USING A TRANSPORTABLE TANDEM MASS SPECTROMETER (GC/MS) SYSTEM: I. FLY-ASH

B. Shushan and A. Ngo., SCIEX®, Thornhill, Ontario
V. Ozvacic, G. Wong, G. DeBrou, B. Bobbie, and R.E. Clement,
Ontario Ministry of the Environment, Toronto, Ontario
B. Chittum, Wellington Environmental Consultants, Guelph, Ontario

INTRODUCTION

The incineration of municipal refuse for the purposes of energy recovery has been linked to the production of undesirable by-products notably polychlorinated-dioxins and -dibenzofurans (PCDD/PCDF). Since these substances are found in incinerator stack gases and fly-ash in miniscule amounts, methods for the analysis of these trace chemicals must therefore be sensitive and selective. This is currently accomplished by time and resource consuming wet chemical clean-up steps followed by gas chromatography mass spectrometric (GC/MS) analysis. The goal of obviating the time and resource consuming clean-up stages by using more specific analytical methods is a desirable one since much of the cost for such sample analyses is in these clean-up stages. Furthermore, if analyses could be performed more cheaply and faster, more information could be gained which would lead to a better understanding of the processes involved in the formation of substances like PCDD/PCDF.

The goals of the present work were to investigate GC/MS/MS analysis of rapidly derived extracts of municipal refuse incinerator fly-ash. Tandem mass spectrometry (MS/MS) has demonstrated high specificity for the analysis of trace substances and since its introduction of the world's first commercially available tandem triple quadrupole MS/MS system, SCIEX® has been involved in investigating novel ways of applying this new technology to solve problems in trace chemical analysis more rapidly. This type of development work has been carried out by SCIEX® in the past for the analysis of tetrachlorodibenzodioxin (TCDD) in soils under contract with the US-EPA (Region VII) and for the detection of polychlorinated biphenyls (PCBs) in stack gases under contract with MOE for example.

The scope of work performed by SCIEX® in this study was to:

(i) Develop a rapid "jar"-extraction* method for municipal refuse incinerator fly-ash which: (a) has the highest possible relative extraction efficiencies, (b) requires minimum sample handling, and (c) is amenable to GC/MS/MS analysis;

(ii) Determine whether crude (i.e. rapidly derived) fly-ash extracts exhibit interferences during GC/MS/MS analysis;

(iii) Compare "jar"-extraction efficiencies with those of conventional (Soxhlet) extraction methods using a variety of fly-ash types; and

(iv) Determine the reproducibility of the procedure.

EXPERIMENTAL

Three types of fly-ash samples were used in this development program: types C (Commissioner Street), A (Ashbridges Bay) and S (SWARU). Jar-extract method development was carried out using a sample of well characterised fly-ash of type C supplied to SCIEX® by MOE-LSB. This was used to ascertain which solvent systems supplied the best relative extraction efficiencies. The absolute extraction efficiencies would be tested by comparing jar-extracts to extracts derived by conventional 18h Soxhlet extraction methods. The conventional extracts were supplied by MOE-LSB and the other contract laboratory (Wellington Environmental Consultants (WEC)) involved in this study.

---

* The term "jar"-extraction means simply a method of extraction requiring only the mixing of the matrix (fly-ash) with a suitable extracting solvent and mixing prior to analysis.

An extracting solvent comprised 2 parts toluene and 1 part methanol was found to provide relatively good extraction efficiencies for the majority of PCDD/PCDF congeners (see Figures 1 and 2). A flow chart for the jar-extraction procedure is provided in Figure 3.

The tandem mass spectrometer used in the present work was the TAGA® 6000E tandem triple quadrupole MS/MS system manufactured by SCIEX®. A GC is directly coupled to the MS/MS system's ion source for sample introduction. The ion source is a Glow Discharge ion source at 200°C which uses Zero Air as the reagent gas at 35 ml/min flow providing a source pressure of some 1 Torr. The N_2/O_2 reagent gas mixture provides an efficient charge transfer medium for the ionization of aromatic hydrocarbons such as PCDD/PCDF while the oxygen acts in a cleansing fashion keeping ion source parts clean by "burning" off carbon deposits. Thus, crude extracts can be analyzed without having to clean the ion source after use. The discharge current was 1.2 mA and the molecular ions created in the source and selected by Quadrupole 1 (the first mass spectrometer) were fragmented in the quadrupole collision cell (Quad 2) by 65 eV collisions with Argon at 4×14^{14} atoms/cm^2 target gas thickness (see Schematic Figure 4). Daughter ions, specific to PCDD/PCDF are mass selected in Quadrupole 3 and detected by pulse counting. The GC conditions are outlined in Table 1. A summary of GC/MS/MS analytical conditions is found in Table 2. The ^{13}C-PCDD/PCDF labelled components were added in the jar-extraction procedure in known amounts and act as internal standards for quantitation purposes. GC/MS/MS data were acquired 6.5 minutes into the GC run after injection of the crude jar extract. As Table 2 summarises, there were 7 groups of Q1/Q3 parent ion/daughter ion pairs covering the whole range of PCDD/PCDF congeners and the isotopically labelled internal standards. The quadrupole mass spectrometer settings and all other instrumental parameters are under computer control. The times for switching ion sets were determined by injection of a previously analysed fly-ash extract. This type of GC/MS/MS analytical procedure is termed multiple reaction monitoring (MRM) since the instrument is detecting the products of collisionally activated decomposition (CAD) ion-molecular reactions occurring between the mass resolving quadrupoles. The detection limits for the GC/MS/MS system are summarized in Table 3 and were found to be in the sub picogram (pg) to 3 pg range for the injection of PCDD/PCDF standards.

The jar-extraction efficiencies were compared to conventional extraction methods for fly-ash sample C1 and the result is shown in Table 4. The relative extraction efficiency was reasonably good for the lower chlorinated congeners but dropped off rapidly as the degree of chlorination increased.

The reproducibility of the techniques was demonstrated by analysing three C4 jar-extracts. The results are summarized in Table 5 and demonstrate an average standard deviation of ±11%.

In addition to the test of analytical reproducibility, QA/QC samples, comprised of crude and cleaned-up extracts of C1 and S1 fly-ash samples (derived by conventional extraction methods and furnished by MOE-LSB (lab A) and WEC (lab B) respectively) were analysed by GC/MS/MS and the results compared (see Table 6).

QA/QC sample handling protocols are summarised in Table 7. The C1 and S1 samples were provided to SCIEX® in a significantly preconcentrated state unlike the jar-extracts which were run without significant preconcentration. Thus the "S1" QA/QC sample detection limits were relatively low (Table 6) since 20 mg equivalents of fly-ash (per ul) were injected for GC/MS/MS analysis compared to 1.8 mg equivalents for the "C1" QA/QC sample and 0.375 mg equivalents for all jar-extract samples. In fact, the significant levels of PCDD/PCDF in the S-type fly-ash sample shown in Table 6 went undetected in the jar-extract of the same sample, due primarily to this concentration factor and secondarily to the fact that the S-type fly-ash presented a difficult matrix to extract PCDD/PCDF using the jar-extraction method. No PCDD/PCDF were detected for A-type fly-ash samples.

The levels of PCDD/PCDF between crude and cleaned-up conventional extracts of C1 and S1 shown in Table 6 indicate that both the other participating laboratories (MOE-LSB and WEC) produced extracts comprising comparable levels of PCDD/PCDF even though their degree of clean-up was substantially different, i.e. MOE-LSB supplied a crude extract (no clean-up) while WEC took its extract through an extensive clean-up procedure. The fact that the GC/MS/MS results showed comparable levels for both crude and cleaned-up extracts (for C1) indicates that the GC/MS/MS analytical technique is unperturbed by the other chemical constituents which make up the bulk of the fly-ash matrix.

CONCLUSIONS

The jar-extraction procedure followed by GC/MS/MS analysis is a rapid technique for the determination of PCD/PCDF in fly-ash requiring less than 2 hours per sample. Although the reproducibility is within reasonable limits (± 11%) the extraction efficiencies for C-type fly-ash samples were somewhat lower than those of conventional methods. The extraction efficiencies were found to be inversely proportional to the degree of chlorination and ranged from 75% for dichloro- species to 24% for octachloro-species. Not all fly-ash samples were amenable to the jar-extraction procedure. Type S fly-ash exhibited much lower extraction efficiencies and was, upon visual inspection, higher in carbon content. The crude C- and S- type extracts derived by conventional extraction exhibited no significant interferences when run by GC/MS/MS which bodes well for eliminating clean-up steps. Furthermore, the fact that the TAGA® 6000E MS/MS system is capable of transport within a mobile laboratory makes the jar-extraction GC/MS/MS analytical scenario amenable to on-site determinations of PCDD/PCDF at their source of production. Unfortunately, the other phase of this program, the analysis of municipal refuse incinerator stack gas samples, is currently on-going and cannot be reported on at this time.

The results of the first phase of this research program were, however, positive enough to represent a significant increase in analytical capability in the area of PCDD/PCDF analysis. The cooperation between the MOE and SCIEX® has contributed substantially to the applications' development of tandem triple quadrupole GC/MS/MS technology, an example of high-technology analytical equipment manufactured in Ontario. This research has benefited SCIEX® by expanding the application base of its technology as well as providing a more rapid and cheaper method of determining dangerous environmental contaminants such as PCDD/PCDF.

FIGURE 1.
Jar Extraction: Fly Ash

Methanol Content vs. Extraction Efficiency for PCDD

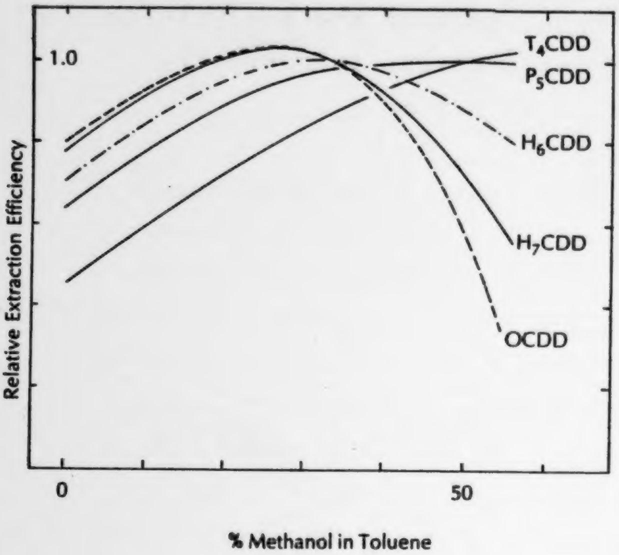

FIGURE 2.
Jar Extraction: Fly Ash

Methanol Content vs. Extraction Efficiency for PCDF

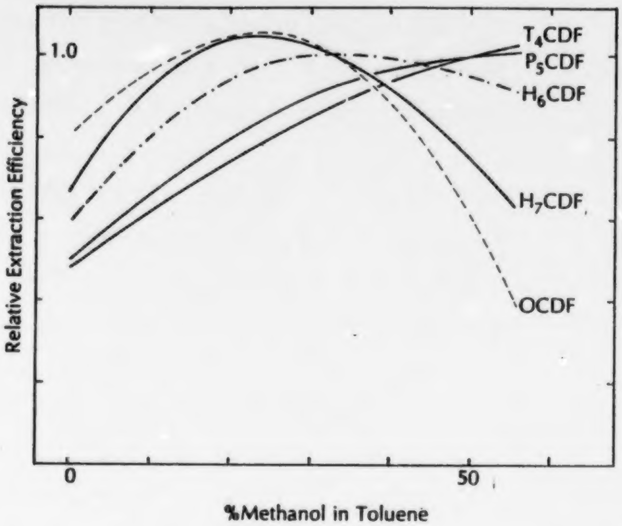

FIGURE 3.
FLOW CHART OF THE "JAR EXTRACTION" PROCEDURE FOR FLY ASH

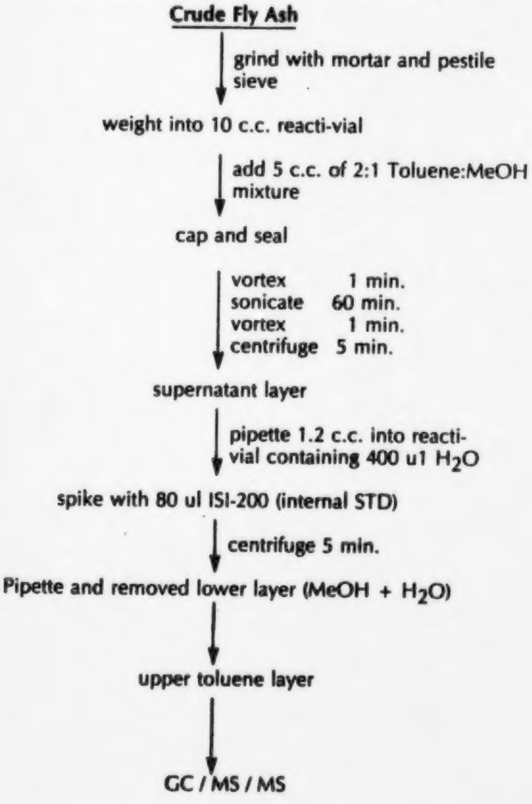
Crude Fly Ash
grind with mortar and pestile
sieve
weight into 10 c.c. reacti-vial
add 5 c.c. of 2:1 Toluene:MeOH
mixture
cap and seal
vortex 1 min.
sonicate 60 min.
vortex 1 min.
centrifuge 5 min.
supernatant layer
pipette 1.2 c.c. into reacti-
vial containing 400 u1 H$_2$O
spike with 80 ul ISI-200 (internal STD)
centrifuge 5 min.
Pipette and removed lower layer (MeOH + H$_2$O)
upper toluene layer
GC / MS / MS

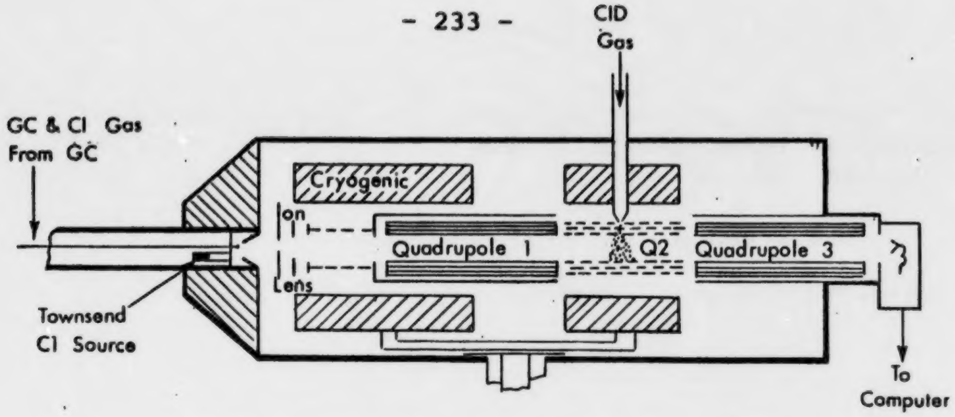

FIGURE 4. Schematic of the TAGA 6000E GC/MS/MS system.

TABLE 1: Gas Chromatography Conditions

GC: HP5840A

Injector: Grob-type, splitless, capillary

Column: 15 m., DB-5 capillary (J & W), 0.32 mm. ID

GC Operating Conditions:
- Injection volume: 1.0 ul with 1.2 ul syringe wash
- Carrier gas: N_2, 15 psig
- Injector temperature: 250°C.
- Capillary split / sweep: Open after 0.5 min.
- GC / MS / MS interface temperature: 280°C.

Temperature Program:
- Initial temperature: 100°C.
- Initial time: 0.5 min.

Level I:
- Program rate: 20°C. / min.
- Final temperature: 160°C.
- Final time: 0 min.

Level II:
- Program rate: 10°C. / min.
- Final temperature: 280°C.
- Final time: 5 min.

TABLE 3: Results of Fly Ash Jar Extract Analysis (GC / MS / MS): Detection Limits

Congener	Reagent Blank[a] (pg)	Estimated Detection Limit[b] (pg)
PCDFs:		
D_2CDF	<0.7	0.8
T_3CDF	<0.4	0.5
T_4CDF	<0.4	0.5
P_5CDF	<0.9	1.0
H_6CDF	<1.2	1.4
H_7CDF	<1.6	1.8
OCDF	<1.9	2.1
PCDDS:		
D_2CDD	<0.5	0.6
T_3CDD	<0.5	0.6
T_4CDD	<0.7	0.8
P_5CDD	<1.2	1.4
H_6CDD	<1.4	1.6
H_7CDD	<2.7	3.0
OCDD	<2.1	2.4

---

a - based on detection limits and an injection size of 0.375 mg - equivalents of fly ash

b - pg of a single isomer injected for response of 3 times the standard deviation

TABLE 2: GC / MS / MS Analysis Summary

	Congener	Q1 (m/z)[a]	Q3 (m/z)	Dwell[b]	Time (sec.)
Group I	D_2CDF	238	175	200	54
	D_2CDD	252	189		
Group II	T_3CDF	270	207	200	49.2
	T_3CDD	286	223		
Group III	T_4CDF	304	241	100	66
	T_4CDD	320	257		
	$^{13}C_{12}$-T_4CDF	316	252		
	$^{13}C_{12}$-T_4CDD	332	268		
Group IV	P_5CDF	340	277	200	79.2
	P_5CDD	356	293		
Group V	H_6CDF	374	311	100	72
	$^{13}C_{12}$-H_6CDF	386	322		
	H_6CDD	390	326		
Group VI	H_7CDF	408	345	200	63
	H_7CDD	424	361		
Group VII	OCDF	442	379	200	36
	OCDD	458	395		
	$^{13}C_{12}$-OCDD	470	406		

---

a - nominal mass setting

b - dwell time at Q1 / Q3 mass setting; milliseconds

TABLE 4:

Comparison of PCDD/PCDF Levels for Jar - and Conventional Extraction Methods Using C1 Fly Ash and GC / MS / MS

Congener	Sample and Concentration (ppb)		
	C1 (Jar Extract)[a]	C1 (Conventional)[a]	Relative Extraction Efficiency (%)
PCDFs:			
D_2CDF	97	128	76
T_3CDF	154	207	74
T_4CDF	142	273	52
P_5CDF	146	355	41
H_6CDF	391	1071	37
H_7CDF	138	400	35
OCDF	40	169	24
PCDDs:			
D_2CDD	24	40	61
T_3CDD	58	123	48
T_4CDD	210	603	35
P_5CDD	260	936	28
H_6CDD	420	1695	25
H_7CDD	613	2486	25
OCDD	234	1167	20

a - crude extract analysed

TABLE 5:

Results of Fly Ash Jar Extract Analysis (GC / MS / MS): Reproducibility

Congener	Sample and Concentration (ppb)[a,b]			
	C4 N° 1	C4 N° 2	C4 N° 3	Average + S.D.
PCDFs:				
D_2CDF	151	148	168	156 ± 11
T_3CDF	285	279	322	295 ± 23
T_4CDF	369	348	388	368 ± 20
P_5CDF	413	303	334	350 ± 57
H_6CDF	758	715	780	751 ± 33
H_7CDF	162	146	136	148 ± 13
OCDF	36	32	38	35 ± 3
PCDDs:				
D_2CDD	62	73	102	79 ± 21
T_3CDD	343	283	301	309 ± 31
T_4CDD	1161	886	1193	1080 ± 169
P_5CDD	1182	965	955	1034 ± 128
H_6CDD	1272	895	1101	1089 ± 189
H_7CDD	816	775	701	764 ± 58
OCDD	255	219	232	235 ± 18
				Average S.D. + 11%

a - Sum of isomers in congener series (ug / kg.)

b - 0.375 mg. — equivalent of Fly Ash injected.

TABLE 6:

Results of QA / QC Sample Analyses by (GC / MS / MS): Comparison of Cleaned-up and Non Cleaned-up Extracts

Congener	Sample and Concentration (ppb)[a,c]					
	"C" Detection Limits	C1[d] (A)	C1[e] (B)	"S" Detection Limits	S1[d] (A)	S[e] (B)
PCDFs:						
D_2CDF	0.44	128	97	0.04	11.3	18.8
T_3CDF	0.29	207	174	0.03	14.4	33.3
T_4CDF	0.29	273	267	0.03	11.9	30.5
P_5CDF	0.56	355	524	0.05	11.9	33.7
H_6CDF	0.78	1071	1160	0.07	25.5	43.9
H_7CDF	1.00	400	537	0.09	5.0	12.4
OCDF	1.17	169	177	0.11	2.6	2.7
PCDDs:						
D_3CDD	0.33	40	28	0.03	2.9	2.2
T_3CDD	0.33	123	115	0.03	13.6[b]	5.5
T_4CDD	0.44	603	643	0.04	7.4	17.4
P_5CDD	0.78	936	1353	0.07	7.9	21.8
H_6CDD	0.89	1695	1908	0.08	11.6	31.1
H_7CDD	1.67	2486	3410	0.15	13.3	34.3
OCDD	1.33	1167	1196	0.12	4.8	9.1

a - based on 3-sigma response and 1.8 and 20 mg-equivalent of Fly Ash injected for "C" and "S" samples respectively (units of ppb in Fly ash).

b - suspected interference.

c - conventional Soxhlet extration.

d - crude extract

e - multi-column clean-up

TABLE 7: QA / QC Samples

Fly Ash (Lab) Type	Fly Ash Equivalents As Received	Fly Ash Equivalents As Analyzed[a]	Cleanup	Additional Spike[b]
S1 (A)	20 mg/ul	20 mg/ul	No	No
S1 (B)	100 mg/ul	20 mg/ul	Yes	No
C1 (A)	20 mg/ul	1.8 mg/ul	No	Yes
C1 (B)	2 mg/ul	1.8 mg/ul	Yes	Yes

---

a - All samples with the exception of S1 (A) required dilution before GC / MS / MS.

b - The C1 sample required an additional spike of isotopically labelled internal standards prior to analysis.

BLOOD LEAD AND ASSOCIATED RISK FACTORS IN ONTARIO CHILDREN - 1984

L.F. Smith, C. Duncan and J. O'Heany
Ontario Ministries of Health, Environment and Labour

Key words: Blood Lead Survey, Lead Exposure, Environmental Health, Exposure Assessment, Air Pollution.

ABSTRACT

Lead exposure from the external environment as well as the home has received much attention in the past decade. In the absence of information on the blood lead levels of Ontario children who are not exposed to a known source of industrial emissions, the Ministries of Labour, Environment and Health undertook the Ontario Blood Lead Study. The purpose of this study was to determine blood lead levels in Ontario children and to identify those demographic, environmental and lifestyle characteristics related to higher blood lead levels.

1315 children aged 7 and younger in selected urban, suburban, and rural areas of Ontario were sampled for analysis of blood lead. Blood lead concentration was determined in finger prick blood samples by graphite furnace atomic absorption spectrophotometry. Measurement of lead in air where children live, lead in tap water at their school, and lead in soil in areas where they play was carried out. Traffic density was measured at the largest intersection nearest to the children's school. A random sub-sample of 800 families of children tested for blood lead was assessed for the presence of risk factors which may be associated with elevated blood lead concentrations.

Urban children had higher geometric mean blood lead levels (12.0 ± 4.4 ug/dl) than suburban children (10.0 ± 3.5 ug/dl), and they in turn had higher blood lead levels than rural children (8.9 ± 3.9 ug/dl), a statistically significant difference. 4.3% of all children were at or above the alert level of 20 ug/dl; the proportion above the alert level did not differ between urban, suburban and rural children. Blood lead levels were slightly higher for males than females and for pre-schoolers aged 3 and 4, compared to school age children aged 5 and 6. The distribution of blood lead levels among these children was lower than that of children in point source areas.

Multivariate statistical modelling resulted in a set of characteristics which best explained the differences in children's blood lead levels: younger age, lower family socio-economic status, hot water radiator heating in the home, number of gas stations within six blocks of residence, number of industries within six blocks of residence, residence within one block of a major highway, and geographic site (Toronto, Windsor, Etobicoke, Scarborough, Longwoods, Nanticoke-Walpole). Environmental measurements of lead in air and soil, together with neighbourhood traffic density, were equivalent to "geographic site" in their ability to predict variations of blood lead levels among children. These environmental measurements and neighbourhood characteristics were meaningful surrogates for "site" in being able to estimate the potential contribution to the lead burden of children.

Five of the seven factors most closely related to children's blood lead levels are measures of lead in the physical environment. The prime contributor to air lead in the areas tested was lead in gasoline. Reduction of lead in leaded gasoline may be expected to produce some reduction of blood lead levels in children in Ontario.

BLOOD LEAD AND ASSOCIATED RISK FACTORS IN ONTARIO CHILDREN 1984

Introduction and Background

Lead exposure from the external environment as well as the home has received much attention in the past decade. In the absence of information on the blood lead levels of Ontario children who are not exposed to a known source of industrial emissions, the Ministries of Labour, Environment and Health undertook the Ontario Blood Lead Study. The purpose of this study was to determine blood lead levels in Ontario children and to identify those demographic, environmental and lifestyle characteristics related to higher blood lead levels.

The study was designed to sample for blood lead, 1600 children, ages six and under, and to assess by interview 800 families (assuming a 50% consent rate), for the presence of demographic, residential, environmental, and lifestyle factors which may be associated with blood lead levels.

Study sites were selected by the Ministry of the Environment as representative of urban, suburban, and rural environments without point sources of lead emissions and in close vicinity to an ambient air monitoring station.

Four to six schools in each of six sites were chosen: Toronto, Windsor, Scarborough, Etobicoke, Nanticoke-Walpole and Longwoods. First grade, junior and senior kindergarten children and younger siblings were accessed through the schools.

Measurement of lead in air where children live, lead in tap water at their school, and lead in school soil in areas where they play was carried out. Traffic density was measured at the largest intersection nearest to the children's school.

The proportion of lead in air generated from leaded gasoline was calculated for five of the six sites. Measurements for the Scarborough site were not available.

A total of 1,315 children, aged seven and younger in selected urban, suburban, and rural areas of Ontario were sampled for analysis of blood lead. Of these, 1,269 were ages six and under. Blood lead concentration was determined in duplicate finger prick blood samples by graphite furnace atomic absorption spectrophotometry.

A random sub-sample of 800 families of children tested for blood lead was assessed for the presence of risk factors which may be associated with elevated blood lead concentrations.

RESULTS

ENVIRONMENTAL MEASUREMENTS:

Water Lead

Water lead levels were uniformly low. There were no differences in lead concentrations among sites tested. The highest reading was 18 ug/L with all other values being from <1 to 7 ug/L. No water lead level was above the Ontario maximum allowable concentration for lead in drinking water (50 ug/L). Geometric means for first and second draw samples are shown in Table 1.

TABLE 1: WATER LEAD LEVELS FOR ALL SITES

	GEOMETRIC MEAN (ug/L) FIRST DRAW	SECOND DRAW
Windsor	2.5	1.8
Toronto	11.4	2.9
Scarborough	12.8	1.2
Etobicoke	8.0	5.0
Nanticoke-Walpole	7.1	1.2
Longwoods	9.6	1.3

Air Lead

Air lead levels, shown in Table II, were different for each site. Each site was intended to be representative of urban, suburban and rural air lead levels.

TABLE II: AIR LEAD LEVELS FOR ALL SITES

	NO. OF MONTHS SAMPLED	GEOMETRIC MEAN (ug/m^3)
Windsor	5	.2
Toronto	5	.7
Scarborough	5	.2
Etobicoke	5	.2
Nanticoke-Walpole	4	.1
Longwoods	4	.1

The differences among urban (.4 ug/m^3), suburban (.2 ug/m^3) and rural (.1 ug/m^3) air lead levels are significantly different. All levels in this study were below the Ministry of the Environment's air quality criterion of 2.0 ug/m^3 calculated as a geometric mean for a 24-hour period.

Soil Lead Levels

Soil lead levels were significantly different among urban, suburban and rural sites, although all levels were relatively low, and the differences not clear cut when individual sites are considered. The Ontario Ministry of the Environment's "upper limit of normal" contaminant guidelines for lead in soil are 500 ppm fcr urban locations and 150 ppm for rural locations. Rural Nanticoke-Walpole was slightly higher than suburban Scarborough while suburban Etobicoke was slightly lower than rural Longwoods. However, Nanticoke- Walpole readings were elevated because of the unusually higher readings of two Dunnville schools. When there were excluded, Nanticoke-Walpole soil lead levels were in keeping with the Longwoods (rural) site. Levels are shown in Table III.

TABLE III: SOIL LEAD LEVELS

	GEOMETRIC MEAN (ug/gm, dry-weight) (sandy soils excluded)
Windsor	72
Toronto	54
Scarborough	22
Etobicoke	20
Nanticoke-Walpole	42
Longwoods	15
Nanticoke-Walpole (excluding Dunnville)	16

Lead in Air Attributable to Leaded Gasoline

The proportion of air lead attributable to leaded gasoline varied by site with higher proportions in more heavily urbanized and higher traffic density areas: 67% ± 5% in Nanticoke-Walpole, 77% ± 5% in Etobicoke, 85% ± 5% in Toronto and 80% ± 5% in Windsor.

Blood Lead Levels in Children

Urban children had higher geometric mean blood lead levels (12.0 ± 4.4 ug/dl) than suburban children (10.0 ± 3.5 ug/dl), and they in turn had higher blood lead levels than rural children (8.9 ± 3.9 ug/dl), a statistically significant difference. Results are summarized in Table IV.

Blood lead levels were slightly higher for males than females and for pre-schoolers aged 3 and 4, compared to school age children aged 5 and 6. The distribution of blood lead levels among these children was lower than that of children in point source areas.

Information obtained from the sample of 800 families interviewed for risk factor assessment was used in the subsequent statistical analysis. Nearly 100 risk factors were assessed.

When analysed one-by-one, many characteristics were associated with blood lead levels and they follow:

- Age;
- Sex;
- Socioeconomic Status;
- Type of Heating;
- Presence of a fireplace;
- Presence of an air filter;
- House vs apartment;
- Type of flooring in child's room;
- Condition of paint in child's room;
- Type of flooring in child's favourite play area;
- Number of major industries within six blocks;
- Number of four lane roads within one block;
- Number of minor highways within one block;
- Number of major highways within one block;
- Number of major industries within one block.

When assessed in more complex models, several risk factors lost significance while others continued to be predictors of higher blood lead levels.

Multivariate statistical modelling resulted in a set of characteristics which best explained the differences in children's blood lead levels:

- Age;
- Family socioeconomic status;
- Heating in home;
- Number of gas stations within six blocks of residence;
- Number of industries within six blocks of residence;
- Residence within one block of a major highway;
- Geographic site (Toronto, Windsor, Etobicoke, Scarborough, Longwoods, Nanticoke-Walpole).

These characteristics were able to explain 20% of the variance in children's blood lead levels.

When actual measurements for lead in air, soil and neighbourhood traffic density were substituted for "site" in the statistical model, residence within one block of a major highway became statistically non-significant and the model could account for 19% of the variance in children's blood lead levels.

Thus, these environmental measurements and neighbourhood characteristics were meaningful surrogates for "site" in being able to estimate the potential contribution of "site" to the lead burden of children.

Five of the eight factors most closely related to children's blood lead levels are measures of lead in the physical environment. The prime contributor to air lead in the areas tested was lead in gasoline.

We concluded from this study that children in typical urban, suburban and rural areas of Ontario had overall blood lead levels lower than children in point source areas (10.36 ± 4.2). Urban children had higher levels than suburban children, and rural children had the lowest levels. Within each area, younger children had higher blood lead levels than older children and boys had higher levels than girls.

Air, water, and soil lead levels were low. But soil and air lead levels varied from site to site with an uban-suburban-rural gradient of high to low.

Lead in air could be attributed in large part to lead in gasoline.

Risk factors which could serve as predictors for blood lead and accounted for 19% of the variability of blood lead levels were socioeconomic status, age, and five factors related to lead in the physical environment: air lead, soil lead, traffic density, and number of gas stations and industries within six blocks of residence.

Dietary intake of lead was not assessed quantitatively and likely contributed significantly to children's lead body burden. It could be expected that the elimination of the environmental sources of lead assessed will produce some decrease in children's blood lead levels. The clinical significance of this potential decrease remains to be evaluated.

TABLE lV

GEOMETRIC MEAN LEVELS AND DISTRIBUTION OF BLOOD LEAD CONCENTRATIONS BY RESIDENCE AMONG SAMPLED ONTARIO CHILDREN AGED SIX AND UNDER

		BLOOD LEAD CONCENTRATION								
	GEOMETRIC MEAN(±SD) (ug/dl)	umol/L	0-.23	.24-.47	.48-.71	.72-.96	.97-1.20	1.21-1.44	≥1.45	Total # Children Tested
RESIDENCE		ug/dl	0-4	5-9	10-14	15-19	20-24	25-29	≥30	
URBAN										
# (%)	12.02(±4.4)		2 (0.5)	112 (28.6)	180 (45.9)	76 (19.4)	15 (3.8)	5 (1.3)	2 (0.5)	392
SUBURBAN										
# (%)	9.95(±3.5)		13 (2.6)	250 (49.3)	194 (38.3)	31 (6.1)	11 (2.2)	5 (1.0)	3 (0.6)	507
RURAL										
# (%)	8.91(±3.9)		27 (7.3)	207 (55.9)	98 (26.5)	25 (6.8)	10 (2.7)	0 (0.0)	3 (0.8)	370
TOTAL										
# (%)	10.36(±4.2)		42 (3.3)	569 (44.8)	472 (37.2)	132 (10.4)	36 (2.8)	10 (0.8)	8 (0.6)	1269

THE DISPERSAL OF AIR PARTICULATES ON A SHORT AND LONG-TERM TIME SCALE

J.D. MacArthur, G.R. Palmer and Xin-Pei Ma
Department of Physics, Queen's University

Key words: Particulates, Air Quality Monitoring, Multielement Analysis, Lead, Air Filters, X-ray Analysis.

ABSTRACT

Two streak filters, having a time resolution of 2 hours, have been used to monitor the air particulates near an intersection in Kingston over a two-week period in June. One filter was placed $\sim$100 m from the intersection while the second was placed $\sim$700 m away in the backyard of a home. The local meteorological conditions were determined with a micro-processor based weather station which formed part of the sampling device. Wind speed and direction, temperature, rainfall and humidity were sampled every 7 seconds and averaged over a half-hour so that the conditions under which the air particulates were collected were known.

The particulates on filters were analyzed for their elemental composition with particle induced X-ray emission (PIXE) using the Queen's Van de Graaff accelerator. Each filter contained a deposit for one week and two of these for the same week, one from each site, have been analyzed. Al, Si, S, Cl, Ca, Cr, Mn, Fe, Cu, Zn, Br and Pb were found in measurable quantities at both sites. The average levels for all the elements except Br and Pb were the same at the two monitoring sites, indicating that elements from natural sources and from fossil fuels are distributed uniformly in this region. Near the intersection, the ratio of Br to Pb was 0.21, indicative of automobile emission. In the backyard, the concentrations of Br and Pb were lower by factors of 4 and 2 respectively. As previously observed, high Pb concentrations (up to 0.6 ug/cm^{2}) correlate strongly with vehicular traffic especially for the station nearer the intersection. There is some indication that the wind velocity, as measured by the station near the intersection, can account for the difference in the high lead levels between the two stations although this is not completely clear. Further evidence for this will be obtained when the filters from the second week are analyzed.

The Dispersal of Air Particulates on a Short and Long Term Time Scale

G.R. Palmer, P.J. Harvey, J.D. MacArthur and Xin-Pei Ma

Department of Physics, Queen's University, Kingston

Two streak filters, having a time resolution of 2 hours, have been used to monitor the air particulates near an intersection in Kingston over a two week period in June. One filter was placed ~ 100m from the intersection while the second was placed ~350 m away in the backyard of a home. The local meteorological conditions were determined with a micro-processor based weather station which formed part of the sampling device. Wind speed and direction, temperature, rainfall and humidity were sampled every 7 seconds and averaged over a half hour so that the conditions under which the air particulates were collected were known.

The particulates on filters were analyzed for their elemental composition with particle induced X-ray emission (PIXE) using the Queen's Van de Graaff accelerator. Each filter contained a deposit for one week and two of these for the same week, one from each site, have been analyzed. Al, Si, S, Cl, Ca, Cr, Mn, Fe, Cu, Zn, Br and Pb were found in measurable quantities at both sites. The average levels for all the elements except Br and Pb were the same at the two monitoring sites indicating that elements from natural sources and from fossil fuels are distributed uniformly in this region. Near the intersection the ratio of Br to Pb was 0.21 indicative of automobile emission. In the backyard the concentrations of Br and Pb were lower by factors of 4 and 2 respectively. As previously observed, high Pb concentrations (up to 0.6 ug/cm2) correlate strongly with vehicular traffic especially for the station nearer the intersection. There is some indication that the wind velocity, as measured by the station near the intersection, can account for the difference in the high lead levels between the two stations although this is not completely clear. Further evidence for this will be obtained when the filters from the second week are analyzed.

Introduction

This project is a continuing study of pollution dispersal on a hourly time scale, specifically the movement of automotive pollutants from a busy traffic zone in Kingston into nearby residential areas. One-week records of air particulates are collected on a moving Nucleopore filter with a time resolution of two hours. This streak sampler incorporates a microprocessor-controlled weather station to record air flow through the filter in addition to wind, rain, humidity, temperature and light intensity at the sampling site. Elemental analysis of the particulates is later performed by particle-induced x-ray analysis (PIXE) using the Van de Graaff accelerator at Queen's University. Details of the streak sampler, weather station and PIXE method have been published (MacArthur and Palmer, 1983, Palmer et al, 1984).

Our previous studies have identified Pb associated with Br in particulates collected at the study area. Although 24-hour averages were well below those in larger cities, on the 2-hour time scale, order of magnitude fluctuations in Pb and Br concentrations were detected.These Pb and Br levels appeared correlated with traffic patterns when winds were favorable for carrying automotive exhaust to the sampler. The Pb was attributed to gasoline combustion since the Br/Pb ratio in the particles matched that in exhaust. A comparison between the streak sampler and a dichotomous sampler was performed to investigate the particle size collected on the streak filter. The study showed the streak sampler collected mainly small (<2.5 um) particles generally considered to be of anthropogenic origin and capable of being injested deep into the lung. Thus it appeared the Pb being detected might be a health concern.

Results

To further study the dispersion of Pb from the traffic zone, a second sampler with accompanying weather station was constructed for the present study. Both samplers were operated for two weeks (June 3-17, 1985) at the sites mapped in Figure 1. One was located beside a school 100 m SW of a busy intersection and 6 m W of the N-S road leading into the intersection while the second was in a residential backyard 350 m SSW of the intersection. The heavy traffic zone of concern is to the NE of the samplers. Both filters from the first week have been analyzed and will be discussed in this paper.

The Importance of Local Wind Measurements.

Often air pollution studies rely on airport weather records taken several km from the sampling site. In the present study of short range dispersion from a local source, wind conditions near ground level at the site were considered responsible for pollutant dispersion. Therefore wind readings 10 m above ground at the Kingston airport, which is 6.5 km W of the study area, were obtained for comparison with wind data recorded simultaneously by the samplers at 1.5 m above ground . All three wind records in Figure 2 reveal higher daytime horizontal winds which accompany increased vertical turbulence and elevated mixing height resulting from solar heating (Stern, 1976).

However, large differences were noted between the airport winds and those at the samplers. The average airport speed for the week was nearly 6 times that at the school which in turn was twice that in the more sheltered backyard. The standard power law expression for the variation of wind speed with sampling height and surface roughness was used to predict the difference between the average speeds. This expression is given as (Stern, 1976, p 411)

$$u_2=u_1*(z_2/z_1)^m \tag{1}$$

where u_1 and u_2 are wind speeds at heights z_1 and z_2 respectively, and m is a constant taken as 0.3 for typical urban surface roughness and neutral atmospheric stability conditions. Using equation (1), only about a factor of 2 difference in average wind speed is expected between the airport and sample sites.

When reduced to N and E components, Figure 3 indicates only weak correlation (r=0.50) between the N components at the airport and school and even less correlation (r=0.39) between the E components. Similar results were obtained between airport wind components and those in the backyard. This comparison between local and prevailing winds stresses the need for on-site meteorological measurements when studying dispersion from localized pollution sources.

Lead Levels

Table 1 presents the elements consistently detected on the filters with corresponding average and maximum concentrations in air throughout the week. Also the minimum detection limits (MDL) for these elements at the school are shown to indicate the confidence levels at which they were detected. The MDL values are calculated as 3*sqrt(background) where background under a peak is defined for one FWHM. The average levels are similar to those previously measured in the study area (MacArthur and Palmer, 1983, Palmer et al, 1984). The average Pb concentration was nearly twice that in the backyard, reflecting the proximity of the school to the traffic zone. Also the average Br/Pb level at the school (0.24) is more representative of that in exhaust (0.12-0.29) than is the ratio in the backyard (0.1). The loss of Br may indicate aging of the exhaust (Paciga et al, 1975).

Figure 4 shows one-week scans of Pb and Br for both filters. The background level of Pb is attributed to general city traffic. High Pb levels at the school show more correlation with east winds than do the levels in the backyard which suggests the fluctuating local Pb source is the traffic zone NE of the school. Also the Pb peaks at the school appeared more correlated to peak periods of traffic than was the case in the backyard. However the Pb peaks rise 5-10 times above background which cannot be attributed entirely to source increases since traffic densities at the intersection increase only about a factor of two during rush hours (Kingston traffic department). Late evening Pb and Br peaks are evident in Figure 4. Such late peaks were not observed in our earlier study at the school however the previous measurements were made in winter before construction of the two 12-story apartment complexes near the school as drawn on Figure 1.

Particle Size

Previous studies (MacArthur and Palmer, 1983) in which the streak sampler was compared to a dichotomous sampler have indicated the streak method collects the small fraction (<2.5 um) of respirable air particulates. To further investigate the size, the school filter was analyzed by scanning electron microscopy (SEM). Very few particles larger than 2.5 um were observed as shown by a typical photo in Figure 5. An average particle diameter of 0.2 um was obtained. The particle density on the photos, combined with the average flow rate of 0.3 l/min through the 2X4 mm collection nozzle, predicts a particle number density in air of $4*10^8/m^3$. Assuming a particle density of 2 g/cm^3 (Stern, 1976, p 88), the mass concentration in air was calculated to be 3 ug/m^3 in accordance with the total average concentrations of 2.7 and 3.8 ug/m^3 from Table 1 detected in the schoolyard and backyard, respectively. This total mass concentration is consistent with that collected in the fine urban particulate fraction composed mainly of S, Pb and Br (Cahill et al, 1977).

Soil Lead

A study was conducted to investigate the Pb levels in soil near the samplers. Soil cores, 1.5 cm in diameter to a depth of approximately 6 cm, were obtained at the school at distances of 1, 6, 15 and 20 m from the adjacent road. The sampler was positioned 6 m from the road. A core was taken in the backyard to obtain a background value and also fine road dust was collected at the school. The cores and road dust were analyzed by PIXE to obtain Pb concentrations in soil at various depths for the two sites. The results are plotted in Figure 6. The relatively low Pb concentration in the road dust may result from vehicle turbulence which forces even large exhaust particles to the roadside (Chock, 1980). The highest Pb levels were in the soil 1 m from the road where the concentration appeared constant throughout the depth sampled. In the core beside the school sampler positioned 6m from the road, the Pb level was lower, with the highest concentration at the surface. At 15 m from the road, Pb levels were reduced to the background value in backyard soil and likely reflect the extent of vehicular turbulence. Moreover the backyard soil, as well as cores furthest from the road, showed no depth profile in the Pb concentration. These measurements showing the decline of soil Pb away from the road and limited penetration of Pb into roadside soil are in general agreement with other studies near roadways (Walter et al, 1977).

Statistical Analyses

Statistical methods including factor analysis, correlation (auto and cross) and multiple regression have been applied to the records of element concentrations and accompanying meteorological scans to further identify sources of the elements detected. Factor analysis (Alpert and Hopke, 1981, Heidam, 1982, Wolff et al, 1985) has been one of the most useful methods for reducing the scans of 15-20 interrelated element and weather variables, into a manageable number (approximately 5) 'factors' or groups of correlated parameters. These independent factors are linear combinations of the original variables. In the procedure all parameter scans are reduced to a matrix of correlation coefficients and a reduced number of factors are deduced which best explain the correlations observed. Each of these independent factors may often be associated with a single pollutant source.

Sources for three major factors were identified from the analysis of the one-week scans at both sites. The rotated (varimax) loadings in which 5 factors were forced on the the school data are presented in Table 2. Factor 1 consisting of Fe, Al, Si, Mn and Ca which were not correlated with either north or east wind components, explained 29.4% of the variance. These elements are associated with "soil". No source could be attributed to factor 2 comprised of Cu and Zn. Pb and Br formed a third factor accounting for 15% of the variance, which as previously discussed, has an "automotive" origin. East winds contributed more to the loading of this group than the north component which is further evidence that the local source of automotive Pb is the traffic zone to the east of the samplers. Factor 4 merely indicates both components contributed to most wind readings. A fifth factor was S which showed strongest correlation ($r=0.42$) with south winds. This sulphur likely arises from "industrial" fossil fuel combustion and is probably partially due to long range transport.

Multiple regression was performed to investigate the parameters contributing to Pb concentrations at both sites. The most successful model was a linear dependence of Pb on The N and E wind components, an equation of the form

$$Pb=a*N +b*E +c \tag{2}$$

where c is a background constant and a and b are coefficients giving the influence of the N and E components, respectively. For the school data the analysis yielded values of 0.008, 0.003 and 0.194 for a, b and c, respectively with corresponding standard errors of 0.002, 0.002 and 0.013. Therefore it appears the east component influences the Pb levels more strongly than does the north component. A similar multiple regression on the backyard data gave a, b and c as 0.003, 0.003 and 0.106 with respective standard errors of 0.001, 0.001 and 0.008. Therefore the backyard Pb is not stongly influenced by either wind component which reflects the greater distance of this sheltered site from concentrated traffic.

To identify periodic trends in the element scans, autocorrelation was applied to the data. Typical autocorrelation plots of Pb and Br are shown in Figure 7 for the school site and similar results were obtained for the backyard. Two peaks indicating 12 and 24-hour periodicities in Pb are evident, however the 12-hour period is significantly reduced for Br. Figure 4 supports this finding in that Br appears relatively lower in the late evening peaks. To investigate this phenomenon further, Br/Pb ratios for the two sites were calculated for the week and these Br/Pb scans were then autocorrelated to search for periodicities in the ratio. A weak periodicity in the ratio was observed at 10-12 hours. This phenomenon of reduced nighttime Br warrants further study since Br in exhaust particulates may be photo-reactive (Paciga et al, 1975).

Studies have been initiated using cross correlation to identify time lags between arrival of pollutant peaks at the samplers. Such time lags may help identify sources. Better time definition in the data is needed, however initial results are encouraging. When scans of "soil" elements such as Si, Ca and Fe at the school were cross correlated against the corresponding records in the backyard, no delays were detected. On the contrary, when scans of Pb were cross correlated between the two sites, a 2-hour delay was discovered. A similar delay was noted when school records of wind speed and Pb levels were cross correlated. Better time definition on future filters will be effected to determine if such delays are significant. Also the time resolution on future filters will be reduced to 0.5 hour to aid in these time delay studies.

Discussion and Future Studies

Several significant observations were made in this report. Airport wind records were shown unsuitable for urban studies of pollutant dispersion from localized sources. This result emphasizes the advantage of the streak filter apparatus with its high time resolution and on-site meteorological station. Further evidence was obtained from SEM studies that the streak sampler collects the small fraction of respirable particulates.

Previously detected Pb was confirmed to be from automotive exhaust. Some progress was made in ascertaining the contribution of local traffic patterns to Pb detected in that the levels were somewhat correlated with winds from the traffic zone. A late evening Pb peak was detected which cannot be explained at this time. Br concentrations associated with this evening peak appear diminished relative to daytime peaks which may be due to "photo-aging" of the exhaust.

Statistical methods, especially factor analysis, were successful in identifying sources of the elements detected. Three major factors were identified. A "soil" component independent of wind was associated with Fe, Al, Si, Mn and Ca. An "automotive" factor consisting of Pb and Br was correlated more with the east wind component than with the north. The third identifiable factor was considered to be of "industrial" origin and consisted of S which correlated best with south winds.

Future studies will concentrate on determining the actual contributions of Pb particulates by the various traffic patterns in the immediate vicinity of the sampling sites by using dispersion modelling. Gaussian plume models (Bullin et al, 1980, Dobbins, 1979, Hamilton Study, 1982) have been successfully applied to dispersion from point, line and area pollution sources which are applicable to the roadways and intersections near the study area. Initial application of these models to the Pb records from this study indicate that a much larger data base of Pb concentrations, wind speeds and insolation values is required before source strengths can be assigned using the models.

References

Alpert D.J. and P.K. Hopke (1981), A Determination of the Sources of Airborne Particles Collected During the Regional Air Pollution Study, Atmos. Envir., 15, 675-687.

Bullin J.A., J.C. Polasek and N.J. Green (1980), Analytical and Experimental Assessment of Highway Impact on Air Quality: Data Analysis and Model Evaluation, Research Report 218-5F, Study 2-8-75-218, Texas Transportation Institute, State Department of Highways and Public Transportation.

Cahill T.A., L.L. Ashbaugh,J.B. Barone, R.A. Aldred, P.J. Feeney, R.G. Flocchini, C.Goodart, D.J. Shadoan and G.W. Wolfe (1977), Analysis of Respirable Fractions in Atmospheric Particulates via Sequential Filtration, J. of A.P.C.A., 27, 675-678.

Chock D.P. (1980), General Motors Sulphate Dispersion Experiment: An Analysis of the Wind Field Near a Road, Boundary Layer Meteorology, 18, 431-451.

Dobbins R.A. (1979), "Atmospheric Motion and Air Pollution", Wiley & Sons, New York.

Hamilton Study (1982), An Assessment of Street Dust and Other Sources of Airborne Particulate Matter in Hamilton Ontario, Ontario Ministry of the Environment, ARB-28-82-ARSP.

Heidam N.Z. (1982), Atmospheric Aerosol Factor Models, Mass and Missing Data, Atmos Envir, 16, 1923-1931.

Kingston Traffic Department, Traffic Counts for Sept, 29, 1982.

MacArthur J.D. and G.R. Palmer (1983), The Dispersal of Air Particulates on a Short and Long Term Basis, Proceedings, Ontario Ministry of the Environment Technology Transfer Conference No 4, 657-679.

Paciga J.J., T.M. Roberts and R.E. Jervis (1975), Particle Size Distributions of Lead, Bromine and Chlorine in Urban Industrial Aerosols, Envir. Sci. and Tech., 9, 1141-1144.

Palmer G.R., J.D. MacArthur and P.P. Wilson (1984), The Dispersal of Air Particulates on a Short and Long Term Basis, Proceedings, Ontario Ministry of the Environment Technology Transfer Conference No 5, 691-716.

Stern A.C. (1976), "Air Pollution" 3rd edition, Vol 1, Academic Press, New York.

Walter R.L., R.D. Willis, W.F. Gutknecht and R.W. Shaw (1977), The Application of Proton-Induced X-Ray Emission to Bioenvironmental Analyses", Nuc. Inst. and Methods, 142, 181-197.

Wolff G.T., P.E. Korsog, N.A. Kelly and M.A. Ferman (1985), Relationships Between Fine Particulate Species, Gaseous Pollutants and Meteorological Parameters in Detroit, Atmos. Envir., 19, 1341-1349.

Table 1

Element concentrations detected on two streak filters during one week

Element	Avg Conc($\mu g/m^3$)		MaxConc($\mu g/m^3$)		MDL($\mu g/m^3$)
	School	Backyard	School	Backyard	at School
Al	0.21	0.32	2.9	9.4	0.05
Si	0.74	1.6	14.0	46.0	0.04
S	0.70	0.92	2.5	5.4	0.03
Cl	0.10	0.07	0.42	0.20	0.02
Ca	0.45	0.39	1.8	4.6	0.03
Cr	0.009	0.01	0.04	0.03	0.01
Mn	0.006	0.01	0.08	0.20	0.01
Fe	0.19	0.36	2.1	6.8	0.01
Cu	0.009	0.004	0.33	0.02	0.002
Zn	0.02	0.02	0.33	0.05	0.002
Br	0.04	0.008	0.16	0.05	0.004
Pb	0.18	0.10	0.65	0.41	0.01
Total	2.7	3.8			

Table 2

Factor analysis of element concentrations and wind components at the school.

ROTATED LOADINGS

	1	2	3	4	5
FE2	0.980	-0.032	-0.087	-0.063	-0.038
AL	0.969	0.016	-0.110	-0.041	-0.114
SI	0.958	0.005	-0.175	-0.012	-0.119
MN	0.873	-0.032	-0.006	0.059	-0.191
CA	0.654	0.041	0.429	-0.169	0.185
CU	0.003	-0.982	-0.019	-0.062	0.046
ZN	0.009	-0.980	0.055	-0.061	0.125
PB	-0.062	0.011	0.958	0.108	0.015
BR	-0.118	-0.050	0.931	0.108	-0.065
NORTH	-0.045	0.069	-0.031	0.902	-0.138
EAST	-0.040	0.061	0.235	0.863	-0.006
CL	0.278	0.031	-0.100	-0.266	-0.723
S	0.029	-0.218	-0.121	-0.099	0.694
CR	-0.069	0.043	0.020	-0.217	0.547

VARIANCE EXPLAINED BY ROTATED COMPONENTS

1	2	3	4	5
4.111	1.990	2.102	1.756	1.445

PERCENT OF TOTAL VARIANCE EXPLAINED

1	2	3	4	5
29.366	14.216	15.017	12.542	10.319

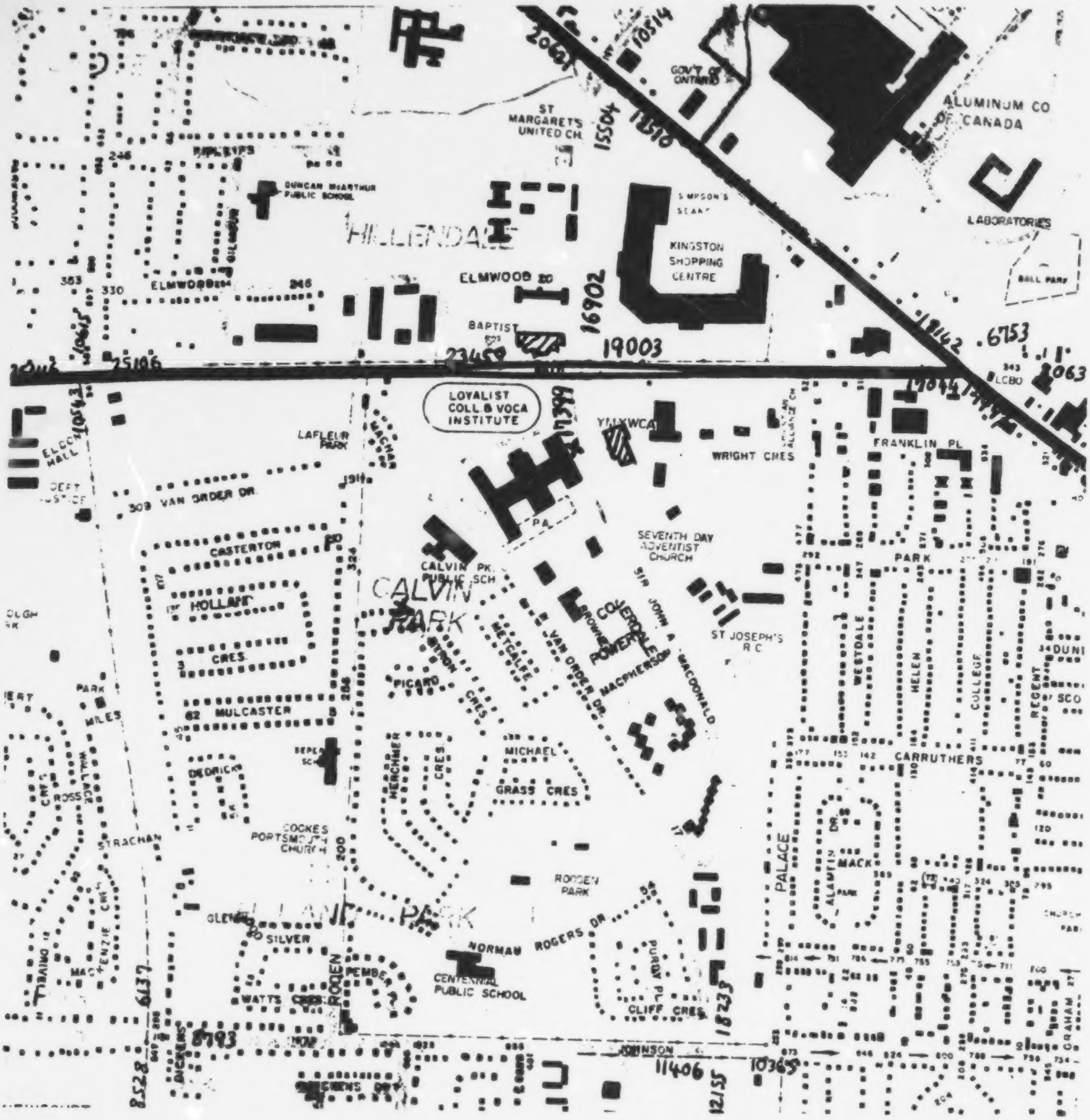
20621
10514
GOV'T OF ONTARIO
ALUMINUM CO OF CANADA
ST MARGARETS UNITED CH.
15504
13510
DUNCAN McARTHUR PUBLIC SCHOOL
HILLENDALE
SIMPSON'S SEARS
KINGSTON SHOPPING CENTRE
LABORATORIES
BALL PARK
ELMWOOD
ELMWOOD RD
BAPTIST
16902
19003
18142
6753
2063
LCBO
25186
23459
LOYALIST COLL. & VOCA INSTITUTE
17399
Y.M.-Y.W.C.A.
LAFLEUR PARK
WRIGHT CRES
FRANKLIN PL
309 VAN ORDER DR.
CASTERTON
HOLLAND
CRES.
MULCASTER
CALVIN PK. PUBLIC SCH
CALVIN PARK
SEVENTH DAY ADVENTIST CHURCH
SIR JOHN A MACDONALD
ST JOSEPH'S R C
PARK
WESTDALE
HELEN
COLLEGE
REGENT
BYRON
METCALFE
E VAN ORDER DR.
POWER
MACPHERSON
PICARD
CRES
MICHAEL
GRASS CRES
HERCHMER
CARRUTHERS
PALACE
ALAMEIN
MACK
DEDRICK
STRACHAN
COCKES PORTSMOUTH CHURCH
RODDEN PARK
HOLLAND PARK
NORMAN ROGERS DR
CENTENNIAL PUBLIC SCHOOL
PURDY PL
CLIFF CRES
18233
RODEN
WATTS CRES
SILVER
PEMBROKE
GRAHAM
JOHNSON
6137
8793
8528
11406
10365
12155
CROSS
MILES

Fig 1 Kingston map showing locations (x) of samplers near center of diagram. North is towards the top and magnification is 1:7480. One sampler was in the schoolyard at Loyalist Collegiate and Vocational Institute, 15 m from the building and 6 m from Sir John A Boulevard; the second was in a residential backyard on Byron Crescent, 350 m to the SW. Average annual daily traffic counts (Kingston traffic department) are written on the major intersections near the samplers. Two 12-story apartment complexes constructed near the school in 1984 are drawn on the map.

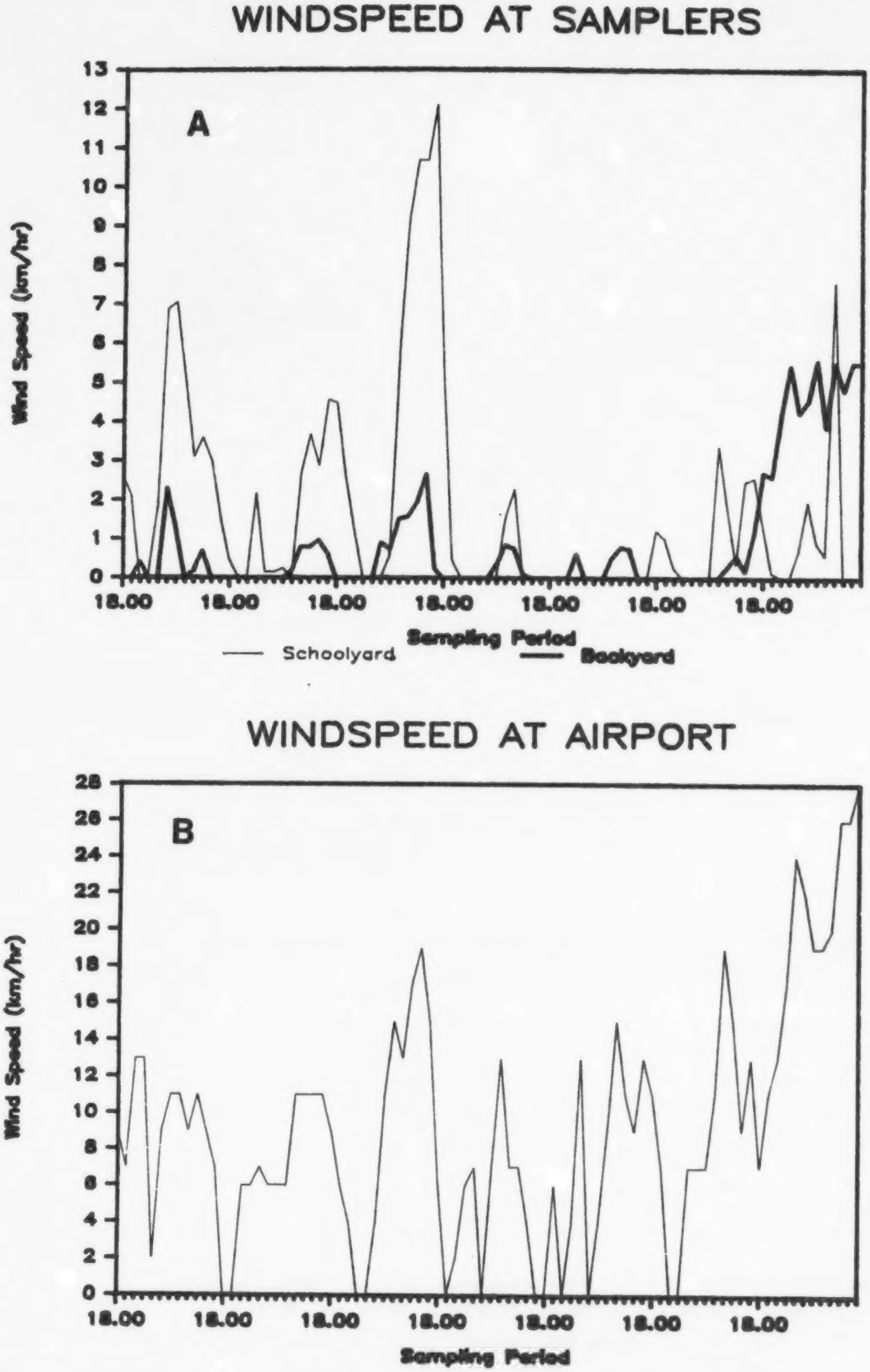

WINDSPEED AT SAMPLERS

WINDSPEED AT AIRPORT

Fig. 2 Comparison of anemometer wind speeds measured a) 1.5m above ground at the samplers in the schoolyard and backyard and b) 10 m above ground at the Kingston airport. Average speeds were 1.8, 0.9 and 10 km/hr at the schoolyard, backyard and airport respectively. Sampling extended from 18:00 hours on Mon June 3 to 18:00 hours on Mon June 10 with 18:00 hours indicated each day.

NORTH COMPONENT OF WIND

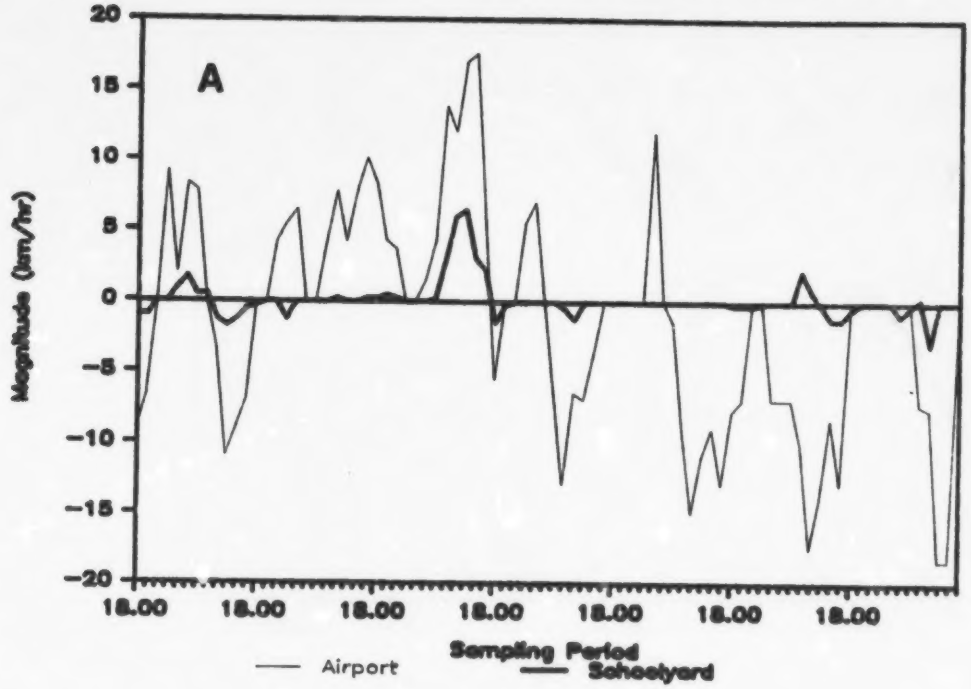

EAST COMPONENT OF WIND

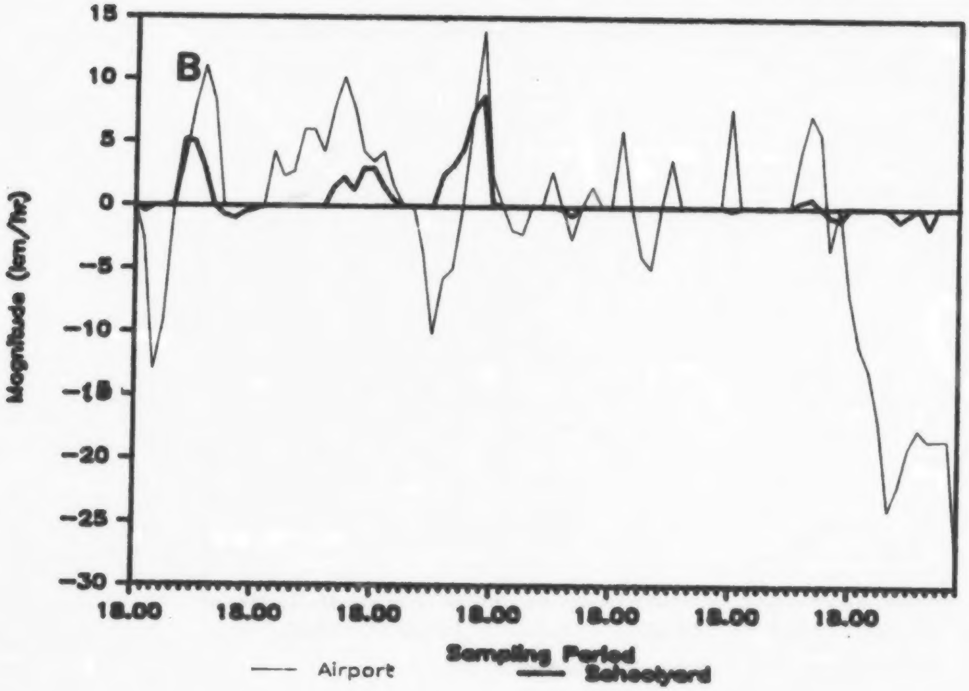

Fig. 3 Airport and schoolyard measurements of a) the north and b) the east component of wind. Each day 18:00 hours are indicated. Correlation coefficients were 0.5 and 0.39 for the north and east components, respectively.

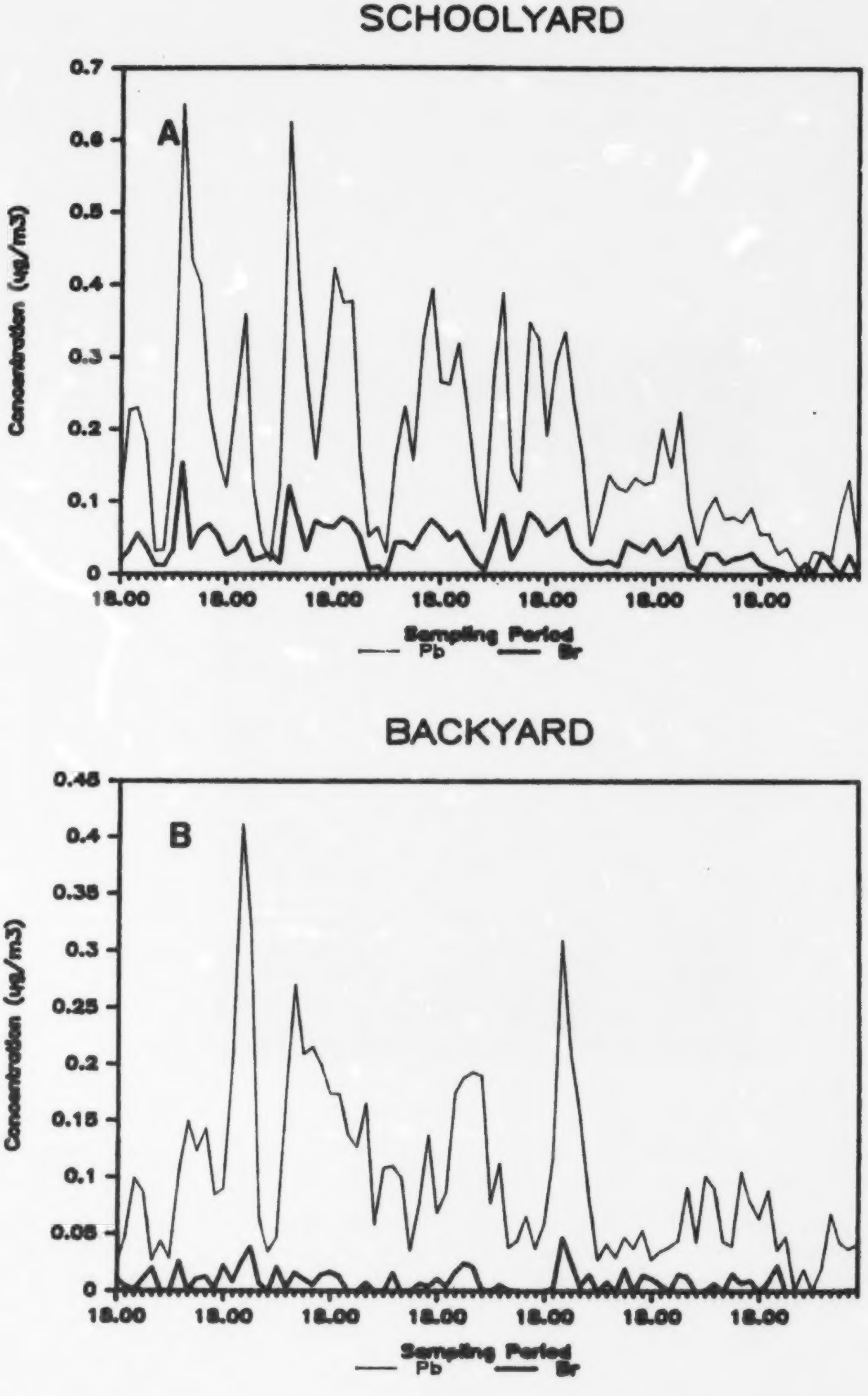

Fig. 4 Pb(—) and Br(▬) concentrations in air at a) the schoolyard and b) backyard. Each day 18:00 hours are indicated.

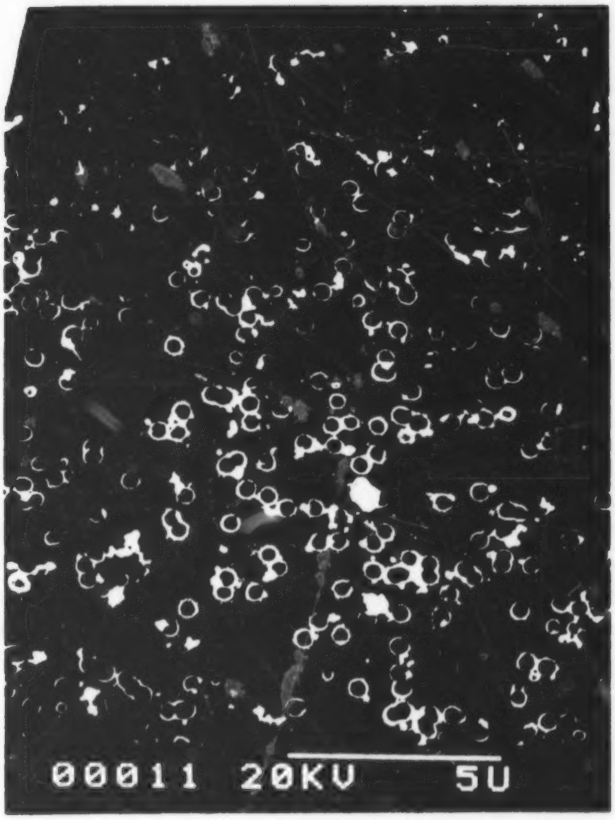

Fig. 5 Typical SEM photograph of air filtate collected at the school. A 5 µm scale is shown. Dark circles are the 0.4 µm pores in the Nucleopore filter whereas the white irregular shapes are air particulates.

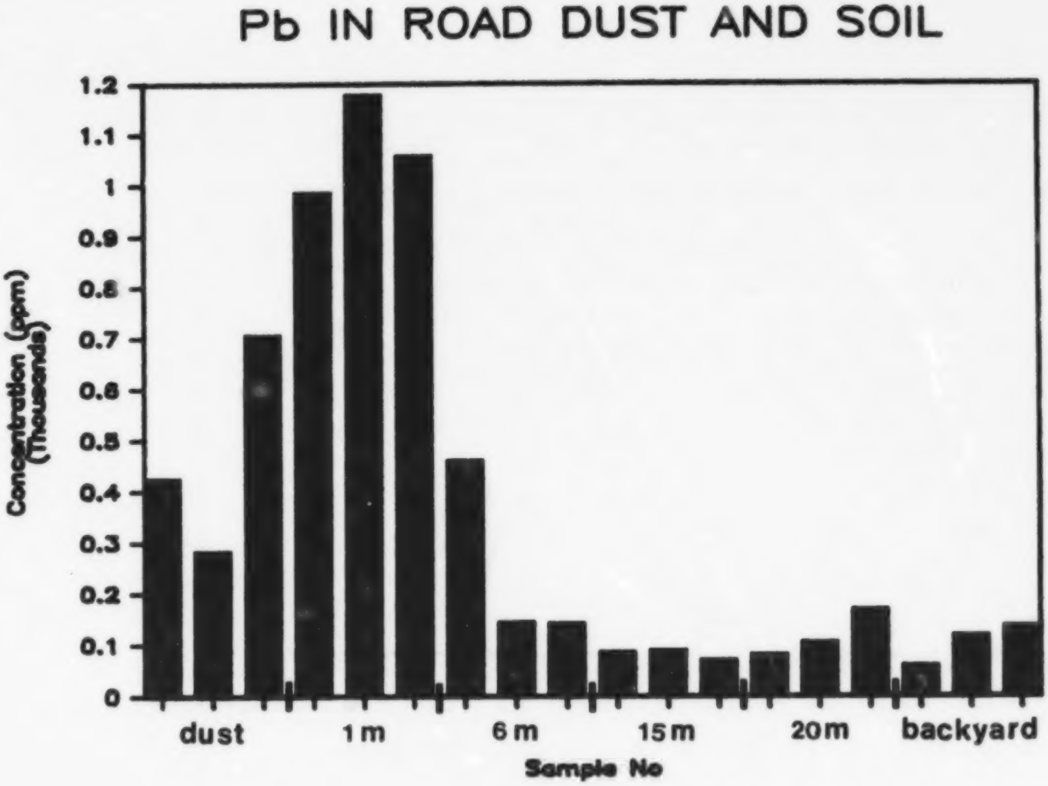

Fig. 6 Pb concentrations in fine dust from road adjacent to the school sampler and in soil cores from the schoolyard and backyard. Four cores were taken in the schoolyard at distances of 1, 6, 15 and 20 m from the road. The three measurements on dust were duplicates whereas those for each core were at the surface and at the 3 and 6 cm depths. For each core measurements at increasing depth proceed to the right in the plot.

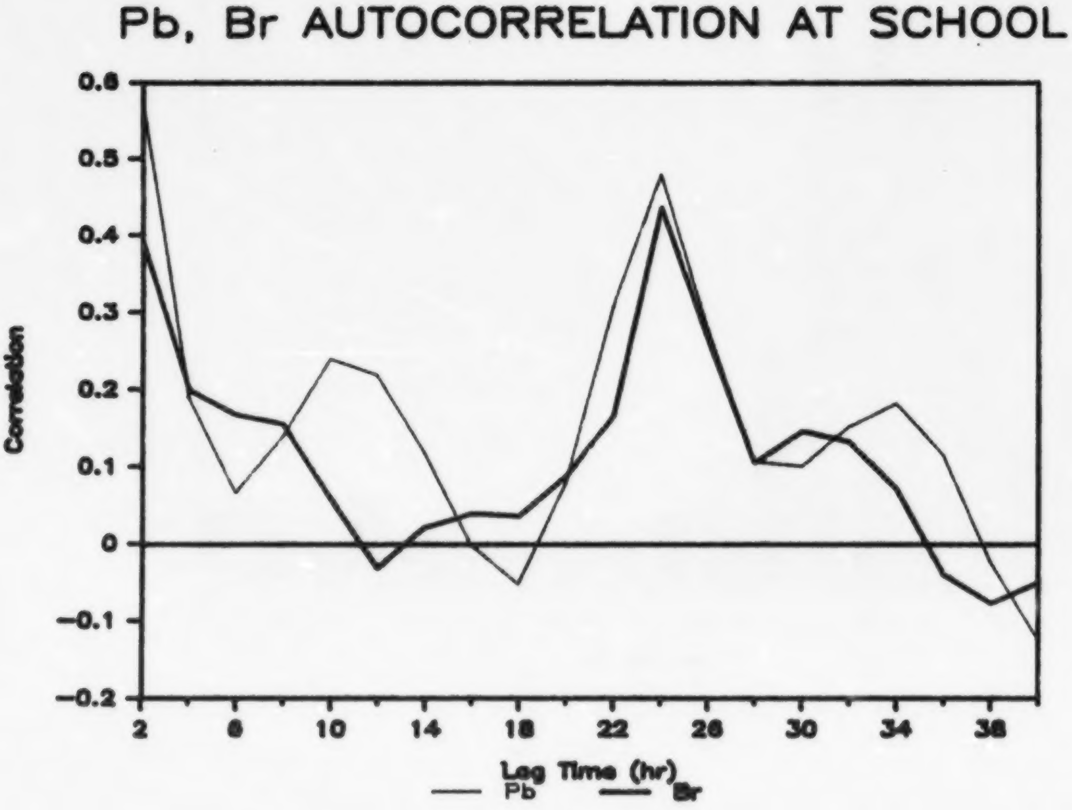

Fig. 7 Autocorrelation plots of Pb and Br concentrations at school. Both elements show a daily (24-hour) periodicity whereas only Pb has a strong 12-hour periodicity.

DOSE-RESPONSE STUDIES OF GASEOUS POLLUTANTS ON FOOD CROPS

Douglas P.L. Ormrod and Jane M. Petitte
Department of Horticultural Science, University of Guelph

Key words: Ozone, Agriculture, Food Crops, Air Pollution Effects.

ABSTRACT

Controlled environment ozone dose-response studies were performed on several food crop species using cultivars widely cultivated in Ontario. Two or three week old cabbage, carrot, and tomato plants were exposed to 0, 0.1, 0.2, or 0.3 ul/l for one 7-hour period. Two-week old "Cherry Belle" radish plants were used as the indicator species in the experiments. Immediately following exposure and also 3 days later, the plants were rated for injury. Three days following ozone exposure, leaf area and leaf and/or stem fresh and dry weights were measured where applicable. For carrot and tomato, significant negative linear dose-response relationships were determined for all growth parameters at both ages at all ozone levels. The reactions of cabbage to ozone differed according to age. The results of the 2-week old plant growth studies indicated a quadratic response to dose with no significant leaf growth reduction occurring until ozone reached 0.2 ul/l. However, no significant ozone effects were observed in the three-week old plants. Field studies in open-top chambers were conducted during the summer using the same species and treatment regimes to determine what type of comparison can be made between indoor and outdoor ozone studies.

Asparagus plants were subjected to the same ozone treatments as previously described. Frond and spear areas, and fresh and dry weights and injury were determined. No significant differences in growth were found. An experiment was performed using 2- and 3-week old carrot plants to determine dose-response to ozone at 0, 0.06, 0.12 or 0.18 ul/l for one 7-hour exposure. A significant ozone effect was observed at both growth stages with growth significantly reduced at 0.18 ul/l. A long-term study to determine ozone effects on carrot shoot growth and root productivity was conducted. Beginning at 16 days of age and once each week for 5 consecutive weeks, the plants were exposed to one 7-hour period of ozone (0, 0.06, 0.12, or 0.18 ul/l). Data analyses and interpretation of data have not been completed at this time, but will be by the time of the Technology Transfer Conference.

Two experiments were conducted with 2-week old tomato plants to determine if imidazolidinyl urea (IDU), a compound similar in structure to EDU, would serve as an ozone protectant. In one experiment, IDU levels of 0, 100, 500, or 2500 ug/ml were sprayed on plants 3 days prior to ozone exposure (0, 0.1, 0.2, or 0.3 ug/l). No evidence was observed for protection against ozone injury. A second experiment also indicated no protection from 0.2 ul/l of ozone with spray applications of 2500 or 10000 ug/ml of IDU applied 0, 1, or 3 days prior to exposure.

DOSE-RESPONSE STUDIES OF THE EFFECTS OF OZONE ON VEGETABLE CROPS

D. P. Ormrod and Jane M. Petitte
Department of Horticultural Science, University of Guelph,
Guelph, Ontario N1G 2W1

ABSTRACT

Controlled environment ozone dose-response studies were performed on several food crop species using cultivars widely grown in Ontario. Two or 3 week old cabbage, carrot, and tomato plants were exposed to 0, 0.1, 0.2, or 0.3 $\mu\ell\ \ell^{-1}$ ozone for one 7 hr. period. Two week old 'Cherry Belle' radish plants were used as the indicator species in the experiments. Immediately following exposure and also 3 days later, the plants were rated for injury. Three days following ozone exposure, leaf area and leaf and/or stem fresh and dry weights were measured where applicable. For carrot and tomato significant negative linear dose-response relationships were determined for all growth parameters at both ages at all ozone levels. The reactions of cabbage to ozone differed according to age. The results of the 2-week-old plant growth studies indicated a quadratic response to dose with no significant leaf growth reduction occurring until ozone reached 0.2 $\mu\ell\ \ell^{-1}$. However, no significant ozone effects were observed in the

3-week-old plants. Field studies in open-top chambers were conducted during the summer using the same species and treatment regimes to determine what type of comparison can be made between indoor and outdoor ozone studies.

Asparagus plants were subjected to the same ozone treatments as previously described. Frond and spear areas, and fresh and dry weights and injury were determined. No significant differences in growth were found. An experiment was performed using 2- and 3-week-old carrot plants to determine dose-responses to ozone, 0, 0.06, 0.12 or 0.18 $\mu\ell\ \ell^{-1}$, for one 7 hr. exposure. A significant ozone effect was observed at both growth stages with growth significantly reduced at 0.18 $\mu\ell\ \ell^{-1}$. A long term study in controlled environments to determine ozone effects on carrot shoot growth and root productivity was conducted. Beginning at 16 days of age and once each week for 5 consecutive weeks, the plants were exposed to one 7 hr. period of ozone (0, 0.06, 0.12, or 0.18 $\mu\ell\ \ell^{-1}$). Data analyses and interpretation of data have not been completed at this time. The result of this experiment will be included in a future report.

Two experiments were conducted with 2-week-old tomato plants to determine if imidazolindinyl urea (IDU), a compound similar in structure to EDU, would serve as an ozone protectant. In one experiment, IDU levels of 0, 100, 500, or 2500 $\mu g\ m\ell^{-1}$ were sprayed on plants 3 days prior to ozone exposure (0, 0.1, 0.2, or 0.3 $\mu\ell\ \ell^{-1}$). No evidence was observed for protection against ozone injury. A second experiment also indicated no protection from 0.2 $\mu\ell\ \ell^{-1}$ of ozone with spray applications of 2500 or 10,000 $\mu g\ m\ell^{-1}$ of IDU applied 0, 1, or 3 days prior to exposure.

INTRODUCTION

Southern Ontario crop production areas are subjected to recurring episodes of elevated ozone concentration during the growing season. These ambient ozone episodes are known to result in crop growth and yield reductions in sensitive plants. Sensitivity to ozone is known to vary among species and among cultivars within species. Some of the commercial crops in southern Ontario have had considerable study in the past in both controlled exposure and field experiments. Other important crops have had little or no attention.

Experiments to quantify the effects of ozone on crop growth were needed to permit evaluations of the differences in sensitivity among species and among cultivars, as well as to provide dose-response relationships for the prediction of field effects of ozone episodes. This research program utilized a standardized procedure for the determination of dose-response relationships. Plants were grown and exposed to ozone in controlled environment facilities. The controlled environment responses are being compared with responses in open-top field chambers.

Species under study include cabbage, carrot, tomato, radish, and asparagus. While tomato and radish have been studied in the past, little attention has been given to cabbage and none to carrot and asparagus. The commercial production of cabbage, carrot, tomato, radish and asparagus is an important horticultural activity in Ontario with about Ω10 million, Ω87 million, Ω1.2 million, and Ω3.8 million cash value to farmers, respectively, each year (Ontario Ministry of Agriculture and Food, 1985). In addition all these species are important home garden vegetables.

The objectives of the research reported herein were to determine the responses of selected vegetable crops to the gaseous air pollutant ozone and to develop response equation methodology for displaying data on the effects of ozone on plant growth. This research and these objectives represent only a part of the research underway and planned in a multiyear study.

MATERIALS AND METHODS

Experiment 1.

---Plant Culture

Seeds of cabbage 'Market Prize', carrot 'Spartan Bonus', tomato 'New Yorker', or radish 'Cherry Belle' were planted in 10 cm green plastic pots filled with moist Promix BX (1 part vermiculite:1 part perlite:3 parts sphagnum peat moss). The plants were watered daily with one-half strength complete nutrient solution.

The plants were grown in Conviron Model E8 growth chambers under the following conditions: day/night temperature, $25/20 \pm 1^{o}C$; relative humidity, 70 ± 5%; photosynthetic photon flux, 325 ± 10 μmol m^{-2}s^{-1} for 16 hr.d^{-1} (5 a.m. to 9 p.m.) with 75% and 25% input wattage from cool white fluorescent and incandescent lamps, respectively. About 7 days after seeding, plants were thinned to one plant per pot.

---Ozone treatment

Fourteen days after seeding for cabbage and radish and 16 days after seeding for carrot and tomato, the plants were exposed to 0, 0.1 0.2, or 0.3 $\mu\ell\ \ell^{-1}$ ozone for one 7 hr. period in continuously stirred tank reactor (CSTR) chambers. About 24 hr. prior to the exposure, the plants were moved from the growth chambers to the CSTR chambers to permit acclimation to the CSTR enviroment. Conditions in each CSTR were similar to those described for the growth chambers except for irradiance; 50% was supplied by a high pressure sodium lamp and 50% by a metal halide lamp. Ozone was supplied by a Grace high-voltage generator and was continuously monitored by a Dasibi ozone analyzer calibrated with a Thermo Electron Series 101 Dyanmic NO, NO_2, O_3 calibrator.

---Plant Measurements

Covariate measurements were made on all plants one day prior to ozone exposure, to permit adjustment of growth data for differences in plant size prior to exposure. Planar leaf area was quantified on all 4 species while hypocotyl diameter was also measured on radish.

A 12-category scoring system was utilized to rate the leaves of all plants for chlorotic and necrotic injury occurring immediately and 3 days following the 7 hr. exposure to ozone. Plants were moved back to the growth chamber following the first rating and harvested 3 days later. The following parameters were measured: leaf area, fresh, and dry weights on each of the 4 species; stem fresh and dry weights on cabbage and tomato; and hypocotyl diameter, fresh and dry weights on radish.

---Experimental Design and Data Analysis

The experimental design for carrot, radish, and tomato was a 4x4 Latin square replicated 4 times designed to remove variability over time as well as between CSTR chambers. A randomized complete block design replicated 3 times was used for cabbage. Four subsamples were used per treatment per replication. The means of the 4 subsamples per treatment per replication were used in the analyses of variance. Prior to statistical analyses, all growth parameters were converted to natural logarithms. The means were adjusted for initial differences in plant size by utilization of planar leaf area or hypocotyl diameter, where applicable. The means were then detransformed for reporting purposes after analysis of variance was conducted.

Experiment 2.

Seeds of all cultivars used in Experiment 1, except for radish, were planted in 12.5 cm green plastic pots and grown under the conditions as previously described. Twenty-one days after seeding, the plants were exposed to ozone using a 4 x 4 Latin square design as described previously and harvested 3 days following exposure. Fourteen day old radish 'Cherry Belle' plants were used as an indicator species, but were not harvested.

Experiment 3.

---Plant Culture

During the summer of 1985, an experiment was conducted in open top field chambers at the Cambridge Research Station. Seeds of cabbage 'Market Prize,' carrot 'Spartan Bonus,' or tomato 'New Yorker' were planted in 15 cm green plastic pots filled with moist Promix BX. The plants were watered approximately every 4 days with complete nutrient solutin. During the other days an automatic system supplied water from an irrigation pond on the farm.

All plants, except those grown under ambient conditions, were grown in open-top chambers. Ambient plants were not contained in a chamber during the growth phase. Seventeen- and 24-day-old cabbage plants and 19- and 24-day-old carrot and tomato plants were exposed to either 0, 0.1, 0.2, or 0.3 $\mu\ell\ \ell^{-1}$ ozone for one 7 hr. period in the open-top chambers. Ambient plants were exposed to ambient air during the exposure period up until harvest. Ozone was supplied by a Grace high-voltage generator and was continuously monitored by a Dasibi ozone analyzer calibrated with a Thermo Electron Series 101 Dynamic NO, NO_2, O_3 calibrator.

---Plant Measurements

The covariate, planar leaf area, was measured on all plants immediately prior to ozone exposure. A 12-category scoring system was used to rate the leaves of all plants for chlorotic and necrotic injury 3 days following the 7 hr. exposure to ozone. Plants were harvested and parameters were measured as described in Experiment 1.

---Experimental Design and Data Analyses

The experimental design was a randomized complete block replicated 3 times designed to remove variability over time. The 3 ozone levels as well as the ambient conditions were compared to the 0 ozone treatment. Four subsamples were used per treatment per replication. The means of 4 subsamples per treatment per replication were used in the analyses of variance. Data was handled as described in Experiment 1.

Experiment 4.

Carrot 'Spartan Bonus' and tomato 'New Yorker' plants were grown as described in Experiments 1 and 2. The ozone treatments were 0, 0.06, 0.12, or 0.18 $\mu\ell\ \ell^{-1}$, and the experimental design was a 4x4 Latin square. Planar leaf area was determined for each plant immediately prior to exposure and was utilized as a covariate in the final analyses.

RESULTS

Experiments 1 and 2

---Cabbage

The sensitivity of 14-day-old cabbage plants exposed to 7 hr of ozone was quite different from that of the 21-day-old plants. At 14 days, the dose response was quadratic (i.e. injury increasing more than linearly with increasing concentration) for all measured leaf growth parameters (Table 1). Leaf fresh weight was most sensitive to ozone at 0.3 $\mu\ell\ \ell^{-1}$. With the addition of one week to the age of the plants, leaf growth became insensitive to ozone up to and including 0.3 $\mu\ell\ \ell^{-1}$ (Table 2).

---Carrot

The dose response curves were very similar for the 16- and

21-day-old carrot plants (Tables 3 and 4). As the ozone concentration increased, all measured leaf growth parameters significantly decreased. Specific leaf area decreased significantly at 0.2 and 0.3 $\mu\ell\ \ell^{-1}$ ozone in the 16- and 21-day-old plants. Leaf dry matter content linearly increased with increasing ozone concentrations in the 16-day-old plants.

Mean percent leaf injury differed according to the age of the plant. The older plants had much more injury at the highest level of ozone. Even though no significant injury was observed at 0.1 $\mu\ell\ \ell^{-1}$ ozone, leaf fresh weight was reduced at both ages.

---Radish

'Cherry Belle' is rated as a sensitive radish cultivar. Quadratic dose-response curves described the response of leaf area to ozone while leaf fresh and dry weight decreases were linear, as were hypocotyl growth responses. Leaf fresh and dry weights decreased at a slower rate than hypocotyl weights. Hypocotyl growth appeared to be more sensitive than leaf growth at 0.2 and 0.3 $\mu\ell\ \ell^{-1}$ ozone. At 0.1 and 0.2 $\mu\ell\ \ell^{-1}$, the injury on the day of exposure increased in 3 days by about 6 and 4.5%, respectively. At 0.3 $\mu\ell\ \ell^{-1}$, injury appeared to decrease slightly during that same time period.

---Tomato

The dose-response curves of some growth parameters differed according to the age of the plant. In the 16-day-old plants, linear decreases in leaf area, fresh and dry weights and stem fresh and dry weights were observed (Table 6). Specific leaf area decreased quadratically while leaf dry matter content increased quadratically with increasing ozone concentration. Injury immediately following exposure increased quadratically with increasing ozone concentration, whereas 3 days later a linear increase was observed. Over the 3 day period, injury increased in all ozone treatments.

The 21-day-old plants had a quadratic decrease in leaf dry weight with increasing ozone concentrations (Table 7). Leaf area and fresh weight decreased linearly. No significant differences between the ozone treatments and the control were observed in specific leaf area, percent leaf dry matter content, or the stem parameters. Leaf growth appeared to be more sensitive to ozone than stem growth. Quadratic relationships were calculated for mean percent injury immediately and 3 days following exposure. At 0.1 $\mu\ell\ \ell^{-1}$ ozone, leaf dry weight was significantly decreased, whereas stem weights were not affected until 0.2 $\mu\ell\ \ell^{-1}$ ozone was applied.

Direct comparison of species responses revealed that cabbage 'Market Prize' was relatively insensitive and carrot "Spartan Bonus' and tomato 'New Yorker' were as sensitive as or more sensitive to ozone than radish 'Cherry Belle' (Table 8). As the latter cultivar is considered to be sensitive to ozone, the relatively sensitive response of the carrot and tomato cultivars studied has been established in a standardized comparison. On the other hand, cabbage is relatively insensitive according to the present study.

Experiment 3.

---Cabbage

No significant differences were observed in any of the measured leaf parameters in the 17- or 24-day-old plants (Table 9). Some insect injury was seen on all plants prior to ozone exposure.

---Carrot

No significant differences were observed in any of the measured leaf parameters of the 19- or 24-day-old plants (Table 10). A significant linear response was calculated for leaf injury in the 24-day-old plants.

---Tomato

Leaf area, leaf fresh weight, and leaf dry weight of the 19- and 24-day-old plants had significant decreasing linear responses to increasing ozone concentrations (Table II). The 19-day-old plants had increasing linear leaf dry matter content as ozone concentration increased. No significant differences were observed in the stem fresh and dry weights of the 19-day-old plants. However, in the 24-day-old plants increasing ozone concentration caused a decreasing quadratic response in these stem parameters. Mean plant injury increased linearly in both ages with increasing ozone concentration.

Experiment 4.

---Carrot

Negative quadratic responses were calculated for leaf area at 16 and 21 days, and fresh weight at 21 days of age (Table 12). Specific leaf area in the 16-day-old plants had a significant quadratic response to increasing ozone concentration. Injury in the 16- and 21-day-old plants increased linearly with increasing ozone concentration 3 days following exposure.

---Tomato

Significant differences between the control and the ozone treatments were observed only in leaf growth parameters of the 16-day-old plants (Table 13). Specific leaf area differed significantly from the control in the 0.12 and 0.18 $\mu\ell\ \ell^{-1}$ ozone treatments, while leaf fresh weight and leaf dry matter content differed significantly at the 0.18 $\mu\ell\ \ell^{-1}$ level. Significant linear relationships were calculated for the above mentioned leaf parameters.

DISCUSSION

The similarity between the results obtained in the field and those obtained in indoor controlled environment studies was dependent upon the particular species observed.

In cabbage, overall dose responses of the leaf growth parameters were similar when comparing the older plants grown under field or growth chamber conditions (Tables 2 and 9). The younger plants in the field, however, were much less sensitive than their indoor counterparts (Tables 1 and 9). The 3 day difference in age (17 vs. 14 days) may have allowed for the response difference, since age appeared to be a factor in ozone sensitivity indoors. The reason for allowing the plants an additional 3 days of growth can be seen when scanning the results of harvested leaf areas. An attempt to obtain field plants comparable in size to indoor grown plants was not feasible within the time limits of the summer. Therefore, the field plants were smaller than the indoor plants at the time of exposure. It also may be possible that a previous stress, such as insect attack, may have physiologically allowed the plant to be less sensitive to other later stresses, e.q. ozone.

The second species studied in the field, carrot, showed no indications of significant growth reductions due to ozone (Table 10). These results were totally opposite of those significant decreased growth effects observed in the laboratory (Tables 3 and 4). The only comparable result was that of visible leaf injury between 21 and 24 day old plants.

In tomato, the overall leaf growth and injury responses were similar between the field and indoor experiments for both ages of plants (Tables 6, 7, and 11). As in cabbage and carrot, field tomato plants were smaller. Age did not play a significant role in the sensitivity of leaves to ozone in the indoor grown plants as observed in cabbage. This lack of age effect was also noted in the field grown tomatoes.

More studies must be conducted with other species and different cultivars of the same species in order to determine the feasibility of using indoor pollution studies to determine the sensitivity of a plant to a pollutant grown under field conditions. As indicated by the previously described results, several factors may predetermine a plant's pollutant sensitivity including size, age, and previous stresses. Future indoor and field research should utilize these factors to better understand plant responses to air pollution stress.

An additional experiment was conducted to determine the effect of lower ozone levels (0, 0.06, 0.12, or 0.18 ul 1^{-1}) on 16 and 21 day old carrot plants. At these levels, 0.18 ul 1^{-1} was the critical level for reducing leaf area, fresh weight, and specific leaf area in the 16 day old plants, while leaf injury significantly increased 3 days following exposure (Table 12). When observing the results of the experiment where the ozone levels of 0 to 0.3 ul 1^{-1} were used (Table 3), 0.2 ul 1^{-1} appeared to be the critical level. The observation that can be made when considering both of the experiments is that in order to determine pollutant levels which reduce plant growth, a wide range of pollutant concentrations may first have to be studied before narrowing to a set of levels which may contain the threshold concentration for a particular plant species or cultivar. In the case of 'Spartan Bonus' carrot the threshold for ozone injury probably lies between 0.12 and 0.18 ul l^{-1} for 7 hr.

Asparagus plants which were exposed to 0, 0.1, 0.2, or 0.3 ul l^{-1} of ozone for 7 hours were observed to have no significant differences in frond or spear growth. Even though a covariate of planar leaf area was utilized to decrease plant to plant variation in the statistical analyses, too much variability existed to permit detection of significant differences between treatments.

A long term indoor study to determine ozone effects on carrot shoot and root growth was conducted. Data analyses have not been completed.

A compound named imidazolindinyl urea (IDU), which is similar in structure to ethylene diurea (EDU), was sprayed on 2-week-old tomato plants at various concentrations. The plants were then exposed to various ozone levels to determine IDU action as an ozone protectant. No visible evidence for protection against ozone injury was observed.

TABLE 1. Growth responses to cabbage 'Market Prize' (14 days old) exposed to one 7 hr period of ozone and harvested 3 days following exposure.

Variable	Ozone (µℓ ℓ$^{-1}$) 0.0	0.1	0.2	0.3	Curve[z]
Leaf area (cm2)	92[y]	91	89	75 ***[x]	Q ***
Leaf fresh weight (g)	4.14	4.10	3.97 **	3.40 ***	Q ***
Leaf dry weight (g)	0.327	0.328	0.319 *	0.276 ***	Q **
Specific leaf area (cm^2 mg^{-1})	0.281	0.278	0.281	0.272	ns
Leaf dry matter content (%)	7.92	8.00	8.03	8.14	ns
Stem fresh weight (g)	0.100	0.101	0.098	0.094	ns
Stem dry weight (g)	0.0080	0.0087	0.0085	0.0076	ns
Mean plant injury (%)					
--- day of exposure	0	0	0	3.5	ns
--- 3 days after exposure	0	0	0	2.5	ns

[z] Dose response curve: L - linear; Q - quadratic; C - cubic.

[y] Geometric mean on a per plant basis.

[x] Level of significance: ns, *, **, *** - not significant, p>0.10, p>0.05, p>0.01, respectively.

TABLE 2. Growth responses of cabbage 'Market Prize' (21 days old) exposed to one 7 hr period of ozone and harvested 3 days following exposure.

Variable	Ozone ($\mu\ell\ \ell^{-1}$) 0.0	0.1	0.2	0.3	Curve^z
Leaf area (cm^2)	532	530	534	523	ns
Leaf fresh weight (g)	28.87	29.54	28.56	28.27	ns
Leaf dry weight (g)	2.133	2.085	2.121	2.114	ns
Specific leaf area ($cm^2\ mg^{-1}$)	0.249	0.254	0.252	0.249	ns
Leaf dry matter content (%)	7.40	7.06	7.43	7.44	ns

^{z}See TABLE 1 for explanation.

TABLE 3. Growth responses of carrot 'Spartan Bonus' (16 days old) exposed to one 7 hr period of ozone and harvested 3 days following exposure.

	Ozone ($\mu\ell\ \ell^{-1}$)				
Variable	0.0	0.1	0.2	0.3	Curve^{z}
Leaf area (cm^2)	9.50	8.13	6.77 ***	4.89 ***	L ***
Leaf fresh weight (g)	0.333	0.280	0.248 **	0.209 ***	L ***
Leaf dry weight (g)	0.037	0.032 **	0.030 **	0.025 ***	L ***
Specific leaf area ($cm^2\ mg^{-1}$)	0.253	0.252	0.220 **	0.193 ***	L ***
Leaf dry matter content (%)	11.16	11.53	11.93 *	12.16 **	L ***
Mean plant injury (%)					
--- day of exposure	0	0	0	3	ns
--- 3 days after exposure	0	1.0	13 ***	14 ***	L ***

^{z}See TABLE 1 for explanation.

TABLE 4. Growth responses of carrot 'Spartan Bonus' (21 days old) exposed to one 7 hr period of ozone and harvested 3 days following exposure.

Variables	Ozone (μℓ ℓ$^{-1}$) 0.0	 0.1	 0.2	 0.3	Curve^z
Leaf area (cm^2)	48	42 *	37 ***	28 ***	L ***
Leaf fresh weight (g)	1.48	1.30 ***	1.16 ***	0.95 ***	L ***
Leaf dry weight (g)	0.171	0.152 *	0.143 **	0.121 ***	L ***
Specific leaf area (cm^2 mg^{-1})	0.285	0.275	0.258 **	0.227 ***	L ***
Leaf dry matter content (%)	11.50	11.46	12.30	12.79	ns
Mean plant injury (%)					
--- day of exposure	0	2	4	26 ***	Q ***
--- 3 days after	0	0	10 **	35 ***	Q ***

^{z}See TABLE 1 for explanation.

TABLE 5. Growth responses of radish 'Cherry Belle' (14 days old) exposed to one 7 hr period of ozone and harvested 3 days following exposure.

Variables	Ozone ($\mu\ell\ \ell^{-1}$)				Curve^z
	0.0	0.1	0.2	0.3	
Leaf area (cm^2)	106	108	83 **	60 **	Q **
Leaf fresh weight (g)	3.94	3.92	3.08 **	2.39 ***	L ***
Leaf dry weight (g)	0.293	0.292	0.274	0.240 *	L *
Specific leaf area (cm^2 mg^{-1})	0.365	0.368	0.298 ***	0.233 ***	Q ***
Leaf dry matter content (%)	7.43	7.46	9.06 ***	10.46 ***	Q ***
Hypocotyl fresh weight (g)	6.58	6.18	4.24 **	3.04 ***	L ***
Hypocotyl dry weight (g)	0.361	0.320	0.217 **	0.141 ***	L ***
Hypocotyl diameter (mm)	18	17	15 **	13 ***	L ***
Hypocotyl dry matter content (%)	5.50	5.22	5.13	4.78	ns
Leaf:hypocotyl fresh weight ratio	0.60	0.61	0.87	0.78	ns
Leaf:hypocotyl dry weight ratio	0.806	0.900	1.470 ***	1.757 ***	L ***
Mean plant injury (%)					
--- day of exposure	0	1	34 ***	56 ***	Q **
--- 3 days after exposure	0	7 *	39 ***	49 ***	L ***

^{z}See TABLE 1 for explanation.

TABLE 6. Growth responses of tomato 'New Yorker' (16 days old) exposed to one 7 hr period of ozone and harvested 3 days following exposure.

Variable	Ozone (µℓ ℓ$^{-1}$) 0.0	0.1	0.2	0.3	Curve^z
Leaf area (cm^2)	120	106 *	84 ***	68 ***	L ***
Leaf fresh weight (g)	3.41	2.89 **	2.16 ***	1.76 ***	L ***
Leaf dry weight (g)	0.305	0.258 **	0.211 ***	0.186 ***	L ***
Specific leaf area (cm^2 mg^{-1})	0.395	0.411 *	0.400 **	0.368 ***	Q
Leaf dry matter content (%)	8.94	8.91	9.82 ***	10.66 ***	Q **
Stem fresh weight (g)	1.054	1.022	0.884 **	0.764 ***	L **
Stem dry weight (g)	0.047	0.044	0.036 **	0.031 ***	L ***
Mean plant injury (%)					
--- day of exposure	0	1	10 ***	26 ***	Q *
--- 3 days after exposure	0	9 ***	21 ***	29 ***	L ***

^{z}See TABLE 1 for explanation.

TABLE 7. Growth responses of tomato 'New Yorker' (21 days old) exposed to one 7 hr period of ozone and harvested 3 days following exposure.

	Ozone ($\mu\ell\ \ell^{-1}$)				
Variable	0.0	0.1	0.2	0.3	Curve^z
Leaf area (cm^2)	519	454	406 **	320 **	L ***
Leaf fresh weight (g)	17.48	15.22	13.53 **	10.51 ***	L ***
Leaf dry weight (g)	1.49	1.28 **	1.13 ***	1.07 **	Q ***
Specific leaf area ($cm^2\ mg^{-1}$)	0.351	0.357	0.361	0.300	ns
Leaf dry matter content (%)	8.49	8.41	8.33	10.15	ns
Stem fresh weight (g)	6.51	5.97	5.42	4.88	ns
Stem dry weight (g)	0.276	0.248	0.213	0.199	ns
Mean plant injury (%)					
--- day of exposure	0	4	13 ***	35 ***	Q ***
--- 3 days after exposure	0	5 *	17 ***	38 ***	Q ***

^{z}See TABLE 1 for explanation.

TABLE 8. Comparative sensitivities of cabbage 'Market Prize', carrot 'Spartan Bonus', radish 'Cherry Belle', and tomato 'New Yorker' to ozone, leaf area (cm^2) basis.

Species	Age (days)	Ozone ($\mu\ell\ \ell^{-1}$)				
		0.0	0.1	0.2	0.3	Curve[z]
Cabbage	14	92	91	89	75 ***	Q ***
	21	532	530	534	523	ns
Carrot	16	9.50	8.13	6.77 ***	4.89 ***	L ***
	21	48	42 *	37 ***	28 ***	L ***
Radish	14	106	108	83 **	60 **	Q **
Tomato	16	120	106 *	84 ***	68 ***	L ***
	21	519	454	406 **	320 **	L ***

[z] See TABLE 1 for explanation.

TABLE 9. Growth responses of cabbage 'Market Prize' (17 or 24 days old) exposed to one 7 hr. period of ozone in open top field chambers and harvested 3 days following exposure.

Variable	Age (days)	Ozone ($\mu\ell\ \ell^{-1}$)					Curve
		0.0	0.1	0.2	0.3	ambient	
Leaf area (cm^2)	17	25.43	22.49	29.43	17.94	28.35	ns
	24	52.25	49.50	42.28	45.10	51.01	ns
Leaf fresh weight (g)	17	1.122	1.012	1.112	0.815	1.229	ns
	24	2.541	2.314	2.040	2.145	2.377	ns
Leaf dry weight (g)	17	0.101	0.093	0.109	0.085	0.111	ns
	24	0.255	0.238	0.216	0.229	0.269	ns
Specific leaf area (cm^2g^{-1})	17	253	242	274	209	255	ns
	24	208	213	198	195	190	ns
Leaf dry matter content (%)	17	9.06	9.23	9.75	10.4	9.06	ns
	24	10.05	10.22	10.51	11.08	11.40	ns
Mean plant injury (%)	17	1	1	3	8	1	ns
	24	1	1	3	6	1	ns

[z] See TABLE 1 for explanation.

TABLE 10. Growth responses of carrot 'Spartan Bonus' (19 or 24 days old) exposed to one 7 hr. period of ozone in open top field chambers and harvested 3 days following exposure.

Variable	Age (days)	Ozone ($\mu\ell\ \ell^{-1}$)					Curve
		0	0.1	0.2	0.3	ambient	
Leaf area (cm^2)	19	1.26	0.83	0.58	0.83	1.30	ns
	24	2.85	2.24	1.84	2.77	2.22	ns
Leaf fresh weight (mg)	19	63.9	53.9	42.2	49.6	72.0	ns
	24	134.4	108.0	100.2	142.5	105.5	ns
Leaf dry weight (mg)	19	6.40	8.69	5.43	6.30	8.67	ns
	24	18.84	15.93	16.81	24.18	23.29	ns
Specific leaf area ($cm^2 mg^{-1}$)	19	0.203	0.125	0.106	0.128	0.156	ns
	24	0.153	0.140	0.115	0.120	0.103	ns
Leaf dry matter content (%)	19	10.19	17.18	12.88	12.76	11.96	ns
	24	14.02	14.68	17.27	15.67	33.30	ns
Mean plant injury (%)	19	1	3	5	9	0	ns
	24	2	7	15**	28***	0	L***

[z] See TABLE 1 for explanation.

TABLE 11. Growth responses of tomato 'New Yorker' (19 or 24 days old) exposed to one 7 hr. period of ozone in open top field chambers and harvested 3 days following exposure.

		Ozone (ul l^{-1})					
Variable	Age (days)	0	0.1	0.2	0.3	ambient	Curve
Leaf area (cm^2)	19	12.32	11.75	7.94*	6.03*	17.78	L***
	24	28.76	25.74	17.81*	14.72**	26.79	L***
Leaf fresh weight (mg)	19	530	323**	211***	223***	598	L***
	24	911	798	586**	506***	953	L***
Leaf dry weight (mg)	19	41.3	35.5	29.6**	29.2**	58.8**	L**
	24	109.5	87.7	80.9**	77.1***	122.4***	L***
Specific leaf area (cm^{2}mg^{-1})	19	0.30	0.34	0.27	0.21	0.30	ns
	24	0.26	0.29	0.22	0.19	0.22	ns
Leaf dry matter content (%)	19	10.0	10.7	13.3*	14.2**	9.8	L**
	24	12.0	10.9	13.8	15.3	12.9	ns
Stem fresh weight (mg)	19	96.0	97.3	90.6	92.7	120.5	ns
	24	276	226	243**	238*	279*	Q*
Stem dry weight (mg)	19	6.18	5.56	4.98	5.11	7.58	ns
	24	19.53	15.66	16.35**	16.93**	21.89*	Q**
Mean plant injury (%)	19	0	13**	23***	28***	0	L***
	24	0	18	32**	39***	0	L***

[z] See TABLE 1 for explanation.

TABLE 12. Growth responses of carrot 'Spartan Bonus' (16 or 21 days old) exposed to one 7 hr. period of ozone and harvested 3 days following exposure.

Variable	Age (days)	Ozone ($\mu\ell\ \ell^{-1}$)				Curve
		0	0.06	0.12	0.18	
Leaf area (cm^2)	16	6.96	7.76	6.68	4.33*	Q*
	21	2.33	27.5*	25.2	20.7	Q**
Leaf fresh weight (g)	16	0.320	0.339	0.310	0.239*	L*
	21	1.045	1.203*	1.049	0.961	Q*
Leaf dry weight (g)	16	0.034	0.035	0.034	0.027	ns
	21	0.116	0.133	0.125	0.108	ns
Specific leaf area ($cm^2\ g^{-1}$)	16	210	223	197	162**	Q*
	21	222	203	198	189	ns
Leaf dry matter content (b)	16	10.5	10.3	10.9	11.5	ns
	21	10.7	11.0	11.8	11.2	ns
Mean plant injury	(%)					
--day of exposure	16	0	0	0	3	ns
	21	0	0	3	4	ns
--3 days after exposure	16	0	0	5	9 **	L**
	21	0	1	10*	11**	L**

[z] See TABLE 1 for explanation.

USE OF THE DIRECT SAMPLE INSERTION DEVICE FOR SAMPLE VAPORIZATION IN THE INDUCTIVELY COUPLED PLASMA FOR ATOMIC AND MASS SPECTROMETRY

E.D. Salin[1], R.L.A. Sing[1], D.W. Boomer[2], and M. Powell[2]

[1]Department of Chemistry, McGill University and
[2]Laboratory Services Branch, Ontario Ministry of the Environment

Key words: ICP-MS, Multielement Analysis, Sample Insertion Devices.

ABSTRACT

The Direct Sample Insertion Device (DSID) will be described, and its application in several areas will be discussed. For liquid samples, the wire loop DSID has demonstrated sub-ppb detection limits for both Atmomc Emission and Mass Spectrometry. Precision better than 1% appears to be possible using an automatic injection system developed in our laboratory. A number of advantages for both optical and mass spectrometry appear to be provided by the wire loop configuration. These include temporal resolution of possible interfering species and elimination of water vapours. The performance of the liquid wire loop DSID system will be discussed in some detail for both optical and mass spectrometric configurations. The systems will be compared and contrasted.

Solid sample introduction into the inductively coupled plasma for atomic emission spectroscopy will be discussed. Considerable success has been achieved with human hair. Undigested single hair samples have been inserted. Precision of the technique seems to be dependent on hair and not on the DSID for Cu. Some questions remain as to the applicability of the technique for high accuracy determinations; however, the accuracy is quite adequate for surveys. More difficult solid sample types will also be discussed.

Authors: E.D. Salin[1], R.L.A. Sing, D.W. Boomer[2]
and M. Powell[2]
Department of Chemistry
McGill University
801 Sherbrooke St. W.
Montreal, P.Q., Canada
H3A 2K6

1. Speaker
2. Inorganic Trace Contaminants Section
Laboratory Services Branch
Ontario Ministry of the Environment
125 Resources Road
P.O. Box 213
Rexdale, Ontario M9W 5L1

Title: Use of the Direct Sample Insertion Device for Sample Vaporization in the Inductively Coupled Plasma for Atomic and Mass Spectrometry.

This work has been focused around the study of applications of the Direct Sample Insertion Device (DSID) for sample introduction into the inductively coupled plasma (ICP). The DSID consists of a mechanism which allows a sample carrier probe to be inserted directly into the central core of the ICP. Before embarking on the direct analysis of solid samples using the DSID for the ICP it was deemed useful to gain knowledge of the behavior of the DSID with desolvated liquid samples. In attempting to determine the physical temperature of a graphite electrode placed in the plasma by the melting points of metals, it was found that tungsten wire could be inserted into the plasma with no effect other than the embrittlement of the wire. A new direct sample insertion device was designed and constructed to permit rapid placement of a tungsten wire loop into the plasma. This device was pneumatically driven to provide near instantaneous entry of the wire into the plasma as was found necessary by the short vaporization times of the sample elements. This system has since been replaced with a more versatile stepper motor driven system which will also be discussed.

Liquid samples (10ul) placed on the wire are desolvated by placing them at roughly 10 to 30 mm from the bottom of the load coil with the plasma ignited. The heat of the plasma and the flow of gases around the wire ensured rapid (10 to 30 sec) drying of the wire. This drying step is easily monitored since three phenomena are observed during this time: 1) the plasma constricts itself due to the presence of di- and poly- atomic molecules 2) the reflected power increases slightly 3) the signal intensity rises as the plasma is constricted into the viewing zone. Once dry, the wire is released into the plasma with the transient emission signal occurring 50 to 400 ms after insertion and having a half width of approximately 100 ms. Under fixed conditions, the standard deviation on the time occurrence of the analyte peak emission is about 3 ms. The extremely high precision of this occurrence may allow spectrally overlapping lines to be resolved in the time domain. We have observed temporal resolution in at least one case.

With this device, the detection limits listed in Table I have been obtained. In comparison, using the same detection system and conventional sample introduction for the ICP (nebulization), the copper detection limit is 30 ng/ml. We are therefore getting a detection limit improvement on our system of approximately a factor of 100. The linear dynamic range for copper extends over 4 to 5 orders of magnitude. The relative standard deviation of the signal well above the detection limit is typically as good as 1% when automated.

Table I. Wire Loop DSID Detection Limits.

Element	Wavelength	Detection Limit		
		Conc.	Absolute	Fassel (b)
	nm	ng/ml	pg	ng/ml
Copper	324.754	0.2	2	5.4
Zinc	213.856	0.08	0.8	1.8
Cadmium	226.501	0.2	2	3.4
Silver	328.068	0.04	0.4	7
Lead (a)	220.350	20	200	42

(a) A tantalum wire was used as support since the spectral overlap of tungsten was not sufficiently temporally resolved.

(b) Fassel's very complete work is often used as a comparative measure. R.G. Winge, V.J. Peterson, V.A. Fassel, Applied Spectroscopy, 33, 3 , pp 206-219 (1979).

Difficulties have arisen in the use of tungsten as a sample support. A certain amount of tungsten oxidizes during the drying of the liquid sample and because of the large number of tungsten lines spectral overlaps are common. The temporal resolution of the overlaps is not sufficient in many cases (Pb, Bi, Co) and in others, the processing of the data is rendered more difficult. Experiments with tantalum show that it would be preferable to tungsten. Tantalum has fewer lines than tungsten and is less reactive and so should and does provide fewer spectral interferences. Equally, tantalum oxide is the least volatile of the oxides consequently ensuring adequate temporal resolution of spectral overlaps.

The weight, more specifically the total heat capacity, of the sample support has been found to contribute significantly to the performance of the DSID technique which exhibits DC arc type response. With a tungsten wire of twice the mass, the peak occured approximately 1.5 times later and had a half width 1.5 times longer. The S/N level was one half that of the thinner wire. The geometric configuration of the support also plays an important role, it appears that the larger the exposed area, the more rapid the heating and evolution of the analyte. The different elements volatilize at different times, the order of which is quite similar to that found in DC arc spectrometry. This differential volatilization is beneficial in that spectral overlaps are temporally resolved in many cases.

In the presence of high salt concentrations (1000 ppm Ca) the peak heights and shapes are altered, but the peak area remains essentially the same as for the aqueous standards. This indicates a relative freedom from matrix effects, since the total emission signal is directly related to the concentration. Our later work with inductively coupled plasma (ICP) mass spectrometry (MS) confirms these findings.

Wire Loop Introduction for Mass Spectrometry with ICP Sample Vaporization

We speculated that the wire loop-DSID technique would provide the same advantages for ICP-MS that it does for ICP-AES (Atomic Emission Spectrometry) for liquid samples. Probably solid samples can still be run more appropriately with an ICP-AES system. It is quite conceivable that the two capabilities can be combined for certain applications.

In conjunction with Mr. David Boomer of the Inorganic Trace Contaminants Section we designed, built and installed a DSID device for use on their new SCIEX Elan 250 ICP-MS. It was felt by Mr. Boomer and myself that this was an important and logical path for the research to take while we were actively working with the wire loop DSID system. The initial results are very promising. Even with the first generation of software, which is not designed for transient signals, we were able to achieve an order of magnitude improvement in the detection limits. Precision was approximately 6% RSD. As we stated in the previous section, this can certainly be improved upon with an automatic sampling-injection system. In the case of the ICP-MS this would seem to be an especially valuable improvement since the instrument and apparatus are already at the MOE facility. The DSID mechanism has been vastly improved and is now well suited to computer control.

No matrix or mass spectral overlap problems were encountered with either the W or Ta wires. The Ta is unsuitable for horizontal operation since the temperature is just sufficient to allow the wire to soften and bend. Since the liquid sample is dried prior to insertion, the analyte enters the plasma without the water vapor which normally accompanies it with conventional sample introduction by nebulization. This leads to an unexpected benefit. By eliminating the water from the plasma during the sample vaporization, the formation of the oxides of the elements is severely reduced. These oxides are the source of significant mass spectral overlaps in conventional ICP-MS (e.g. ArO on Fe). This is especially important with the molecular O_2 overlap with S^{32}. Sulfur is an important element which can be difficult to determine at low levels by optical methods. The elimination of water also means that more energy appears to be available for ionization and sample breakdown. The temporal resolution may prove advantageous in cases where isotopes overlap.

Wire Loop Stepper Motor Driven Direct Insertion Device

It was apparent that a great deal of flexibility would be required for the DSID system if it was to be used for solid sample analysis. The reason being that an ashing or drying step might be necessary. Since the heating action is achieved by moving the electrode into, or close to, the plasma, a great deal of control over both velocity and position was required. A stepper motor design for the DSID was developed which would provide a velocity sufficient for wire loop DSID work (less than 0.1 s for insertion) and yet provide the flexibility for solid work. The stepper DSID developed uses a 1 inch diameter wheel and reaches a linear velocity of 15 inches/second. Experiments have demonstrated that this is sufficient for wire loop DSID work.

The liquid wire loop system has been further modified by the complete elimination of a sample chamber system. A computer controlled solenoid port now seals the bottom of the DSID torch system. This "door" now opens to allow insertion into the torch. The wire loop or electrode is cooled below the plasma before dropping the wire or electrode down into the atmosphere. The system is now "wide open" and very accessible for either an automatic injector system (for wire loop work) or robot insertion of an electrode for solid sample work.

Solid Sample Analysis

Hair

A number of hair samples were analyzed by a variety of accepted procedures. The results were in good agreement. We now have three standardized hair samples and well developed procedures for new samples.

Our initial work with conventional electrodes was unsatisfactory. A new electrode with a deep well was developed. This allowed the insertion of one or several strands directly into the plasma without any ashing or drying step. Our calibration was carried out using water samples. This is essentially ideal due to the simplicity of water standard preparation (or commercial availability). The peak areas and time behavior of a given element in a hair sample appear to be identical with that in an aqueous sample. This drastically simplifies analysis procedures and requires only a simple standard preparation step.

The precision of the technique was element dependent. Copper had a relative standard deviation (RSD) of 30 % while Zn had an RSD of 10 %. The literature demonstrates that this is to be expected as Cu concentration is often dependent on the distance from the scalp, while Zn is relatively independent. The Cu precision can probably be improved by the insertion of multiple strands in a given insertion. The Zn RSD is typical of the DSID device and can only be improved by multiple insertions.

The accuracy varies from sample to sample. It appears that we had trouble with certain elements with one donor, but other elements with another donor. With the low number of donors it was impossible to make more emphatic statements. In no case was the error worse than 40%. If an average correction value is used, since all values were high, the maximum error drops to 20%. This will be acceptable for some work, e.g. toxicology, but may not be adequate for others. Certainly this is a marvelous rapid survey technique as it stands. More work needs to be done to clarify the accuracy problem.

Sediments

The sediment types recommend by Mr. Boomer of the MOE were acquired. These include BCSS-1, MESS-1 and SRM 1646 . We initiated our work with these after the stepper motor DSID was completed. After initially profiling the samples for detection limits for the toxic elements (see Table II), we began work on stabilizing the signal level for Cu. Copper is an element which we commonly study and is in relatively high concentration in all these samples. Once we have stabilized with Cu, then we expect that we will have improved our precision and accuracy for all the elements. Our precision at this stage is still at such a level that we can not make substantial statements about the need for special standards. Our hope is that graphite standards, usually oxides, will work, however the time behavior is drastically different between each of the sediments and the graphite standards. We also believe at this time that our precision problems arises due to inhomogeneity problems in the G series standards provided by SPEX. Since we only use 1 to 10 mg per insertion, this is quite possible. Our own "home made" standards which are more finely ground (about the same mesh as the sediments) have provided higher precision.

. We believe that it may also be necessary to use either mixed gasses or fluxing agents when preparing the samples. In the matter of sample preparation we believe that the processes can be conveniently and very effectively automated using a commercially available robot. This will be the subject of a later proposal since the same robot can be used for dc arc and other sample preparation procedures as well as incorporated into the DSID process.

Table II. Detection of elements in sediments

Element	Sample	Certified Concentration	Comments
Cu	G4	1 ppm	clearly seen
Cu	MESS1	25.2 ppm	Stable Burn Needed for Good Precision
Pb	G3	10 ppm	Sufficient for Sediments
Ni	G3	10 ppm	Sufficient for Sediments
Cd	MESS1	0.25 ppm	Need Background Correction for Assurance that this is Cd

IDENTIFICATION OF SELECTED PAHs IN A HAMILTON, ONTARIO AIR SAMPLE BY SHPOL'SKII SPECTROSCOPY

S.V. Filseth and C.M. Sadowski, Department of Chemistry
and
G. Parnell and F.J. Morgan, Department of Physics, York University

Key words: PAH, Trace Organics, Atmospheric Emissions, Shpol'skii Spectroscopy, Hamilton.

ABSTRACT

Shpol'skii Spectroscopy is used to establish the presence of selected PAHs, including both benzo(a) and benzo(b) pyrenes, in an air sample taken from the vicinity of steel refineries in Hamilton, Ontario. The selected PAHs are taken from a list of priority PAHs drawn up by the Ontario Ministry of the Environment. The sample analyzed is an HPLC fraction of a Hi-Vol sample provided by IEC Beak Analytical Services and is diluted with n-octane in preparation for analysis by Shpol'skii Spectroscopy. The dilute solution is flash frozen in liquid nitrogen and then cooled to 12°K. Preliminary identification is made by first obtaining a fluorescence spectrum of the environmental sample using a pulsed nitrogen laser at 337 nm as the excitation source and then comparing this with reference spectra from a library of fluorescence spectra of authentic PAHs in n-octane matrices. To confirm the tentative identification, use is made of excitation spectra of the environmental sample obtained with the aid of a pulsed tunable dye laser. The fluorescence from the sample is observed with a monochromator set at the wavelengths of individual fluorescence spectral features used to make the preliminary identifications. These excitation spectra are compared to reference spectra in a library of excitation spectra of authentic PAH samples in n-octane matrices. The final identification of PAHs in the environmental sample is compared with that obtained by HPLC analysis of the same environmental sample in the Ministry of the Environment's laboratories.

IDENTIFICATION OF SELECTED PAH'S IN A HAMILTON, ONTARIO AIR SAMPLE BY SHPOL'SKII SPECTROSCOPY

S.V. Filseth and C.M. Sadowski
Department of Chemistry
and
G. Parnell and F.J. Morgan
Department of Physics

YORK UNIVERSITY

Shpol'skii spectroscopy is used to establish the presence of selected PAH's, including benzo[a] and benzo[e]pyrenes, in an air sample from Hamilton, Ontario. The selected PAH's are taken from a list of priority PAH's drawn up by the Ontario Ministry of the Environment. The sample is diluted in n-octane, rapidly frozen and cooled to 12 K. Preliminary identification is made by comparing a nitrogen laser excited fluorescence spectrum of the environmental sample with similar spectra of authentic samples of the selected PAH'S. To confirm the preliminary identifications, use is made of excitation spectra of the environmental sample obtained with a tunable dye laser. These excitation spectra are compared to those of authentic samples of the selected PAH's. The final identification is compared to that obtained by HPLC analysis of the same environmental sample.

1. Introduction

The accumulating literature of environmental toxicology has revealed some potentially significant problems. One of these is that many members of the class of environmental pollutants known as polynuclear aromatic hydrocarbons (PAH) are mammalian carcinogens and/or mutagens. Some PAH have been determined to be highly carcinogenic and others, differing perhaps only subtly in their structure, are innocuous. Thus for example, 7, 12-dimethyl benzo[a]anthracene belongs to the former group and its isomer 1, 2-dimethyl benzo[a]anthracene to the latter.

The most important source of environmental PAH appears to be incomplete combustion of fossil fuels (e.g. coal) and thus current energy strategies which call for a renewed emphasis on abundant coal reserves may be cause for concern. Some of the most pressing unanswered questions continue to be the kind answered by analytical chemists: to what concentrations are we exposed and to what specific compounds ? The fact that simple structural modifications within a group of very similar PAH can cause enormous variations in biological activity places a premium on analytical specificity. The fact that ambient levels in many cases are quite low from an analytical viewpoint (not necessarily from a toxicological viewpoint) places a premium on sensitivity.

While conventional analytical techniques have been applied with increasing sophistication and success to the analysis of complex mixtures of similar PAH there remains interest in exploring alternatives. We have been investigating the usefulness of a modern application of one of the oldest of analytical procedures-optical spectroscopy.

The spectra of atoms while undeniably complex even for the simplest of atoms are characterized by one convenient simplicity: spectral features consist of narrow (perhaps 0.0005 nm in the visible at room temperature) well-separated lines. The spectra of molecules-even triatomic molecules-on the other hand are characterized by a daunting richness of structure at room temperature. This is due to the additional degrees of freedom unavailable in an isolated atom-nuclear rotation and vibration. In the case of complex molecules such as PAH, the low rotational constants and vibrational frequencies lead to a spectroscopy so complex at room temperature that spectra consist of broad features without useful discrete structure. Thus even though the optical spectra of two molecules which differ from one another in the slightest structural detail are in principle entirely unique and distinct, in practice the broad features from one may be indistinguishable from those of others in a mixture at room temperature.

The optical spectra of large molecules can be quite dramatically simplified by bringing the molecule to a very low temperature where only a few rotational and vibrational levels are populated. There are several ways to do this in low temperature matrices and one way to it in the vapor phase. Our work has concentrated upon the former approach but initial results have also been obtained with the latter and will be described briefly at the end of this report.

Perhaps the simplest way to lower the temperature of a PAH sample at concentrations typical of environmental samples is to freeze a very dilute solution and reduce the temperature in a cryogenic device. When the solute molecule is locked rigidly in a frozen matrix, vibrational and rotational motion in the solute is enormously reduced or eliminated respectively. If, in addition, the temperature is lowered to the vicinity of 10 K, matrix vibration is reduced to a very low level. Finally, if a solvent molecule is chosen which (1) is of similar structural proportion to the solute molecule, and, (2) freezes in a regular repeating lattice array, residual spectral broadening due to orientational effects is greatly reduced. It is under these conditions that we may expect to see the fewest and narrowest spectral features. Indeed this expectation is realized in a technique in which PAH are the solutes and saturated alkanes are the solvents. This technique has been referred to as Shpol'skii spectroscopy in recognition of the Soviet spectroscopist responsible for much of the early work [1].

2. Background

Our preliminary experiments on the analytical potential of Shpol'skii spectroscopy have been summarized most recently at a previous Technology Transfer Conference [2]. We have profited in this work by communication with other groups active in the same field most notably those of Colmsjo [3] and DiSilva [4]. Our initial efforts have been devoted to apparatus construction and the assembly of spectral databases to support qualitative analysis of environmental air samples. During this work we discovered the importance of sample holder design in achieving reproducibly low temperatures. In addition, a protocol has been developed for the investigation of authentic air samples. This has been tested against a synthetic PAH mixture and finally applied to an unknown air sample from Hamilton, Ontario.

Two types of spectra are obtained in this work depending upon whether it is the wavelength of the exciting radiation or the resulting fluorescent radiation which is varied as a spectrum is recorded. In the former case the result is called an excitation spectrum and it is a record of fluorescence intensity at a specific fluorescent wavelength (selected by a monochromator) as the tunable dye laser which excites fluorescence is scanned through the absorption spectrum of the PAH molecule. This is an absorption spectrum using fluorescence as a detector. As illustrated in Figure 1, such an experiment measures the energy separation between excited vibronic states of the molecule.

The second type of spectrum obtainable with the apparatus which will be described below is a fluorescence spectrum. In this case the wavelength of excitation is fixed and the resulting fluorescence is dispersed in a scanning monochromator. As illustrated in Figure 1, this experiment measures the energy separation between vibronic states in the ground electronic state of the molecule.

One of the features of the condensed phase spectra of large molecules can be used to advantage in this work. This is the often cited "mirror-image" relationship between excitation spectra and fluorescence spectra. This reflection symmetry arises because of rapid internal conversion in the excited state. When a molecule is excited to higher-lying vibrational levels in the excited state, this additional energy (relative to the origin of the excited state) is lost by efficient internal conversion leaving the metastable molecule at the origin within a time period much less than fluorescence lifetimes. At that point the molecule subsequently radiates in transitions controlled by the values of Franck-Condon factors which display a mirror-image symmetry to excitation Franck-Condon factors. Thus irrespective of the excitation wavelength we expect to see (and do see) essentially identical fluorescence spectra (see Figure 1). This makes it possible to produce a preliminary qualitative diagnostic fluorescence spectrum with a single light source containing wavelengths absorbed by many different PAH. In our experiments this source was a nitrogen laser as described below.

3. Experimental

The apparatus employed in this work has changed in several significant respects from earlier versions. A schematic diagram is given as Figure 2. Basically, a dilute sample is contained in a cuvette which can be reduced in temperature to near 10 K and then illuminated with a tunable dye laser or nitrogen laser, the resulting fluorescence being dispersed with a 0.3 m monochromator. Some details of the operation have been described previously [2] and only significant alterations are described here.

Sample temperature has been a matter of conern since our earliest experiments [2]. Because sample and sample holder heat capacities are quite low near 10 K it is important to ensure good thermal contact between the sample holder and the cold head of the closed cycle He refrigerator. Our initial arrangement in which the sample was contained in a glass tube held snugly in a copper clamp proved entirely inadequate with sample temperatures several tens of degrees in excess of cold head temperatures. A very significant improvement was achieved by injecting liquid alkane solutions directly into a pre-cooled copper plug equipped with a quartz window and then inserting the plug into a matching recptacle on the cold head. Recently we have found that this arrangement becomes progressively less satisfactory with repeated use of the same copper plug. We attribute this to work-hardening of the copper following many temperature cycles. This problem has been overcome by injecting very small quantities (tens of microliters) of a liquid hydrocarbon, isopentane, into the annular space which surrounds the copper plug when it is positioned within the matching receptacle. The isopentane freezes immediatly and apparently provides good thermal contact between plug and receptacle.

Our early spectra were recorded with a simple RC network and a picoammeter. More recent spectra have been processed with a boxcar integrator-basically a gated RC network. This permits discrimination against prompt scattered dye laser fluorescence, laser induced optics fluorescence and photomultiplier tube dark current. Typically integrator time constants set near one microsecond with gate widths between 50 and 100 nanoseconds are employed with dye laser or monochromator scan rates determined by these choices, the repetition rate of 10 Hz and the spectral resolution of 0.1 to 0.2 nm.

Seven PAH were chosen for study in the qualitative phase of these experiments. These compounds, selected in consultation with the Ministry, are: pyrene, perylene, benzo[a]pyrene, benzo[e]pyrene, benzo[ghi]perylene, benzo[b]fluoranthene, and, benzo[k]fluoranthene. For purposes of subsequent reference, these compounds are abbreviated, Py, P, BaP, BeP, BghiP, BbF, and BkF respectively. Authentic samples of these materials were obtained commercially with stated purities of typically 99 % and were used as dilute solutions in spectra quality n-octane without further purification.

Two laser dyes (BPBD and BBQ from Exciton) were used to excite fluorescence in these PAH solutions as dictated by their regions of absorption. Typically fluorescence is excited somewhat to shorter wavelengths than the band origin of each PAH in order to diminish the contributions of scattered dye laser light to the fluorescence signal.

4. Results

The following two-step laboratory protocol has been developed for the identification of the presence of one or more of the seven database compounds in an environmental sample.

(1) A nitrogen laser excited fluorescence spectrum is obtained over a wavelength interval which spans the fluorescence features of all seven compounds as determined separately from authentic samples.

On the basis of a comparison of this fluorescence spectrum with those of the seven database compounds, a preliminary identification is made of the PAH's which appear to be present.

(2) The fluorescence monochromator is fixed at a wavelength corresponding to a prominent fluorescence line of the suspected compound. A tunable dye laser excitation spectrum is obtained over the wavelength interval corresponding to that associated with that compound in the database of excitation spectra.

This procedure is repeated for each compound that is suspected to be present in the environmental sample and the correspondence or lack of it between excitation spectra in the database and in the sample determines whether a given compound is identified as present or absent.

The extent of the database itself, the validity of the protocol and the results of its application to an environmental sample are summarized below.

4.1 Database

The core of our database on the seven PAH emphasized in this work now consists of 21 spectra-three for each PAH corresponding to (1) nitrogen laser excited fluorescence, (2) tunable dye laser excited fluorescence, and, (3) tunable dye laser excitation spectra. For illustration, six of these spectra are given for two compounds as Figure 3 a,b,c for P and as Figure 4 a,b,c for BkF. These spectra are not all free of detector or transition saturation (primarily the former). This has little consequence when the experimental objective is a qualitative identification but will be eliminated in forthcoming quantitative work.

4.2 Protocol validation

A commercially available [4] standard sample was obtained which was certified to contain the following ten PAH's, each at a concentration of 0.5 mg/ml in toluene: anthracene, benzo[a]anthracene, BaP, BeP, chrysene, fluoranthane, P, phenanthrene, Py, and triphenylene. Thus the sample contains four of the compounds present in our database and the remaining six may be regarded as a source of possible interference to be overcome by a successfull procedure. The nitrogen laser excited fluorescence spectrum of this sample diluted by a factor of 5000 in n-octane is given in Figure 5.

Three quasiline features are identified by numerals 1-3 in this Figure. Their wavelength position suggests that lines 1 and 3 are due to the presence of Py and BeP respectively. This is confirmed when tunable dye laser excitation spectra are obtained for each of these fluorescent features. The excitation spectrum of peak 3 and that of an authentic sample of BeP are presented in Figure 6a and b respectively. An excitation spectrum of feature 2 in Figure 5 is not similar to any of the spectra in our database and presumably corresponds to one of the six other PAH present in this sample.

In summary, through the use of this protocol all four of the PAH's in the commercial sample which are part of our current database were successfully identified [5] in the presence of an additional six PAH's which are not part of the database. These conclusions were confirmed by an HPLC analysis performed on the sample by the Pesticides Analytical Laboratory Branch of the Ministry of the Environment.

4.3 Environmental Sample

A previously extracted environmental sample dissolved in acetonitrile was supplied by Concord Scientific and identified as F-7. It had been obtained by Hi-Vol filtration of the air in the vicinity of the Stelco steel plant in Hamilton. A ten-fold dilution of this sample in n-octane led to a fractionation of the PAH content between the two phases. It is not known whether the PAH was quantitatively transferred to the octane phase. Presumably it was not but this does not pose a problem since the objective was simply to establish the presence or absence of the seven database compounds in this sample.

As with the commercial standard sample, a nitrogen laser excited fluorescence spectrum of the diluted environmental sample was obtained as an initial diagnostic. The spectrum is given as Figure 7. Several features are identified on the basis of their wavelengths as possible PAH's contained in our database. As an illustration the tunable dye laser excitation sepectrum of feature number 4 is given in Figure 8a together with the excitation spectrum of an authentic sample of BkF as Figure 8b. The comparison of these two spectra is not facilitated by the difference in wavelength direction and scale between the two. Nonetheless it is clear that BkF is present in the environmental sample.

In a similar fashion, a total of six of the seven database PAH's were found to be present in the Hamilton environmental sample.The seventh, BbF, is apparently not present and two, Py and BeP, are present near our detection limit. An HPLC analysis of part of the original F-7 sample confirmed these conclusions with two exceptions: BeP was not detected and P was not analysed for. In addition, the presence of additional PAH not present in our data base was established by the HPLC analysis.

5. Conclusion

With these experiments, which have recently been described in detail [5], we have demonstrated a viable analytical method for the identification of PAH in environmental samples. Both the nitrogen and dye lasers produced distinctive spectra of the several PAH chosen for examination. Nitrogen laser excitation alone is sufficient to identify the origin of spectral features which are isolated from other features. However, when a feature is quite weak or is part of a cluster of other features, dye laser excitation spectra are required for final confirmation.

6. Work in Progress

Further work on PAH analysis is underway in our group as summarized below.

(1) Quantitative Analysis of Air Samples. The work described here which was conducted by Mr. Gary Parnell as part of his Physics M.Sc. thesis project is being continued by Mr. Harold Malle, a Chemistry M.Sc. student. The objective of his work will be to devise procedures which will permit us to establish concentration levels in environmental samples.

(2) Identification of Pentacenes. Several pentacene isomers have been identified in cigarette smoke fractions [6]. As a further demonstration of the Shpol'skii technique we are attempting to show that we can quantitatively analyse for pentacenes in these fractions.

(3) Spectroscopy in Supersonic Jets. It has been shown [7] that expansion of a dilute mixture of a PAH in an inert gas produces rotational and vibrational cooling in the PAH. The spectra of such molecules can be as simple as those obtained in Shpol'skii matrices as can be seen in Figure 9 a and b which shows tunable dye laser excitation spectra of 9-methyl anthracene in supersonic jet and in Shpol'skii matrix in n-octane.

The unique advantage of the supersonic jet spectra is that we are not restricted to compounds which possess structural similarities to the Shpol'skii hydrocarbon solvents. An additional advantage is that solubility in any solvent is not an important factor. On the other hand, PAH vapor pressures become very important and elevated temperatures are necessary. Our work in this area is being conducted by Mr. John Lai, a Chemistry M.Sc. student. Hiw work is directed at a comparison of range of applicability and absolute sensitivity with the Shpol'skii method.

7. Acknowledgement

The authors are pleased to acknowledge the support of the Ontario Ministry of the Environment in the conduct of this work.

References

1. E.V. Shpol'skii. (1959). Soviet Physics Uspekhi 2, 378-392.
2. F. Morgan, G. Parnell, S. Filseth and C. Sadowski. (1984). Proc. Tech. Transf. Conf. No. 5, Ontario Ministry of the Environment, 871-894.
3. A. Colmsjo. (1981). "The Practice and Utility of the Shpol'skii Effect in Chemical Analysis", Univ. Stockholm.
4. Supelco 4-9155 PAH standard.
5. G.P. Parnell, M.Sc. Thesis, York University, Department of Physics and Faculty of Graduate Studies, 1985.
6. D. Hoffman, I. Schmeltz, S.S. Hecht, and E.L. Wynder, (1978) "Tobacco Carcinogenisis", Chapter 4 in Polycyclic Hydrocarbons and Cancer, Vol. 1, Acad. Press., 85-117.
7. J.A. Warren, J.M. Hayes, G.J. Small, (1982). Anal. Chem. 54, 138-140.

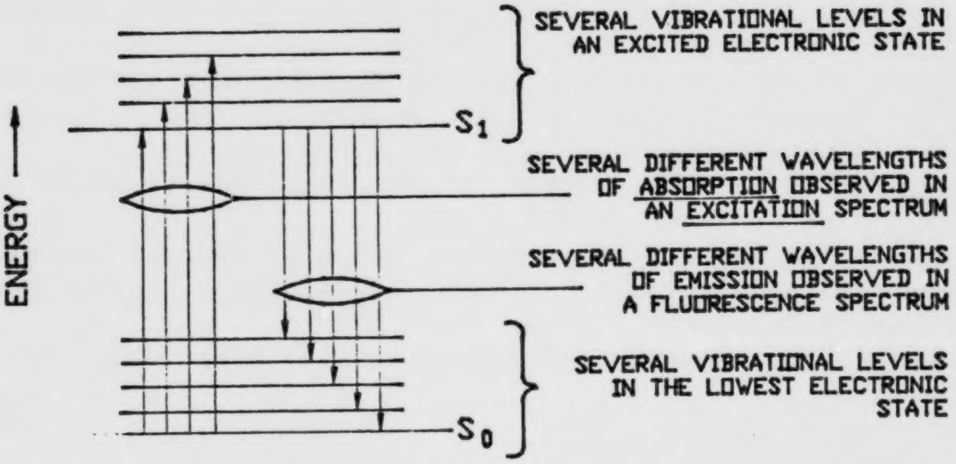
SEVERAL VIBRATIONAL LEVELS IN AN EXCITED ELECTRONIC STATE
S_1
ENERGY
SEVERAL DIFFERENT WAVELENGTHS OF ABSORPTION OBSERVED IN AN EXCITATION SPECTRUM
SEVERAL DIFFERENT WAVELENGTHS OF EMISSION OBSERVED IN A FLUORESCENCE SPECTRUM
SEVERAL VIBRATIONAL LEVELS IN THE LOWEST ELECTRONIC STATE
S_0

1

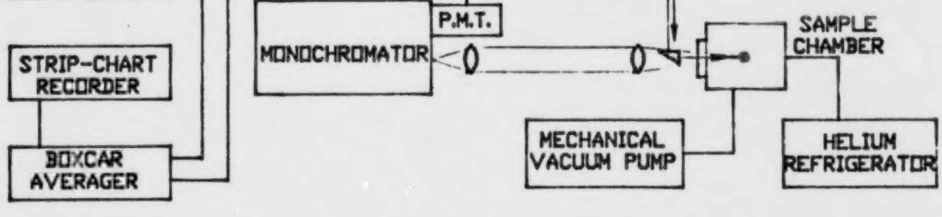
N_2 LASER
TUNABLE DYE LASER
WAVELENGTH CONTROLLER
PHOTODIODE
DELAY/GATE GENERATOR
STRIP-CHART RECORDER
BOXCAR AVERAGER
MONOCHROMATOR
P.M.T.
SAMPLE CHAMBER
MECHANICAL VACUUM PUMP
HELIUM REFRIGERATOR

2

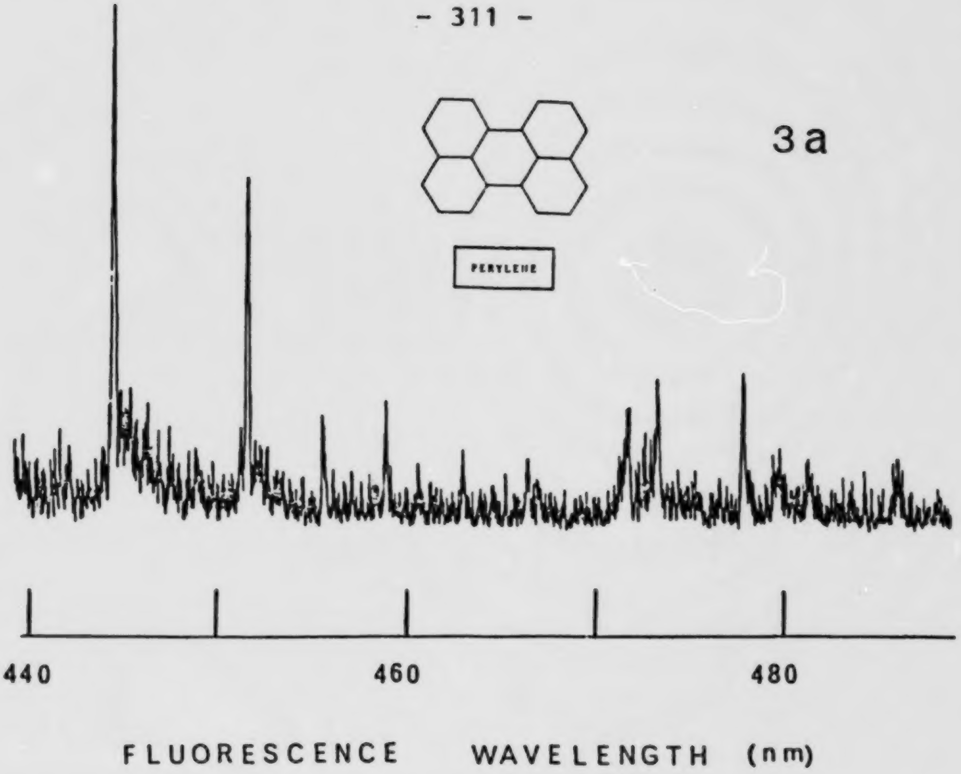

Fluorescence spectrum of Perylene, 135 ng/mL in n-octane, N_2 laser excitation at 337.1 nm.

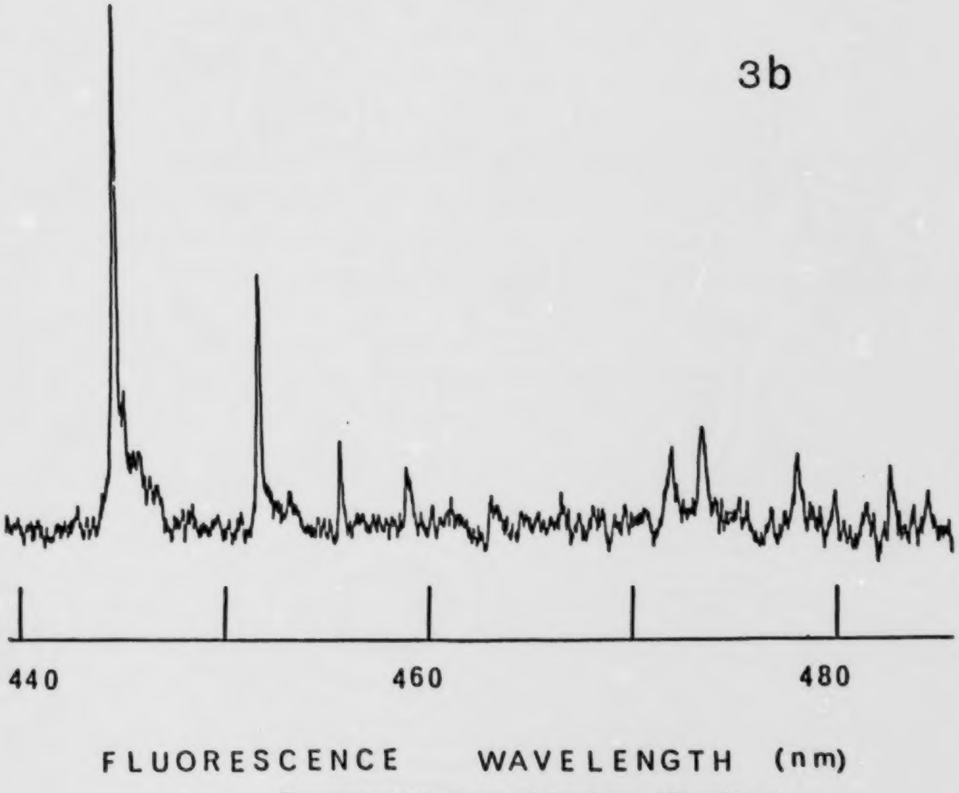

Fluorescence spectrum of Perylene, 180 ng/mL in n-octane, excitation wavelength = 394.4 nm.

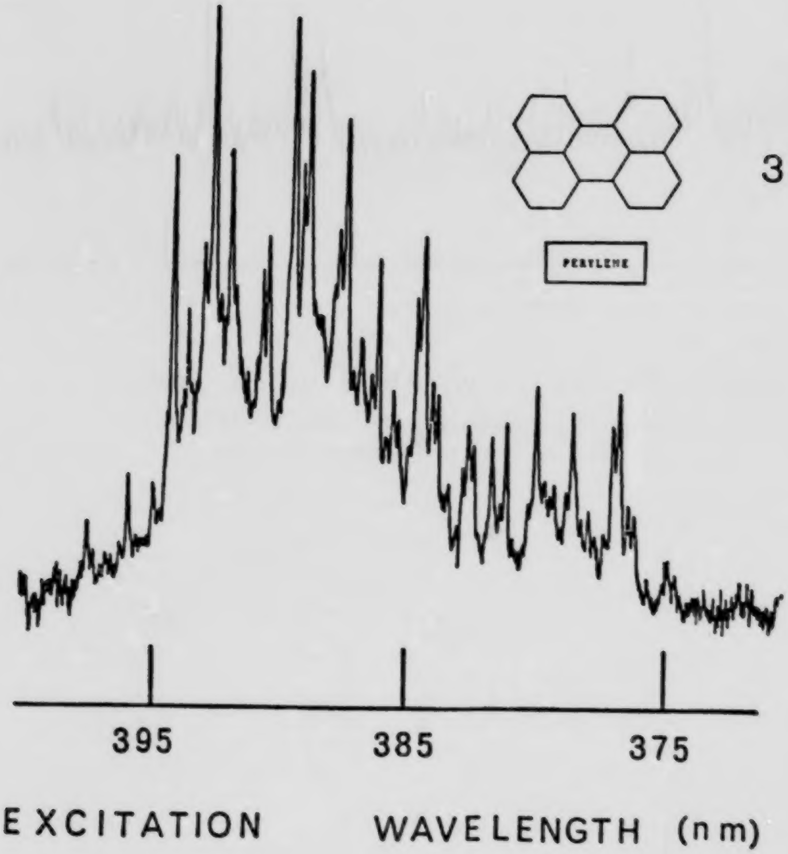

3C

Excitation spectrum of Perylene, 190 ng/mL in n-octane, observation wavelength = 445.1 nm.

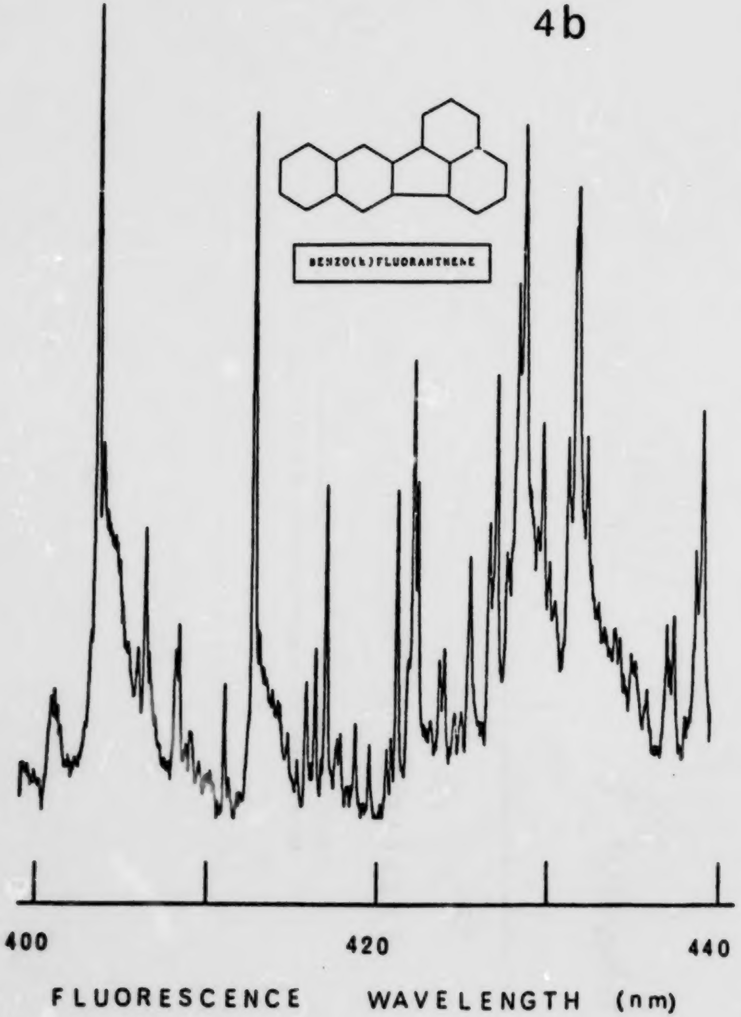

Fluorescence spectrum of Benzo(k)Fluoranthene, 290 ng/mL in n-octane, excitation wavelength = 395.2 nm.

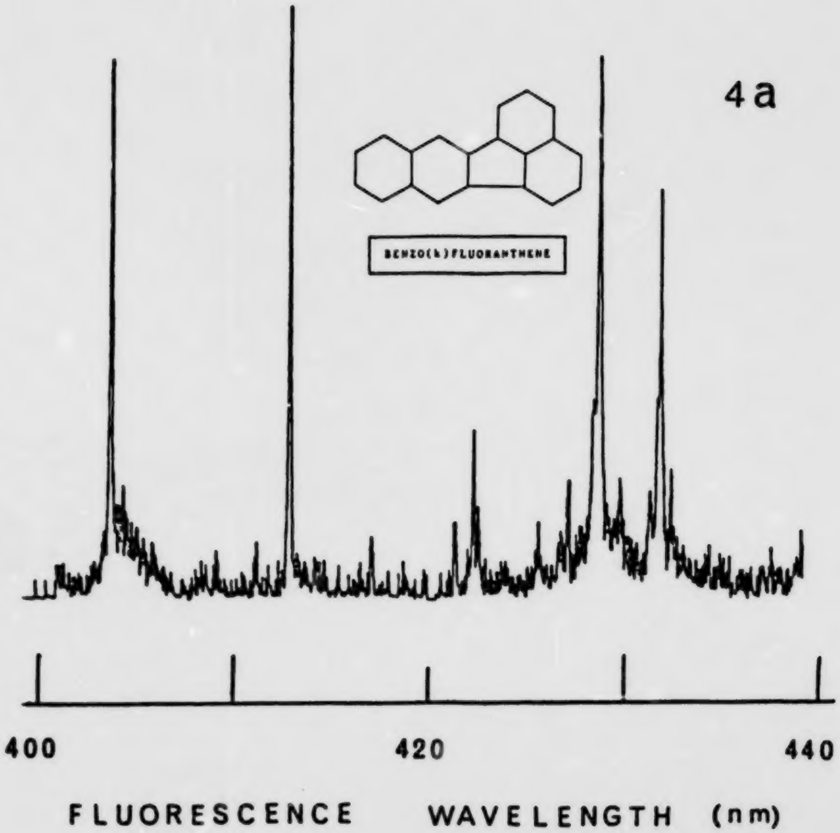

Fluorescence spectrum of Benzo(k)Fluoranthene, 290 ng/mL in n-octane, N_2 laser excitation at 337.1 nm.

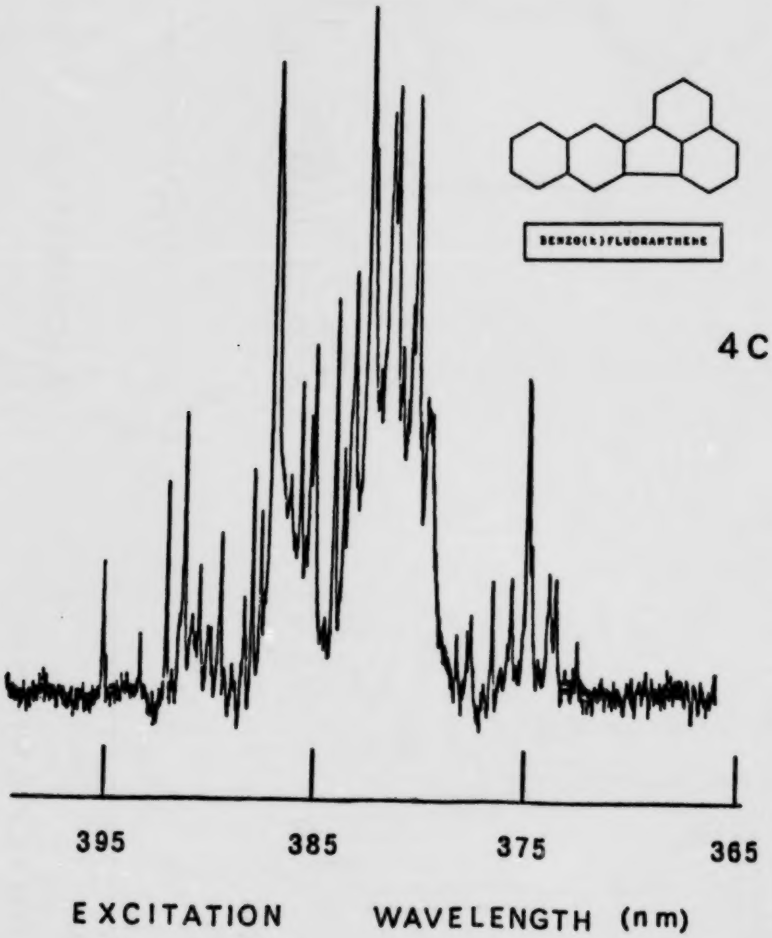

4C

Excitation spectrum of Benzo(k)Fluoranthene, 290 ng/mL in n-octane, observation wavelength = 404.5 nm.

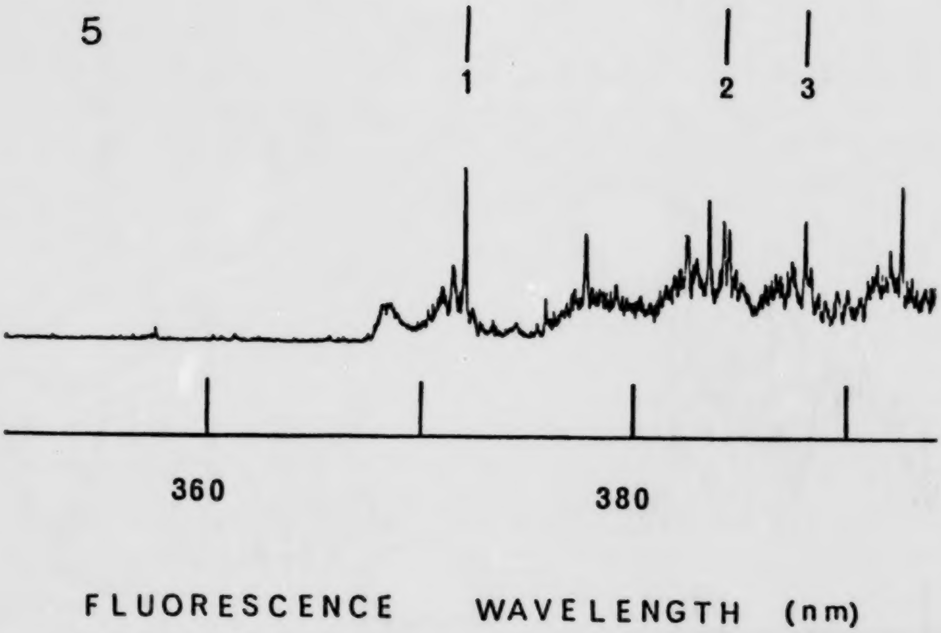

Fluorescence spectrum of Supelco Standard PAH Mixture 4-9155, 100 ng/mL of each PAH, N_2 laser excitation at 337.1 nm.

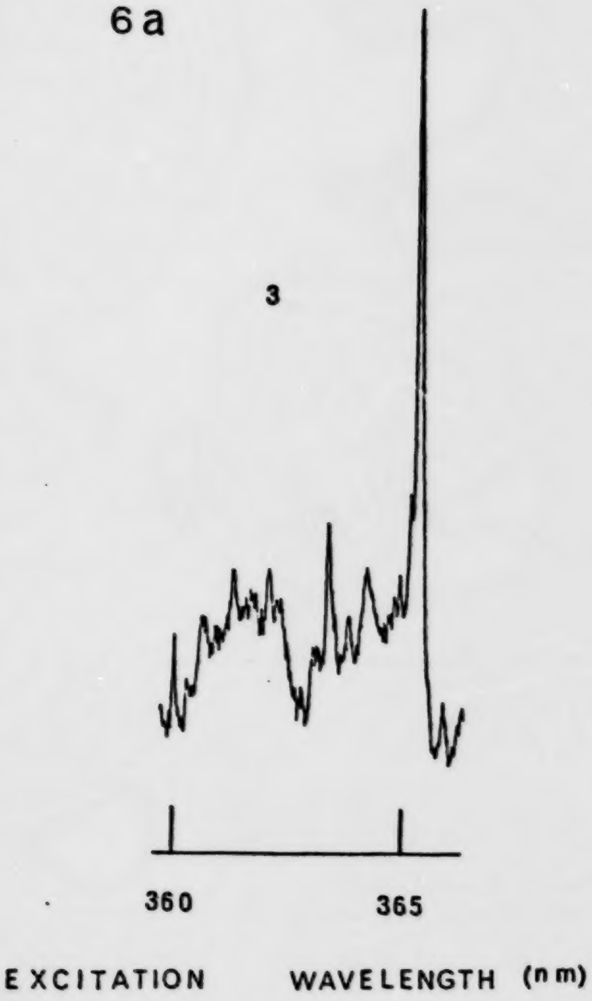

Excitation spectrum for Feature 3 observation wavelength = 388.9 nm.

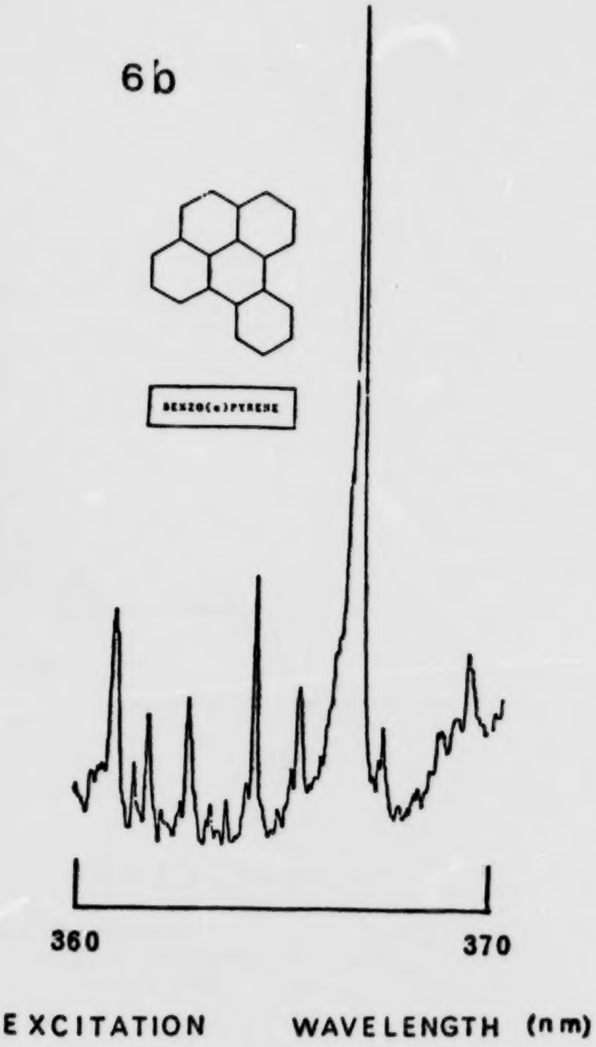

Excitation spectrum of Benzo(e)Pyrene, 1240 ng/mL in n-octane, observation wavelength = 389.3 nm.

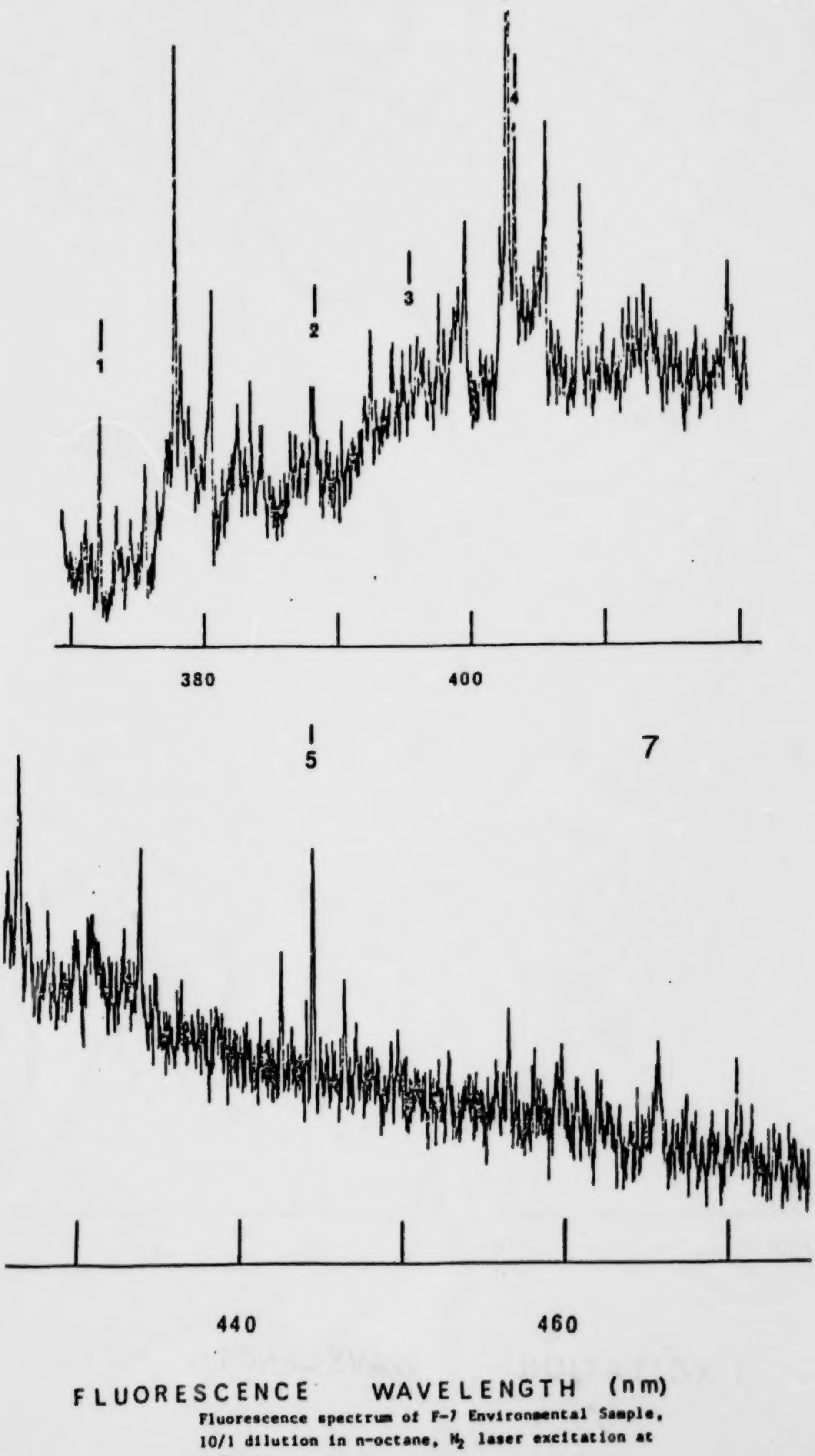

Fluorescence spectrum of F-7 Environmental Sample, 10/1 dilution in n-octane, N_2 laser excitation at 337.1 nm.

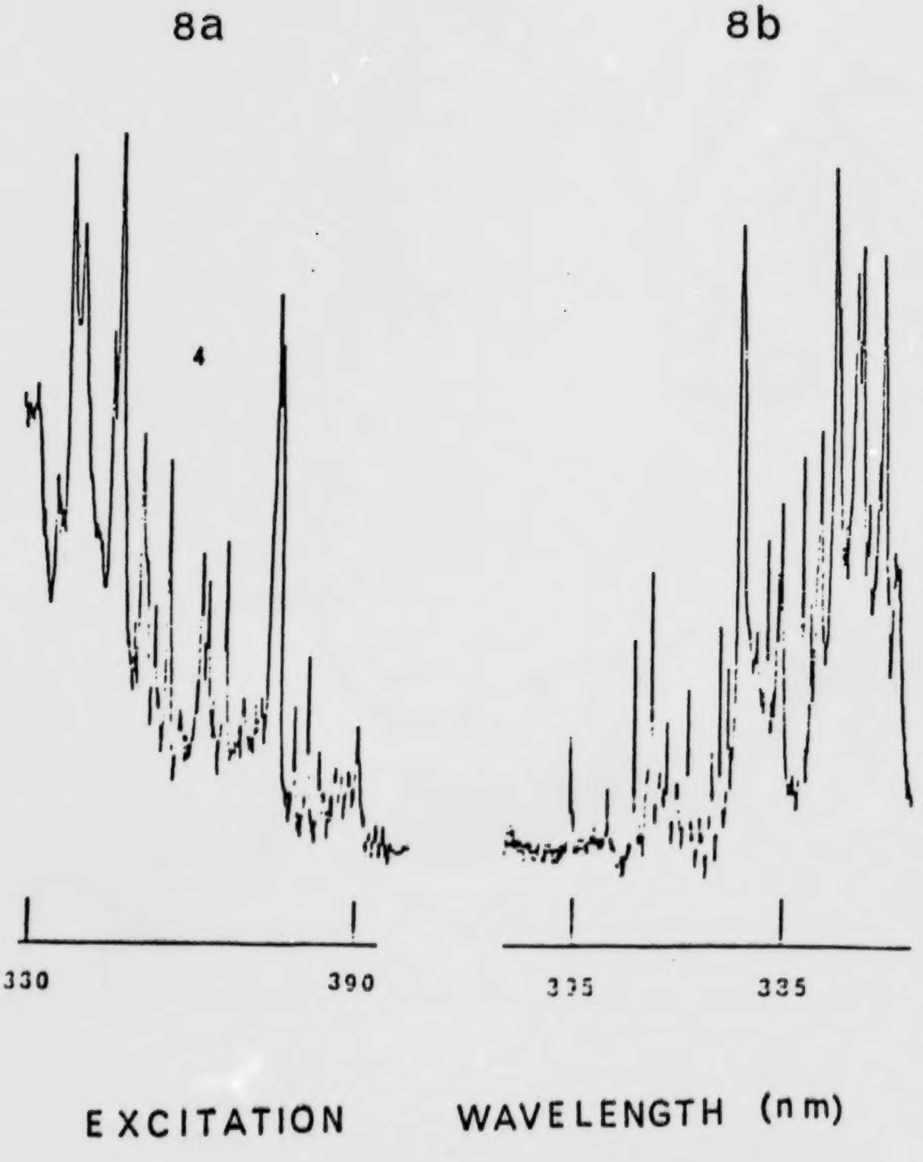
8a
8b
4
330
390
335
335
EXCITATION WAVELENGTH (nm)

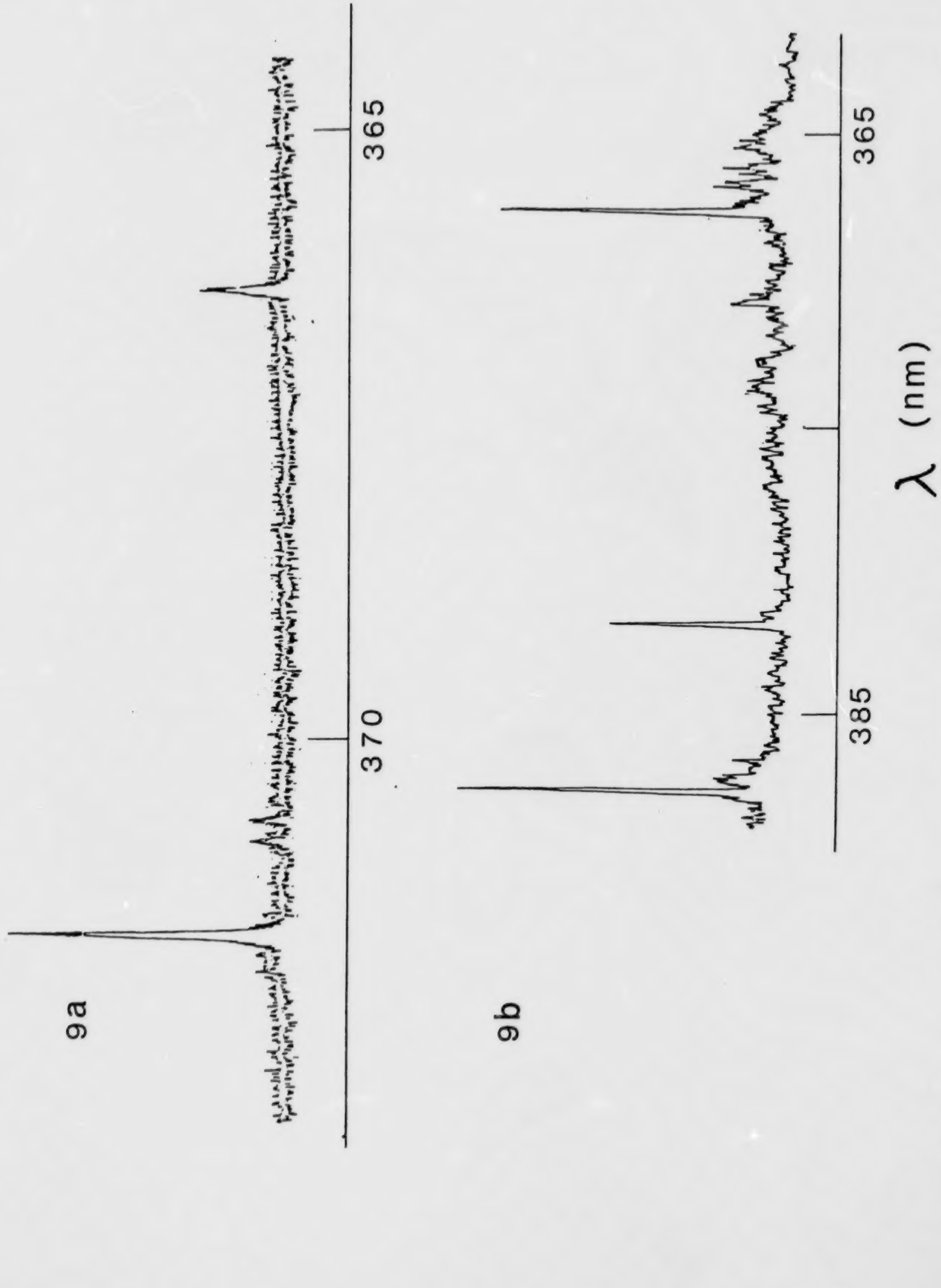
9a
370
365
9b
385
365
λ (nm)

THE EXCHANGE OF AIR PARTICULATES BETWEEN THE INSIDE AND OUTSIDE OF A BUILDING

J.D. MacArthur, G.R. Palmer and Xin-Pei Ma
Department of Physics, Queen's University

Key words: Particulates, Air Quality, Multielement Analysis, Indoor-Outdoor Air.

ABSTRACT

The element composition of air particulates collected simultaneously inside and outside a school has been determined with particle induced X-ray emission (PIXE) using the Queen's Van de Graaff accelerator. The indoor stations were placed in three sections of a school which are ventilated separately and which are more or less isolated from each other, one a classroom, the second an office and the third a workshop.

The particles were collected on streak filters operating with a time resolution of two hours so that time correlations between the indoor and outdoor air could be monitored. Two filters at each position, each of one week duration, were collected. One indoor, from the classroom, and one outdoor filter from the same time period have been analyzed, and the other six filters will be analyzed shortly.

Al, Si, S, Cl, Ca, Cr, Mn, Fe, Cu, Zn, Br and Pb were observed both inside and outside the school. The levels of Al, Si, Ca, Br and Pb were all lower by a factor of 2 - 3 inside the school than outside, Cl appeared to be higher and the others the same. Besides Pb and Br which were expected to have elevated levels of short duration due to the traffic pattern at the intersection, several other elements showed high levels of short duration outside the school and so the exchange of air into and out of the building could be determined. If a high level appeared outside the school, an elevated level inside the school was measured within two hours, the time resolution at which the system was operated. The actual level inside the school was not always the same fraction of that which appeared outside the building and this is not understood. Generally, the level inside this classroom was about a third of that outside. Whether this is the same for the other locations will be determined when the other filters are analyzed.

The Exchange of Air Particulates
Between the Inside and Outside of a Building

J.D. MacArthur, P.J. Harvey, G.R. Palmer and Xin-Pei Ma

Department of Physics, Queen's University, Kingston

Abstract

The element composition of air particulates collected simultaneously inside and outside a school has determined with particle induced X-ray emission (PIXE) using the Queen's Van de Graaff accelerator. The indoor stations were placed in three sections of a school which are ventilated separately and which are more or less isolated from each other, one a class room, the second an office and the third a workshop.

The particles were collected on streak filters operating with a time resolution of two hours so that time correlations between the indoor and outdoor air could be monitored. Two filters at each position, each of one week duration were collected. One indoor, from the class room, and one outdoor filter for the same time period have been analyzed and the other six filters will be analyzed shortly.

Al, Si, S, Cl, Ca, Cr, Mn, Fe, Cu, Zn, Br and Pb were observed both inside and outside the school. The levels of Al, Si, Ca, Br and Pb were all lower by a factor of 2 - 3 inside the school than outside, Cl appeared to be higher and the others the same. Besides Pb and Br which were expected to have elevated levels of short duration due to the traffic pattern at the intersection, several other elements showed high levels of short duration outside the school and so the exchange of air into and out of the building could be determined. If a high level appeared outside the school an elevated level inside the school was measured within two hours, the time resolution at which the system was operated. The actual level inside the school was not always the same fraction of that which appeared outside the building and this is not understood. Generally, the level inside this classroom was about a third of that outside. Whether this is the same for the other locations will be determined when the other filters are analyzed.

Introduction

People living in urban communities spend a very large fraction of their lives indoors(Yoccum 1982). Consequently, the air quality inside buildings is of considerable interest. Among the various substances which determine the air quality are air particulates which, if smokers are not present, probably come from outside the building. In order to investigate this problem, we have used a streak air filter and particle induced X-ray emission to measure the concentration of the elements in the air particulates collected simultaneously inside and outside a school in Kingston.

In his summary, Yoccum(1982) reports on many aspects of the indoor/outdoor relationships and the problems associated with the interpretation of the results. As might be expected, smokers influence significantly the quantities of certain pollutants in a building, including respirable particulates, such that indoor/oudoor ratios much larger than one are the norm. Even in residences without smokers and in office buildings where air conditioning exists, Yoccum calculates from the data of Moschandreas et al.(1981) that the indoor/outdoor ratio is > 1 for respirable particulates. In the case of lead, Halpern(1978) measured the indoor/outdoor ratio in New York city using, in series, two nucleopore filters with different pore sizes and concluded that there was no "homeostatic balance between indoor and outdoor pollutant levels". For sulphates, in a study using a streak filter to obtain the time relationship, Moschandres et al.(1979) found, inside homes, slightly smaller levels of this pollutant which they considered to be in the form of ammonium sulphate.

In a Canadian study Pengelly et al (1984) measured the total suspended particulates and found that the indoor/outdoor levels are close to unity or even > 1 if there are several smokers present. However, not all particulates are of equal concern since only the fine fraction (particles with aerodynamic diameters <2.5 μm) enters the gas transfer area of the human respiratory tract. In a previous test of a streak filter(MacArthur and Palmer 1983), we inferred that this device preferentially collected the fine fraction and therefore is well suited for a study of the transfer of respirable air particulates between the inside and outside of a building. Furthermore, a preliminary observation of the daily average of the levels inside a school compared to that outside indicated that the levels were quite measureable with this technique.

For a time relationship to be established, changes in element levels must be available. Previously we established that there were sharp increases in the Pb and Br levels with increased traffic density. Consequently, these can serve as time references for a study of this type. As this study progressed, other pollution incidences with very rapid changes in element levels were also observed so that there are many oppurtunities to measure time delays.

The Situation

Three streak filters were placed (fig. 1) in a school which has at least three separate parts with independent ventilation. This afforded an opportunity to study how sections with different activity levels might respond to outside disturbances. One filter was placed in the main office where there is a high level of activity; another was placed in a "business" room which was used by relatively few students; and the third was placed in a drafting-modelling room which was close to an outdoor filter and one of the main traffic arteries. A streak filter with accompanying weather station was placed in the school yard.

The air particulates were collected on 0.45 μm Nuclepore moving at 1mm/hr past a 2x4 mm^2 nozzle which drew the air upwards at ~0.3 l/min. The air flow through the filters inside the school was monitored daily and found to be constant to better than 10%, while a microprocessor, measuring the weather parameters, also measured and recorded, half hourly, the flow through the outdoor filter.

The Analysis

An external beam of 3 MeV protons from the Queen's University Van de Graaff accelerator was used to analyze the deposited layer of air particulates at 2 mm intervals along a filter. The protons excite the atoms of the deposit which emit X-rays characteristic of the element. These X-rays are observed with two Si(Li) detectors, one more sensitive to low energy X-rays and the other more sensitive to higher energy X-rays. In the resulting spectra, the counting rates for each peak are a measure of the amount of the corresponding element present. This PIXE technique has a sensitivity of ~1 ppm but, more importantly, in this application requires very small amounts of material. At a typical spot along the filter, 10 ng of deposit is analyzed at any one time and this is 10 to 100 times the minimum detectable limit for a counting time of a few minutes and a beam of moderate intensity (~3 nA).

Fig 2 shows an X-ray spectrum and is presented to show the level at which different elements are present as well as to give an indication of how reliable statements about the presence of any element might be. This spectrum is actually the sum of 24 spectra of lower statistical accuracy and is equivalent to what would be observed if the air particulates were collected on a daily average rather than the two-hourly basis used in this study. Clearly present are S, Fe, Pb etc. These are not unexpected since sources of such elements are well known. However, small peaks due to Mn and Cr are also seen. (These are quite distinctly seen in the second, larger detector which is more sensitivity to higher energy X-rays). Since any explanation of why these are present is more difficult, one needs to be convinced that these elements are observed before concluding that there is a source of such elements.

For quantitative results to be given, the efficiency at which each element is detected must be determined for the particular experimental arrangement used to obtain the spectrum. This efficiency varies smoothly with atomic number because of the excitation process and was determined with thin layers of known thickness for a range of elements. This procedure has been found to provide reproducible results, of ~10%, on the same sample in different experimental arrangements. Consequently, the accuracy of the concentration for most elements is determined by the counting statistics and any error in the peak fitting routine.

Results

The results of such scans are the simultaneous concentrations of many elements inside and outside the building. As an illustration of such results, Fig 3 gives the concentration of S and Pb, two of the more interesting elements, measured in the business room and outside for one week. Average values of all elements measured in the business room and the outside are given in table 1 for the week. The indoor-outdoor ratio (I/O) is also given and shows that most of the elements exist at lower concentrations inside than outside. This suggests that the outdoors is the source of the pollutants. The ratios are similar to the values given by Alonza et al.(1979) for the situation in homes where the windows are wide open. Since there is a continuous intake of the air from the outside for the school, this seems the most appropriate comparison to make.

Table 1

Element	Inside	Outside	I/O	a	σ_a	b	σ_b
Al	0.21	0.074	0.26	0.051	0.012	0.112	0.026
Si	0.74	0.158	0.21	0.105	0.029	0.071	0.014
S	0.70	0.65	1.08	0.025	0.074	0.888	0.075
Cl	0.008	0.031	3.9	0.024	0.004	0.854	0.196
Ca	0.45	0.21	0.47	0.059	0.064	0.343	0.107
Cr	0.007	0.004	0.57	0.006	0.001	-.145	0.119
Mn	0.004	0.004	1.00	0.004	0.001	0.120	0.081
Fe	0.19	0.12	0.64	-.053	0.096	1.158	0.280
Cu	0.010	0.003	0.30	0.003	0.001	-.008	0.025
Zn	0.018	0.020	1.1	0.022	0.011	-.064	0.288
Br	0.038	0.014	0.37	0.009	0.002	0.146	0.049
Pb	0.179	0.061	0.34	0.038	0.009	0.132	0.040

A very simple empirical model(Klienbaum and Kupper, 1978) for the indoor-outdoor relationship is $C_i = bC_o + a$ where C_i and C_o are the indoor and outdoor concentrations respectively. When analyzed with this model, values of the coefficients a and b shown in columns 5 and 7 of table 1 result while columns 6 and 8 give the standard errors on a and b respectively. Most of the elements which are easily measured, have values of b which are distinctly non zero and therefore the inside concentrations are related to the outside levels. Only Cu and Zn have b indistinquishable from zero which indicates that there is no relationship between the indoor and outdoor levels. Had the weekly scans for these elements been presented, high concentrations of these elements would have been noticed for a few time periods, different ones for the inside and outside scans, while, for most of the week, the levels were very low. A possible explanation for these observations is that these measurements are due to a rare large particle (~10 μm diameter) during the time period and therefore, no correlation would be expected between the arrival of a large particle inside and outside at the same time. Since the constants for S, Ca and Fe are consistent with zero, it appears that the inside concentration for these elements is due completely to the outside level.

Dockery and Spengler(1981) interpret the constant, a, in this model as a source term, and the coefficient, b, as a measure of the filtration, b=1-F, where F is the efficiency of the ventilation system. An examination of the table reveals that the value for the efficiency must vary between ~0 and ~90% for the different elements. Whether the actual value for a specific element is an indication of the size of the particle can only be speculative. However, as an example, if S is associated with very small particles formed when SO_2 is changed to a sulphate, then these small particles might be expected to pass through the filters of the ventilation system. The reason that source terms are present for most of the elements might be due to the fact that particles containing these elements are deposited in the room and then resuspended with activity in the room. Thus, they would appear continuously in the room as a source.

This simple model gives clear indications that the pollutants, found inside the school, enter from the outside. However, it does not give the source of the pollutants. The multivariant statistical procedure, factor analysis, has been used to identify the sources. This is a receptor model since no *a priori* information of what sources are producing the pollutants is assumed. Instead, correlations between the levels of the many observed elements are used to deduce a smaller number of independent variables or factors from the eigenvalues of the correlation matrix for all the measurements. The particular elements in each of these factors is usually suggestive of a possible source. This procedure requires a decision to be made on how many factors are, in fact, present. A common criterion(Wolff and Korsog, 1985; Hopke, 1982; Heidam, 1982) is to retain factors which have an eigenvalue >1. Table 2 shows the results of the factor analysis on both the indoor and outdoor samples. With the criterion stated, only 4 factors were needed to represent the outdoor data. However, we allowed the factor analysis to proceed with an eigenvalue cutoff of 0.95 in order to include a fifth factor because its value was 0.97 which is relatively close to 1, the eigenvalue for the sixth factor is significantly less than one and the presence of 5 factors means that a comparison between the inside and outside sources has some symmetry. After a varimax rotation was performed in this analysis, the fifth factor had an eigenvalue >1 which is additional justification for retaining this factor(Hopke, 1981).

Table 2

	Inside					Outside				
Factor	1	2	3	4	5	1	2	3	4	5
Element										
Al	0.81					0.97				
Si	0.92					0.96				
Cl	0.61					0.30				
Ca	0.88					0.67				
Mn		0.54				0.86				
Br		0.86					0.97			
Pb		0.91					0.94			
Fe			0.99			0.98				
Zn			0.98					0.98		
S				0.89					0.88	
Cr					0.81					0.97
Cu					0.76			0.99		

As with all statistical analyses, the results in this table must be evaluated with care. Nevertheless, this table shows a number of features which other studies(Alpert and Hocke, 1981; Wolff and Korsog,1985) have observed; namely a soil source (factor 1) containing Al, Si, Cl and Ca, an automobile source (factor 2) containing Br and Pb, and a combustion source (factor 4) containing S. The other factors, although relatively well defined from the statistical analysis are not readily identified with sources. This is particularly true for the "Cr" factor since Cr is not an element which is normally observed. Its concentration is low but it is consistently present in the spectra, it does not appear to be a contaminant and it has not been established as an artifact of the system. Why Cu should associate with it inside the school is not apparent. There are differences between the inside and outside factors. For example Mn and Fe are observed outdoors in the soil factor which is the source usually attributed to these elements, while inside Mn is associated with the automobile exhaust. It has already been pointed out that the ventilation system does not filter Fe as well as Al, Si and Ca and so the appearance of Fe in a different factor inside the school may be understandable.

The results show clearly that the elements found in the business room depend significantly on outside sources. Furthermore, the time scans of the elements (fig 3) show significant changes in levels over short time intervals. Therefore, in order to obtain some indication of the time relationship between the inside concentrations and those outside, a cross correlation analysis was preformed. Fig 4 shows the results for most of the readily measured elements. No clear time delay is discernible and this is not unreasonable since (1) the resolution of the streak filter is two hours due to the size of the noozle (2 mm wide) and the speed (1 mm/hr) at which the filter moves and (2) the position of the 1 mm proton beam relative to the beginning of track is uncertain to about 0.5mm. However there is a hint of some delay for S, Fe and Pb since the centre of the distribution of the cross correlation coefficient is delayed ~ one measurement position (2 hours) relative to the Al, Si and Cl distributions which show no delay. A time delay of two hours between the inside and outside concentrations seems excessive when the outdoor measurements are made immediately adjacent to the building. Only further data of this nature with higher time resolution will give a more definitive result.

Conclusions

The simultaneous measurement of the indoor and outdoor concentrations of the elements in air particulates has shown that this is a useful way to determine the relationship between the levels both qualitatively and quantitatively.

The sources of the particulates were determined to be the same for the outdoors and this business room where the indoor measurements were made. The indoor levels for soil related and automobile related particulates are a factor of ~4 or 3 lower than the outdoor levels which is somewhat comforting if Pb were considered a problem. The sulphate level inside the school whether it is due to local combustion or long range transport was not diminished as compared to the outside level. Whether there is a delay for the particulates entering this business room has not been established.

References

J. Alonza, B.L. Cohen, H. Rudolph, H.N. Jow and J.O. Frohliger, "Indoor-outdoor relationship for airbourne particulate matter of outdoor origin", Atmos. Environ. 13 55 1979.

D.J. Alpert and P.H. Hopke, "A determination of the sources of airbourne particles collected during the regional air pollution study", Atmos. Environ. 15 675 1981.

D.W. Dockery and J.D. Spengler, "Indoor-Outdoor relationships of respirable sulphates and particles", Atmos. Environ. 15 335, 1981.

M. Halpern, "Indoor/Outdoor air pollution exposure relationships", J. Air Pollution Control Assoc., 28, 689 1978.

N.Z. Heidam, "Atmospheric aerosol factor models, mass and missing data", Atmos. Environ. 16 1923 1982.

P.K. Hopke "The application of factor analysis to urban aerosol resolution", American Chemical Society Series, No. 167 Atmospheric Aerosol: Source/air Quality Relationships ed. E.S. Macias and P.K. Hopke, 1981.

P.K. Hopke, Comments on "Trace element concentrations in summer aerosols at rural sites in New York State and their possible sources", Atmos. Environ. 16 1279 1982.

D.G. Klienbaum and L.L. Kupper *Applied Regression Analysis and Other Multivariate Methods*, Duxbury press, North Scituate, Mass

J.D. MacArthur and G.R. Palmer, Proceedings of the Ontario Ministry of the Environment Technology Transfer Conference #4, 657 1983.

D.J. Moschandreas, J.W. Winchester, J.W. Nelson and R.M. Burton, "Fine particle residential indoor air pollution", Atmos. Environ. 13 1413 1979.

D.J. Moschandreas, J. Zabransky and D.J. Pelton, "Comparison of indoor and outdoor air quality", Electric Power Research Institute, Report EA-1733, Palo Alto, CA, 1981.

L.D. Pengelly, C.H. Goldsmith, A.T. Kerigan, S.A. Toplack and H. McCage, "The Hamilton Study: Refinement of SO2 and particulate data for exposure estimation", Proceedings of the Ontario Ministry of the Environment Technology Transfer Conference #5, 683 1984.

G.T Wolff and P.E. Korsog, "Estimates of the concentrations of sources of inhalable particulate concentrations in Detroit", Atmos. Environ. 19 1399 1985.

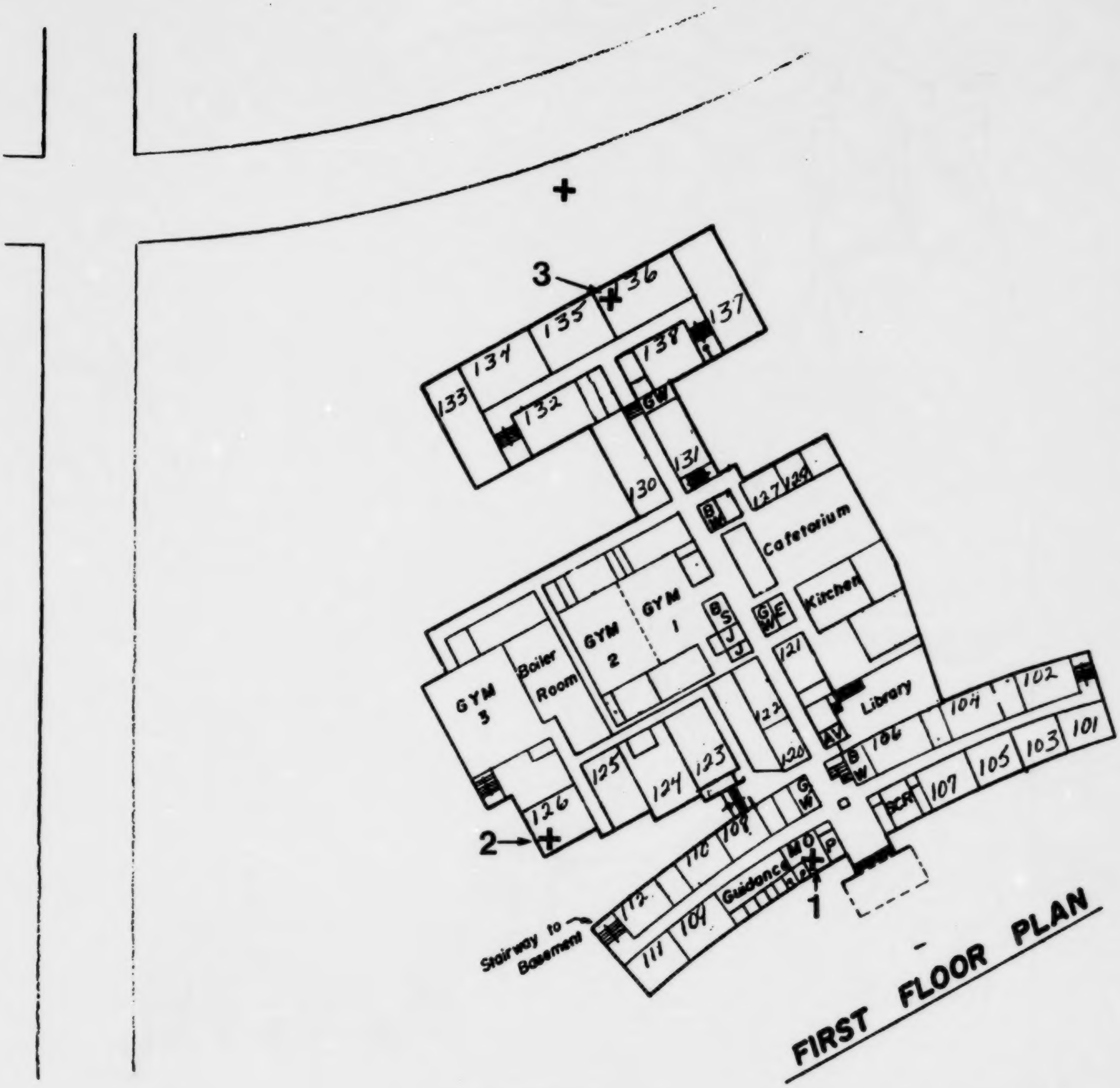
3
136
137
135
134
133
132
138
GW
131
130
127
129
B W
Cafetorium
Kitchen
GYM 1
GYM 2
GYM 3
Boiler Room
B S J J
G W
E
121
122
120
Library
AV
102
104
101
103
105
106
107
B W
SCR
125
124
123
126
G W
109
110
112
Guidance
M O
P
2
1
104
111
Stairway to Basement
FIRST FLOOR PLAN

Fig. 1 The location of the filters inside and outside the school. The nearby main traffic arteries are also shown. Inside filter 1 was placed in the main office; filter 2 was placed in a "business" room well separated from the main activity of the school; and filter 3 was placed in a drafting-modelling room.

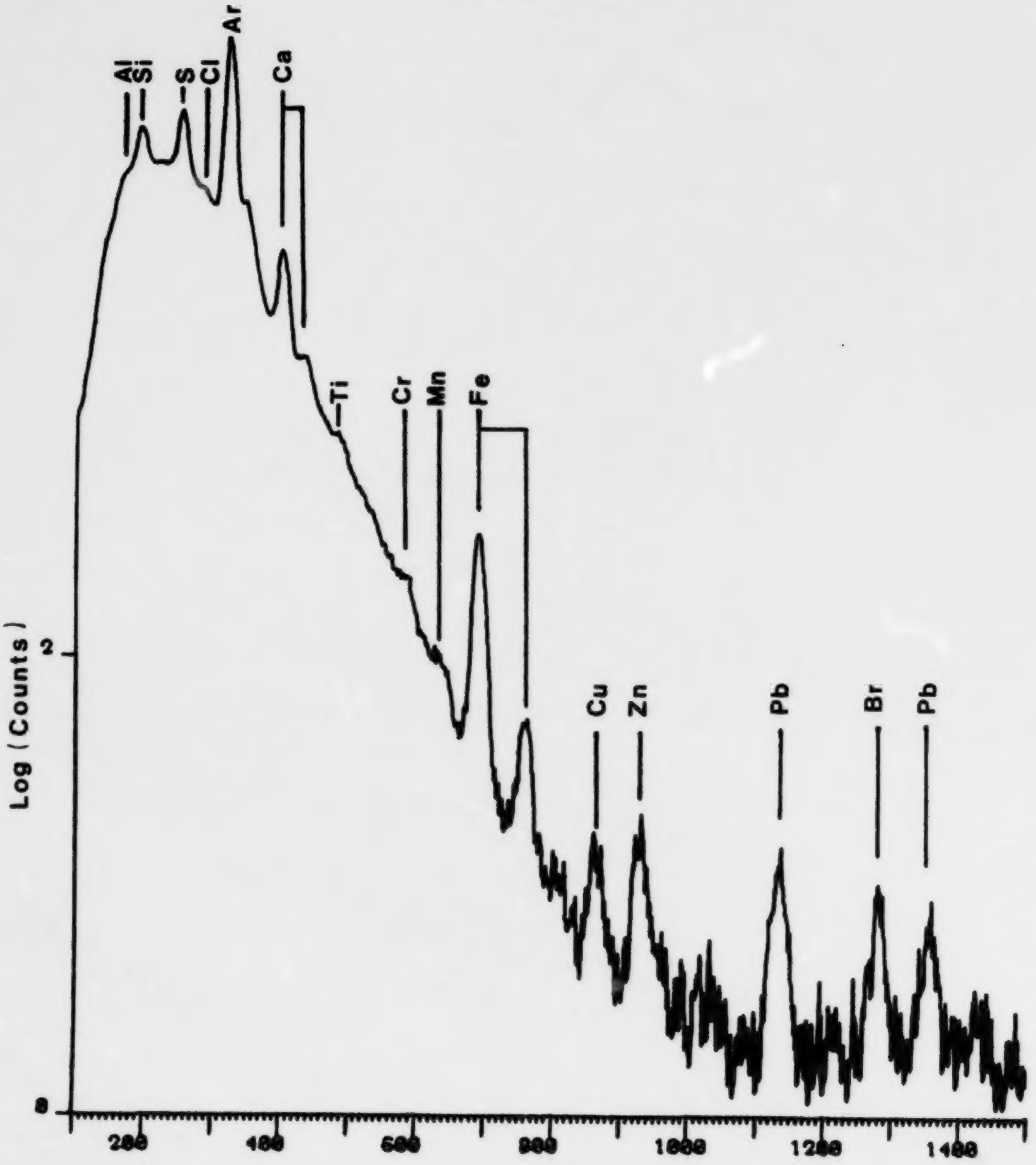

Fig. 2 A spectrum taken with the detector more sensitive to low energy X-rays. The peaks are identified with element producing the X-ray. This spectrum is the summed of 24 succesive spectra spanning a two day period.

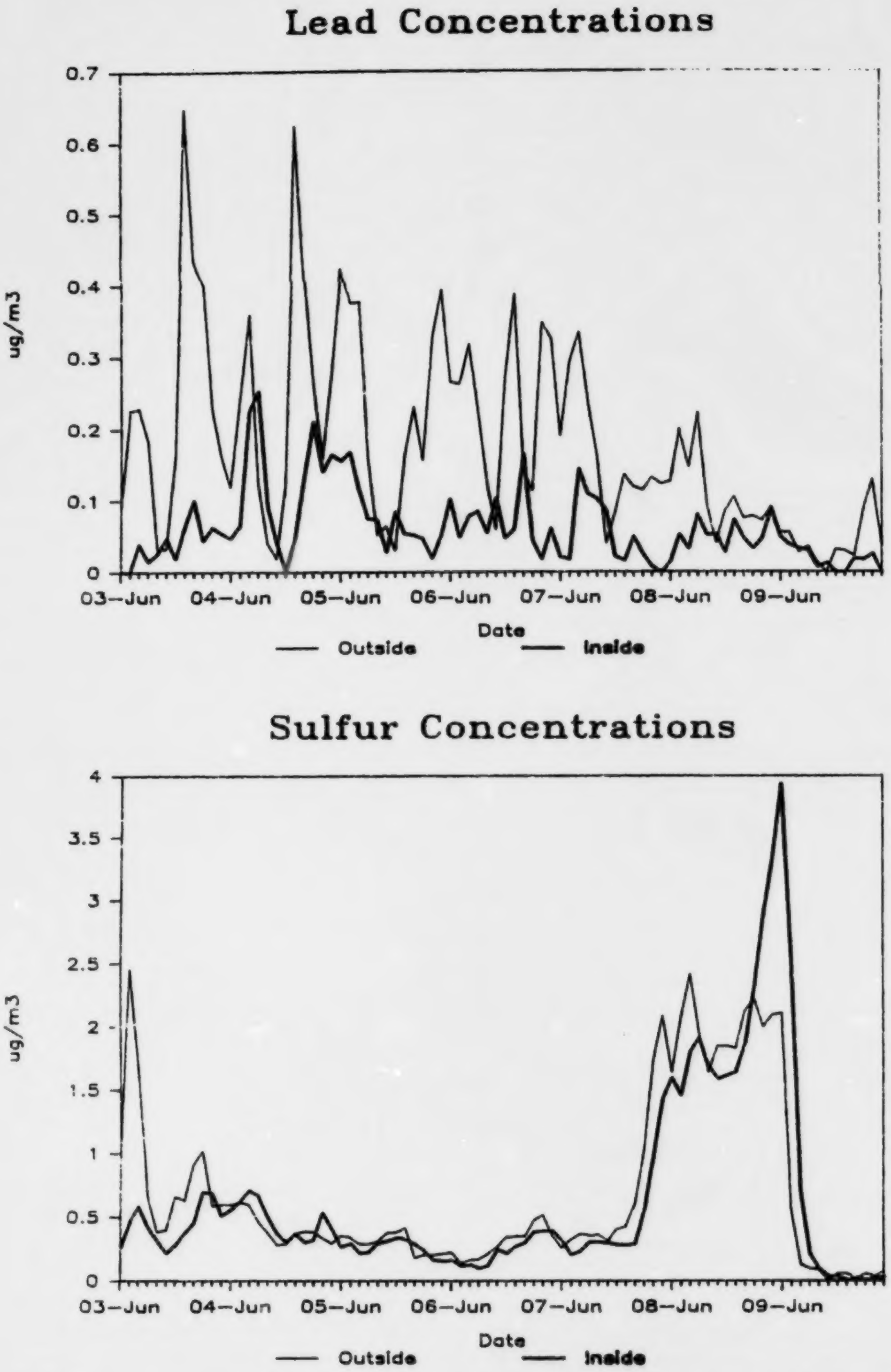

Fig. 3 Weekly time scans for S and Pb from the outside station and the filter in the business room. Significant changes in level are observed and there is a good correlation between the inside and outside levels.

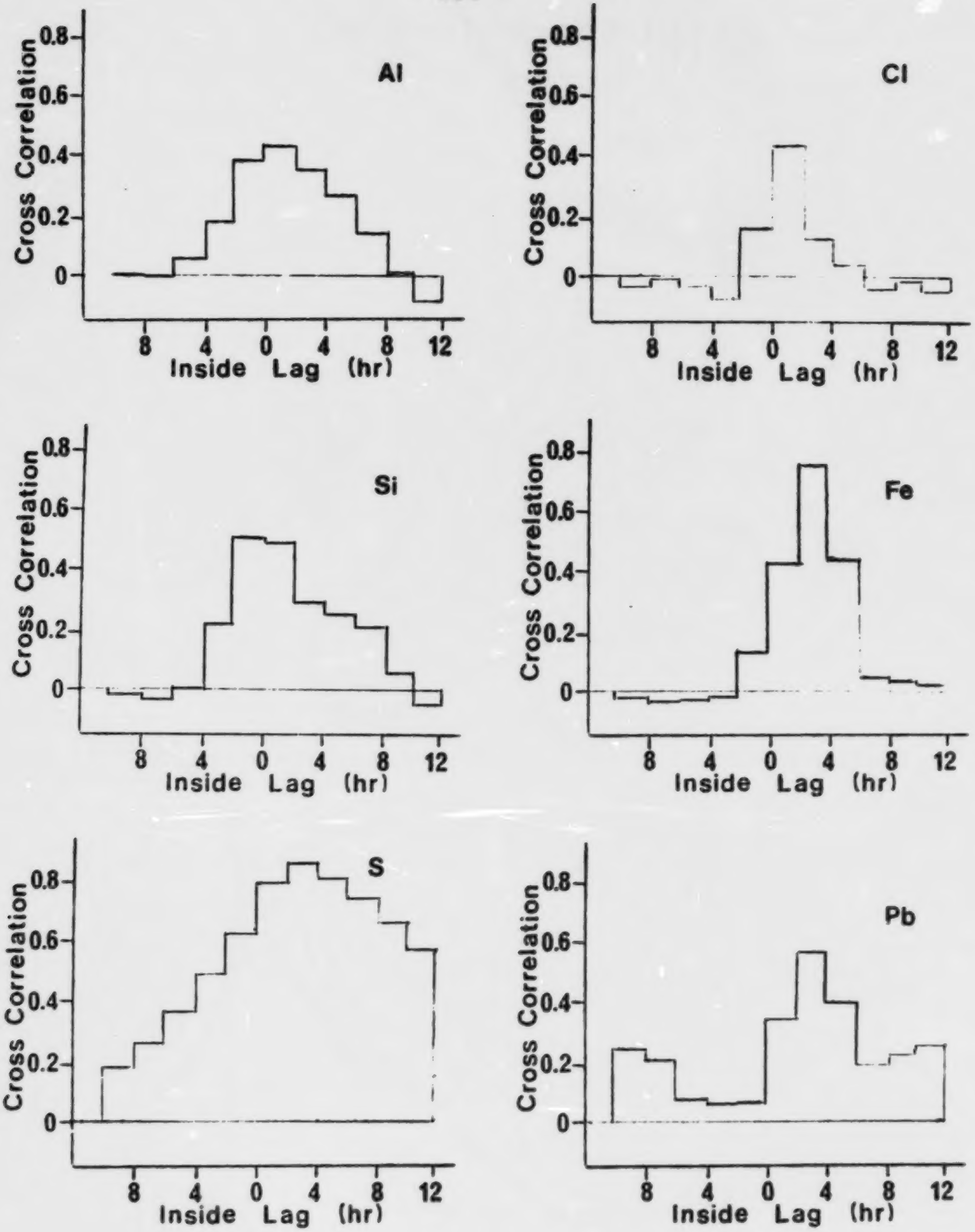

Fig. 4 Cross correlations between levels in the business room and the outside for several elements. Although there are indications of a delay for some elements to reach the inside of the school the time resolution of the present system is not sufficiently good to establish the delay.

FEASIBILITY OF DETERMINING SO_2 MASS EMISSION FLUXES BY STACKSCANNING

R.C. Mitchner and R.A.H. Buxton. MONITEQ Ltd.

Key words: Stack Emissions. Emissions Monitoring. Sulphur Dioxide.

ABSTRACT

The MONITEQ PLUMETRACKER has a proven record for being able to remotely measure SO_2 concentrations in overhead plumes several kilometers downwind of a stack. During 1984, with the assistance of the Ontario Ministry of the Environment, MONITEQ undertook a study to assess the feasibility of using a PLUMETRACKER from a stationary platform to measure SO_2 emissions at the mouth of a stack. A 5-metre high test stack normally used by the Ministry to train personnel to measure plume opacity was used for these investigations. Parameters studied included varying SO_2 concentrations, plume opacities, background sky conditions and the effects of the sun and sight elevation angles. The SO_2 concentrations exiting from the stack were verified using an in-stack continuous emission monitor (CEM).

The work established that there is a strong correlation between the CEM value and the PLUMETRACKER value, but that the nature of the correlation varied from experiment to experiment. The correlation desired is a linear, one-to-one relationship between the CEM measurement and the PLUMETRACKER measurement (as was obtained in an initial laboratory comparison). The field results obtained did yield linear relationships, but they showed three forms of variation from the ideal: an offset; a slope other than one; and scatter in the points. This behaviour is ascribed to several causes, including instrumental effects and those related to the experimental procedure.

The principal instrumental effect is believed to be caused by a variation in response within PLUMETRACKER's rectangular field of view. Such performance, if true, is not noticeable in the instrument's normal mode of operation wherein the angular extent of the plume (some distance downwind of the source stack) greatly exceeds that of the instrument's field of view (FOV), but is significant under the stationary conditions of this study wherein the plume size at the stack mouth is much smaller than the instrument's FOV. The effects of the other parameters under study were small in comparison to the aforementioned and it was therefore not possible to quantitatively determine their impact upon the measurement.

The study concluded that the PLUMETRACKER and the measuring technique can be modified to overcome the variable response problem of the PLUMETRACKER FOV. The proposed solution is to reduce the instrument's FOV and adopt a true scanning technique whereby the instrument's FOV is uniformly scanned across the mouth of the stack.

ABSTRACT

The study presented was designed to assess the feasibility of using the MONITEQ PLUMETRACKER from a fixed platform to remotely determine SO_2 emission levels from point sources. The study was conducted using a test stack for which the parameters to be examined could be controlled and their effect on the measurement accuracy determined. The results showed a reasonable correlation between the measured and actual emissions. However, the relationship varied significantly for each series of measurements. The variance in the data made it difficult to accurately determine the effect on the measurement of the parameters to be studied. The variance in the data was most likely due to spatial variations within the PLUMETRACKER field of view. Consequently an alternative measurement technique to reduce the effect is presented.

INTRODUCTION

At present, the determination of SO_2 emission levels from stacks or other stationary sources is usually made from in-stack measurements and/or from mass balances based upon fuel sulphur content. These methods usually require, at the very least, the co-operation of the stack operator and in many instances real time emission information is not possible. There are a few instruments available which allow the measurement to be made remotely. However, the accuracy of the measurement by these instruments is largely dependent upon detailed knowledge of the plume direction and velocity (Ref. 1). Consequently, current remote techniques usually require the services of several personnel and are generally time consuming (Ref. 2).

An instrument which can perform an accurate remote measurement with relative ease would be of great benefit to the monitoring industry. With such a device, stack emission levels could be verified rapidly at the discretion of the monitoring personnel, and, in most cases, the measurements could be obtained from outside the plant boundary.

The objective of this study was to assess the feasibility of using the MONITEQ PLUMETRACKER to make such a measurement. In addition, the study evaluated the influence of specific parameters, such as plume opacity, background sky conditions, sun angle, etc., on the accuracy of the measurement.

EXPERIMENTAL

Instrumentation

The MONITEQ PLUMETRACKER is a remote sensor which simultaneously measures ambient burdens of SO_2 and NO_2. Utilizing the sun as the source of UV radiation, the measurement is achieved by measuring the absorption of SO_2 and NO_2 at specific wavelengths. The wavelength chosen is one at which the target gas has strong absorption, yet absorption by other gases is minimal. Changes in source intensity are compensated for by also measuring the intensity of radiation at nearby wavelengths known to have little absorption to the target gas.

For purposes of this study, it was necessary to modify the rectangular field of view of the PLUMETRACKER, nominally 1.6 by 60 mrad, such that the longer dimension was located on a horizontal plane. To avoid complicated instrument modifications, this was accomplished by simply rotating the instrument 90^o and operating it on its side. A telescopic sight was added to the instrument to allow the operator to visually align the PLUMETRACKER on the intended target.

In order to control as many of the parameters as possible, a portable test stack provided by the Ontario Ministry of the Environment was utilized throughout the study. This twelve foot high, one foot diameter, stack was equipped with a combustion chamber, opacity monitor and a fan capable of delivering an output air velocity of approximately twenty feet per second.

Actual in-stack concentrations of SO_2 were measured using a continuous emission monitor also provided by the Ontario Ministry of the Environment. The instrument utilizes infrared absorption of SO_2 to make the measurement and was capable of measuring SO_2 concentrations up to 3000 ppm.

Study Methodology

A typical field arrangement is illustrated in Figure 1. The required SO_2 emission levels were obtained by controlling the rate at which pure SO_2 gas was introduced into the air intake system. The actual SO_2 emission levels were verified by sampling the gas near the stack mouth using the continuous emission monitor.

Plume opacity was achieved through the controlled burning of toluene inside the combustion chamber adjacent to the stack air intake. The combustion products were mixed with the air and SO_2 being drawn into the system, and the entire mixture was then exhausted out through the stack. Since this was a small stack, no harmful effects were caused by the release of SO_2.

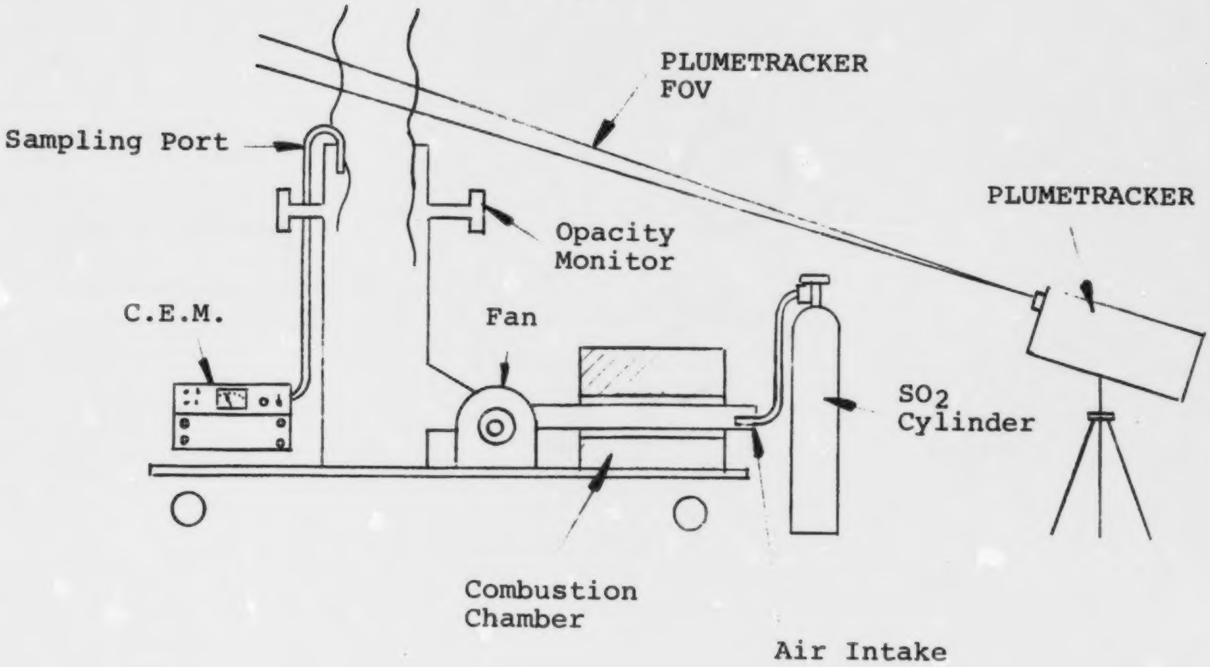
PLUMETRACKER FOV
Sampling Port
PLUMETRACKER
Opacity Monitor
C.E.M.
Fan
SO_2 Cylinder
Combustion Chamber
Air Intake

Figure 1: Typical Field Arrangement

Measurement Technique

The orientation of the PLUMETRACKER field of view with respect to the stack mouth is illustrated in Figure 2. Prior to each series of measurements, the PLUMETRACKER was aligned such that the stack emissions were located within the horizontal dimensions of the field of view (Figure 2a). The instrument's field of view was also aligned in the vertical direction so that the emissions a few cm's above the stack mouth were monitored (Figure 2b). Typical dimensions of the field of view at the stack mouth are shown in Figure 2. The actual dimensions are dependent upon the distance between the stack mouth and the PLUMETRACKER, and were varied throughout the study.

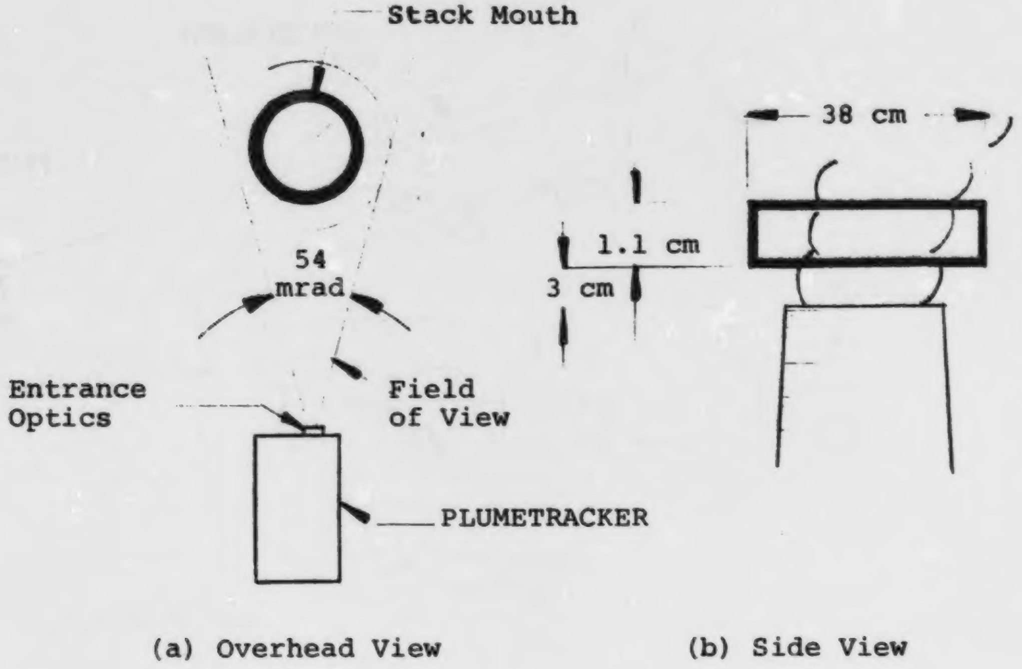

(a) Overhead View (b) Side View

Figure 2: Orientation of the PLUMETRACKER Field of View

Calculation of Plume Concentration

The PLUMETRACKER measures the total absorption due to SO_2 within its field of view. The units of the measurement are commonly expressed in parts per million-meter (ppm-m) and represent the product of the average SO_2 concentration over the total optical pathlength. For the purpose of this study, where the absorption of SO_2 outside of the stack region was not of interest, a background or 'zero' reading was obtained by shutting off the flow of SO_2 prior to each series of measurements. The actual in-stack SO_2 concentrations were calculated from the PLUMETRACKER reading by correcting for the field of view coverage, the viewing angle and the plume geometry. Since the PLUMETRACKER was viewing an area immediately above the stack mouth, a cylindrical plume having a diameter equal to the stack diameter was assumed.

RESULTS

Laboratory Calibration

Twice during the field program, both the PLUMETRACKER and the CEM were calibrated in the laboratory. Following their individual calibrations, both analysers were connected in series to the calibration arrangement and their responses compared. The results of the laboratory comparison are shown in Figure 3, which illustrates an almost ideal 1:1 relationship between the two.

Field Study Without Wind Shield

The initial objectives of the field study were to determine the effects of the field of view coverage and the PLUMETRACKER elevation angle upon the accuracy of the measurement. This was accomplished by conducting measurements with the PLUMETRACKER at varying distances from the stack mouth. A plume opacity of zero was maintained throughout this series of tests. A typical result of the comparison between the measured and the actual in-stack SO_2 concentrations is shown in Figure 4. In general the results showed a reasonable correlation between the two measurements ($r > 0.90$). However, the relationship between the two was not 1:1 as expected. The actual relationship (PLUMETRACKER:In-Stack) was found to vary from as little as 0.9:1 to greater than 3:1.

The reason for the varying relationships was not discovered until measurements involving plume opacity were attempted. With the plume visible, it was possible to see the effect of the ambient wind on the plume rise. For the most part, with wind speeds in excess of 5 km/hr., the plume rise was less than one or two cm. Quite often, a significant portion of the plume was forced below the exit level of the stack.

FIGURE 3

Laboratory Comparison
November 19, 1984
~~Correlation Coefficient: 0.99~~

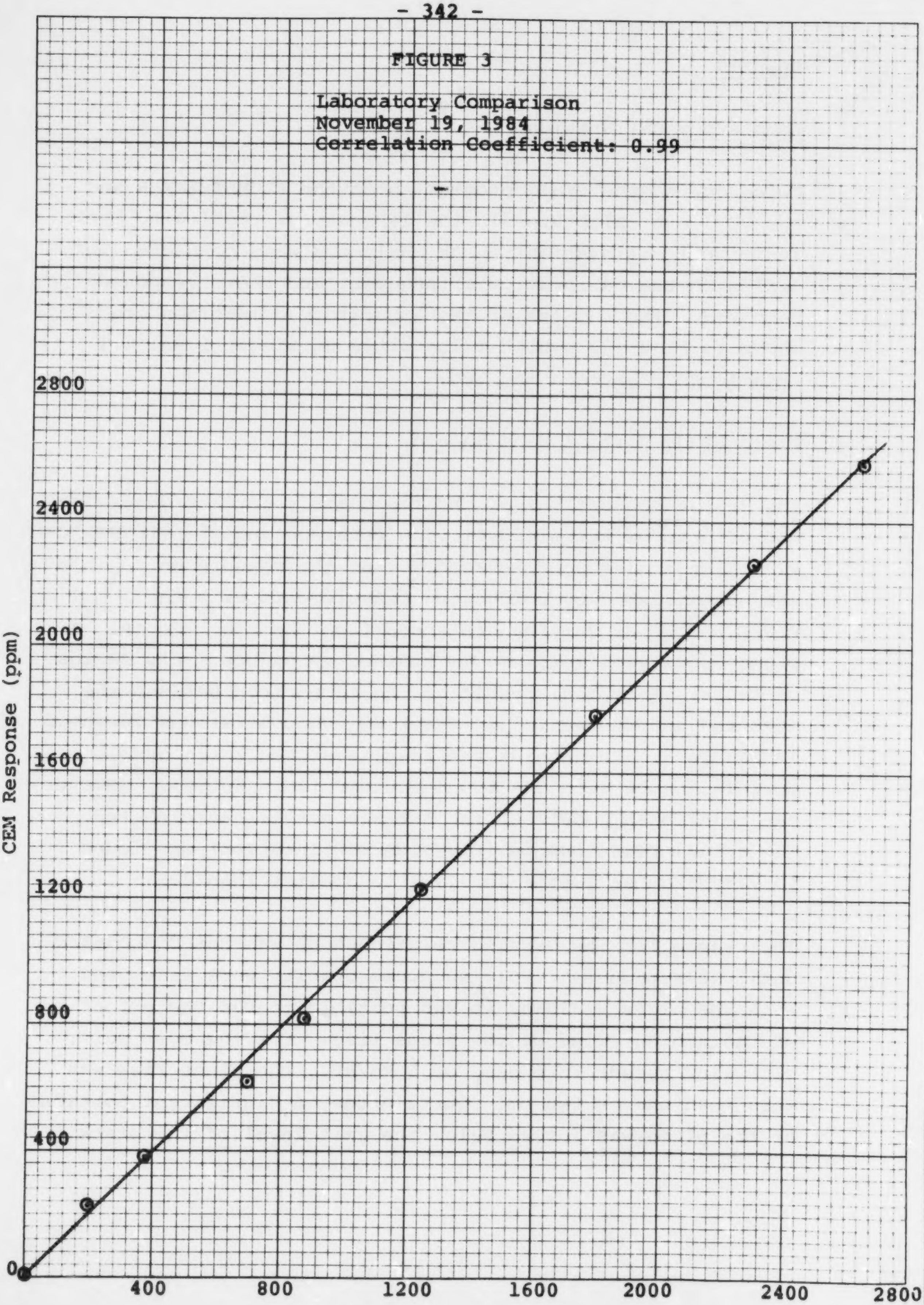

K•E 10 X 10 TO THE INCH • 7 X 10 INCHES
KEUFFEL & ESSER CO. MADE IN U.S.A.
46 0700

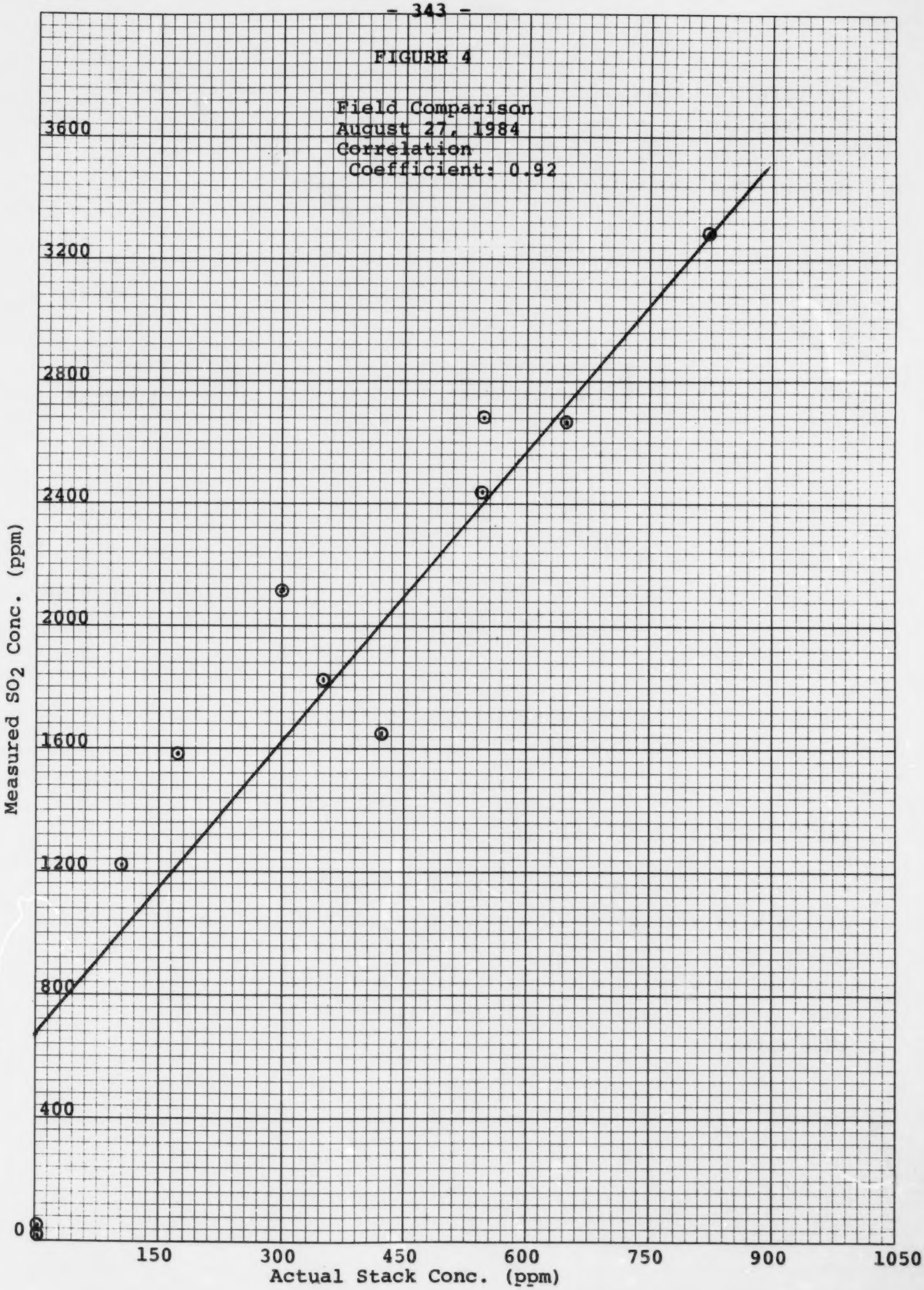

FIGURE 4

Field Comparison
August 27, 1984
Correlation
Coefficient: 0.92

46 0700
K&E 10 X 10 TO THE INCH • 7 X 10 INCHES
KEUFFEL & ESSER CO. MADE IN U.S.A.

The effect on the remote measurement is illustrated in Figure 5. Insufficient plume rise results in a greater portion of the FOV being covered which in turn results in an increased absorption being detected by the PLUMETRACKER.

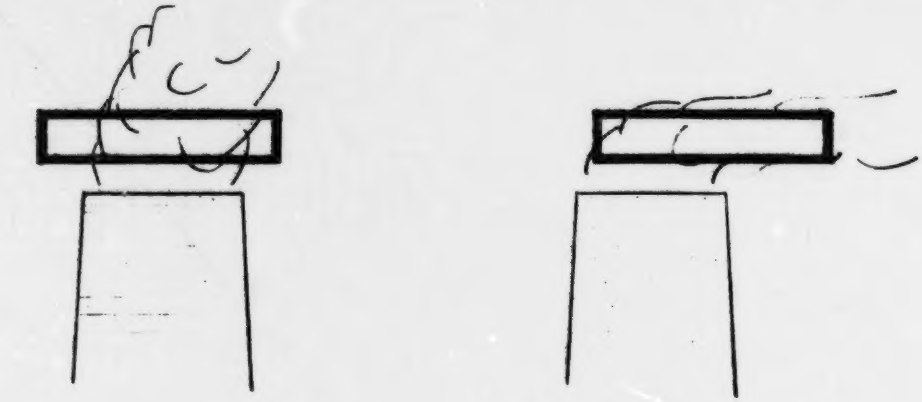

Sufficient Plume Rise
Expected FOV Coverage

Insufficient Plume Rise
Excessive FOV Coverage

Figure 5: Effect of Wind on Plume Rise

Field Study With Wind Shield

To avoid the problems associated with insufficient plume rise a wind screen was constructed, and was placed up wind of the stack. In addition, the remainder of the field program was carried out only during low to moderate wind conditions to ensure a sufficient plume rise of greater than 6 cm.

In general the results showed an improved correlation (r > 0.97) between the measured and actual concentrations. However, the relationship between the two was found to vary from 2:1 to 3:1. On only one occasion was the measured to actual relationship found to remain constant between two successive series of measurements. This occurred on the final study day when two sets of measurements were undertaken without changing the position of the PLUMETRACKER (Figure 6).

DISCUSSION

The general lack of repeatable results made it difficult to draw any definite conclusions with respect to the parameters under study. A review of the data does show, however that the single most important factor contributing to the lack of consistent results was the re-positioning of the PLUMETRACKER between each series of measurements. On the one occasion when the PLUMETRACKER was not re-positioned, the two sets of measurements were almost identical even though the plume opacity and sun angle had been varied.

The most probable explanation for this observation is that the response of the PLUMETRACKER is dependent upon the location of the plume within the instrument's field of view. In its normal mode of operation and during the laboratory calibration, the PLUMETRACKER field of view is fully covered and this effect is not observed. It appears that the variation in responsivity is only observed when the target source is smaller than the instrument field of view. Such behaviour could be caused by several mechanisms including; spatial variations in the photomultiplier responsivity or a variety of optical aberrations within the spectrometer.

Generally the background sky conditions had little effect on the measurement as long as there was a sufficient amount of UV radiation. Factors which effect the available amount of

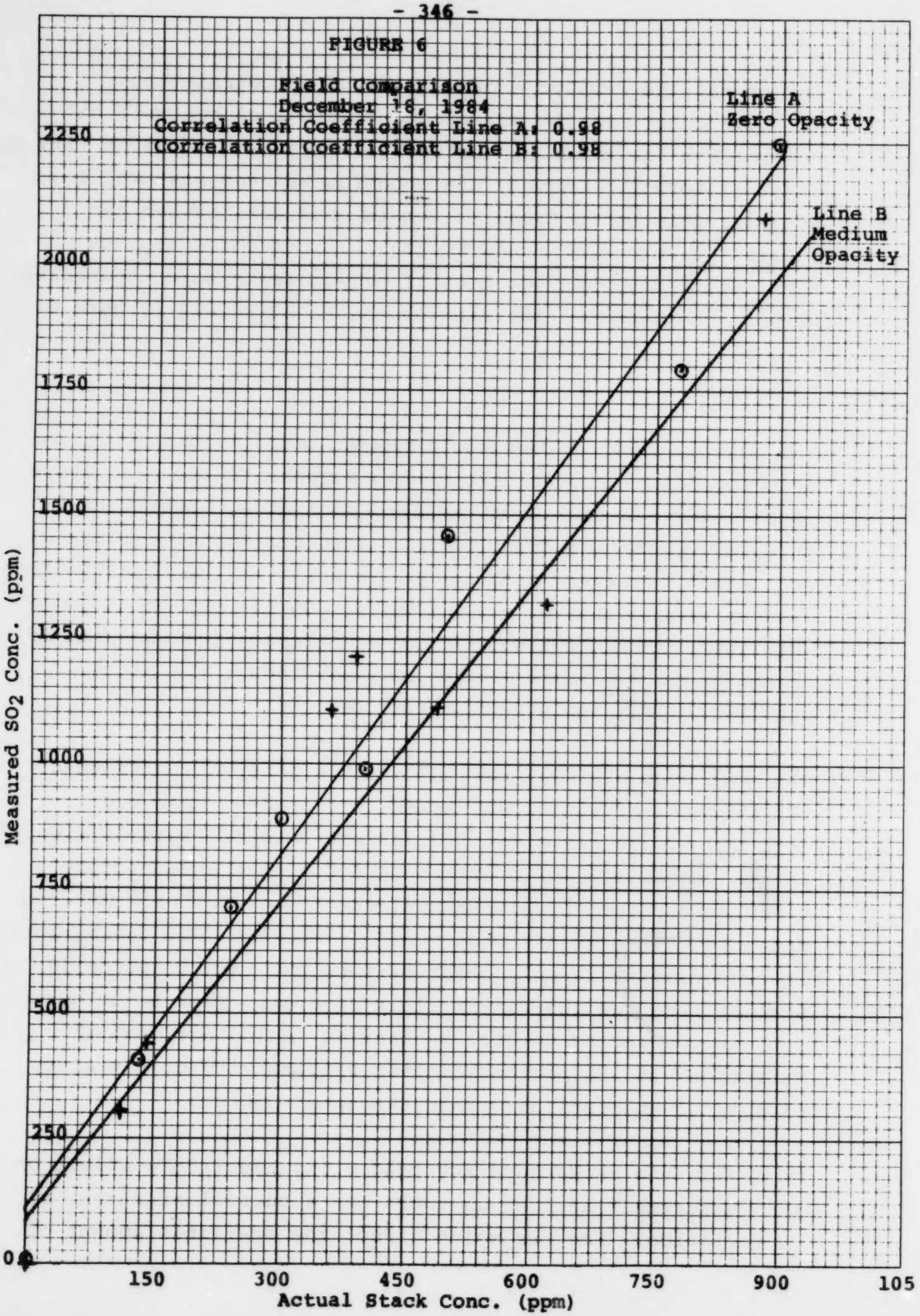

FIGURE 6

Field Comparison
December 18, 1984
Correlation Coefficient Line A: 0.98
Correlation Coefficient Line B: 0.98

46 0700

K+E 10 X 10 TO THE INCH • 7 X 10 INCHES
KEUFFEL & ESSER CO. MADE IN U.S.A.

UV radiation include; the sun angle, the position of the sun relative to the sky viewed by the PLUMETRACKER and the cloud cover. During the summer months sufficient UV radiation is available during normal daylight hours even with the presence of a heavy cloud cover. The low sun angle during the winter months, however limited the operation of the PLUMETRACKER to approximately four hours under conditions of light to moderate cloud cover.

The only results which allow for conclusions concerning the effect of plume opacity are those which were obtained on the final study day. The data does indicate that there is little if any effect on the measurement for plume opacities up to 20%. With respect to SO_2 concentration, the study shows that a reasonable correlation exists between those results obtained from the PLUMETRACKER and the actual in-stack concentrations up to approximately 3000 ppm.

The exact nature of the relationship, however was not 1:1 as expected and except for the final study day, a significantly different relationship was found for each series of measurements.

CONCLUSIONS

The results of study suggest that the use of the PLUMETRACKER from a fixed platform offers promise for the remote measurement of stack emissions.

The lack of consistent results and the non ideal 1:1 relationship are likely attributable to the spatial variations of the plume within the PLUMETRACKER field of view when the instrument was re-positioned for each series of measurements.

In future, spatial variations can be overcome by combining a scanning technique using a motor driven platform with a modified PLUMETRACKER optical arrangement. This should eliminate any effects due to spatial variations within the instrument's field of view and result in an improved correlation between the measured and actual in-stack concentrations.

Of the parameters studied, background sky conditions and plume opacity were expected to have the greatest effect on the measurement. Although the variability of the data makes it difficult to draw any definite conclusions, the results suggest that these paramters have little if any effect on the accuracy of the measurement.

ACKNOWLEDGEMENTS

This study was supported by the Ontario Ministry of the Environment whose assistance and support are gratefully acknowledged. We also wish to acknowledge the assistance of Ontario Hydro on whose property the study was conducted.

REFERENCES

1) T.V. Ward, S.C. Jain, "Determination of Mass Flux of Sulphur Dioxide by Using Optical Remote Sensing Spectroscopy", MONITEQ Report prepared for ARB, OME (1980).

2) S.C. Jain, T.V. Ward, S. Onlock, "A Demonstration of the Feasibility of Using Remote Sensing to Measure Specific SO_2 Source Emissions", MONITEQ Report for Environment Canada (1979).

GAS PHASE PHOTOCHEMISTRY OF POLYCHLORINATED BIPHENYLS

Nigel J. Bunce and Jo-Anne Langshaw
Department of Chemistry and Biochemistry, University of Guelph

Key words: PCBs, Photodecomposition, Air Pollution, Contaminant Transport, Aromatic Hydrocarbons.

ABSTRACT

The quantum yields of photodecomposition of a series of polychlorinated benzenes and polychlorinated biphenyls have been determined in the vapour phase. Most of the compounds studied decompose with a photochemical efficiency in the range of 10 - 20%. By making use of literature data on typical ambient concentrations of PCBs in urban air, and literature data on the variation of the solar intensity with wavelength, it has been concluded that photodecomposition of these substances is very slow in absolute terms. Consequently, chlorinated aromatic hydrocarbons are able to travel through the atmosphere and to be deposited unchanged far from their point of emission into the atmosphere. These conclusions are in line with practical experience. Details of the methods used for the actinometry and for the calculations will be discussed.

Vapour phase photochemistry of chlorinated aromatic hydrocarbons

Nigel J. Bunce, James P. Landers and Jo-Anne Langshaw
Department of Chemistry & Biochemistry
University of Guelph, Guelph, Ontario N1G 2W1

Final Report to the Ontario Ministry of the Environment: Project 107RR.

Chlorinated aromatic hydrocarbons are widespread and persistent pollutants. The EPA priority pollutant list (1978) mentions chlorobenzene, the three dichlorobenzenes, 1,2,4-trichlorobenzenes, hexachlorobenzene, and the polychlorinated biphenyls (PCB's) as examples of priority pollutants. DDT is an example of a chlorobenzene derivative.

In addition to the many studies of the biological chemistry of these chlorinated hydrocarbons, there have also been numerous photochemical studies. The justification for these photochemical studies has been that because these chlorinated hydrocarbons absorb light in the region of the solar spectrum (although very inefficiently) there may be a chance that sunlight assisted degradation is one of the routes by which these substances disappear from the environment.

Pollutants such as the PCB's may be found in locations very remote from any industrial activity. They have, for example, been found in the snows of Antarctica(1). It follows that they must have reached this location by transport through the atmosphere. This is reasonable, given the relatively high volatility of many of these compounds. Recent estimates of the amounts of PCB's in the atmosphere (over the United States) are estimated to be of the order of 18 tonnes at any time, which translates to 900 tonnes cycled through the atmosphere per year when the residence time is assumed to be 1 week[2]. Volatilization from landfills is thought to be a much more important source of atmospheric PCB's than incinerations[2,3].

Previous liquid phase studies

Most of the previous photochemical studies of chlorinated aromatic compounds have been made in the liquid phase, usually in solution. The primary photochemical act is usually cleavage of the carbon-to-chlorine chemical bond (eq. 1); this is the weakest bond in the molecule.

e.g. 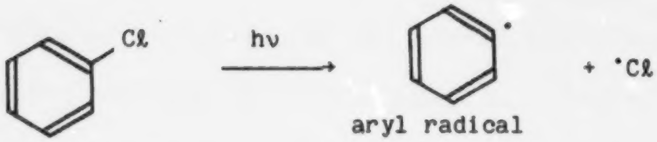 [1]

The products of this initial cleavage are free radicals, which are very reactive. In solution, the final products depend upon what other compounds are available to undergo reaction with these radicals. Removal of hydrogen giving eventual dechlorinative products, and addition to aromatic solvents, are typical fates of the free radicals.

The photochemical efficiency of the bond cleavage is strongly dependent on the energetics of eq. [1](4). The excited state involved is usually a triplet; if the energy of the state above the ground state is comparable with, or greater than, the C-Cℓ bond energy, dissociation occurs efficiently (high quantum yield). If the excited state energy is too low the reaction is very inefficient. Most estimates place the C-Cℓ bond energy in the region of 330 kJ mol^{-1}; Table 1 gives the triplet energies of some representative aryl chlorides.

Table 1. Triplet energies of aromatic systems

System		Triplet Energy, kJ mol^{-1}
Phenyl		350
Naphthyl		250
Biphenyl	not o-substituted	280
	o-substituted	330

Chlorinated benzenes and o-chlorinated biphenyls (Figure 1) tend to undergo dissociation with high efficiency ϕ 0.1-0.6. On the other hand, chlorinated napthalenes and non-o-chlorinated biphenyls are very resistant to photolysis, $\phi < 10^{-3}$. This is a steric effect. The ground state of biphenyl is best described as having a single bond between the two benzene rings (Figure 1a); a comparable description of the excited state has the rings coplanar (Figure 1b). Substitutents larger than hydrogen cause steric compression, which is relieved when the substituent (chlorine) departs. Additionally, the energy content of the o-excited state is higher, again because of steric compression (Table 1). This point is discussed in more detail in reference 5.

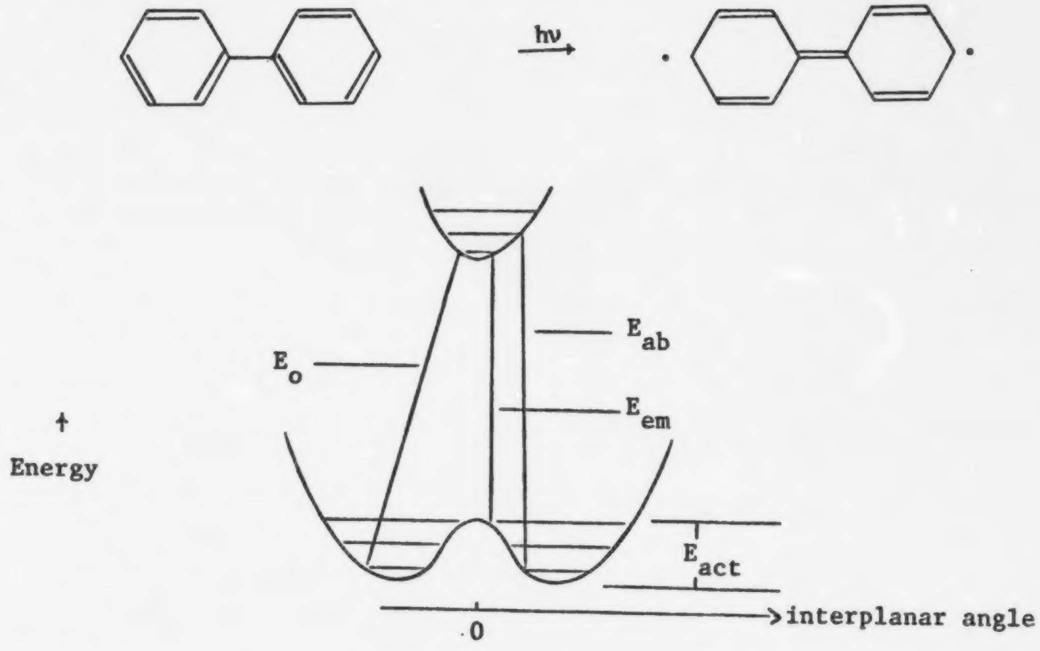

Figure 1: Ground and excited states of PCB's

Previous vapour phase studies

Only one report of the gas phase photochemistry of chlorobenzene has appeared(6). In that work, Ichimura and Mori photolysed chlorobenzene in an atmosphere of ethane. The products observed were benzene, HCℓ, and butane. It is clear that under these conditions the reaction is exactly analogous to that observed in solution with, for example, cyclohexane. The products are explained by Scheme 1.

Scheme 1

$$PhC\ell^* \longrightarrow Ph^\cdot + C\ell^\cdot$$

$$Ph^\cdot + C_2H_6 \longrightarrow PhH + C_2H_5^\cdot$$

$$C\ell^\cdot + C_2H_6 \longrightarrow HC\ell + C_2H_5^\cdot$$

$$2C_2H_5^\cdot \longrightarrow C_4H_{10}$$

For the present purposes, what is significant is that the quantum yield of reaction (0.4) is very similar to that found in solution. In solution, there could be cage recombination (eq. 2) which would make the observed quantum yield of decomposition smaller than the primary quantum yield of decomposition.

$$(C\ell^\cdot + Ph^\cdot) \longrightarrow PhC\ell \qquad [2]$$

The similarity of quantum yields suggests that this is not a problem in practice; more importantly, it suggests a primary $\phi_{decomp.}$ of ca 0.4 should be observed in any gas phase reaction of chlorobenzene. Therefore in ordinary air, we would expect that the first formed radicals in scheme 1 should disappear by reaction with oxygen, eq. 3.

e.g.

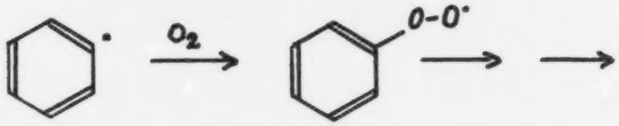

phenols [3]

The expectation of eq. 3 appears to be fulfilled in the chlorobiphenyl series, where the only published gas phase study, that of Hustert and Korte(7), indeed gave a phenolic product eq. 4.

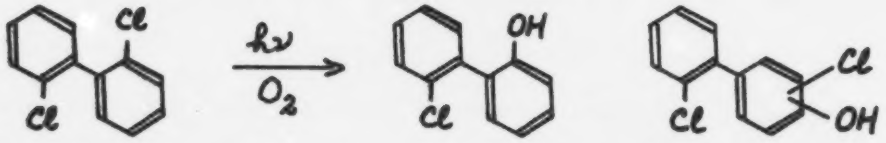

[4]

In this study, 2,2'-dichlorobiphenyl underwent photodecomposition to afford two products. In one of them, hydroxyl replaced one of the chlorine substituents, presumably by some reaction analogous to eq. 3. The other product was incompletely identified, but contained a hydroxyl function additional to the two chlorines. We would expect, again by analogy with the solution phase studies, that PCB's containing ortho chlorines should be much more photolabile in the gas phase than those without.

Among chloro compounds which are not aromatic, a research group at Dow Chemical Co. has studied the simulated atmospheric photodecomposition of simple aliphatic chlorides such as chlorinated ethenes and ethylenes(8). These reactions were carried out with 10 ppm of the organic compound in the presence of ca. 5 ppm of NO to simulate a polluted atmosphere. Under conditions controlled to imitate bright sunlight, all the mono-, di-, and trichloroethylenes had half lives for decomposition $\tau_{1/2}$ of 5-12 h. Chlorobenzene is mentioned briefly in this paper, its $\tau_{1/2}$ was ca. 9 h. No products were identified.

EXPERIMENTAL PROCEDURES

Our preliminary experiments have not been designed to simulate natural sunlight. Instead we are using mercury arc lamps as the UV sources, and equipment constructed out of quartz or Pyrex glass. The rationale for this approach is that typical aryl chlorides have very poor spectral overlap between their absorption spectra and the solar spectrum at the Earth's surface. Environmentally only the tail of the aryl chloride absorption overlaps the shortest wavelength UV-B part of the solar spectrum. Since the same absorption band is excited by the quartz-filtered mercury arc, the chemistry should remain the same, but the reactions occur at a more conveniently rapid rate.

REACTION CHAMBERS

A: The first reaction chamber consisted of a 12 litre flask equipped with three ground glass joints. The largest of these (60/50) accommodated an immersion well apparatus which projected into the flask. The lamp, a 450 W "Hanovia" medium pressure mercury arc, rested in the centre of the immersion well and was cooled by a flow of water. We have available both quartz and Pyrex immersion wells; the former transmits all radiation λ >220 nm, the latter only λ >290 nm.

The remaining inlets to the flask were used to admit and remove gas. The chloroaromatic compound was placed in a reservoir, which was heated if necessary. Gas (N_2 or O_2) was passed slowly through the reservoir, and entrained some of the vapour of the chlorocompound. After the gases left the reaction chamber, they were condensed at -78°C in a dry ice cold trap. After reaction the contents of the trap and the reaction flask were separately dissolved in a suitable solvent, and analysed by vapour phase chromotography and GC-mass spectrometry.

B: Because photolysis times with the above mentioned equipment were inconveniently long, most of the work was carried out in 500 ml 3 necked flasks. The central neck accommodated a 7.5W low pressure mercury lamp equipped with 24/40 standard taper (inner) ground glass joint. In later experiments a similar 4.6 W lamp was held in the central neck by means of a tapered Teflon plug. For most of the work a Pyrex 500 ml flask was used, but for the actinometry (see below) a specially constructed quartz flask was needed so that the UV radiation would penetrate through the flask and into the surrounding actinometer.

GAS CHROMATOGRAPHY

The instrument was a Carle model 211 gas chromatograph equipped with flame ionization detector. The column was 6 ft x 1/8 inch packed with 10% SE 30 on 60/80 mesh acid-washed Chromosorb W. A Hewlett-Packard model 3390A integrator was used to determine peak areas. Quantitation of samples was done using the external standard method, in which a known amount of reference substance of convenient retention time was added to the sample immediately prior to gas chromatographic analysis. The addition was made by taking an aliquot of fixed volume of the reference substance. Since the amount of the reference substance was constant for each analysis, the ratio of the areas [substrate/reference] could be used to calculate the amount of substrate present.

GC-MS AND PRODUCT STUDIES

Gc-ms analysis employed a VG Analytical model MM 12000 equipped with model 250 data system. It was interfaced to a Hewlett Packard 5790 gas chromatograph which was temperature programmed to allow elution of compounds of differing volatility. The chromatography column was a J&W DB-5 Fused Silica quartz capillary of length 50 m. The mass spectrometer was operated in the E.I. mode with scans taken every 1.0 sec. Eluted compounds were compared with library spectra of authentic materials. In all cases, because of the extreme sensitivity of the gc-ms equipment, the starting materials were also analysed to confirm that the observed products were not merely impurities in the starting materials.

The photolysis products were observed for several chlorinated benzenes and biphenyls under an atmosphere of air, and also in an oxygen free atmosphere of nitrogen. Charts 1 and 2 summarise a number of photolysis runs.

The products formed in the photolysis of the chlorinated benzenes and biphenyls in the presence of oxygen were largely biphenyl and hydroxybiphenyls. Under the nitrogen environment, the products of photolysis were much more varied, with few, if any phenol or hydroxybiphenyl products detected.

Chart 1. Products observed from selected chlorinated aromatic hydrocarbons upon gas phase photolysis under an atmosphere of air[a].

	Products (M^+)		
Reactant	BP[b](154)	BP-OH(170)	BP(OH)Cl(204)
o-$C_6H_4Cl_2$	+	+	
1,3,5-$C_6H_3Cl_3$	+	+	
o-BP-Cl	+	+	
m-BP-Cl	+	+	+
p-BP-Cl	+	+	

a - other products looked for but not observed included chlorobenzene, phenol, chlorophenol, dichlorobiphenyl, trichlorobiphenyl and quaterphenyl.

b - BP = biphenyl, BP-OH=hydroxybiphenyl, BP(OH)Cl=chlorohydroxybiphenyl

Chart 2. Products observed from selected chlorinated aromatic hydrocarbons upon gas phase photolysis under an atmosphere of N_2[a].

	Products (M^+)										
Reactant	C_6H_5Cl (112)	$C_6H_4Cl_2$ (146)	$C_6H_3Cl_3$ (180)	C_6H_4ClOH (128)	$C_6H_3Cl_2OH$ (162)	BP[b] (154)	BP-Cl (188)	$C_6H_2Cl_4$ (216)	BP-Cl_2 (222)	BP-Cl_4 (290)	QP (306)
o-$C_6H_4Cl_2$	+		+	tr[c]		+	++[d]				
1,2,4-$C_6H_3Cl_3$		+++			tr[c]	+	++				
1,3,5-$C_6H_3Cl_3$	+	+					+	+			
o-BP-Cl		+				+			++		tr[e]
m-BP-Cl						+			+++		
p-BP-Cl		+	+			+					

a - other products looked for but not observed included phenol, hydroxybiphenyl, chlorohydroxybiphenyl, dichlorodihydroxy-biphenyl, trichlorobiphenyl

b - BP = biphenyl, BP-Cl=chlorobiphenyl, BP-Cl_2=dichlorobiphenyl, BP-Cl_4=tetrachlorobiphenyl, QP=quaterphenyl

c - trace amounts of phenols were detected, but were probably due to small amounts of oxygen present in the flask

d - each + indicates a different isomer

e - trace amounts of quaterphenyl were observed

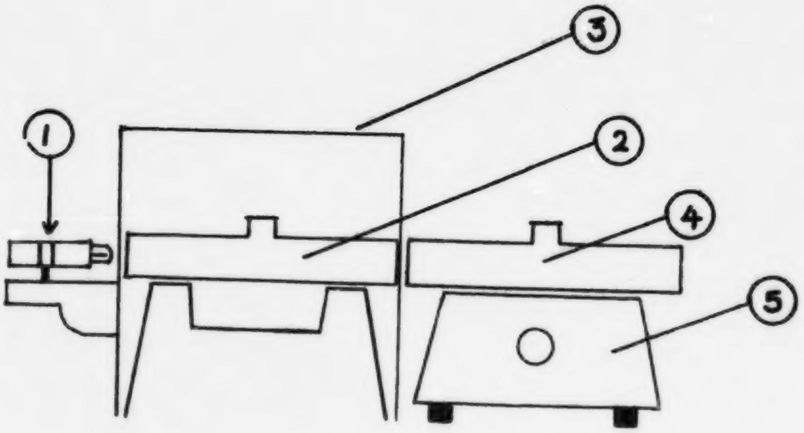

Fig. 2

1. lamp
2. cell 1, contains the vaporized ArCl
3. insulated thermostatted "hot-box"
4. cell 2, contains actinometer
5. stirrer

The procedure was as follows:

a) With cell 1 empty, monitor the output of the lamp using actinometer in cell 2.

b) With cell 1 filled with the vapour of the chloro compound, monitor the light transmitted through cell 1 using the actinometer in cell 2. The light absorbed in cell 1 is the difference between the two readings of the actinometer in cell 2.

c) Condense the organic material in cell 1, add organic solvent, remove the solution from the cell and analyze for disappearance of reactant using gas chromatography.

The disadvantage of this method was that the light beam could not be properly collimated. Consequently more light was received in cell 1, even when empty, than could be monitored in cell 2.

Method 2

The apparatus, shown in Fig. 3, consisted of a 500 mL 3-necked quartz flask. The lamp, a 4.6 W, low pressure mercury lamp, 5.4 cm long, was placed in the central neck. Originally, the other two necks were used as a method of introducing and removing the chloro compound without exposing it to the air. Ultimately this was found to be unnecessary, and the compound was simply introduced in a weighed amount in a small (approx. 1 cm diameter x 0.5 cm high) glass vial, and vaporized out of the vial in situ by applying heat. Liquid samples were injected directly, using a microsyringe.

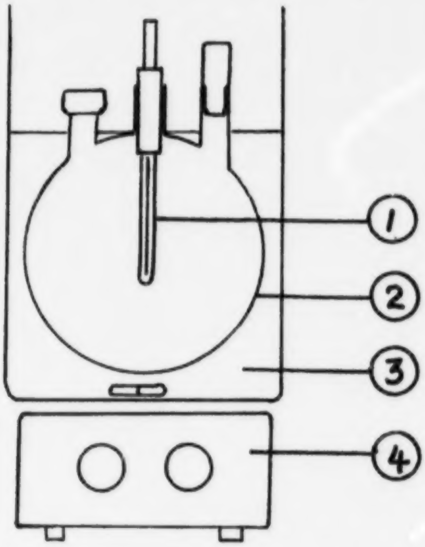

Fig. 3

1. lamp
2. 500 mL quartz flask, containing vaporized ArCl
3. $K_3Fe(C_2O_4)_3$ actinometer solution
4. heater - stirrer

The 3-necked quartz flask was positioned as far as possible from the sides and bottom of a 2 L beaker. The beaker was then filled with the actinometer solution (1 L) so that the actinometer solution rose to a level higher than the top of the rounded part of the flask. The contents of the beaker were heated to 50°C (so that the chloro compound would not condense) and stirred (for homogeneity of the mixture).

In method 2 the actinometer solution was azoxybenzene in ethanolic solution. This actinometer has $\phi_{254\,nm}$ 0.017 and is temperature independent$^{(9)}$. The method consisted of measuring the absorbance of 5 mL aliquots of solution (a) before reaction (b) after irradiation through an empty flask (c) after irradiation through the flask filled with the vapour of the chloro compound. Determination (b)-(a) gives the total lamp output and (c)-(b) gives the radiation not absorbed by the sample. Accordingly, the radiation absorbed by the sample is the difference (b-a)-(c-b). As in method (1) the loss of chloro compound upon irradiation was monitored by condensing the irradiated sample, dissolution, and analysis by gas chromatography.

Method (2) was inapplicable to our system because the low sensitivity of the actinometer meant that the absorbances developed by the actinometer solution [reading (b-a) and (c-b)] were inconveniently small for irradiations that led to convenient percentage reaction of the chloro compound.

Method 3

The apparatus and protocol were identical to those of method (2) except that potassium ferrioxalate$^{(10)}$ was substituted for azoxybenzene as the actinometer. Because potassium ferrioxalate is sensitive to visible as well as to ultraviolet light, the whole experiment had to be carried out in a dark room, by the illumination of a photographic safe-light.

Although potassium ferrioxalate is well established as a general purpose actinometer, its applicability at elevated temperatures appears not to have been studied. We found that the actinometer was stable in the dark at 50°C (but not above 70°C), and that its quantum yield of reaction was the same ±3% at 50°C as at 22°C.

The photoreaction of potassium ferrioxalate proceeds as follows.

$$2Fe^{3+} + C_2O_4^{2-} \rightarrow 2Fe^{2+} + 2CO_2 \qquad [5]$$

At 254 nm, the wavelength of the output of the low pressure-arc, $\phi(Fe^{2+})$ is reported to be 1.25(10).

The Fe^{2+} produced in the photoreaction is determined by forming a phenanthroline complex.

$$Fe^{2+} + 3\ \text{"phen"} \xrightarrow[\text{pH3.6}]{\text{buffer}} [Fe(phen)_3]^{2+} \qquad [6]$$

The red complex has ε 11,100 at its absorption maximum of 510 nm and may therefore be estimated spectrophotometrically.

Determination of ϕ_r for azoxybenzene

Through previous work in our laboratory the solution phase quantum yield for azoxybenzene is known to be 0.017(9). Using the same apparatus, the quantum yield of an ethanolic solution of azoxybenzene was determined. Azoxybenzene (3.0 mg) was dissolved in 500 ml of 95% ethanol. Since azoxybenzene is a much less reactive actinometer than ferrioxalate, it was irradiated for 15 min. This produced an 8% conversion of the azoxybenzene. In duplicate attempts, the quantum yield for azoxybenzene was determined to be 0.019 ± 0.0015. This is similar to the previously determined value, and thus gives us confidence in the reliability of the methodology used.

Sample Calculation: ϕ_r for 1,2,4-trichlorobenzene

Volume of actinometer solution 1000 mL

(a) Removed a 1.0 mL aliquot before irradiation. To 1.0 mL of the aliquot added 2.0 mL phenanthroline solution and 2.0 mL buffer to a final volume of 10.0 mL. Absorbance at 510 nm: = 0.069

(b) Irradiated for 3.0 min. with an empty flask in position. Removed a 1.0 mL aliquot. Absorbance at 510 nm after identical treatment to (a) = 0.310

(c) Introduced the chlorocompound to the flask and vaporized it. Irradiated for 3.0 min. with substance in flask. Removed a 1.0 mL aliquot. Absorbance at 510 nm after identical treatment to (a) = 0.473

(d) mol L^{-1} Fe^{2+} in solution (a)

$$\text{concentration of diluted solution} = A/\varepsilon l = \frac{0.069}{11,100 \times 1.0} = 6.22 \times 10^{-6} \text{ mol L}^{-1}$$

therefore concentration of original solution (a)= 6.22×10^{-5} mol L^{-1}

Similarly mol L^{-1} Fe^{2+} in solution (b) = 2.79×10^{-4} mol L^{-1}

mol L^{-1} Fe^{2+} in solution (c) = 4.26×10^{-4} mol L^{-1}

(e) Mol L^{-1} Fe^{2+} produced in irradiation through empty flask

= (b) - (a) = 2.17×10^{-4} mol L^{-1}

Mol L^{-1} Fe^{2+} produced in irradiation through sample

= (c) - (b) = 1.47×10^{-4} mol L^{-1}

(f) Photon output by lamp in 3.0 min = 2.17×10^{-4} mol L^{-1} x 1.00 L/ϕ_r

$$= \frac{2.17 \times 10^{-4}}{1.25} = 1.74 \times 10^{-4} \text{ mol}$$

Similarly, photons transmitted by sample in 3.0 min

$$= \frac{1.47 \times 10^{-4}}{1.25} \text{ mol} = 1.18 \times 10^{-4} \text{ mol}$$

(g) Photons absorbed by sample

$$1.74 \times 10^{-4} - 1.18 \times 10^{-4} = 5.60 \times 10^{-5} \text{ mol}$$

Quantum Yields of Reaction: Calculations

The quantum yield ϕ_r is defined as follows:

$$\phi_r = \frac{\text{Amount of substance undergoing reaction (moles)}}{\text{Photons of radiation absorbed by the substance (moles)}} \qquad [7]$$

The quantum yield is thus a dimensionless quantity; it is the fraction of all the photons absorbed that cause reaction. The fraction $(1-\phi_r)$ thus represents the photons that are "wasted" (degraded to heat).

At very low conversions of the chlorinated reactant, ϕ_r is obtained very simply as

$$\phi_r = \frac{\text{mol ArCl (time zero) - mol ArCl (time t)}}{\text{Photons absorbed (mol)}} \qquad [8]$$

The procedures for obtaining moles of substance consumed (gas chromatography) and moles of photons absorbed (actinometry) have been described. However at very low conversions of ArCl, the numerator of eq.[8] is ill defined (difference of two large numbers). At higher conversions, competing light absorption by reactant and products occurs. We have shown previously$^{(11)}$ that under these conditions, eq. [9] gives a better value of ϕ_r

$$\phi_r = \frac{n_o \ln(n_o/n)}{\text{photons absorbed (mol)}} \qquad [9]$$

In eq. [9] n and n_o are the moles of chlorocompound in the flask after irradiation and before irradiation respectively. Eq. [9] was used throughout this work to obtain the reported quantum yields. Thus, for the sample calculation shown previously

(a) Glc results show that the initial # moles of sample was 2.40×10^{-5} and after irradiation, final # moles = 8.61×10^{-6}

(b) $$\phi_r = \frac{2.40 \times 10^{-5} \ln (2.40 \times 10^{-5}/8.61 \times 10^{-6})}{5.60 \times 10^{-5}} = 0.44$$

Appendix(10)

(1) Prep. of $K_3Fe(C_2O_4)_3 \cdot 3H_2O$

3 volumes 1.5 M $K_2C_2O_4$

1 volume 1.5 M $FeCl_3$

Mix with vigorous stirring, and a precipitate of $K_3Fe(C_2O_4)_3.3H_2O$ forms. Recrystallize two times in warm water. Carry out the preparation in diffuse light and store the crystals in the dark.

(2) Prep. of 0.006M $K_3Fe(C_2O_4)_3 \cdot 3H_2O$ solutions for irradiation.

In dark: dissolve 2.947 g of $K_3Fe(C_2O_4)_3 \cdot 3H_2O$ in 800 mL distilled H_2O and add 100 mL of 0.5 M H_2SO_4. Dilute to 1.0 L.

(3) Prep. of 0.5M H_2SO_4

Pipette 27.78 mL of conc. H_2SO_4 into distilled H_2O. Dilute to 1.0L.

(4) Prep. of 0.1% phenanthroline

Fisher 1,10-phenanthroline(monohydrate) was used.

For 0.1% by weight solution, weigh out 0.10 g and dilute to 100 mL with distilled H_2O.

(5) Prep. of buffer

Mix: 60 mL 1M NaO_2CCH_3

36 mL 0.5 H_2SO_4

dilute to 100 mL

UV Absorption Spectra

These were measured in the vapour phase and in cyclohexane solution for the following representative compounds of the two series: chlorobenzene, m-dichlorobenzene, 1,2,4-trichlorobenzene, o-chlorobiphenyl, m-chlorobiphenyl. Fig. 4 and 5 are representative spectra. It may be seen that the loss of solvation as the substance moves from solution into the gas phase is accompanied by a small shift in the spectrum to shorter wavelength (higher energy). The significance of this shift is twofold:

(i) the excited state has more energy with which to undergo any photochemical reaction

(ii) there is poorer overlap between the absorption spectrum of the compound and the solar sectrum in the troposphere in the vapour phase than there is in solution.

Absorption spectrum of Aroclor 1254

This was measured in cyclohexane over the range 290 nm -325 nm. Tabulated extinction coefficients are given in Table 4 (see discussion section).

RESULTS AND DISCUSSION

A. Products and reaction mechanism

Charts 1 and 2 contain some typical product studies. These suggest strongly that the photochemical reactions of chloroaromatic compounds are free radical processes, as they are in solution. The most probable primary event, which is actually the only photochemical process, is shown as eq. 10.

$$\mathrm{ArCl} \xrightarrow{h\nu} \mathrm{Ar}^{\cdot} + \mathrm{Cl}^{\cdot} \qquad [10]$$

The final products are formed by ground state (thermal) reactions of the resulting free radicals. Scheme 2 postulates how some of the observed products arise (o-dichlorobenzene chosen as substrate for illustration).

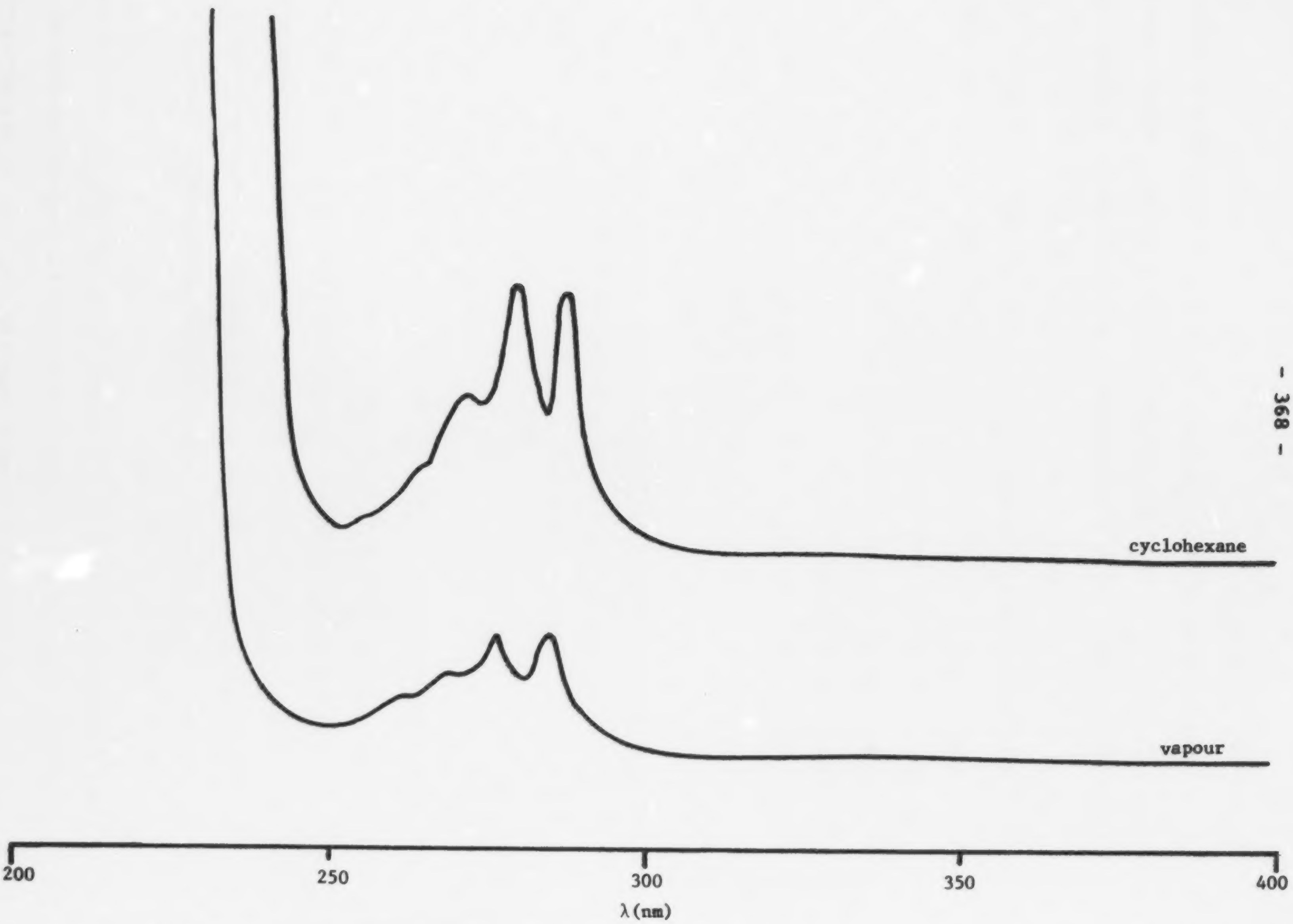

Figure 4: UV absorption spectrum of 1,2,4-trichlorobenzene in the vapour phase and in cyclohexane solution

Figure 5: UV absorption spectrum of o-chlorobiphenyl in the vapour phase and in cyclohexane solution

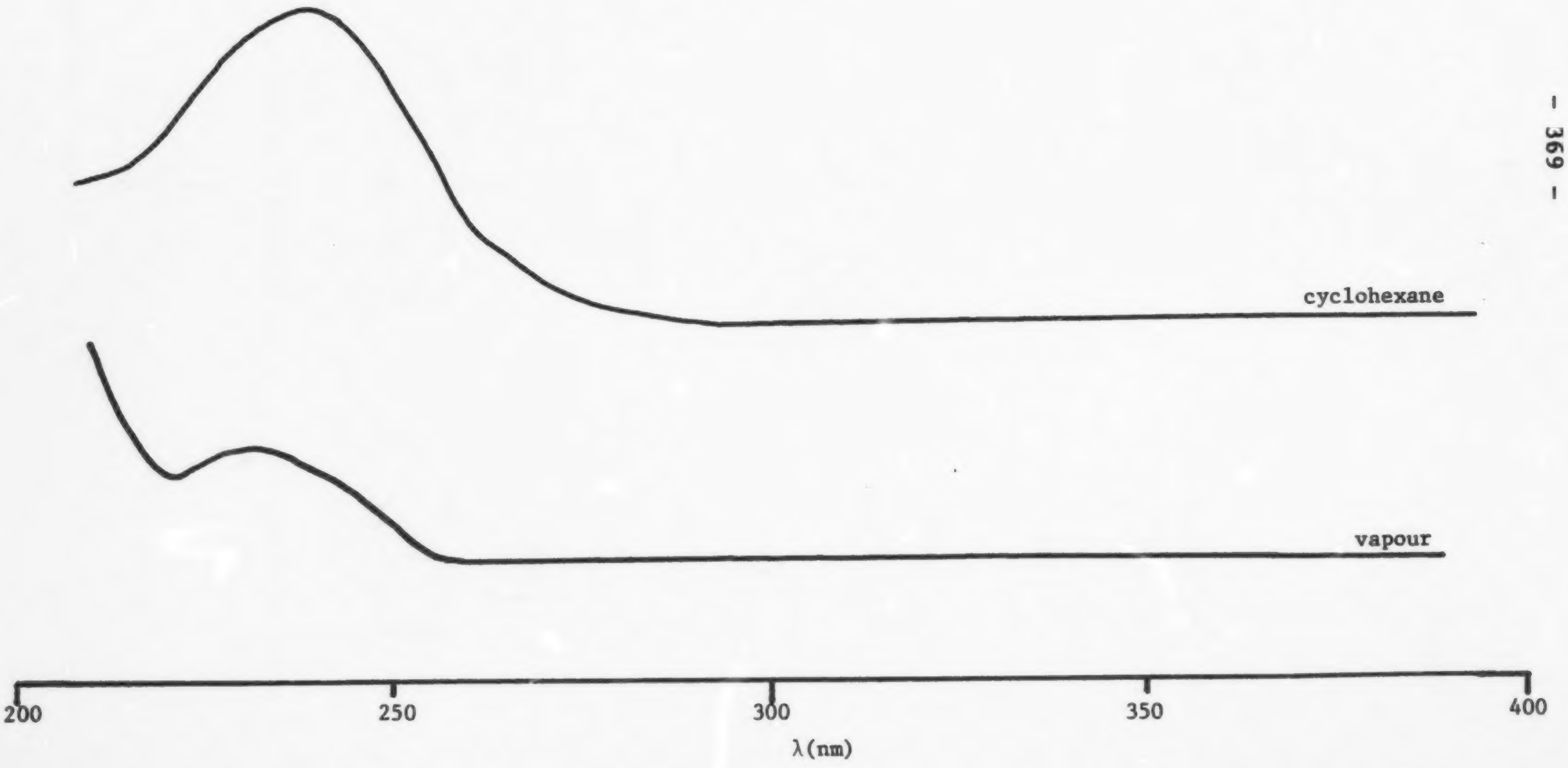

Scheme 2:

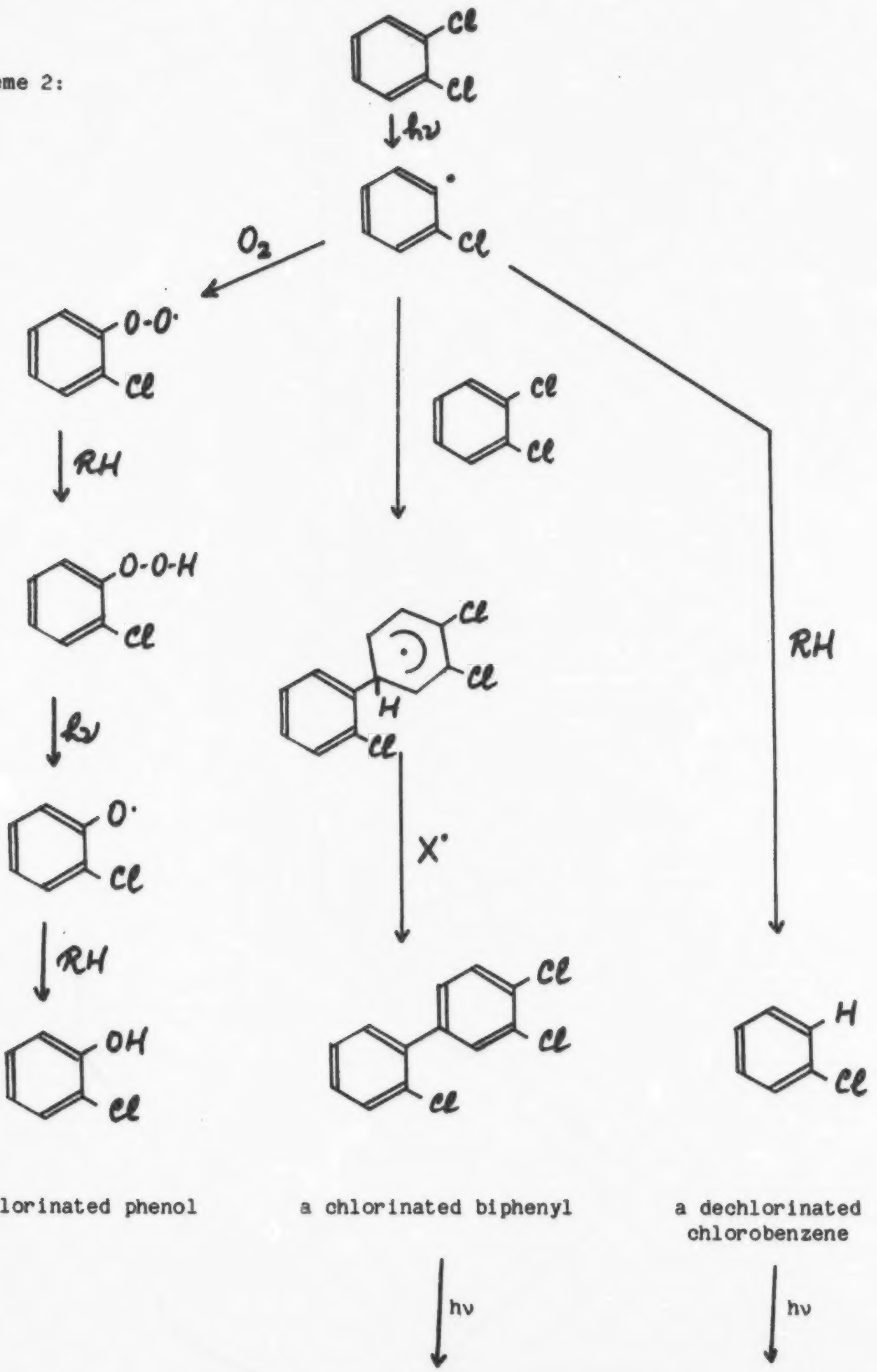
Cl
Cl
hν
Cl
O2
O-O·
Cl
RH
O-O-H
Cl
hν
O·
Cl
RH
OH
Cl
Cl
Cl
Cl
Cl
H
Cl
X·
Cl
Cl
Cl
RH
H
Cl
hν
hν

a chlorinated phenol

a chlorinated biphenyl

a dechlorinated chlorobenzene

Further photochemical reactions

We anticipate that the difference between our laboratory studies and the actual environment is that the reactions involving two molecules of the chloro compound (the right hand half of Scheme 2) will be very unlikely in the natural atmosphere (except possibly where the pollutants are adsorbed on particles). This is because the concentrations of the pollutants are too low for bimolecular processes to occur. However, we stress that the change in product spread will have no effect on rates (and hence quantum yields) of disappearance of the chloro compound, since this is determined only by the rate and efficiency of eq. [10]. Evidence supporting this point of view was obtained by carrying out rate studies. These are shown in Table 2.

Table 2. Observed first order rate constants for photolysis of 1.0μl of chlorinated aromatic hydrocarbons under identical conditions.

Compound	k_{obs}, min^{-1}
C_6H_5Cl	0.28
1,2-$C_6H_4Cl_2$	0.55
1,3-$C_6H_4Cl_2$	0.30
1,4-$C_6H_4Cl_2$	0.43
1,2,4-$C_6H_3Cl_3$	0.31
1,3,5-$C_6H_3Cl_3$	0.33
1,2-$C_6H_4Cl.C_6H_5$	0.29
1,3-$C_6H_4Cl.C_6H_5$	0.10
1,4-$C_6H_4Cl.C_6H_5$	0.09

Because the disappearance behaviour is in every case kinetically of the first order, this is consistent with the reaction of eq. [10] being the rate-limiting process of the overall reaction. Hence the processes occurring subsequently to reaction [10] do not affect the rate of chloro compound degradation.

B. Quantum Yields

The quantum efficiency ϕ was defined above as eq. [7]. It is a dimensionless quantity, which corresponds to the chemical yield of product in a chemical reaction. The quantum yield is, in fact, the yield of product based upon photons as the starting material.

Measurement of a quantum yield requires two independent determinations. These are the amount of starting material reacting while the irradiation source is on, and the amount of light actually absorbed by the reactant (as opposed to the total output of the lamp). A sample calculation was given under "Experimental Procedures".

Quantum yields for disappearance of several chlorinated benzenes and chlorinated biphenyls in the gas phase are given in Table 3. Comparative literature values for solutions of these same substances in hydrocarbon solvents are also given.

Table 3 ϕ_r for several chloroaromatic compounds

Chlorinated benzenes[a]	ϕ_r(vapour)	ϕ_r(solution)
C_6H_5Cl	0.33±0.01	0.31
1,2-$C_6H_4Cl_2$	0.63±0.04	0.78
1,3-$C_6H_4Cl_2$	0.52±0.02	0.46
1,2,4-$C_6H_3Cl_3$	0.47±0.03	0.63
1,3,5-$C_6H_3Cl_3$	0.65±0.04	0.14
Chlorinated biphenyls[b]		
2-Cl biphenyl	0.32±0.02	0.35
3-Cl biphenyl	0.056±0.002	0.001
4-Cl biphenyl	0.078±0.004	0.0006

[a] Solution values, in cyclohexane, from ref. 12

[b] Solution values, in isooctane, from ref. 13

For the chlorinated benzenes, most of the quantum yields are similar in both gas and solution phases. This also supports the idea that the same process (eq. 10) is the primary event in both phases. Since these dissociations are believed to take place from the triplet state of the chloro compounds(4,12), the small differences in photochemical efficiency between phases may well be due in part to changes in the efficiency of singlet-to-triplet intersystem crossing between the phases.

UV spectroscopy has shown (experimental) that the excitation energies of the chloro compounds under study are slightly higher in the gas phase than in solution. Energetic analysis (Table 1) shows how the triplet states of chlorinated benzenes and o-chlorobiphenyls have sufficient energy to allow the cleavage reaction, eq. [10] to occur. However, m- and p-chlorobiphenyl are both substantially more photolabile in the vapour phase than in solution. These compounds have excited states insufficiently energetic to allow facile photocleavages. We suspect, but cannot prove at this time, that cleavage is occurring from a vibrationally excited variant of the electronic triplet excited state. The absence of solvent lengthens the time period which the vibrationally "hot" excited state requires to reach the lowest vibrational levels, and as a result this increases the chance that cleavage can occur while the excited state is still "hot".

ENVIRONMENTAL SIGNIFICANCE OF RESULTS

The key question to be answered is, "Does the solar degradation of chlorinated aromatic compounds take place in the gas phase at such a rate that photodegradation of atomospheric chlorinated aromatic compounds is a significant sink for these compounds?" We need the following input:

1. Intensity of solar radiation
2. Absorption characteristics of chlorinated aromatic compounds
3. Quantum yield information
4. Ambient concentrations of chlorinated aromatic compounds

We will first consider the case of the PCB's. Item (1) is available from tables(14) for the latitude 40°N. We will use this as an approximation to Ontario conditions. Data for mid-summer and midwinter are available. Items (2) and (3) are more of a problem, in that different PCB congeners have individual absorption spectra and quantum yields of reaction. As a compromise we will consider the absorption behaviour of the commercial mixture Aroclor 1254, and take the ϕ_r value determined in our laboratory for 2-chlorobiphenyl, because most of the substances in the commercial mixture contain at least one ortho chlorine. For item (4) we take two extreme values of PCB concentrations reported for ambient air in the U.S.(15), namely 0.0001 $\mu g\ m^{-3}$ and 0.036 $\mu g\ m^{-3}$. We will assume that this material is Aroclor 1254, which has approximate composition $C_{12}H_5Cl_5$ and approximate molar mass 330 $g\ mol^{-1}$.

Calculations

a) Molar concentration of PCB's.

$$c,\ mol\ L^{-1} = conc.\ (\ \mu g\ m^{-3}\ ) \times \frac{1g}{10^6\ \mu g} \times \frac{1m^3}{1000L} \times \frac{1\ mol}{330g}$$

$$= 3.0 \times 10^{-16} \text{ to } 1.0 \times 10^{-13}\ mol\ L^{-1} \text{ of air.}$$

b) Absorption of light at any wavelength.

$$\text{Beer's law: } \frac{I(transmitted)}{I(incident)} = 1 - \frac{I(absorbed)}{I(incident)} = 1 - I_{abs}/I_o = 10^{-\varepsilon cl}$$

$$\text{Thus } I_{abs}/I_o = 1-10^{-\varepsilon cl} = 1 - e^{-2.3\ \varepsilon cl}$$

$$\text{For small absorbances } e^{-2.3\ \varepsilon cl} \simeq 1-2.3\ \varepsilon cl$$

$$\text{Thus } I_{abs}/I_o \simeq 2.3\ \varepsilon cl = 2.3A \quad (A = \text{absorbance})$$

$$I_{abs} = 2.3\ AI_o$$

If ℓ is taken over 1 dm (10 cm) then I and I_o each refer to 1 dm² of the Earth's surface when c is in mol dm^{-3}. Because, as seen below, the absorbances are extremely small, we have not corrected the I_o values for any absorption by PCB's at higher levels in the atmosphere.

c) By definition $\phi_r = \dfrac{\text{PCB reacting, mol L}^{-1}}{\text{photons absorbed, mol L}^{-1}}$

If we assume that ϕ_r is independent of wavelength, since all the photochemistry involves the same absorption band of the PCB compound

$$\sum_\lambda c_{\text{PCB reacted}} = \phi \sum_\lambda c_{\text{photons absorbed}}$$

$$= 2.3\phi \sum_\lambda A_\lambda (I_o)_\lambda = 2.3\phi c l \sum_\lambda \varepsilon_\lambda (I_o)_\lambda$$

Tables 4 and 5 give the results of these calculations for the following scenarios:

low PCB concentration, summer
low PCB concentration, winter
high PCB concentration, summer
high PCB concentration, winter

The wavelength window of interest is quite narrow: 295-315 nm. Radiation λ<295 nm does not reach the Earth's surface, while beyond 315 nm, the absorption of Aroclor 1254 is imperceptibly small.

Table 4. Light absorption by Aroclor 1254

λ,nm	ε^a	I_o^b		$\varepsilon_\lambda I_{o(\lambda)}$	
		Summer	Winter	Summer	Winter
<298	650	4.2×10^{-7}	~0	2.7×10^{-4}	~0
298-303	240	5.6×10^{-6}	2.3×10^{-7}	1.3×10^{-3}	5.5×10^{-5}
303-308	63	2.8×10^{-5}	3.3×10^{-6}	1.8×10^{-3}	2.1×10^{-4}
308-313	9	7.2×10^{-5}	1.4×10^{-5}	6.5×10^{-4}	1.3×10^{-4}
313-318	~0	1.2×10^{-4}	3.3×10^{-5}	~0	~0
			$\ell\Sigma\varepsilon_\lambda I_{o(\lambda)}{}^c$	4.0×10^{-2}	3.9×10^{-3}

a units ℓ mol^{-1} cm^{-1}

b units mol dm^{-2} h^{-1}. The data of Zepp and Cline (Table II of reference (11) were taken with $I_{o(\lambda)} = W_\lambda/0.93$

c units h^{-1} = 10$(\varepsilon)^a(I_o)^b$

Table 5. Ranges for the rate of decomposition of Aroclor 1254 in air.

	Summer Low	Summer High	Winter Low	Winter High
$\ell\Sigma\ \varepsilon_\lambda I_{o(\lambda)}$, h^{-1}	4.0×10^{-2}	4.0×10^{-2}	3.9×10^{-3}	3.9×10^{-3}
c, mol L^{-1}	3.0×10^{-16}	1.0×10^{-13}	3.0×10^{-16}	1.0×10^{-13}
Rate of[a] Decomposition	8.3×10^{-18}	2.8×10^{-15}	8.1×10^{-19}	2.7×10^{-16}
% Decomposed per hour[b]	2.8	2.8	0.27	0.27

[a] units mol L^{-1} h^{-1} = $2.3\phi c\ell\Sigma\varepsilon_\lambda I_{o(\lambda)}$ with $\phi = 0.3$

[b] $2.3\phi\ell\Sigma\varepsilon_\lambda I_{o(\lambda)} \times 100$. Note that at these low concentrations, this quantity is independent of the initial concentration.

Table 6 shows a corresponding calculation for 1,2,4-trichlorobenzene. Because of the lower extinction coefficient for this compound than for Aroclor 1254, the overall decomposition of 1,2,4-trichlorobenzene is even less on a percentage basis, than that of the Aroclor.

Table 6. Light absorption and photodegradation of 1,2,4-trichlorobenzene

λ, nm	ε	$\varepsilon_\lambda I_{o(\lambda)}$ Summer	$\varepsilon_\lambda I_{o(\lambda)}$ Winter
<298	19	8.0×10^{-6}	0
298-303	2.4	1.3×10^{-5}	5.5×10^{-7}
303-308	0.2	5.6×10^{-6}	6.6×10^{-7}
308-313	0	0	0
	$\lambda_\lambda I_{o(\lambda)}$	2.7×10^{-5}	1.2×10^{-6}
% Decomposed per hour[a]		0.029	0.0013

(a) See note (b) of Table 5.

A similar calculation was carried out for 2,4,5-trichlorophenol, Table 7. In this case the percent decomposition is calculated to be higher. For neither the trichlorobenzene nor the trichlorophenol were atmospheric concentrations available, so only the percent decompositions, and not the actual rates, were calculable.

Table 7. Light absorption and photodegradation of 2,4,5-trichlorophenol

λnm	ε	$\varepsilon_\lambda I_{o(\lambda)}$	
		Summer	Winter
<298	2540	1.0×10^{-3}	0
298-303	2100	1.2×10^{-2}	4.8×10^{-4}
303-308	330	9.2×10^{-3}	1.1×10^{-3}
308-313	33	2.4×10^{-3}	4.6×10^{-4}
	$\Sigma\varepsilon_\lambda I_{o(\lambda)}$	2.5×10^{-2}	2.0×10^{-3}
	% Decomposed per hour[a]	5.7	0.5

(a) as note (b) of Table 5 with ϕ assumed to be 0.1.

The results of these calculations show that, even making rather favourable assumptions, the results of direct irradiation of chlorinated aromatic compounds by solar radiation will not lead to rapid destruction of the pollutants. (Indirect photolysis, such as attack by singlet oxygen, hydroxyl radicals, or other trace atmospheric constituents is not considered in this work). Among these assumptions perhaps the most important concerns the solar intensity. Not only are these quoted for 40°N, but they refer to the solar intensity found under clear skies at midday. These then are the maximum rates of photodegradation; averaged over a 24 h period, and realizing that the shortest wavelengths are attenuated the most as the zenith angle increases away from midday, the daily rates may well amount to no more than a few percent of these maximum rates.

References

1. R.W. Risebrough, W. Walker, T.T. Schmidt, B.W. de Lappe, and C.W. Connors, Nature 264, 738 (1976).
2. T.J. Murphy, L.J. Formanski, B. Brownawell, and L.A. Meyer, Environ. Sci. Technol. 19, 942 (1985).
3. R.G. Lewis, B.E. Martin, D.L. Sgontz, and J.E. Howes, Environ. Sci. Technol. 19, 986 (1985).
4. N.J. Bunce, M.D. Bergsma, J.P. Bergsma, W. De Graaf, Y. Kumar, and L. Ravanal, J. Org. Chem. 45, 3708 (1980).
5. N.J. Bunce, Chemosphere 11, 701 (1982).
6. T. Ichimura and Y. Mori, J. Chem. Phys. 58, 288 (1973).
7. K. Hustert and F. Korte, Chemosphere 4, 153 (1974).
8. W.L. Dilling, C.J. Bredeweg, and N.B. Tefertiller, Env. Sci. Technol. 10, 351 (1976).
9. N.J. Bunce, J. La Marre, and S.P. Vaish, Photochem. Photobiol. 39, 531 (1984).
10. C.G. Hatchard and C.A. Parker, Proc. Roy. Soc. A235, 518 (1956).
11. N.J. Bunce, J. Photochem. 15, 1 (1981).
12. N.J. Bunce, P.J. Hayes, and M.E. Lemke, Can. J. Chem. 61, 1103 (1983).
13. N.J. Bunce, Y. Kumar, L. Ravanal, and S. Safe, J. Chem. Soc. Perkin Trans. 2, 880 (1978).
14. R.G. Zepp and D.M. Cline, Environ. Sci. Technol. 11, 359 (1977).
15. J.J. Richard and G.A. Junk, Environ. Sci. Technol. 15, 1095 (1981) and references there cited.

A FUNDAMENTAL STUDY ON THE DEPOSITION OF AEROSOLS ON CYLINDERS IN TURBULENT CROSS FLOWS

S. Ilias and P.L. Douglas
Computer Aided Process Design Laboratory, Department of Chemical
Engineering, Queen's University

Key words: Aerosol, Deposition Rates.

ABSTRACT

The deposition of aerosols on non-streamlined surfaces such as cylinders and spheres in ideal flow (viscous or inviscid flow) has been studied in some detail. Under such flow conditions, the deposition process has been modelled in terms of the inertial impaction, interception and Brownian diffusion collection mechanisms. Carefully designed experiments to test these models have shown them to be adequate for the conditions under which they were developed.

However, recent experimental results on the deposition of aerosols on single wires in turbulent cross flow yielded significantly higher collection efficiencies than the values predicted by the classical mechanisms. To explain the increased collection efficiency, it is necessary to consider eddy diffusion of the particles due to the free stream turbulence as a prime mechanism.

Based on the concept of eddy diffusivity, a turbulent diffusion model has been developed to predict the experimentally observed deposition rates. The model is essentially the solution of the continuity equation and equations of motion for the particles, with the assumption that within the boundary layer the fluid-particles closely follow the fluid streamlines. From physical reasoning, the eddy diffusivity profile within the boundary layer is assumed to have the same shape as that near a flat plate.

The model equations are solved with the solution of the boundary layer equation in which the external flow is assumed to be for potential or for experimental flowlines. Computed deposition rates are in good agreement with the experimental results when the solution of the turbulent diffusion model is based on the solution of boundary layer equations where experimental flowlines are used for external flow instead of potential flow conditions. A single parameter, known as the turbulent Schmidt number, was obtained which adequately characterizes the system.

A FUNDAMENTAL STUDY ON THE DEPOSITION OF AEROSOLS ON CYLINDERS IN TURBULENT CROSS FLOWS

S. Ilias and P.L. Douglas
Computer Aided Process Design Laboratory
Department of Chemical Engineering
Queen's University
Kingston, Ontario
Canada K7L 3N6

INTRODUCTION

In recent years, the problem of removing particulates from gases has become important because of stringent environmental regulations to reduce health hazards, limit nuisance dust, and recover valuable products. A wide variety of commercial equipment used for collecting aerosols rely on aerosols depositing on surfaces which are then cleaned or removed. Typical examples are scrubbers which use liquid droplets, fibrous filters which use cylindrical elements and electrostatic precipitators which use plane or cylindrical surfaces to capture the aerosol particles. In each of the devices, a realistic analysis of the deposition process would require a detailed analysis of the fluid flow field around the object or target.

In the hydrodynamic sense, the deposition of aerosols on surfaces can be discussed under two broad classifications. In the first classification, the bulk flow is considered parallel to the surface on which the deposition takes place. Typical examples are walls of a duct or pipe containing the aerosol laden gas, or flow past a flat plate. Such surfaces are often termed streamlined surfaces. In the second classification, the surface is placed normal to the bulk flow and is often called a non-streamlined surface. The flow of a dust laden gas stream normal to a cylinder, sphere, or ribbon immersed in the flow are classical examples of deposition on non-streamlined surfaces.

The deposition of aerosols on non-streamlined surfaces plays an important role in gas filtration and gas scrubbing. Usually in modelling fibrous filters a cylindrical element is taken as a model collector while in wet scrubbers, a sphere is taken as a model for water droplets. The deposition of aerosols on non-streamlined surfaces such as cylinders and spheres in ideal flow (viscous or inviscid flow) has been studied in some detail. Classically, for these cases, the deposition process has been modelled in terms of inertial impaction, interception and Brownian diffusion collection mechanisms [1,2,3,4]. Carefully designed experiments to test these models have shown them to be adequate for the specific conditions under which they were developed.

It is important to note that these models are essentially based on either inviscid or viscous flow fields. But in a real situation, the flow field lies between these two extreme limits. Any realistic analysis of the deposition process on surfaces would require a detailed analysis of the fluid flow field around the object or target. Usually the flow field is very complex and in most practical situations, deposition occurs under turbulent flow conditions. When compared with available experimental data for the inertial deposition of aerosols on cylinders and spheres in non-turbulent cross flow, the collection efficiency based on the viscous flow model grossly underestimates the measured efficiency while the model based on potential flow field overestimates the measured efficiency. Our recent calculations based on the full solution of the unsteady Navier-Stokes equation has shown a significant improvement in predicting measured collection efficiency when compared with the classical models based on potential or viscous flow fields [5].

Although nearly all particulate control devices operate in the turbulent flow regime, there has been little reference in the literature to the deposition of aerosols on non-streamlined surfaces. There has been a systematic study on the deposition of aerosols on streamlined surfaces, such as in pipe flows and over flat plates under turbulent flow conditions [6,7]. An excellent review on this subject may be found elsewhere [8].

Recent experimental results on the deposition of aerosols on single wires in turbulent cross flow yielded significantly higher collection efficiencies than the values predicted by classical mechanisms [9,10]. To explain the increased collection efficiency, it is necessary to consider the eddy diffusion of the particles due to free stream turbulence as a prime mechanism. In this paper the development of a turbulent diffusion model for the deposition of aerosols on isolated cylinders in turbulent cross flow along with some experimental results are presented.

TURBULENT DIFFUSION MODEL

The development of turbulent diffusion model for the deposition of aerosols on cylinders in turbulent cross flow is based on the continuum concept for gas-solid systems. This continuum concept will only be valid as long as the aerosol concentration is low enough so as not to influence the hydrodynamics of the gas phase. The limiting concentration is to be a volume fraction, $\phi << 0.1$ [11]. In most practical situation, this condition is always satisfied.

The continuity equation for the aerosols in an orthogonal coordinate system, as shown in Figure 1, in the absence of production or depletion terms in two dimensions for steady state conditions may be written as:

$$\frac{\partial N_x}{\partial x} + \frac{\partial N_y}{\partial y} = 0 \qquad (1)$$

where N is the total mass flux in the subscripted direction, x is the distance from the stagnation point along the contour of the cylinder and y is the normal distance from the cylinder surface.

The mass fluxes are given by:

$$N_x = u_p c - (D_b + \varepsilon)\frac{\partial c}{\partial x} \tag{2}$$

$$N_y = v_p c - (D_b + \varepsilon)\frac{\partial c}{\partial y} \tag{3}$$

where c is the particle concentration in the gas phase, ε is the particle eddy diffusivity due to turbulence, D_b is the molecular or Brownian diffusion coefficient, and u_p and v_p are the velocity components of aerosol particles in the x and y directions, respectively.

The solution of continuity equation (1) with appropriate boundary conditions yields a concentration profile, c = f(x,y), enabling one to compute the mass flux towards the surface from equation (3). However, the solution of equation (1) as given is extremely difficult. In order to get a reasonable solution without losing the physical realities, the following simplifying assumptions are made:

1. $\varepsilon \neq f(x)$ i.e. the eddy diffusivity is a function of distance measured normal to the surface only and any vari-

ation due to the thickening of boundary layer with x can be neglected.

2. $\varepsilon >> D_b$ and particle and gas diffusivity are equal

3. $\partial^2 c/\partial x^2$ is neglected, being small

4. u_p and v_p may be replaced by fluid velocities u and v for fine particles, with the assumption that within the boundary layer the fluid-particles closely follow the fluid streamlines.

With assumptions (2) and (4), equations (2) and (3) may be simplified to:

$$N_x = uc - \varepsilon\frac{\partial c}{\partial x} \tag{4}$$

$$N_x = vc - \varepsilon\frac{\partial c}{\partial y} \tag{5}$$

Invoking assumptions (1) and (3) and using the simplified flux equations (4) and (5), the continuity equation (1) reduces to:

$$\frac{\partial^2 c}{\partial y^2} - \frac{1}{\varepsilon}\left(v - \frac{\partial \varepsilon}{\partial y}\right)\frac{\partial c}{\partial y} - \frac{u}{\varepsilon}\,\frac{\partial c}{\partial x} = 0 \tag{6}$$

Equation (6) is transformed into dimensionless form by introducing the following dimensionless variables:

$$\bar{c} = \frac{c}{C_0}\ ; \quad \varepsilon = \frac{\varepsilon}{\varepsilon_0}\ ; \quad \bar{x} = \frac{2x}{D_c}\ ; \quad \bar{y} = \frac{2y}{D_c}\,Re_c^{\frac{1}{2}}$$

$$\bar{u} = \frac{u}{U_0} \; ; \quad \bar{v} = \frac{v}{U_0} \, Re_c^{\frac{1}{2}}$$

where C_0, U_0, and ε_0 are the free stream aerosol concentration, gas velocity, and eddy diffusivity, respectively. Re_c is the Reynolds number based on cylinder diameter ($Re_c = D_c U_0/\nu$).

With the above dimensionless variables, equation (6) reduces to:

$$\frac{\partial^2 \bar{c}}{\partial \bar{y}^2} - \frac{1}{\bar{\varepsilon}}\left(0.5 \; Sc \; \bar{v} - \frac{\partial \bar{\varepsilon}}{\partial \bar{y}}\right)\frac{\partial \bar{c}}{\partial \bar{y}} - \frac{0.5 \; Sc \; \bar{v}}{\bar{\varepsilon}} \frac{\partial \bar{c}}{\partial \bar{x}} = 0 \tag{7}$$

where Sc is the turbulent Schmidt number ($Sc = \nu/\varepsilon_0$). The numerical solution of equation (7) requires two boundary conditions. The appropriate boundary conditions are:

B.C. 1: at $\bar{y} = 0$ $\quad \bar{c} = 0$ (8)

B.C. 2: at $\bar{y} = \infty$ $\quad \bar{c} = 1$ (9)

The numerical solution of equation (7) subject to the above boundary conditions (8) and (9), requires the prior knowledge of the eddy diffusivity profile, $\bar{\varepsilon} = f(\bar{y})$ and velocity profiles within the boundary layer. Velocity profiles near the cylinder are obtained from the solution of boundary layer equations:

$$\frac{\partial \bar{u}}{\partial \bar{x}} + \frac{\partial \bar{v}}{\partial \bar{y}} = 0 \tag{10}$$

$$\bar{u}\,\frac{\partial\bar{u}}{\partial\bar{x}} + \bar{v}\,\frac{\partial\bar{u}}{\partial\bar{y}} = \bar{U}\,\frac{d\bar{U}}{d\bar{x}} + \frac{\partial^2\bar{u}}{\partial\bar{y}^2} \qquad (11)$$

subject to boundary conditions:

B.C. 1: at $\bar{y} = 0$ $\bar{u} = 0;\ \bar{v} = 0$ (12)

B.C. 2: at $\bar{y} = \infty$ $\bar{u} = \bar{U}(\bar{x})$ (13)

Levich [12] and Schlichting [13], both claim the boundary layer near the front of a cylinder is very similar to the boundary layer on a flat plate or duct wall. However, the thickness of the boundary layer on a duct wall is usually much greater than that on a cylinder in cross flow. Therefore, the most logical approach is to assume that the shape of the eddy diffusivity profile on a flat plate and on a duct wall is the same as the eddy diffusivity profile in the boundary layer near the front of a circular cylinder. In other words, the normalized eddy diffusivity profiles on both surfaces are equal. Figure 2 shows the eddy diffusivity profile in fully developed turbulent flow [14] while the normalized eddy diffusivity profile is shown in Figure 3. At $\bar{y} = 0$, $\bar{\varepsilon} = 0$, and molecular diffusivity prevails. At the other end of the plot which is the outer edge of the boundary layer, the eddy diffusivity is equal to the free stream eddy diffusivity.

In the above analysis, it is worth mentioning that although we assumed turbulent flow normal to the cylinder, the boundary layer near the cylinder surface is treated as a laminar boundary layer. Therefore in treating the effects of free stream turbulent eddy diffusion in the boundary layer, we note that the influence of turbulent eddy diffusion has not disappeared in the boundary layer, although it decreases as the surface of the cylinder is approached. It is the turbulent eddies which contribute considerably in projecting the aerosol particles towards the cylinder surface.

SOLUTION ALGORITHM

The numerical solution of the continuity equation (7) subject to boundary conditions (8) and (9) requires prior knowledge of the velocity profiles and the eddy diffusivity profile within the boundary layer. Velocity profiles within the boundary layer is obtained from the boundary layer equations (10) and (11) subject to boundary conditions (12) and (13). To solve the boundary layer equations, one has to specify the velocity profile at the outer edge of the boundary layer. For a give external velocity profile, the boundary layer equations may be solved by either the Blasius Method or finite difference solutions [13,15].

The turbulent diffusion model, equation (7), which is a second order partial differential equation in y may be reduced to an ordinary differential equation by replacing the x-derivative by a finite difference approximation. The basic scheme is shown in Figure 4. The solution domain in the x-direction is divided into number of regions bounded by lines $\bar{x}_n$, $\bar{x}_{n-1}$, $\bar{x}_{n-2}$ etc. It is assumed that the solution has been obtained at all stations up to and including $\bar{x}_{n-1}$, which implies that $\bar{c}(\bar{y})$ and its derivatives are fully known at these stations. The problem is to find the solution $\bar{c}(\bar{y})$ at the new station $\bar{x}_n$.

The x-derivative in equation (7) is replaced by finite difference Lagrangian formulas for three points as follows:

$$\left.\frac{\partial \bar{c}}{\partial \bar{x}}\right|_n \cong \left(\frac{1}{\bar{x}_n-\bar{x}_{n-1}}+\frac{1}{\bar{x}_n-\bar{x}_{n-2}}\right)\bar{c}_n - \frac{\bar{x}_n-\bar{x}_{n-2}}{(\bar{x}_n-\bar{x}_{n-1})(\bar{x}_{n-1}-\bar{x}_{n-2})}\,\bar{c}_{n-1}$$

$$+\frac{\bar{x}_n-\bar{x}_{n-1}}{(\bar{x}_{n-1}-\bar{x}_{n-2})(\bar{x}_n-\bar{x}_{n-2})}\,\bar{c}_{n-2} \qquad (14)$$

Thus, equation (7) then reduces to an ordinary second order differential equation in the y-direction, which may be solved by various methods, i.e. Runge-Kutta, predictor-corrector, etc. In this work, equation (7) was integrated by the fourth order Runge-Kutta method and a search technique was used to find the missing boundary condition of $(\partial\bar{c}/\partial\bar{y})_{\bar{y}=0}$ such that the second boundary condition was satisfied. Once the concentration profile was obtained, the local collection efficiency (η_{TD}) and overall collection efficiency ($\bar{\eta}_{TD}$) were calculated from the following equations:

$$\eta_{TD} = \frac{2}{ScRe_c^{\frac{1}{2}}} \bar{\varepsilon} \frac{\partial \bar{c}}{\partial \bar{y}} \bigg|_{\bar{y}=0} \times 100 \qquad (15)$$

$$\bar{\eta}_{TD} = \frac{2}{D_c} \int_0^{\theta_s} \eta_{TD}(\theta) d\theta \text{ --} \qquad (16)$$

where θ_s is angle of separation of the boundary layer from the forward stagnation point.

EXPERIMENTAL AND THEORETICAL RESULTS

The deposition of aerosols on cylinders due to inertial impaction has been studied in the past both theoretically and experimentally under potential or viscous flow conditions. Another important area in aerosol mechanics is the deposition of aerosols under turbulent flow conditions. The deposition of aerosols on cylinders in turbulent cross flow is totally different from inertial impaction mechanism and this is important because in most practical situations deposition occurs under turbulent flow condition. In Figure 5, we present the available experimental data on collection efficiency versus inertial impaction parameter for the deposition of aerosols on cylinders in cross flow for both laminar and turbulent flow conditions [2,10]. Experimental details on inertial and turbulent deposition of aerosols on cylinders in cross flows are given in the above references and are not presented here. Although the data show a lot of scatter, the results clearly indicate that collection efficiency increases with increasing inertial impaction parameter. It may be noted that in Figure 5, the potential flow model tends to overestimate the measured inertial collection efficiency while the viscous flow model grossly underestimate the measured efficiency. Our recent calculations based on the full solution of the Navier-Stokes equation [5], as shown in Figure 5, demonstrate a significant improvement in predicting the measured efficiency over the existing models. However, under turbulent flow conditions, none of these model predictions are close to the measured collection efficiencies. Although the critical value of the inertial impaction parameter is known to be $\psi_{cr} = 0.0625$, below which no deposition occurs [2], it may be observed that collection efficiencies under turbulent flow conditions are much greater than zero for values of ε less than 0.0625.

In order to compare the turbulent deposition results with our turbulent diffusion model, the numerical solution of equation (7) was obtained from the solution of the boundary layer equations. The velocity profile at the outer edge of the boundary layer was assumed to that given by Hiemenz [15] for moderate Reynolds numbers:

$$\overline{U}(\overline{x}) = 1.814\overline{x} - 0.271\overline{x}^3 - 0.0471\overline{x}^5 \qquad (17)$$

The computed velocity profiles and the variation of surface shear stress are shown in Figures 6 and 7, respectively. The boundary layer separates at $\theta_s = 80.5$ from the forward stagnation point.

The computed concentration profiles at the stagnation point across the boundary layer are given in Figure 8, for various values of $ScRe_c^{1/2}$. Comparing the concentration profiles in Figure 8 with the velocity profiles in Figure 6, one observes that the concentration boundary layer is much thinner than the momentum boundary layer and a sharp concentration gradient occurs at the surface.

The local collection efficiency of a cylindrical collector as given by equation (15), is calculated from the local concentration gradient at the surface. In Figure 9, the variation of local collection efficiency from forward stagnation point is given for various values of $ScRe_c^{1/2}$. The local collection efficiency first increases and then decreases as the angle θ increases. The local heat and mass transfer coefficients for circular cylinders in cross flow also show a similar variation as discussed above [16,17]. It may be noted that as the diameter of the collector increases, the local collection efficiency increases. However, the overall collection efficiency decreases.

In Figure 10, we compare measured collection efficiencies as a function of inertial impaction parameter for turbulent deposition with the turbulent diffusion model predictions. When one compares the measured and predicted collection efficiencies due to turbulent diffusion with the inertial impaction model (as shown in Figure 5), it clearly demonstrates a significant improvement over classical models. However, the new model tends to overestimate the collection efficiencies. This may be attributed to the fact that in this type of experimental work, the probability of making negative error far exceeds the probability of making positive error. In the model development, the effect of particle-particle cohesion or particle-collector adhesion was not taken into account. Furthermore, the loss of aerosol already deposited on the collector surface can occur by sloughing during the deposition process and also at the time of withdrawing the collector for sampling. Therefore, it is logical to conclude that the true collection efficiency may be the upper boundary of the data envelope of Figure 10 rather than the median curve. Finally, in Figure 11, we present the measured collection efficiency as a function of the characteristic group $ScRe_c^{1/2}$ for 0.86 μm particles along with the new model predictions.

CONCLUSIONS

A new model has been developed to describe the deposition of aerosols on an isolated cylindrical collector under turbulent flow condition. The model is based on the concept of eddy diffusivity and has been tested by comparing the theoretical results with the available experimental data [2,10]. The turbulent diffusion model, which is the solution of the continuity equation for aerosol particles under turbulent flow conditions, can reasonably predict the experimental observations. The numerical solution of the model equations requires the assumption of an eddy diffusivity profile within the boundary layer and a velocity profile at the outer edge of the boundary layer. In this work, the normalized eddy diffusivity profile near the cylinder surface was assumed to have the same shape as the eddy diffusivity profile near a flat plate while the velocity profile at the outer edge of the boundary layer was assumed to be that given by Hiemenz [15] for moderate Reynolds numbers.

ACKNOWLEDGEMENTS

The authors gratefully acknowledge the Ontario Ministry of the Environment and the Natural Sciences and Engineering Research Council for the financial support made in the form of a university research grant and an operating grant respectively.

REFERENCES

1. Fuchs, N.A., Mechanics of Aerosols, The MacMillan Company, New York, 1964.

2. Ranz, W.E. and Wong, J.B., Impaction of Dust and Smoke Particles on Surface and Body Collectors, Ind. Eng. Chem., 44, 1371-1381, 1952

3. Brauer, H., Movement of Single Particles In Various Flow Field. In Majumder A.S. and Mushelkar, R.A. (eds.), Advances in Transport Processes Vol. III, John Wiley & Sons, 1982.

4. Strauss, W., Industrial Gas Cleaning (2nd ed.), Pergamon Press, New York, 1975.

5. Ilias, S. and Douglas, P.L., The Deposition of Aerosols on Cylinders in Crossflow: A Time Dependent Study, Proc. 10th Can. Cong. App. Mech., B-41, 1985.

6. Friedlander, S.K. and Johnstone, H.F., Deposition of Suspended Particles from Turbulent Gas Streams, Ind. Eng. Chem., 47, 7, 1151-1165, 1957.

7. Lui,B.Y.H. and Agarwal, J.K., Experimental Observation of Aerosol Deposition in Turbulent Flow, J. Aerosol Sci., 5, 145-155, 1974.

8. Papavergos, P.G. and Hedley, A.B., Particle Deposition Behaviour from Turbulent Flows, Chem. Eng. Res. Des., 62, 275-293, 1984.

9. Douglas, P.L., Dullien, F.A.L. and Spink, D.R., Particle Agglomeration and Synergism Between Inertial Impaction and Eddy Diffusion, Can. J. Chem. Eng., 61, 776-784, 1983.

10. Douglas, P.L., Ph.D. Dissertation, University of Waterloo, Waterloo, 1980.

11. Soo, S.L., Fluid Dynamics of Multiphase Systems, Baisdell Publishing Co., Waltham, 1967.

12. Levich, V.G., Physicochemical Hydrodynamics, Prentice-Hall Inc., Englewood Cliffs, N.J., 1962.

13. Schlichting, H., Boundary-Layer Theory (6th ed.), McGraw-Hill Book Co., N.Y., 1968.

14. Davies, C.N., Deposition of Aerosols from the Turbulent Floe Through Pipes, Proc. Royal Soc. (London), A 289, 235-246, 1966.

15. White, F.M., Viscous Fluid Flow, McGraw-Hill Book Co., N.Y., 1974.

16. Oosthuizen, P.H., Numerical Study of Combined Convective Heat Transfer from a Cylinder in a Horizontal Flow, Proc. 6th Int. Heat Transfer Conf., MC-4, 19-24, 1978.

17. Mizushina, T., Ueda, H. and Nobuyki, N., Effect of Free-stream Turbulence on Mass Transfer from Circular Cylinder in Cross Flow, Int. J. Heat Mass Transfer, 15, 769-780, 1972.

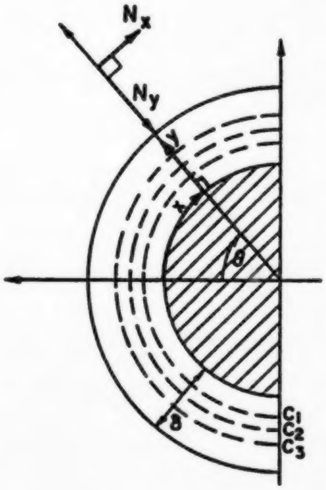

FIGURE 1. Schematic Diagram of Orthogonal Co-ordinates, Concentration Contours and Fluxes to a Cylinder.

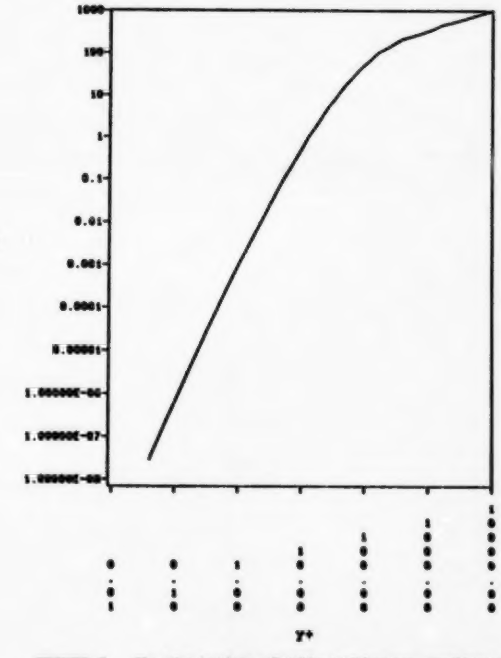

FIGURE 2. The Variation of Eddy Diffusion Coefficient with Distance from the Wall for Fully Developed Turbulent Pipe Flow [14].

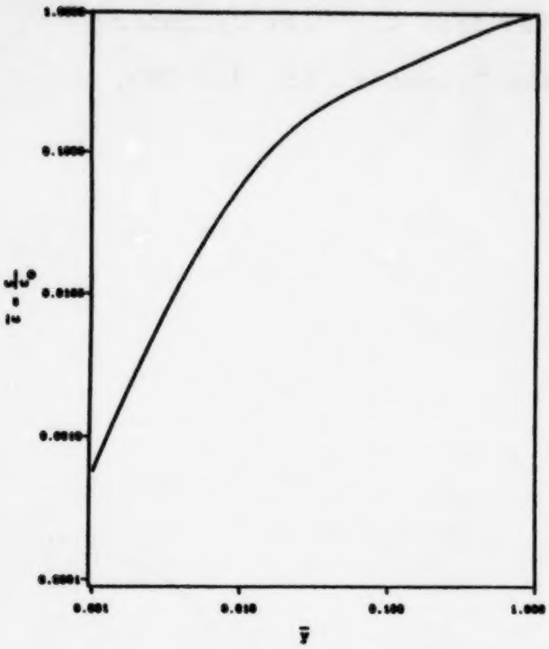

FIGURE 3. Dimensionless Eddy Diffusivity Versus Dimensionless Distance from the Wall.

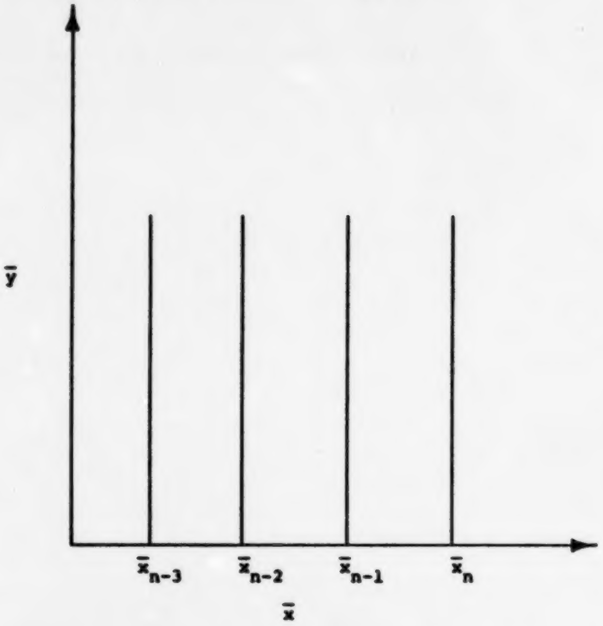
$\bar{y}$
$\bar{x}_{n-3}$
$\bar{x}_{n-2}$
$\bar{x}_{n-1}$
$\bar{x}_n$
$\bar{x}$

FIGURE 4. Coordinate and Notation System.

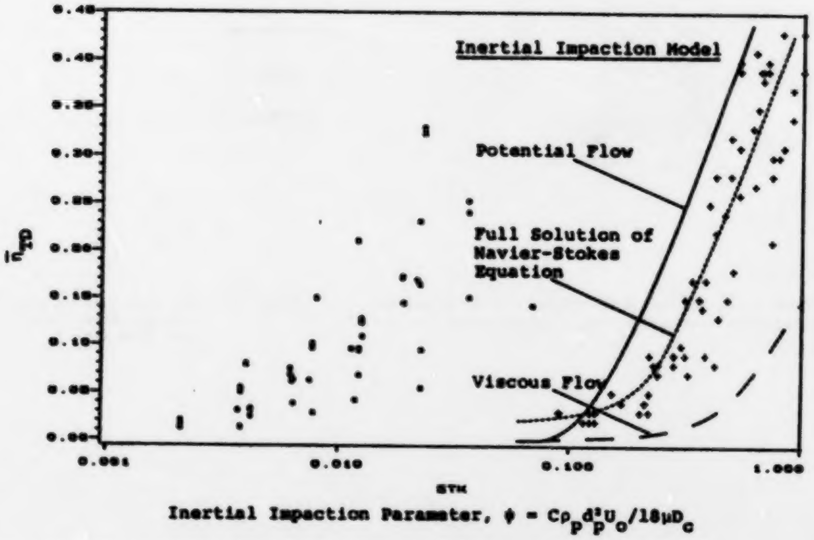

FIGURE 5. Comparison of Various Experimental Data (see Douglas, 1980; +++ Ranz & Wong, 1952) for the Collection of Aerosols on Single Cylinders in Cross Flow with Predictions of Inertial Impaction Models.

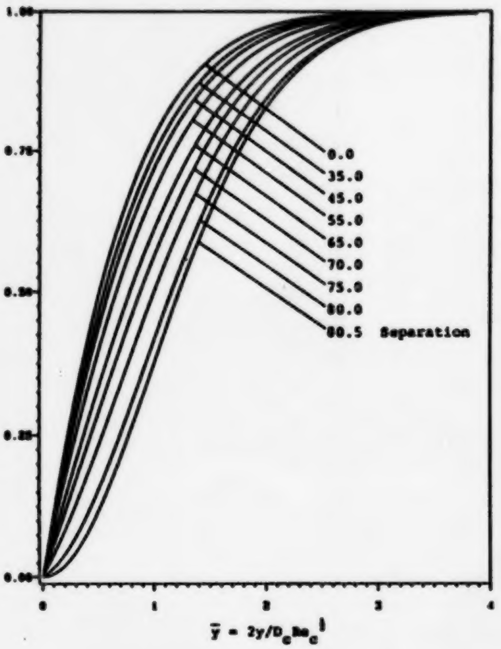

FIGURE 6. Velocity Profiles in the Boundary Layer on a Circular Cylinder Based on Experimental Velocity Distribution.

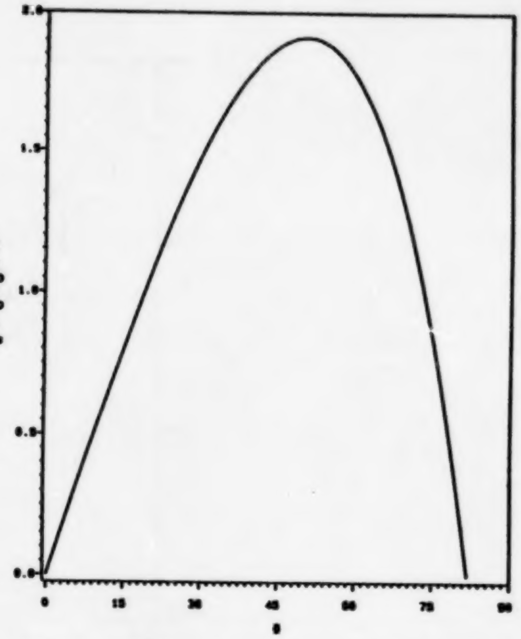

FIGURE 7. Variation of Shearing Stress at the Wall of a Circular Cylinder for a Laminar Boundary Layer.

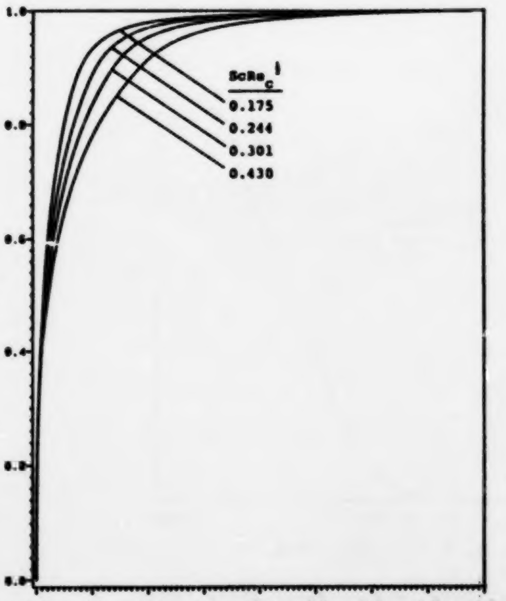

FIGURE 8. Concentration Profiles at the Stagnation Point across the Boundary Layer for Various Values of $ScRe_c^{1/2}$.

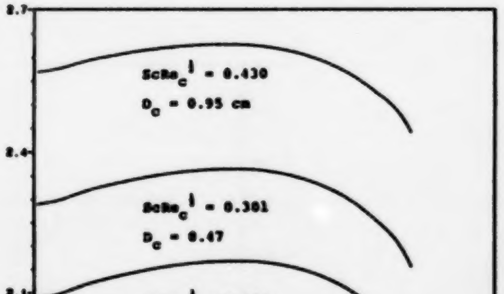

FIGURE 9. Variation of Local Collection Efficiency of Aerosols on Cylinder Surfaces for Various Values of $ScRe_c^{1/2}$.

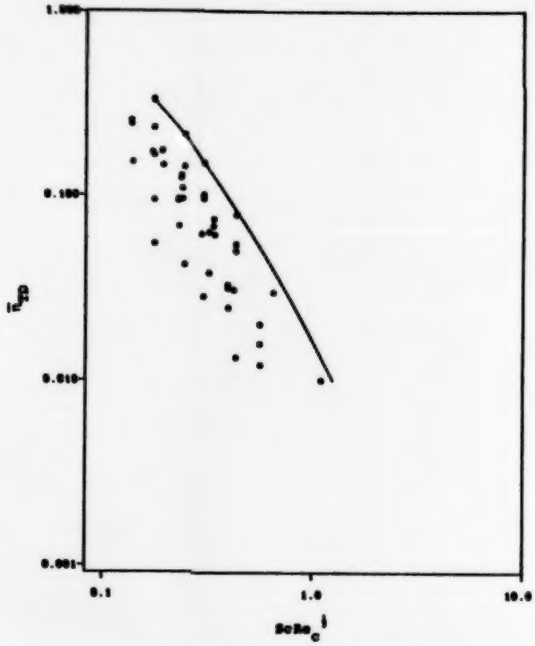

FIGURE 11. Comparison of Measured Collection Efficiency vs. $ScRe_c^{\frac{1}{2}}$ with Turbulent Diffusion Model Predictions.

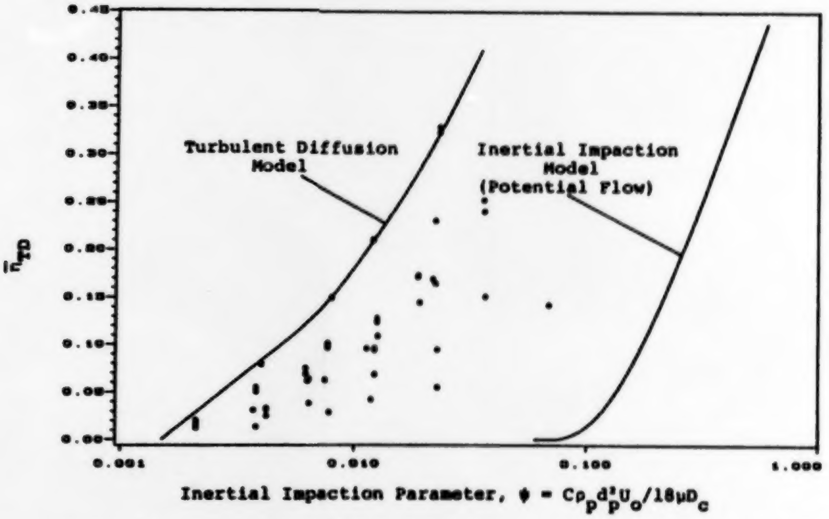

FIGURE 10. Comparison of Experimental Data (see Douglas, 1980) for the Collection of Aerosols on Single Cylinders from Turbulent Flow with Predictions of Turbulent Diffusion Model and Inertial Impaction Model.